CHEMICAL REVIEWS

pubs.acs.org/CR

Review

Photoclick Chemistry: A Bright Idea

Benjamin D. Fairbanks, Laura J. Macdougall, Sudheendran Mavila, Jasmine Sinha, Bruce E. Kirkpatrick, Kristi S. Anseth, and Christopher N. Bowman*

Cite This: *Chem. Rev.* 2021, 121, 6915−6990

Read Online

ACCESS | Metrics & More | Article Recommendations

ABSTRACT: At its basic conceptualization, photoclick chemistry embodies a collection of click reactions that are performed via the application of light. The emergence of this concept has had diverse impact over a broad range of chemical and biological research due to the spatiotemporal control, high selectivity, and excellent product yields afforded by the combination of light and click chemistry. While the reactions designated as "photoclick" have many important features in common, each has its own particular combination of advantages and shortcomings. A more extensive realization of the potential of this chemistry requires a broader understanding of the physical and chemical characteristics of the specific reactions. This review discusses the features of the most frequently employed photoclick reactions reported in the literature: photomediated azide−alkyne cycloadditions, other 1,3-dipolarcycloadditions, Diels−Alder and inverse electron demand Diels−Alder additions, radical alternating addition chain transfer additions, and nucleophilic additions. Applications of these reactions in a variety of chemical syntheses, materials chemistry, and biological contexts are surveyed, with particular attention paid to the respective strengths and limitations of each reaction and how that reaction benefits from its combination with light. Finally, challenges to broader employment of these reactions are discussed, along with strategies and opportunities to mitigate such obstacles.

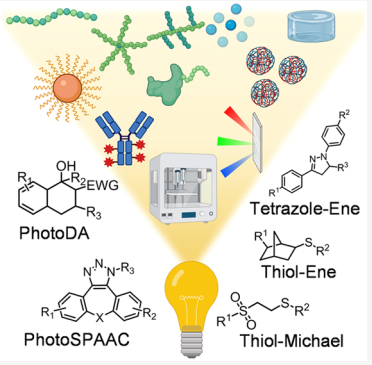

CONTENTS

1. Introduction 6916
1.1. The Click Chemistry Paradigm 6916
1.2. Photochemistry Introduction 6916
1.3. The Concept of Photoclick Chemistry 6920
1.3.1. One Photon, One Event vs One Photon Many Events Reactions 6921
1.3.2. Light Attenuation 6921
1.3.3. Other General Challenges in Photoclick Chemistry and Proposed Criteria for Designation 6922
2. Photoclick Reactions 6924
2.1. Dipolar Cycloadditions 6925
2.1.1. Azide−Alkyne Cycloaddition 6925
2.1.2. Photocaged Nitrile Imines and Nitrile Ylides 6930
2.2. Diels−Alder Reactions 6932
2.2.1. Photoenolization DA Reactions 6933
2.2.2. Inverse Electron Demand Diels−Alder 6934
2.3. Alternating Radical Propagation Chain Transfer Reactions 6935
2.3.1. Thiol−ene 6935
2.3.2. Thiol−yne 6939
2.3.3. Other APT Reactions: Iodo−ene, Silane−ene, and Phosphane−ene 6940
2.4. Photoinduced Click Reactions Based on Thiolate Nucleophiles 6940
2.4.1. Photolatent Base/Nucleophile Catalyzed Thiol−Epoxide Click Reactions 6941
2.4.2. Photolatent Base Catalyzed Thiol−Isocyanate Click Reactions 6942
2.4.3. Photolatent Base/Nucleophile Catalyzed Thiol-Michael Addition 6943
2.4.4. Click Reactions Based on Photolatent Thiols and Other Nucleophiles 6946
2.4.5. Photoinduced Native Chemical Ligation 6950
3. Applications 6951
3.1. Drug Development and Small Biomimetic Molecules 6951
3.2. Oligomerization and Polymerization Reactions 6953
3.3. Macromolecular Modification 6954
3.3.1. Biolabeling 6954
3.3.2. Polymer−Polymer Conjugation 6958
3.3.3. Biomacromolecule−Polymer Conjugation 6960
3.4. Surface Modification and Patterning 6960

Special Issue: Click Chemistry

Received: November 16, 2020
Published: April 9, 2021

https://doi.org/10.1021/acs.chemrev.0c01212
Chem. Rev. 2021, 121, 6915−6990

3.5. Network Polymers 6962
3.5.1. Dental Restoratives 6963
3.5.2. Photolithography and Additive Manufacturing 6963
3.5.3. Optical Materials 6965
3.5.4. Hydrogels and Tissue Engineering 6966
3.5.5. Microparticles and Nanoparticles 6972
3.6. Obstacles in Application of Photoclick Reactions 6974
4. Conclusions 6975
Author Information 6975
Corresponding Author 6975
Authors 6975
Notes 6976
Biographies 6976
Acknowledgments 6976
Abbreviations 6976
References 6977

1. INTRODUCTION

Photoclick reactions combine high yields and selectivity with the advantages of light-triggered conjugation. While these chemistries fall into just a handful of diverse reactions, they do not necessarily share much in common with regards to mechanism for either their respective photochemical processes or their subsequent coupling. It is rather their broad applicability to diverse chemical requirements and their ease of use that defines the category of "photoclick chemistry." While this classification originated in 2008 with the rise in popularity of tetrazole−ene couplings, many reactions described currently as "photoclick" have been in use for decades earlier, and in 2013, Tasdelen et al. reviewed this nascent field.[1] Here, this review expands upon and updates that survey to address recent advances in the field. A brief introduction to click concepts and reactions as well as photochemistry is presented along with a general description of those features common to photoclick reactions. The chemistry of those reactions most frequently described as "photoclick" is then presented followed by a description of the various fields and applications in which those reactions have been used most effectively. Particular attention is given to the specific features of each reaction and how those characteristics are exploited for the respective applications of each chemistry. The review concludes with a discussion of obstacles to broader application of photoclick chemistry and an outlook for the future of this category of reactions.

1.1. The Click Chemistry Paradigm

The concept of "Click Chemistry" is at once potentially transformative and tantalizingly simple.[2] At its most fundamental, this philosophy could be summarized as chemists should use reactions that work well. While this may seem obvious, it is instructive for the community of researchers to identify and give preference to those reactions that are typically more "fool proof" than average so that those who seek to replicate and build on others' past achievements will start their endeavors with the greatest potential for success.

When Sharpless and co-workers elucidated the philosophy of "Click Chemistry," they established criteria requisite for inclusion in this elite class of chemical conjugations. Such reactions, they proposed, should be "modular, wide in scope, give very high yields, generate only inoffensive byproducts that can be removed via nonchromatographic methods," and be carried out via processes that include "simple reaction conditions. . .should be insensitive to oxygen and water. . ., readily available starting materials and reagents, the use of no solvent or a solvent that is benign or easily removed. . ., and simple product isolation."[2] These criteria are summarized in Table 1. Notable is the requirement of "modularity," which indicates the potential of the reactions to be used as part of a strategy for generating complex molecular structures by the independent synthesis and subsequent assembly of smaller subunits. This requirement favors reactions between complementary reactive groups; many dimerization reactions may be extremely efficient but do not otherwise result in modularity. Modularity is also favored by reactions that are orthogonal to other functional groups potentially present in the environment in which the reaction is employed. While all of these click chemistry characteristics are self-evidently beneficial to the ease and success of synthesis of complex, conjugated products, many of them are dependent on the context in which they are employed. What may be an inoffensive, easily removed byproduct in the synthesis of a small molecule, for example, may be detrimental to the application of that chemistry in the presence of living cells or organisms or polymeric species. Conversely, those cells may well tolerate byproducts (thus rendering them "inoffensive") that would otherwise require chromatographic separation.

As an illustration of the context dependence of the utility of click reactions, one may consider the challenge of conjugating or functionalizing macromolecules.[3,4] In some cases, "click" criteria are more easily met in the application of reactions to the coupling of such compounds. A coupling between two small molecules may result in a byproduct that is difficult to separate from the desired small molecule product; the same chemistry applied to the conjugation of two macromolecules may result in the same undesired byproduct which, in this latter case, is easily removed via a quick precipitation of the desired high MW species in a poor solvent (e.g., methanol for highly hydrophobic polymers or diethyl ether for hydrophilic polymers). More frequently, however, the reactions often referred to as "click" in the context of small molecule synthesis, are less effective in macromolecular modification. The high molecular weights of these compounds and the necessity of significant amounts of solvent to dissolve them often preclude the performing of any conjugations in anything but dilute solutions.[4] As a consequence, the polymer research community has designated additional criteria for the designation of "click reactions" for the purposes of polymer modification.[3] These are summarized in Table 1 and include amenability to scalable purification, fast reaction time scales, successful reactions under equimolar conditions, and suitability for generation of polymer−polymer conjugates.

1.2. Photochemistry Introduction

The reactions designated in the literature as "photoclick" proceed via various mechanisms; therefore, it is advantageous to review the fundamentals of photochemistry to establish a solid grounding for subsequent discussion of these reactions.

The electromagnetic spectrum encompasses radiative energy with wavelengths from as small as one picometer to 100 000 km, a range of 17 orders of magnitude. This energy is distributed in quanta referred to as "photons," yet by convention, the term "photochemistry" does not generally include those reactions mediated by highly energetic ionizing

https://doi.org/10.1021/acs.chemrev.0c01212
Chem. Rev. 2021, 121, 6915−6990

Table 1. Original Criteria for Click Chemistry As Defined by Kolb et al.,[2] Supplementary Criteria for Designation of Click Reactions, as Proposed by Barner-Kowollik et al.,[3] in the Context of Polymer Chemistry and Supplementary Criteria for Designation of Photoclick Chemistry Recommended in This Work

2001 original criteria for click reactions *Kolb et al.*[2]	2011 additional criteria for polymer click reactions *Barner-Kowollik et al.*[3]	2021 proposed criteria for photoclick reactions *This work*
• modular • wide scope • high yielding • inoffensive byproducts • stereospecific where applicable • simple reaction conditions (e.g. O_2, H_2O insensitive) • readily available materials • amenable to solvent-free or easily-removed solvent • simple product isolation	• scalable purification • fast reaction timescales • successful reactions under equimolar conditions • suited to polymer-polymer conjugation	• can be performed with easily obtained light exposure instrumentation • avoids use of high energy wavelengths of light • triggerable by relatively low light intensities • fast reaction timescales • high specificity

radiation (below about 150 nm). Very long wavelengths provide inadequate energy to initiate many chemical reactions at all, and thus wavelengths exceeding that of the near-infrared region of the spectrum are generally considered less consequential to the study of photochemistry.

Whereas catalysts decrease the activation energy barrier for a reaction to occur (Figure 1), photochemical reactions are achieved by photoactivation of species "R," providing the reactant alterantive reaction pathways potentially exhibiting lower energy barriers. For more detailed discussion of reaction energy coordinate diagrams of photochemical processes, the reader is directed to this 2016 review by Kärkäs et al.[5] and Turro, Ramamurthy, and Scaiano's book on the principles of photochemistry.[6] This lends some significant advantageous features of photochemical reactions. Many reactions that would otherwise be extremely slow, with the exposure to an appropriate wavelength of light, occur at relatively low temperatures. This is of particular relevance in the management of synthetic polymer waste; solar radiation of polymers such as polybutadiene and polystyrene accelerates their degradation.[7] Another pertinent example especially relevant to the discussion of photoclick reactions, is the decomposition of tetrazoles to nitrile imides, which can be accomplished thermally but may progress much more quickly and with much lower energy input with exposure to appropriate wavelengths of light.[8]

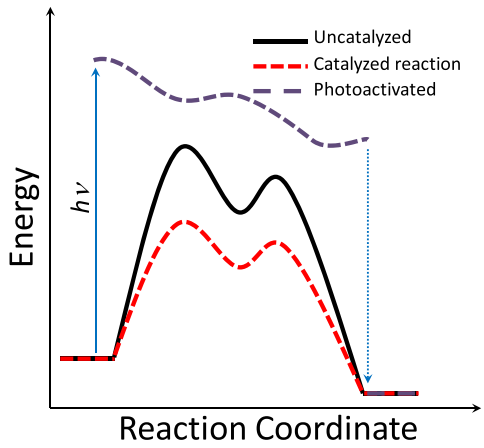

Figure 1. Reaction coordinate plotted against energy for uncatalyzed, catalyzed, and photomediated chemical reactions. Catalysts lower activation energy barriers, facilitating increased reaction rates. In photochemical reactions, absorbed photons put the absorbing species in a higher energy state from which alternative chemical reaction pathways may effectively proceed.

Thus, the application of photochemistry can be exceptionally energy efficient, but the advantages extend well beyond this. The fact that chemical reactions can be performed at lower temperatures and with the selection of particular and appropriate spectra of light exposure provides a specific selectivity or orthogonality to the performing of such reactions; photoreactions can be performed with exposure at one wavelength of light in the presence of other chemical moieties that might be sensitive to the input of thermal energy or even to other wavelengths of light.

The mediation of chemical reactions via light also provides for temporal control. It should be noted that while a specific photochemical reaction proceeds only upon exposure and is arrested by the removal of the stimulus, downstream chemical reactions may persist, potentially mitigating the absolute temporal control over the reaction. For example, light may release a photolatent catalyst that proceeds to facilitate the reaction. When the light is turned off, the catalyst remains potent. In such a case, temporal control only over commencement of the desired reaction is realized, and cessation of the reaction is determined by other aspects of the reaction conditions.

A similar relationship with spatial control is also realized by the application of photochemistry. As with temporal control, spatial occlusion of light exposure provides dimensional control over where the reaction takes place. This restriction is most easily done in two dimensions, at interphases or with three-dimensional projections of two-dimensional images. Sophisticated manipulation of light by focusing, multiphoton excitement, interference, etc., however, has allowed true three-dimensional control over exposure in general and photoclick

https://doi.org/10.1021/acs.chemrev.0c01212
Chem. Rev. 2021, 121, 6915−6990

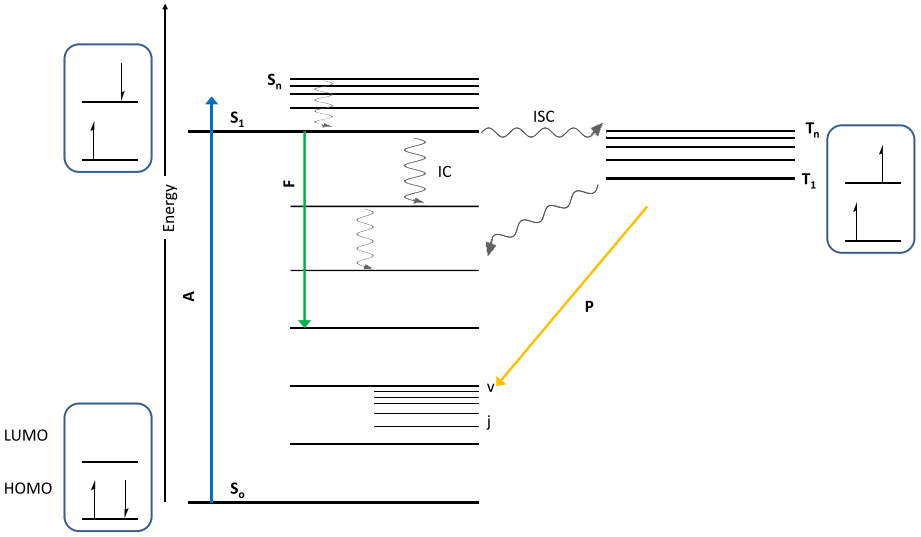

Figure 2. General Jablonski diagram for the possible fates of photonic energy absorbed by a photoactivated molecule. Internal conversion is denoted by IC; intersystem crossing, ISC; fluorescence, F; phosphorescence, P; absorbance, A. Also shown are the electron orbitals and spins. Highest occupied molecular orbital is abbreviated HOMO and lowest unoccupied molecular orbital is abbreviated LUMO.

chemistry in particular. As with temporal control, however, spatial control may be limited by the persistence of products from the photochemical reaction; photoactivated catalysts may diffuse beyond the spatial limits of exposure, decreasing the resolution of the physical boundaries of the reaction space.

For a photochemical reaction to take place, there must be a species that absorbs photons of the wavelength of light to which it is exposed. This guideline is often referred to as the first law of photochemistry or the Grothuss–Draper law.[9] The second law of photochemistry or the Stark–Einstein law states that one absorbed photon can excite only one molecule.[10] Typically, one absorbed photon excites exactly one molecule, though multiphoton activation, wherein the quick succession of sequential absorption of lower energy photons activates a single absorbing species, is an exception to this.

For single photon activation, however, it is the light dose, rather than intensity, that dictates how many molecules will become photoactivated. For the initial stage of the primary photochemical processes, longer exposure times at lower intensity are equivalent to shorter times at a higher intensity. This outcome is limited though because reactions subsequent to the primary photochemical event may have nonlinear relationships with the concentration of light activated species. As such, the end result often does not result in a proportional relationship with light dose. The relationship describing the amount of light of a particular wavelength (A) absorbed by a chromophore is known as the Beer–Lambert law (eq 1), wherein c refers to the concentration of the absorbing species, l refers to the path length of the light, and ε refers to the wavelength (λ) dependent extinction coefficient, a standard measurement of how much light is absorbed by a given concentration of absorbing species at a standard path length. The extinction coefficient typically has units of L/(mole cm),

$$A(\lambda) = \varepsilon(\lambda)\cdot c\cdot l \tag{1}$$

While the Beer–Lambert law indicates a linear relationship between absorption and concentration, it should be noted that this linearity does not always extend indefinitely. A variety of factors cause nonlinear deviation at higher concentrations.[11]

The intramolecular or atomic photophysical processes that occur following absorption of light are often portrayed in what is known as a Jablonski diagram. A general Jablonski diagram portrays the possible energy processes a light absorbing molecule may undergo (Figure 2). Upon absorption of a photon, a molecule or atom may move from its ground state, S_o, to an excited singlet state, S_n. From higher singlet states ($n > 1$), the excited species relaxes to its lowest excited singlet state, S_1, via a radiationless decay process designated "internal conversion" or "IC." The exitation energy lost in this process is converted to thermal energy via vibrational relaxation. From the S_1 state, the remaining energy from the absorbed photon may be dissipated via a number of means as the molecule returns to its ground state. It may be released as a photon of lower energy in the process of fluorescence, or it may be lost via internal conversion to thermal energy. Alternatively, it may undergo another radiationless decay process, "intersystem crossing" or "ISC," that moves the excited species to a triplet state (T_n), from which it undergoes internal conversion to reach its lowest excited triplet state (T_1). This ISC process results in the excited state molecule possessing two unpaired electrons with the same spin. As returning to ground state S_o from T_1 requires a change in electron spin, this transition generally takes more time. Because of the longer triplet state lifetime, many photoreactions occur from the excited triplet state. Indicative of this phenomenon is the difference between radiative decay from the excited singlet state (fluorescence; lifetime from $<10^{-10}$ to 10^{-7} s),[12] which occurs very quickly following irradiation, and the radiative decay from the excited triplet state (phosphorescence; lifetime from 10^{-5} to $>10^{3}$ s),[13] which persists, frequently for minutes, following the cessation of photoexposure.

An excited atom or molecule can undergo a combination of radiative (fluorescence, phosphorescence) and nonradiative (internal conversion and intersystem crossing) processes in its pathway to return to the ground state. In addition, it may undergo bond rearrangement, either intramolecularly or intermolecularly, to generate new products. The fraction of excited molecules that undergoes a particular process is referred to as the quantum yield (φ) and is a measure of the

https://doi.org/10.1021/acs.chemrev.0c01212
Chem. Rev. 2021, 121, 6915–6990

efficiency of a given photochemical process relative to the light absorbed. A quantum yield exists for every potential photochemical process; however, some are frequently negligible. Quantum yield can be defined in terms of the respective first-order reaction rate constants "k" (Figure 3) and the lifetime of

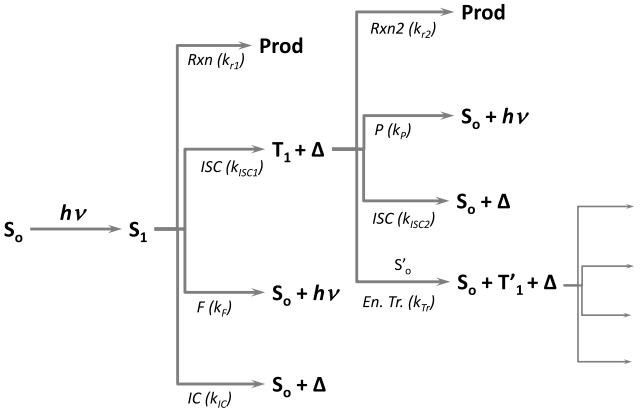

Figure 3. Flowchart showing the processes that an absorbing molecule may take with the accompanying potential products and the reaction constants.

the excited states "τ", which is the inverse of the sum of all possible reactions from that state (eqs 2 and 3, where subscripts S, and T correspond to the singlet and triplet states, respectively, and subscripts r1, ISC1, F, IC, r2, ISC2, P and Tr correspond to the processes of reaction from the singlet state, intersystem crossing to the triplet state, fluorescence, internal conversion, reaction from the triplet state, intersystem crossing to the ground state, phosphorescence, and energy transfer, respectively). The quantum yield for any process is the reaction rate constant of that process multiplied by the lifetime of the excited state from which it occurs whether for fluorescence (eq 4), a photochemical reaction from the triplet state (eq 5), or any of the processes shown in Figure 3.

$$\tau_S = \frac{1}{k_{r1} + k_{ISC1} + k_F + k_{IC}} \quad (2)$$

$$\tau_T = \frac{1}{k_{r2} + k_{ISC2} + k_P + k_{Tr}} \quad (3)$$

$$\phi_F = k_F \cdot \tau_S \quad (4)$$

$$\phi_{rxn2} = k_{r2} \cdot \tau_T \quad (5)$$

In addition to the photochemical processes mentioned above, an excited atom or molecule can transfer energy to another molecule or atom, resulting in that species being elevated to a higher energy state despite having not directly absorbed any photons (Figure 4). The newly excited atom or molecule can undergo similar radiative and nonradiative decay processes from its own excited state (Figure 3).

Photochemical reactions are broadly categorized into six nondiscrete categories (Figure 5). Excited species undergo bond breaking wherein the compound generates one or more chemically distinct products. Examples of such reactions are abundant in both the lab and in many day-to-day experiences. Photolabile groups on reactive side groups during solid phase peptide synthesis have been used for decades as orthogonal protecting groups (Figure 6). Cleavage-type radical photoinitiators are common both in research and in consumer

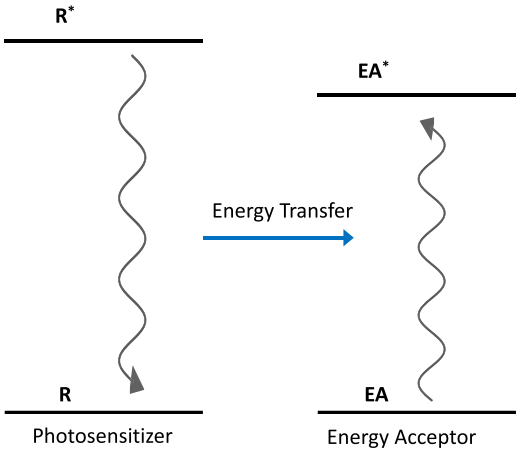

Figure 4. Jablonski diagram for photosensitization wherein an excited molecule transfers energy from its high energy, excited state, to another molecule, placing it in an excited state while the original molecule relaxes to ground state.

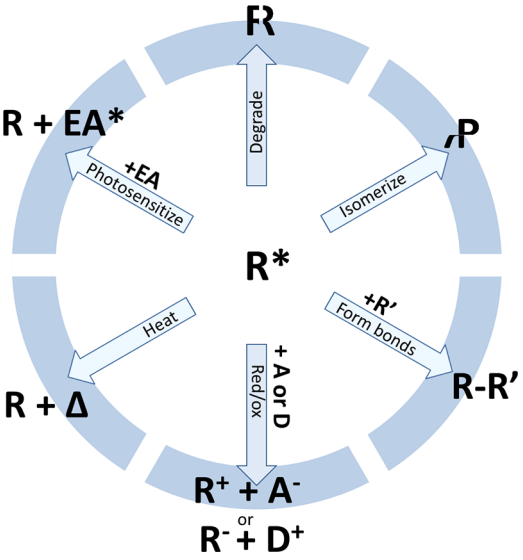

Figure 5. Photoactivated species can participate or initiate chemical reactions via one of these six general mechanisms.

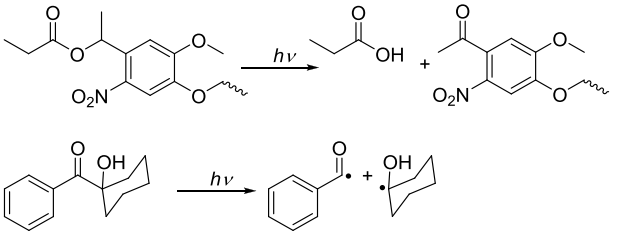

Figure 6. Two examples of photomediated degradation including photodeprotection of a carboxylic acid (top) and photomediated cleavage of 1-hydroxycyclohexyl phenyl ketone.

products (Figure 6). Beer and red wines are frequently stored in green or amber tinted bottles to mitigate the UV-mediated degradation of flavor compounds.

Bond breaking that results in subsequent intramolecular reorganization of those bonds rather than the more permanent scission thereof creates isomers of the ground state compound in photoisomerization reactions. While azobenzene and its

https://doi.org/10.1021/acs.chemrev.0c01212
Chem. Rev. 2021, 121, 6915−6990

derivatives are among the most widely studied compounds prone to photoisomerization (Figure 7), many people are

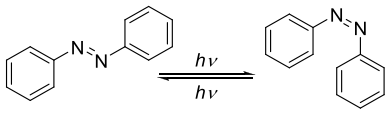

Figure 7. Photoisomerization of azobenzene wherein high energy UV light isomerizes the trans form to the cis form. Exposure to visible light isomerizes the cis form to the trans form.

familiar with photochromic eyeglasses that change absorbance characteristics in sunlight due to photoisomerization. Phototherapy to treat neonatal jaundice employs blue and green lights to photoisomerize bilirubin to a more soluble form for more efficient clearing from the bloodstream.[14]

In the presence of photoexcited species, bonds may break and reform with other molecules to create new bonds in photoinduced reactions. While many photoreactions lead indirectly to bond formation (e.g., frequently cited as an example of photochemistry in introductory chemistry textbooks, the chlorination of methane begins with the photocleavage of Cl_2 to Cl radicals), these are examples of bonds forming as a result of the reactions of photogenerated species rather than the reactions of photoexcited species themselves. Among this class of directly photoactivated bond forming cyclization reactions is the [2 + 2] cycloaddition. First observed in 1908, this reaction consists of the reaction of a photon-absorbing enone with an alkene.[15] Frequently, the enone provides the alkene in the reaction as well with the resulting product being the dimer. The photomediated [2 + 2] cycloaddition of pyrimidine nucleobases (thymine and cytosine)[16] is one of the mutagenic reactions in the DNA of epidermal cells that has been implicated in the development of melanomas (Figure 8).[17]

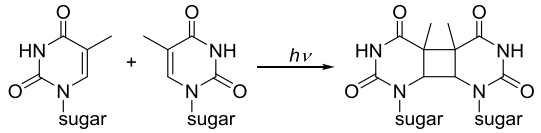

Figure 8. Photodimerization of thymine (shown) and cytosine in DNA has been implicated in the development of skin cancer.

Not all photochemical processes that effect subsequent chemical reactions involve the breaking or rearrangement of covalent bonds within the chromophore itself. Molecules in the S_1 or T_1 state have unpaired electrons in both higher and lower energy orbitals (Figure 2), and they are more prone than their ground state counterparts to participate in electron transfer processes, either as an oxidant or reductant (Figure 9). The donation of electrons or acceptance of electrons results in the formation of a radical ion species without necessarily breaking any chemical bonds. Although subsequent bond breaking is a frequently observed consequence of the photoinduced electron transfer, the photocatalysts is often regenerated by downstream electrochemical processes.[18]

The internal conversion of photonic energy to heat (photothermal) may also mediate chemical reactions among other molecules within proximity without any chemical change of the absorbing species. A common application of photothermal effects involves the introduction of gold or silver

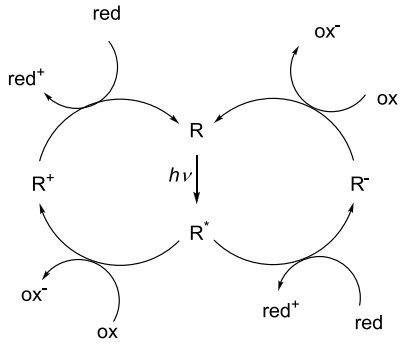

Figure 9. General scheme for photoredox reactions with oxidative quenching shown on the left and reductive quenching shown on the right. In oxidative quenching, the light-activated species loses an electron to an oxidizer, gaining a net positive charge. The photoactive species is regenerated by reduction. In the reductive quenching mechanism, the photoactivated species accepts an electron from a reducer, gaining a net negative charge. The photoactive species is regenerated by oxidation.

nanoparticles with high infrared and near-infrared absorbances (Figure 10). Upon irradiation with NIR and IR light, the

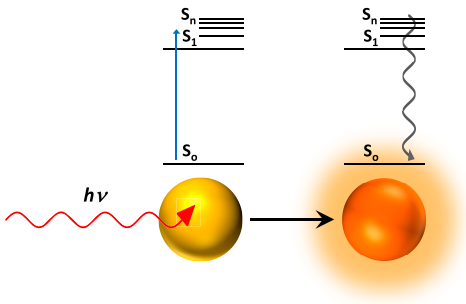

Figure 10. Photothermal relaxation of gold nanoparticles, transitioning absorbed photonic energy into thermal energy via internal conversion.

nanoparticles absorb photons and release the acquired energy via internal conversion to heat. While this heats up the average temperature of the surrounding environment, the local responses of temperature sensitive polymers (e.g., poly(*N*-isopropylacrylamide)) have exhibited temperature dependent responses corresponding to temperatures substantially higher than that of the bulk medium, indicating highly localized thermal effects of the light activated nanoparticles. Similar effects are achieved with IR dyes. In general, photothermal effects provide a means for initiating thermally sensitive reactions via exposure to light.

Finally, as noted above, excited state species may transfer that excitement to other molecules via photosensitization whereupon those newly excited molecules may undergo any of the above-mentioned photochemical and photophysical reactions.

1.3. The Concept of Photoclick Chemistry

While conventional click reactions are often mediated by the addition of catalysts or moderate heating, temporal control over the reaction is frequently limited; once the reactants are all in the reaction vessel, the reaction begins. Photomediated reactions allow at least one element of temporal control over the reaction and frequently, depending on the particular

https://doi.org/10.1021/acs.chemrev.0c01212
Chem. Rev. 2021, 121, 6915−6990

reaction employed, a very high degree of both spatial and temporal control over the reaction.

This combination of advantages leads to photomediated click reactions being of particular benefit to a wide variety of applications, including 3D printing, patterned surface chemistry modification, in situ hydrogel synthesis, and many more described in the applications section of this review. It is not the spatial and temporal control only, however, that dictates the applications of photoclick reactions. High rates relative to nonphotomediated reactions may also be reason to employ photoclick chemistry in particular applications. There are, however, contexts in which photoclick reactions may not be appropriately suited and a better understanding of the features of those reactions will foster informed decisions as to when they can be effectively utilized.

1.3.1. One Photon, One Event vs One Photon Many Events Reactions. In many photomediated reactions, photolatent catalysts are released upon exposure to an appropriate wavelength of light, initiating the reaction. As one photon is capable of activating one catalyst molecule which is in turn capable of facilitating many reactions, this amplification is often referred to as a "one photon, many events" chemistry. Without a mechanism to consume or poison the catalyst, the reaction will continue to completion even after the light is turned off. In some recent examples, photolatent acids have been used to deactivate base catalysts.[19] Similarly, acid-catalyzed reactions could be deactivated upon light exposure of endogenous photolatent bases, thus providing alternative or additional photoelements of temporal control.

Other photomediated reactions occur upon intramolecular activation of the reacting species itself. This might be via deprotection of a reactive functional group, allowing it to participate in an otherwise precluded reaction or via direct absorbance and excitation of that species (e.g., via 2,2-cycloaddition). In these cases, one photon leads directly to at most one reaction (a "one photon, one event" chemistry). As might be expected, absent the photoamplification of a one photon, many events type reaction, a one photon, one event reaction necessarily requires a higher concentration of light-absorbing, photoreactive species and therefore frequently requires higher intensities and significantly longer exposure times. Such reactions are also often subject to significant light attenuation through the thickness of the exposed sample.[20] As a result, "one photon, one event" chemistries are frequently limited to applications with thin geometries and frequently at surfaces. There are advantages, however, to these one photon, one event chemistries. The desired reaction occurs only upon photon absorption so that the removal of the light stimulus causes the reaction to cease, providing a high degree of temporal and spatial control (subject to the practical depth of cure limitations brought about by the relatively high concentration of chromophores).

Radically mediated photoreactions, however, occupy somewhat of a middle ground in this trade-off between photoamplification of reaction and spatial and temporal control. A single initiating radical in a chain reaction may propagate hundreds or thousands of times, but its lifetime is functionally short. While anionic or cationic catalysts and reaction intermediates will not rapidly recombine with other molecules of similar charge, radicals are prone to termination by recombination and disproportionation. Whereas an anionic, photogenerated catalyst, in the absence of a poison, will continue to facilitate reactions indefinitely, actively propagating radicals will terminate and the reaction will cease rapidly unless radicals are replenished. In this way, radical reactions exhibit the photoamplification effect of a one photon, many events chemistry but with limited dark cure and maintenance of a greater degree of spatiotemporal control.

Some related reviews on the subject of photomediated click chemistry in particular fields of research have preferred discussion primarily of those reactions that are self-sufficiently photoreactive.[21−23] Conversely, others have adopted a broader view of the chemistry.[1,24] This review favors the inclusion of reactions that take advantage of the photoamplification of self-perpetuating, photomediated reactions for their obvious benefits in the contexts in which they are used. Click reactions as a whole are put in the click category because of their performance and utility. Similarly, with photoclick reactions, their defining characteristic, provided that that they meet the criteria for click reactions generally, is that they are mediated by the application of light.

1.3.2. Light Attenuation. Despite the significant advantages of photochemical reactions, there are significant intrinsic challenges to effectively and practically conducting such chemistry. Some of these challenges to the broad application of photochemistry include the inescapable problem that the absorbance of photons requisite for photoactivation prevent photoactive molecules farther away from the incident light from being activated themselves, creating a light gradient through the exposed sample. While this is especially consequential, as discussed above, in one photon, one event reactions, it is an issue with one photon, many events reactions as well. Light attenuation may cause inadequate light penetration through the depth of a sample, preventing anything but superficial conversion (Figure 11). Furthermore,

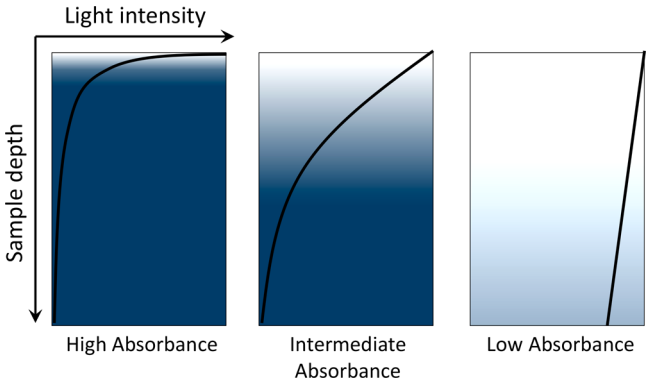

Figure 11. Hypothetical light intensity vs sample depth diagrams for a reaction with high absorbance (left) and low absorbance (right) and intermediate absorbance (middle). Linearity as described by the Beer−Lambert is often not observed at high absorptions.[11]

as chromophores are reacted, their absorption profiles often change in disadvantageous ways; photodegradation products may absorb more light than the species from which they originated, blocking even more light from reaching the reactive molecules below. This outcome makes scalability of reactions a challenge. Options to mitigate such light attenuation include stirring the reaction mixture to distribute either photoactivated catalyst or to increase the median residence time near the incident light of all molecules in the vessel. Flow photochemistry, wherein the reactants are flowed through a thin, transparent polymer tube while exposed to light, also increase the time that molecules spend in proximity to the photo-

https://doi.org/10.1021/acs.chemrev.0c01212
Chem. Rev. 2021, 121, 6915−6990

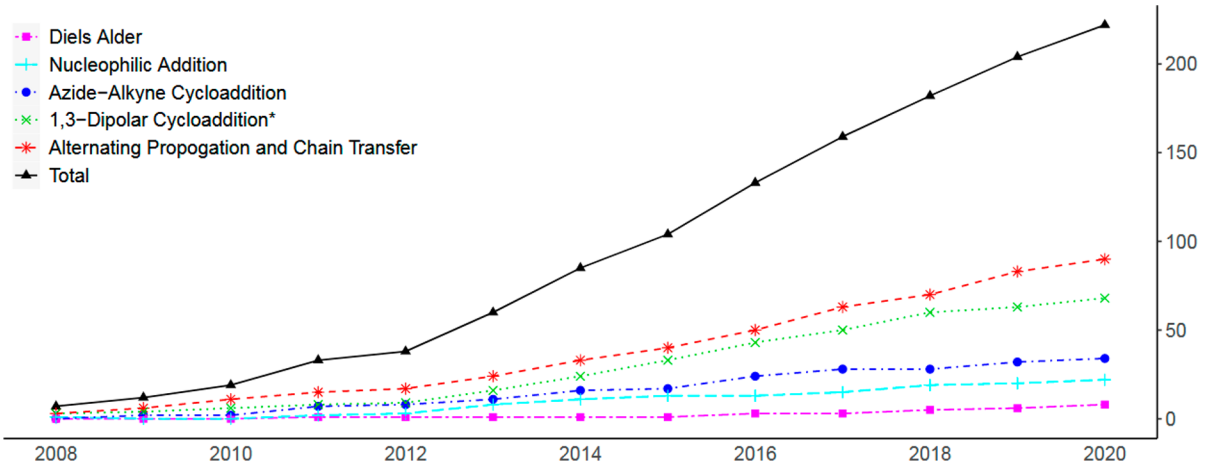

Figure 12. Number of journal articles published by year on photoclick chemistry, divided by class of reaction. *Indicates 1,3-dipolar cylcoadditions other than azide−alkyne cycloadditions.

exposed surfaces. Frequently, however, mechanical agitation is not an option. The choice, therefore, of excitation light exposure is not trivial; sometimes choosing a light with an emission that matches an absorption maximum is counterproductive. A light source with a wavelength that overlaps with the absorption spectrum of the photoactive molecule less than perfectly may serve to better provide effective reaction through the depth of the sample. While the attenuation of light may be a difficult problem to overcome, it should be noted that because of their high efficiency, click reactions are frequently applied to situations where the complementary reactive groups are in very dilute conditions, diminishing the light attenuated by absorbing species. Reaction conditions, therefore, that would disfavor reactions mediated via other means, may promote effective photomediated reactions. For a more in-depth description of the relationship between irradiation/absorption overlap and depth of penetration, the reader is referred to recent work by Barner-Kowollik and co-workers.[25,26]

1.3.3. Other General Challenges in Photoclick Chemistry and Proposed Criteria for Designation. Atom economy is defined as the ratio of the molecular weight of the product of a chemical reaction to the sum of the molecular weights of the reactants. Relatively high atom economy, while not explicitly described in the seminal paper describing click chemistry, is often intuited as a requisite or at least preferred feature, given the established criteria related to byproducts.[27,28] The applicability of this metric varies with context. In many applications of click chemistry (e.g., polymeric and biomacromolecular conjugations), reactants have substantial molecular weights. So long as the molecular weight of the conjugated macromolecules is many times that of any byproducts, the atom economy will necessarily be high, even with a sizable number of unutilized atoms. While atom economy, as defined, may not reflect actual atom utilization efficiency in such contexts, the general feature of generating smaller (or zero) byproducts is a useful one. Yet another important, and related, consideration is the size of the reactive moieties and their contribution to the molecular weight of the product. This is particularly true in the case of photochemical reactions where, in order to modulate light absorbance characteristics, red-shifting substituents are appended to chromophores, considerably increasing the molecular weight of the reactive group. Reactive handles that make up significant fractions of the molecular weight of the reactants can change the physical and biochemical properties of those compounds themselves: physical and biochemical properties, the maintenance of which may be integral to their function in the desired context. Solubility of polymers and proteins may change; new interactions with other components in complex systems may be introduced. Additionally, it should be noted that typically, if not always, larger and more complex reactive moieties represent a more significant synthetic challenge. For these reasons, the size of reactive functional groups is a valid consideration for designation as photoclick chemistry.

Another challenge to the effective application of photochemical techniques is the availability of instrumentation required for carrying them out. Hot plates and thermometers are ubiquitous in chemistry laboratories. High powered light sources of discrete or variable wavelengths and radiometers are less so. Though as LEDs of various wavelengths and intensities have become more available in recent years, the difficulty in obtaining adequate photochemistry instrumentation has been substantially mitigated.

High energy (low wavelength) photons can have deleterious health effects on researchers exposed to them including acute injury (e.g., sunburns, temporary blindness) and disease due to cumulative exposure (e.g., development of macular degeneration, skin cancers). As a result of these hazards, additional PPE is recommended for those employing light-mediated chemistry, including tinted safety glasses, face shields, photoexposure cabinets, etc., but even with such supplementary protection, chemists who perform photochemical reactions should be cognizant of the specific hazards of the particular wavelengths and intensities of light that they employ. It should also be noted that it is not only the chemist who is susceptible to deleterious effects of light. High doses of high energy light can damage other chemical compounds and moieties present in the reaction mixture as well. For these reasons reactions that require low wavelengths of UV light, high intensities, or long exposure times, may not adequately meet the spirit of the original click classification criteria.

The incorporation of photochemistry into the philosophical framework of "click" chemistry introduces new considerations, it is beneficial to consider how photoclick may correlate with the original criteria of "click chemistry." While the application of light generally has proven an invaluable tool in synthetic organic chemistry, polymer chemistry, and biochemistry,

https://doi.org/10.1021/acs.chemrev.0c01212
Chem. Rev. 2021, 121, 6915−6990

Table 2. A List of General Reaction Schemes of Photomediated Reactions Designated As "Photoclick" in the Literature, Grouped by Reaction Mechanism[a]

Reaction	Name	Typical λ (nm)	Typical rxn time	Amplification
1,3-Dipolarcycloadditions				
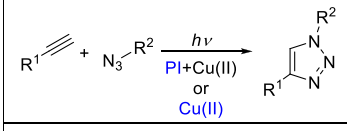	photo-CuAAC[30, 31]	330-500	30 s – 1 h	PA
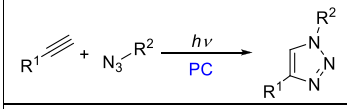	PcAAC[32]	Visible light	>1 h	PC
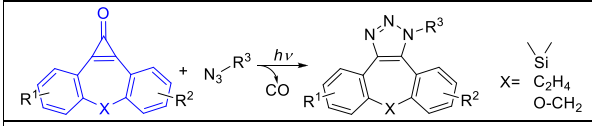	photoSPAAC[33, 34]	350-420	1-10 min	1P1E
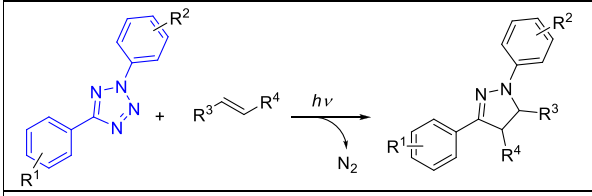	tetrazole-ene[8, 29, 35]	300-405 NIR with TPA	1-10 min	1P1E
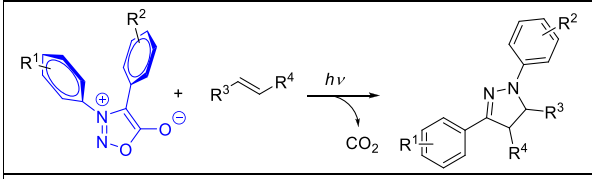	sydnone-ene[36]	300-405	1-10 min	1P1E
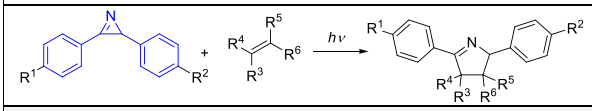	azirine-ene[37]	302-420	1-10 min	1P1E
Diels Alder and Inverse Electron Demand Diels Alder				
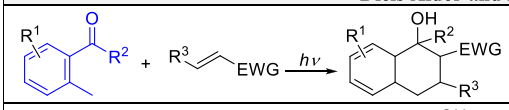	photoenol DA[38]	320-350	100 min	1P1E
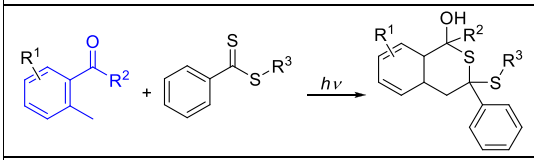	hetero DA[39]	320-350	100 min	1P1E
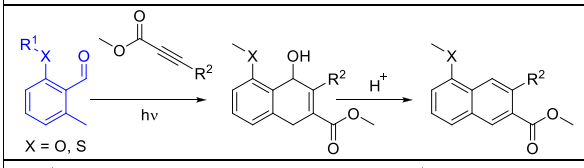	photoenol alkyne DA[40]	320-350	15-60 min	1P1E
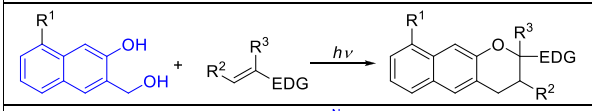	naphtoquin-one methide[41] IEDDA	320-350	15 min	1P1E
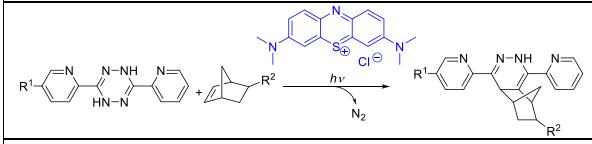	photo Tetrazine IEDDA[42, 43]	600-900	60 s	PC
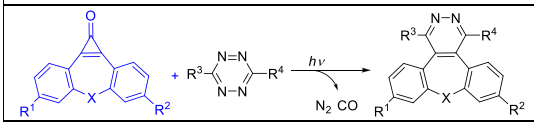	tetrazine Photocyclo-alkyne IEDDA[44]	350-420	5-10 min	1P1E

https://doi.org/10.1021/acs.chemrev.0c01212
Chem. Rev. 2021, 121, 6915−6990

Table 2. continued

Reaction	Name	Typical λ (nm)	Typical rxn time	Amplification
Radical alternating propagation chain transfer reactions				
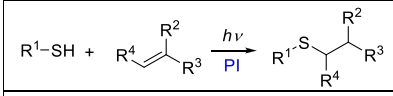	thiol-ene[45, 46]	320-700	30 s – 30 min	PA
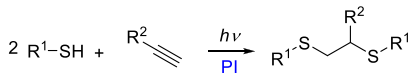	thiol-yne[47, 48]	320-500	5– 30 min	PA
Nucleophilic additions				
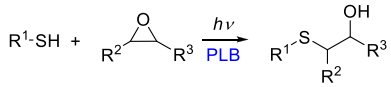	photolatent base- catalyzed thiol-epoxide[49]	320-400	5 -30 min	PA
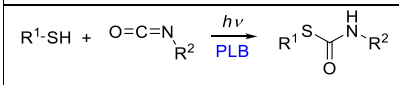	photolatent base-catalyzed thiol-isocyanate[50, 51]	365	1 -30 min	PA
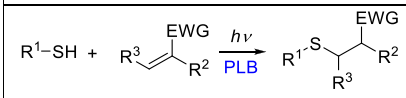	photolatent base-catalyzed thiol-Michael[52, 53]	320-500	5 – 30 min	PA
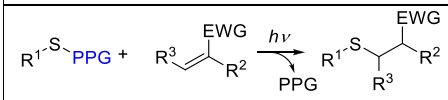	photouncaged thiol-Michael[54, 55]	320-740	1– 60 min	1P1E
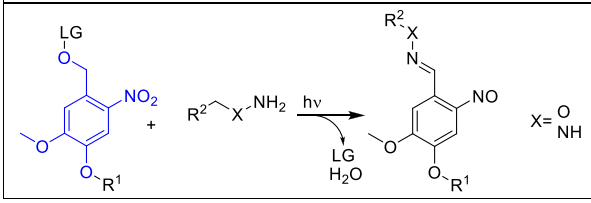	photomediated hydrazone and Oxime ligation[56, 57]	355-370	2 – 30 min	1P1E

[a]The chromophore in each reaction is indicated in blue. Included in the table are relevant features: typical wavelengths at which the corresponding reaction is conducted, typical duration of reaction, and whether the reaction is photoamplified (PA), photocatalyzed but not amplified (PC), or whether the reaction is a one photonone event process (1P1E).

stringent application of standards must be applied to the characterization of "photoclick" chemistry to prevent the phrase from becoming just another synonym for "useful reaction." Just as click reactions are supposed to avoid hazardous reactants, which increase the likelihood of undesired side reactions and present a hazard to the chemist performing the reaction, photoclick chemistry should similarly avoid hazardous reaction conditions like high doses of low wavelength light. Additionally, click reactions originally were intended to employ widely available or easily synthesized reagents and catalysts. If a corollary between the initiating chemical and physical stimuli can be made, then broad accessibility of light instrumentation and mild exposure conditions to carry out the reaction would be necessary for a reaction to qualify as "photoclick." For these reasons, it is proposed that additional criteria be met for a reaction to qualify as a "photoclick" reaction (Table 1).

In the present body of literature on the subject, photoclick reactions generally fall into four general categories: 1,3-dipolarcycloadditions, Diels–Alder and inverse electron demand Diels–Alder additions, radical alternating propagation and chain transfer reactions, and nucleophilic addition reactions. Figure 12 demonstrates the increasing popularity of photoclick reactions generally and of the specific subdivisions as well. This plot was generated from results by the SciFinder (American Chemical Society) search feature with queries of "'[chemistry]" + "photo" + "click" to generate an index of publications, which were then individually examined to verify applicability and to avoid duplicates in counting. As there may be a good number of publications with these various chemistries that may not explicitly employ the term "photoclick," the numbers represented here are necessarily an undercount. However, it is believed that the trends are accurate. With this increase in use and research into these reactions, a thorough examination of their relative strengths and limitations should serve to direct their application to those contexts to which each reaction is most suited.

2. PHOTOCLICK REACTIONS

The characterization of "photoclick chemistry" was first applied to the tetrazole–ene reaction in 2008.[29,35] Since then, the designation has been applied to a number of other photo-mediated reactions. Table 2 shows the general reaction schemes for the most common photoclick reactions along with relevant features of those reactions, such as the role the chromophore plays in the reaction, typical wavelengths, and reaction durations. The table also indicates whether the nature of each reaction is one photon, one event or photoamplified (one photon, many events), which, to a great extent, determines appropriate applications for these reactions. The remainder of this section follows the organization of this table by discussing each reaction in detail and how it meets or fails to meet the photoclick classification, depending on the reaction and the conditions under which it is implemented.

https://doi.org/10.1021/acs.chemrev.0c01212
Chem. Rev. 2021, 121, 6915–6990

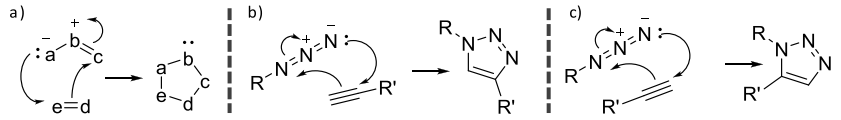

Figure 13. (a) General mechanism for 1,3-dipolar cycloaddition wherein rearrangement of electrons between a 1,3-dipole and dipolarophile results in generation of five-membered ring structure. (b) 1,3-Dipolar cycloaddition between an azide (1,3-dipole) and alkyne (dipolarophile) (Huisgen azide−alkyne cycloaddition), resulting in 1,4 regioisomer, and (c) the cycloaddition, resulting in the 1,5-regioisomer.

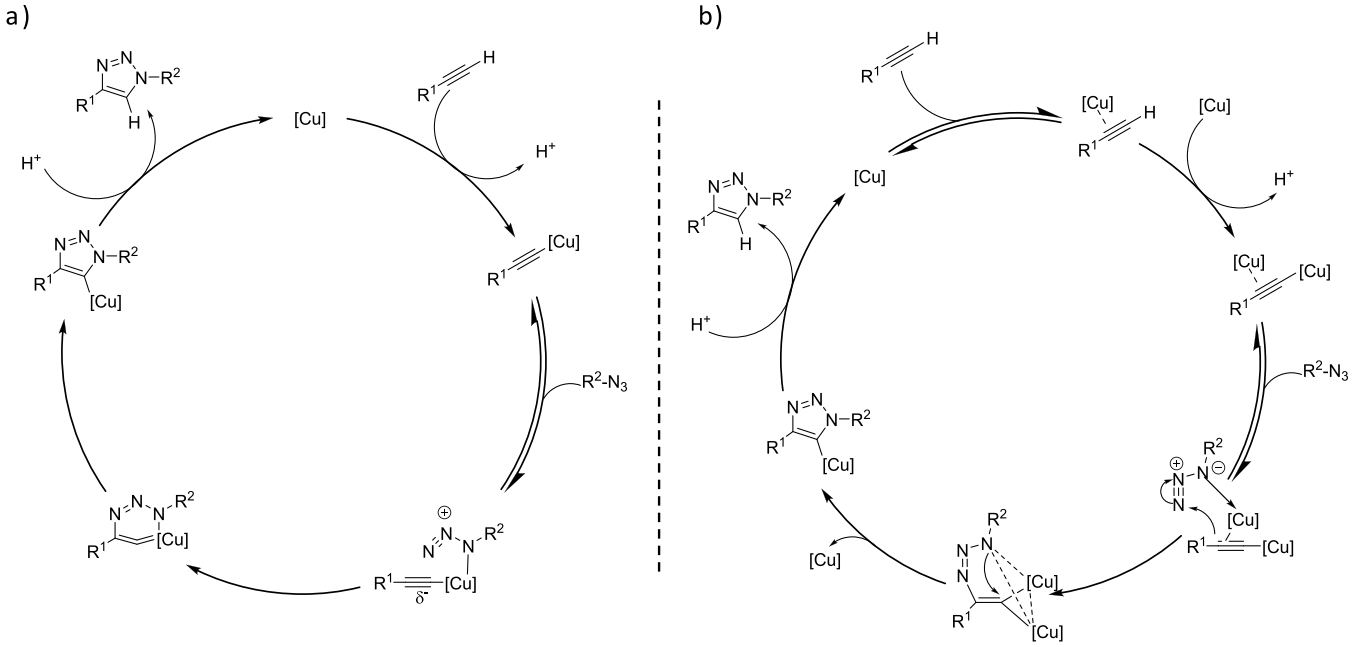

Figure 14. (a) Original proposed mechanism for Cu(I) catalysis of azide−alkyne cycloaddition. Adapted with permission from ref 60. Copyright 2002 John Wiley and Sons. (b) Updated mechanism for Cu(I) catalyzed azide−alkyne cycloaddition, indicating concerted effect of two copper atoms reflecting low experimental yields of copper(I)-acetylide in reactions without exogenous Cu(I). Adapted with permission from ref 61. Copyright 2013 AAAS.

2.1. Dipolar Cycloadditions

Among click reactions generally and photoclick reactions more specifically, 1,3-dipolar cycloadditions constitute a significant number of reactions so categorized. The generalized mechanism of a 1,3-dipolar cycloaddition involves electron rearrangement of a 1,3-dipole and an unsaturated dipolarophile, resulting in the generation of a five-membered ring (Figure 13a).

2.1.1. Azide−Alkyne Cycloaddition. The classic example of such a reaction is the 1,3-dipolar cycloaddition between an azide dipole and an alkyne dipolarophile. This reaction is also known as the Huisgen azide−alkyne cycloaddition in recognition of the work performed by Rolf Huisgen on these cycloaddition reactions.[58] In the absence of a catalyst, the azide−alkyne cycloaddition is accomplished by overcoming the activation barrier thermally. The elevated temperatures required for reaction and the nonregiospecificity of the product (thermal cycloadditions result in approximately equivalent yields of 1,4-substituted and 1,5-substituted products, Figure 13b,c), however, disqualify the solely thermally mediated reaction from a click designation.

The copper catalyzed variant of the 1,3-dipolar cycloaddition between an azide and an alkyne (CuAAC) is currently probably the most recognized click reaction. Terminal alkynes and azides are frequently readily available or easily prepared (although caution is recommended in the synthesis of organic azides as low C:N ratio compounds can pose an explosion hazard). Whereas the thermal Huisgen azide−alkyne cycloaddition is relatively sluggish and results in a mixture of regioisomers, catalysis by copper(I) results exclusively in the 1,4-product with a rate of reaction 10^7 or 10^8 times as high as that of the uncatalyzed reaction.[59] Since its introduction in 2001,[59] the CuAAC reaction has been a flagship for click reactions, having been successfully employed in a wide variety of conditions and frequently resulting in high conversions. Moreover, as azides and alkynes are generally not particularly reactive toward many of the most common functional groups employed in the biochemical and materials laboratories, the CuAAC reaction is tolerant of many reaction environments that might preclude the performance of other coupling chemistries.

While copper(I) salts can be used directly as catalysts, the in situ reduction of copper(II) allows for facile aqueous reactions via the inclusion of water-soluble copper salts (most frequently $CuSO_4$) and a reducing agent (e.g., sodium ascorbate). Frequently, the reducing agent is included in large excesses to disfavor the otherwise rapid oxidation of the Cu(I) back to Cu(II). For a similar reason, chelating ligands have been used to maintain effective Cu(I) concentrations. These strategies greatly mitigate the reactions' otherwise sensitivity to oxygen. While a common class of Cu(I) ligands for the CuAAC reaction include multifunctional tertiary amines, triazole rings have proven among the more effective ligands. Indeed, the products of CuAAC reactions may serve as ligands during the

https://doi.org/10.1021/acs.chemrev.0c01212
Chem. Rev. 2021, 121, 6915−6990

progression of the reaction. Despite its seeming ubiquity, the precise mechanism for the copper catalyzed cycloaddition remains somewhat of a mystery. The mechanism proposed by Rostovtsev et al. in 2002 suggests a single copper atom facilitates the formation of cyclic intermediates and ultimately the triazole (Figure 14a).[60] Subsequent experiments by Worrell, Malik, and Fokin,[61] however, demonstrated that copper coordination to the alkyne was insufficient to explain the increased cycloaddition rates by measuring reaction kinetics of a preformed s-bound copper(I)-acetylide with an organic azide in the presence or absence of an exogenously added copper(I) catalyst. The reaction occurred to an appreciable rate only in the presence of catalysts suggested a two-copper atom mechanism for the cycloaddition (Figure 14b).

Azide−alkyne cycloadditions may also be catalyzed with ruthenium(II) complexes, resulting in the 1,5-substituted triazoles rather than the 1,4-substituted triazoles of the copper catalyzed cycloadditions or the mixture resulting from thermally mediated reactions.[62] Furthermore, whereas the CuAAC reactions are exclusive to terminal alkynes, the RuAAC reaction may be performed with internal alkynes. However, the RuAAC reaction may require elevated temperatures or longer reaction times, and the ruthenium catalysts necessary for these reactions are more expensive or difficult to acquire than are the simple copper salts and vitamin C so frequently used in CuAAC reactions.[62] For these reasons, and perhaps suffering from generally unfavorable comparisons to its copper catalyzed counterpart, RuAAC reactions are seldom referred to as "click reactions".

One additional advantage of employing a copper(I) catalyst is the copper(II) species serving as a latent catalyst, activated by the application of a reducing agent. As described prior, this is typically achieved by physically mixing in the exogenous electron donor, although latent catalyst may also be activated electrochemically.[63]

2.1.1.1. Photo CuAAC and PcAAC. By photochemical means, however, the reducing agent can be generated in situ by activating endogenous photoactive species. In 2006, Ritter and König reported the photoreduction of Cu(II) with the visible light exposure of riboflavine tetraacetate in the presence of an electron donor trimethylamine.[64] To an equimolar solution of alkyne and organic azide (200 mM in acetonitrile) was added 8 mol % $CuCl_2$, 10 mol % TEA, and 4 mol % of the photoactive riboflavine and exposed to visible light irradiation of unspecified intensity. The resulting Cu(I) was capable of catalyzing the CuAAC reaction between an alkyne and an organic azide to above 80% conversion in 20 min. Aqueous reactions were similarly performed with $CuSO_4$ in place of the $CuCl_2$ and benzyl alcohol replacing the triethylamine, achieving lower conversions with longer exposure, reportedly due to the water-promoted disproportionation of Cu(I) to Cu(0) and Cu(II). This was supported by the observation that in aqueous systems, the reaction was arrested upon termination of light exposure, indicating consumption of the catalytic species.

Tasdelen and Yagci were able to generate Cu(I) catalysts by the direct photoactivation of a $Cu(II)Cl_2$ PMDETA (pentamethyldiethylenetriamine) ligand complex.[30] This reaction was achieved with exposure to low intensity (3 mW/cm^2), low energy ultraviolet radiation (350 nm). Despite relatively low concentrations of reactants (0.2 mM in DMSO) and Cu(II) (20 μM), high conversions (93−99%) were reached for a variety of alkynes with benzyl azide at room temperature and open to air. Reaction times varied from 120 to 600 min.

Adzima et al. took a different approach to the photoreduction of Cu(II), taking advantage of the vast work that had been completed in the fine-tuning of radical-generating photoinitiators.[31] Specifically, they employed a cleavage-type radical phosphine oxide photoinitiator (phenylbis(2,4,6-trimethylbenzoyl)phosphine oxide) to generate radical fragments that subsequently reduced Cu(II) by direct electron donation from a radical initiator (Figure 15).

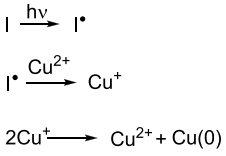

Figure 15. Photogeneration of Cu(I) via direct donation of electron from photogenerated radicals. Also depicted is the disproporationation, resulting in regeneration of Cu(II) and the formation of Cu(0).[31]

This reaction was performed both in model, monofunctional studies, as well as with multifunctional alkynes and azides, resulting in network photopolymerization. The authors noted two seemingly contradictory observations. First, relatively short irradiation times generated enough catalyst to continue the reaction for hours following the shuttering of the light. For example, in one reaction that exhibited only 5% conversion when exposure ceased at 5 min reached approximately 75% after 100 min, indicating the presence of a long-lived catalytic Cu(I) species. Second, the authors demonstrated a relatively high degree of spatial control over photomasked reactions of multifunctional reactants on surfaces with features as small as 4 μm obtained. While the observation of the long dark-reaction of previously irradiated reaction would suggest that the Cu(I) would have sufficient lifetime to diffuse away from the photoexposed regions into masked regions and catalyze reaction there as well, this "dark reaction" apparently did not happen. The failure to do so was explained by the formation of Cu(I) ligands with the triazole products of the photoCuAAC reaction, which remained effective catalysts, but within a 3D network, prevented the diffusion of Cu(I) outside of the irradiated regions. The autoligandization then demonstrated benefits of photogenerated radical and general photolatent catalyst mediated reactions, high resolution spatial control, and postirradiation dark reaction. While initial studies of this photo CuAAC reaction reported reaction times on the order of 1 h, subsequent papers have demonstrated much improved kinetics on the order of seconds to minutes under modest irradiation conditions (e.g., 10 mW cm^{-2}, 365 nm).[65] The copper ligand and anion have significant effects over the reaction kinetics.[66] While preligation of copper with multifunctional aliphatic tertiary amines, such as tetramethylenediamene (TMEDA) and greatly improved reaction rates, pyridine-based ligands showed little improvement. Meanwhile, copper salts with halide anions proved substantially more effective in initiating systems than those with organic anions such as triflates and bistriflimides. Initiator and copper concentrations also have significant effects on the reaction rate, although recent reports have indicated limits to this relationship. El-Zaatari et al. noted that by increasing the copper and initiator concentrations, the reaction reached a threshold at which it transitioned from a

https://doi.org/10.1021/acs.chemrev.0c01212
Chem. Rev. 2021, 121, 6915−6990

first-order to a zero-order reaction with respect to copper and initiator concentrations. This outcome indicated that side reactions, such as the disproportionation of copper (Figure 15), that are negligible at relatively low catalyst concentrations, likely become significant as those concentrations increase.[67] The properties of the radical photoinitiator exhbit significant influence over this reaction, which have been explored in great depth in the context of radical chain addition polymerizations and in radical addition, chain transfer reactions. More attention is given to these compounds in section 2.3.

The reduction of copper was also carried out with photoinduced electron transfer (PET) catalysts.[68] Cleavage type photoinitiators are generally limited to UV and lower wavelength visible light initiators; however, the application of PET catalysts, with their more varied absorption spectra, provides the benefit of being able to conduct the photoinitiated CuAAC reaction with substantially longer wavelength exposure. Kutahya et al. demonstrated effective catalysis of the CuAAC reaction using a NIR cyanine-based PET catalyst with a barbital group in the meso position (Figure 16).[68]

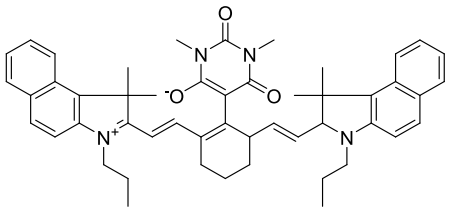

Figure 16. Cyanine-based PET catalyst with a barbital group in the meso position employed in the NIR mediated reduction of Cu(II) to Cu(I) and successful catalysis of CuAAC reaction.[68]

Exposure of the PET catalyst to 790 nm light at 100 mW/cm^2 in the presence of a phenyl acetylene and benzyl azide in equimolar ratios and with PMDETA achieved complete conversion within 2 h. Effective polymer−polymer coupling was also demonstrated via this NIR PET-catalyzed CuAAC in the reaction between a 3000 g/mol polystyrene and a 4000 g/mol polycarpolactone. The product, analyzed by gel permeation chromatography, demonstrated the expected molecular weight and a low dispersity, indicating efficient coupling with relatively little unreacted starting material.

Another means by which the CuAAC reaction may be photomediated is by the photodeprotection of an otherwise unreactive alkyne. Because only terminal alkynes are reactive in CuAAC reactions, reversible protection of the terminal alkyne with a photoremovable group (generally a nitrobenzyl moiety[69]) allows researchers to conduct photomediated CuAAC reactions. Tebikachew et al. generated terminal alkynes by the photolysis of nitrobenzyl arylpropiolates and subsequent decarboxylation in the presence of copper catalysts.[70] While the description of this reaction as "photo-click" may not be accurate (the wavelength of light employed in this reaction was very low, thermal input was needed for decarboxylation, and the atom economy is poor), it does represent an unusual approach to carrying out these conjugations and deserves mention.

Copperless photoredox azide−alkyne cycloaddition has been recently demonstrated by Wu et al. in a process they have called "photocatalyzed azide−alkyne cycloaddition" or PcAAC.[32] While photoredox catalysts are used in this PcAAC reaction, rather than the photoreduction of copper(II) to copper(I), the excited photocatalysts oxidizes the alkyne, generating a radical cation, which is a much more reactive dipolarophile than the original alkyne that reacts with the azide to form a radical cation triazole that is subsequently reduced, regenerating the photocatalyst (Figure 17). While the reaction

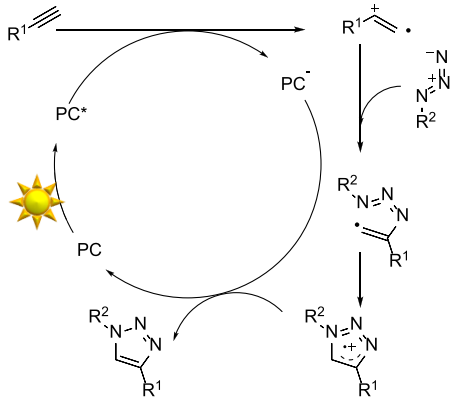

Figure 17. PcAAC mechanism: the photomediated azide−alkyne cycloaddition by direct photooxidation of alkyne and subsequent 1,3-dipolarcycloaddition and regeneration of photocatalyst. Adapted with permission from ref 32. Copyright 2020 John Wiley and Sons.

rates achieved were modest compared to those in which photoreduced copper served as the catalyst, near quantitative yields in model reactions between phenylacetylene and benzyl azide were achieved in as little as 6 h under visible light irradiation. Sunlight also proved an effective light source. In contrast to thermally mediated azide−alkyne cycloadditions, complete regioselectivity was observed, with only the 1,4-disubstituted triazole recovered. The reaction was carried out in DCM and DMF as well as in aqueous solutions and open to air, demonstrating insensitivity toward oxygen and water. According to the authors' data, the most effective photocatalyst screened for the PcAAC was bis(1-phenylisoquinoline)-(acetylacetonate)iridium(III), although significant reaction was achieved with 2,4,6-tris(4-methoxyphenyl)pyrylium tetrafluoroborate as well, demonstrating for the first time a completely metal-free photomediated azide−alkyne cycloaddition without employing ring-strained cycloalkynes.

Photothermal initiation of click reactions is not especially common in the literature. A likely reason for this is the avoidance of relying on highly thermally dependent reactions. Typically, for any reaction to be considered "click", it must exhibit a considerable thermodynamic driving force, a feature even suggested by the moniker "click" as if a gentle push over the energy barrier causes all reactants to simply click into place. Thus, any more than a little added energy to overcome an activation barrier would seem to exclude reactions from a designation as "click" altogether. Photothermal effects, however, potentially being extremely localized, may provide the thermal energy necessary for overcoming the activation barrier of a reaction while heating the bulk reaction medium less than would otherwise be required. While photothermal-mediated click reactions are sparsely reported, there are examples. Sun et al. demonstrated a synergistic photothermal and hot electron mechanism for the reduction of Cu(II) to Cu(I) sufficient to catalyze the azide−alkyne cycloaddition between benzyl azide and phenylacetylene within 90 min with exposure to visible light (420−780 nm).[71] Hot electrons refer to electrons that have a higher kinetic energy and therefore a

https://doi.org/10.1021/acs.chemrev.0c01212
Chem. Rev. 2021, 121, 6915−6990

higher effective temperature of the electrons despite a lower bulk temperature of the material.

2.1.1.2. Photomediated Strain Promoted Azide–Alkyne Cycloaddition (SPAAC). In no small part because of the desire to perform click reactions in the presence of living cells and because of the toxicity of copper, strain promoted azide–alkyne cycloadditions have received considerable attention over the past decade.[72−74] Cyclooctyne, the smallest, stable, and isolable cycloalkyne, undergoes significant release of ring strain when the alkyne, with a preferred bond angle of 180° but exhibiting a bond angle of 163° in its eight-membered ring, is converted to a triazole ring, eliminating the triple bond (Figure 18).[75]

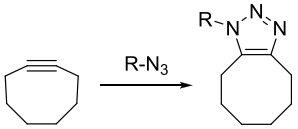

Figure 18. Ring strain in cyclooctyne facilitates fast, room temperature, and copperless cycloaddtion.

Electron withdrawing fluorine atoms further destabilized the alkyne, contributing to greater reactivity in the absence of any catalyst. Greater destabilization still was achieved via a series of dibenzoannulated cyclooctynes with additional ring strain imparted by the presence of multiple sp^2 hybridized atoms in the cycloalkyne ring (Figure 19). Azides and alkynes are generally less reactive toward many functional groups found in the biological context. For this reason, the azide–alkyne cycloaddition reactions have found substantial application in selective labeling of biological structure and macromolecules. Diminishing the stability of alkynes by introducing ring strain, for example, not only increases its reactivity toward azides but toward other functional groups as well. Thiols, for example, are slow to react with most linear, terminal alkynes in the absence of radicals, catalysts, or elevated temperatures but will readily and spontaneously react with cyclooctyne at room temperature.[47,48] This example demonstrates the difficult trade-off between reactivity and selectivity. Click reactions are supposed to be both fast and specific. Achieving both is not a trivial matter.

Cyclopropenones, upon exposure to UV light, decompose into one molecule of carbon monoxide and an alkyne. Highly ring-strained themselves, the conversion of a cyclopropenone to the strained triple bond of a cyclooctyne is still an energetically favorable reaction, allowing for the photodeprotection of strained cycloalkynes for subsequent, spontaneous reaction in azide–alkyne cycloaddition (Figure 20).[33] It should be noted that as in the case of the thermally mediated Huisgen azide–alkyne cycloaddition, a mixture of regioisomers is obtained from the copper-free SPAAC reaction, whether photomediated or spontaneous.

Generally, cyclooctynes are considered the smallest stable cycloalkynes that can be isolated and stored without decomposing. Cyclopropenones serve as a temporary protecting group, the removal of which generates, in situ, cycloalkynes that may be relatively short-lived. In the presence of their reactive azide complement, however, the rate of cycloaddition far exceeds the rate of decomposition, producing the desired product in high yields. A particularly effective example of this ability to generate protected, otherwise unstable cycloalkynes was demonstrated by Sutton et al. in their synthesis of a photocaged cyclooctadiyne (the Sondheimer diyne, Figure 21).[64] This protected diyne is, as would be expected, difunctional, although the quantum yield for the first and subsequent cyclopropenone decompositions are not equal, that for the first decarbonylation is approximately 10 times that of the second at a wavelength of 350 nm. This allows for the selective, sequential reaction of the resulting alkynes with complementary azides.[76,77]

Cycloheptynes (employing heteroatoms such as sulfur, selenium, or silicon, in the alkynyl ring) can also be synthesized to yield even more reactive alkynes. However, working with the highly unstable cycloheptynes can be difficult. Similar to the work with the cyclopropenone-protected octadiyne, cyclopropenone-protected dibenzosilacycloheptynes have been synthesized by Martínek et al. that exhibit very good quantum yield (>0.50) and subsequent cycloaddition reaction rates (Figure 21).[34]

The direct photolysis of cyclopropenones is a one photon, one event reaction; the generation of every reactive cylcoalkyne requires absorption of light. Under dilute reaction conditions, this is not an obstacle to carrying out the reaction. In more concentrated conditions, however, the necessary light will become more attenuated in thicker geometries, preventing reaction from occurring within the bulk of the sample. This is in contrast to photo CuAAC reactions wherein a small amount of photogenerated Cu(I) may catalyze thousands of cycloadditions, allowing the researcher to perform the reaction with very low concentrations of light absorbing chromophore. This limitation has resulted in the photoSPAAC reaction to find particular application in highly diluted reactions, including biological labeling as described subsequently in this review. In such context, however, the potential deleterious effects of significant doses of lower wavelength UV light may be a concern.

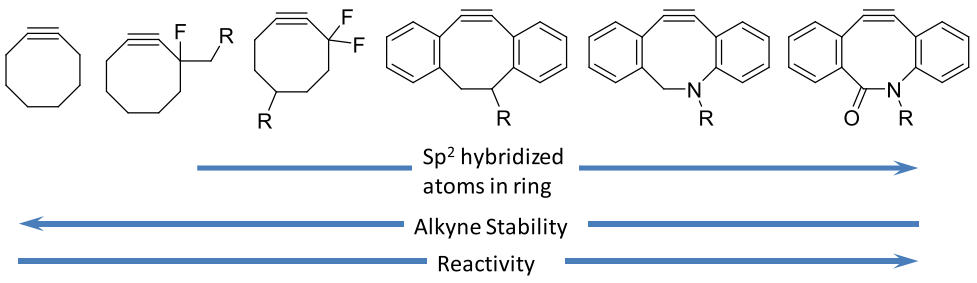

Figure 19. Propensity for cycloaddition with azides is increased in cycloalkynes by the destabilization of the alkyne by proximal electron withdrawing groups (e.g., fluorine atoms) and by the increase of sp^2 hybridized atoms in the ring.

https://doi.org/10.1021/acs.chemrev.0c01212
Chem. Rev. 2021, 121, 6915−6990

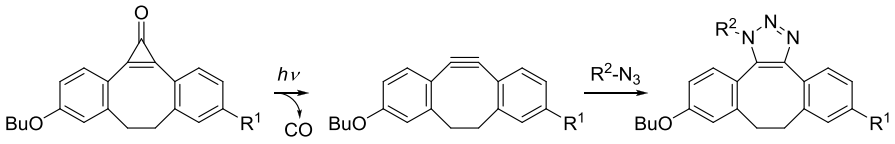

Figure 20. Photouncaging of cyclooctyne for subsequent strain promoted cycloaddition with organic azide.

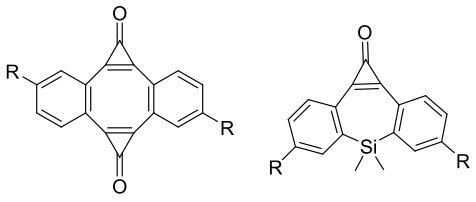

Figure 21. Other notable cyclopropenone-protected strained alkynes, including a photocaged dibenzocyclooctadiyne (dibenzo[*a*,*e*]-dicyclopropa[*c*,*g*][8]annulene-1,6-dione; left)[64] and a photocaged dibenzosilacycloheptyne (6,6-dimethyldibenzo[*b*,*f*]cyclopropa[*d*]-silepin-1(6*H*)-one; right).[34]

To address this requirement for relatively low wavelength light exposure, recently, Mishiro et al. reported an indirect photolysis of cyclopropenones to generate the ring strained cyclooctyne.[78] Prior studies had indicated that the photo-mediated decarbonylation of cyclopropenone occurred from the excited singlet state, and so photosensitization via energy transfer from a lower energy, visible-light sensitizer to a UV-absorbing chromophore would not be possible. The indirect photolysis would, then, necessarily proceed via a wholly different decarbonylation mechanism. The authors demonstrated a photoredox catalyst abstracting an electron from the cyclopropenone, generating an unstable radical cation, opening the ring structure that could then remove an electron from the reduced photocatalyst, regenerating it in the process and subsequently decomposing into carbon dioxide and the desired alkyne.

Although the use of cyclopropenones as photocaging groups for cycloalkynes is favored given its relatively high quantum yields and inoffensive byproducts, there are other potential strategies for the photogeneration of ring strained cycloalkynes. Jedináková et al. have reported photoSPAAC reactions via the synthesis of cyclooctynes via the photodecomposition of cycloota-1,2,3-selenadiazole (Figure 22).[79] This reaction,

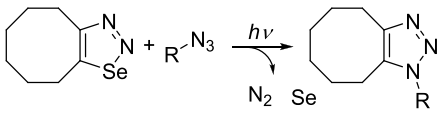

Figure 22. PhotoSPAAC reaction using selenadiazole photocaging group.[79]

however, exhibits a relatively poor quantum yield. Moreover, although selenium is an essential nutrient, in elevated concentrations it may have unpleasant or toxic physiological effects, making the broader application of its use in click reactions problematic. In this respect, selenium is similar to copper, which is also an essential nutrient in trace quantities but toxic at higher concentrations.

A final photoSPAAC reaction that deserves some attention is the photogeneration of benzyne and subsequent reaction with organic azides. Rather than the decarbonylation of cyclopropenone, however, Gann et al. reported the photo-decomposition of 2-(3-acetyl-3-methyltriaz-1-en-1-yl)benzoic acid to produce the strained cycloalkyne (Figure 23).[80] This

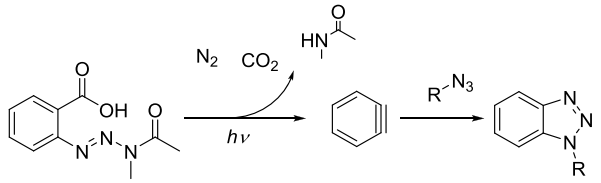

Figure 23. Photogeneration of benzyne via decomposition of 2-(3-acetyl-3-methyltriaz-1-en-1-yl)benzoic acid and subsequent conjugation to organic azide.

photoreaction was accomplished in just a few minutes at 365 nm irradiation. The subsequent reaction with organic azides was rapid and high yielding. Although this reaction provided an efficient and rapid reaction, benzyne is a very reactive compound, particularly toward nucleophiles generally. For this reason, there is concern regarding the specificity and orthogonality of this reaction under a variety of conditions in which photoclick reactions may be employed.

2.1.1.3. Strain Promoted Azide-Alkene Cycloaddition. While most attention in azide dipolarcycloaddition reactions has been focused on the employment of alkyne dipolarophiles, alkenes are frequently the coreactant of choice for other reactions in this category. Alkenes are capable of participating in cycloadditions with azides and that reaction is favored, as it is with alkynes, by strained alkenes. Huisgen noted a hundred-fold increase of the reaction of ring strained norbornene with benzyl azide.[81] In 2018, Singh et al. demonstrated the photosensitization of the isomerization of a cyclooctene to a more highly ring strained conformation and the subsequent reaction with benzyl azide in a 1,3-dipolarcycloaddition.[82] The photosensitizer was a derivative of *fac*-tris-[2-phenylpyridinato-*C*2,*N*]iridium(III) (Figure 24), and the sensitization was

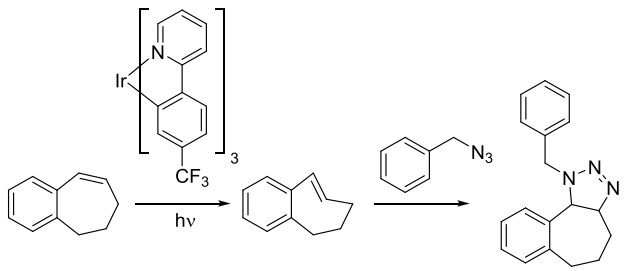

Figure 24. Photosensitized ring-strain generation in cycloheptene, promoting subsequent reaction with benzyl azide.[82]

performed with blue light. While the reaction required 16 h for completion and a slightly elevated temperature (30 °C), near-quantitative conversion was achieved (Figure 24). While the conditions of this reaction were not what might be considered sufficient for a "click" reaction, this demonstration of photogenerated ring-strain to promote dipolarcycloadditions

https://doi.org/10.1021/acs.chemrev.0c01212
Chem. Rev. 2021, 121, 6915−6990

has proven consequential in the development of other photoisomerization-promoted click reactions.

2.1.2. Photocaged Nitrile Imines and Nitrile Ylides. *2.1.2.1. Tetrazole and Sydnone Reactions.* Nitrile imines were first obtained by the thermal decomposition of tetrazoles, releasing N_2 during the process.[83] Exposure to appropriate wavelengths of light (dictated by chromophore substituents), accomplishes the same decomposition, yielding the same reactive intermediate. In the presence of alkenes the nitrile imine may undergo 1,3-dipolar cycloaddition to form the conjugated product linked by a five-membered pyrazoline ring (Figure 25). An interesting and useful feature of the reaction

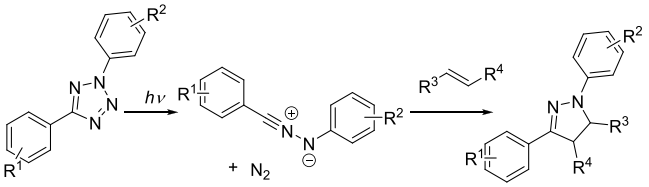

Figure 25. Photomediated decomposition of bisaryl tetrazole to nitrile imine for subsequent participation in 1,3-dipolarcycloaddition.

between alkenes and nitrile imines is that the generation of the fluorophore pyrazoline can serve as an in situ reaction monitoring system, absorbing UV light and emitting visible light as an indication of successful reaction. While a variety of alkenes (e.g., acrylates, styrene derivatives) participate in this reaction, the dipolarophilicity of alkenes is substantially increased by conjugation or by proximal electron withdrawing substituents.[58] This photodecomposition of the tetrazole to the nitrile imine has the advantageous feature of generating only inert N_2 as a byproduct. As is the case with most dipolar cycloadditions, the nitrile imine−alkene reaction is amenable to a variety of solvents including aqueous media. Also, like other 1,3-dipolar cycloadditions, the reaction may not be regiospecific.[84]

The wavelengths at which the reaction is performed are tunable via the choice of substituents. The reaction has been performed from 300 to 420 nm by single photon excitation and at 700 nm with multiphoton excitation.[85] The red-shifting that allowed the 405 nm exposure was accomplished by replacing the benzene ring substituents on either side of the tetrazole with oligothiophene substituents, greatly increasing the absorbance in the visible spectrum (Figure 26).[86] Lederhose et al. accomplished a similar shift in absorbance via synthesis of a pyrene-substituted aryl tetrazole, permitting reaction with exposure to light at wavelengths of 410−420 nm.[87]

One interesting strategy to allow longer wavelengths of light in the performance of tetrazole−alkene photoclick chemistry was the employment of upconverting nanoparticles to generate light capable of photoconversion of a pyrene aryl tetrazole (λ_{max} = 346 nm) upon exposure to NIR light. Photon upconversion is a process distinct from two photon absorption but with significant similarities. Upconverting nanoparticles absorb photons of a particular wavelength and emit photons of a shorter wavelength. Thus, the researchers were able to effect a UV-photomediated reaction with NIR exposure.[88] In contrast to previously described two photon absorption strategies, the aryl tetrazole chromaphore in this example is not absorbing the NIR photons, but rather UV photons emitted by the upconverting nanoparticles; this reaction is still mediated by UV radiation. The potential benefit to employing photon upconversion here is not avoiding exposure to UV light, but rather the avoidance of light attenuation of shorter wavelength photons.

Diaryl tetrazoles are not unique in their photodecomposition to dipolar nitrile imines. Diaryl sydnones similarly form the highly reactive intermediates upon light activation. Zhang et al., in 2018, synthesized a library of diaryl sydnones and noted higher absorbance of the sydnone chromophores at longer wavelengths relative to their tetrazole counterparts, portending beneficial application in biological research where visible light excitation is preferred.[36] Rather than releasing nitrogen, photoconversion of the sydnone, which involves a flipping of the aryl moieties, results in the release of carbon dioxide (Figure 27).

Despite the advantageous features of the photo tetrazole−alkene and sydnone−alkene reactions, the reactive intermediates exhibit a significant lack of reaction selectivity. Recently, researchers have recommended the application of the reaction as a general photo-cross-linking reagent rather than for biorthogonal labeling protocols, citing the relative preference of the photogenerated nitrile imine to react with biologically present functional groups,[89] in particular carboxylic acids,[90] relative to their experimental, more aliphatic alkene moieties. They noted significant reaction with acetonitrile as well when used as a cosolvent for the reaction.

While reactive toward nucleophiles generally, nitrile imides are particularly reactive toward thiols,[91] first observed by Rolf Huisgen in 1962.[92] This reaction can be so fast that the photomediated, addition of thiols to nitrile imides has been compared to other "photoclick" reactions such as the tetrazole−alkene and thiol−ene conjugations. Feng et al. used the photodecomposition of tetrazoles in the presence of thiols to perform polymer−polymer conjugation reactions as

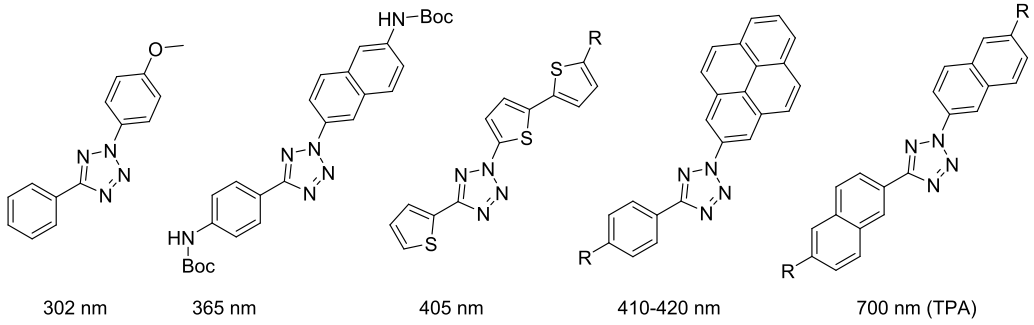

Figure 26. Tuning of photoabsorption profiles can be accomplished by choice of tetrazole substituents.

https://doi.org/10.1021/acs.chemrev.0c01212
Chem. Rev. 2021, 121, 6915−6990

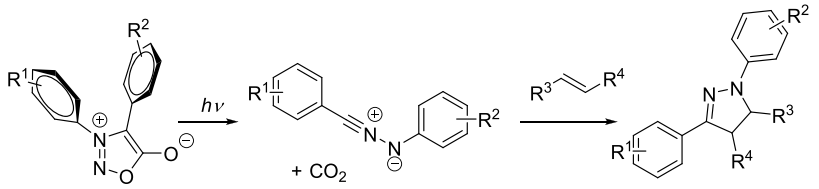

Figure 27. Photoconversion of diaryl sydnone to nitrile imine and subsequent 1,3-dipolarcycloaddition with alkene.[36]

well as surface functionalization, both frequent applications of many click chemistries.[93] The authors suggested that the biological availability of thiols (e.g., in reduced disulfides within proteins) could make the photo tetrazole thiol reaction an effective tool for the selective labeling of biomolecules, noting a much higher rate of reaction of the nitrile imine with thiol than with amines.

Additional dipolarophiles that may react with nitrile imines include alkynes, carbon dioxide, isocyanates, thiocarbonyls, amines, alcohols, and more, although the rates of reaction vary greatly (Figure 28).[84] Yu and co-workers have examined the

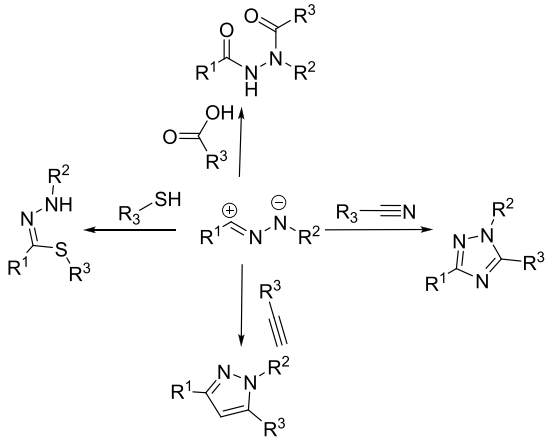

Figure 28. Reactions of nitrile imine 1,3-dipole with thiols and carboxylates as well as other dipolarophiles including nitriles and alkynes.

photoreactions of diaryl tetrazoles and diaryl sydnones with various alkynes.[94,95] While the linear, terminal alkynes yielded no observable product under dilute conditions (0.5−500 μM), ring strained alkynes were converted in high fractions with an excess of coreactants.

As indicated by these results, in addition to conjugation and electron deficiency, ring strain can also improve the reactivity of dipolarophiles to promote the 1,3-dipolarcycloaddition to nitrile imines. Fascinating recent examples of ring-strain promoted reaction were demonstrated by Yu and co-workers, who employed the photoisomerizable cyclic azobenzene-containing compounds such as dibenzo[*b*,*f*][1,4,5]-thiadiazepine (DBTD, Figure 29) as a photoactivatable dipolarophile in reactions with nitrile imines generated by the photodecomposition of either tetrazoles or sydnones.[96,97] In the cis configuration, DBTD exhibits little ring strain energy. Upon irradiation with 405 nm light, the DBTD is isomerized to a predominantly trans configuration, increasing ring strain and increasing the dipolarophilicity of the nitrogen−nitrogen double bond. Cycloaddition is followed by opening of the N−N bridge, resulting in a ten-membered ring (Figure 29). Noteworthy in this reaction is the double role that the light

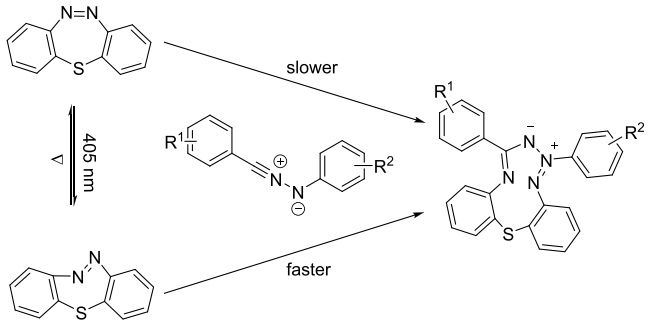

Figure 29. Photoisomerization of cis configuration of DBTD to trans configuration of DBTD by irradiation with 405 nm light permits the addition to photogenerated nitrile imine. In contrast to cis DBTD, trans DBTD proves an effective dipolarophile in the reaction.[81,82]

may play in the reaction, serving both in the generation of the reactive nitrile imine and in creating the ring strain via photoisomerization in the DBTD. In a subsequent report, the same team demonstrated a similar ring-strain by photoisomerization in carbon-bridged octocyclic azobenzene (CBOA) to promote the 1,3-dipolarcycloaddition.[53] In this later study, nitrile imides were synthesized independently and delivered exogenously to isolate the photoisomerization effects independent from the photogeneration of the reactive dipole. Both of these photochemical transformations (the photoisomerization and the photodecomposition of the tetrazole/sydnone) are one photon, one event type reactions, meaning that the concentration of light absorbing chromophores is necessarily twice what would otherwise be necessary for the reaction to take place with a different dipolarophile, recommending applications where low concentrations of reactants are required. Near quantitative conversions were achieved.

The apparent lack of specificity of the tetrazole−ene photoclick reaction could be a cause for concern for those seeking to employ it to precisely modify their particular compounds of interest. As with other "click" reactions, however, the utility of such reactions must take into account the relative rates of competing reactions for participating reactive moieties generally, and not only for those conditions understood to be far from ideal. The side reaction of a photogenerated nitrile imide with acetonitrile cosolvent may be significant when the intended coreactant is a poor dipolarophile, e.g., an alkyl ethylene compound. However, a fumarate used in place of the less effective dipolarophile will likely improve the selectivity of the dipolar cycloaddition.[91] The alkene selection is not the only way in which selectivity of the tetrazole alkene reaction can be improved. A recent report has demonstrated a particularly effective strategy for obtaining higher selectivity for alkenes over carboxylic acids, alcohols, amines, and other potentially nitrile imide-reactive nucleophiles. This was accomplished by the employment of tetrazoles with bulky substituent groups that sterically hinder the

https://doi.org/10.1021/acs.chemrev.0c01212
Chem. Rev. 2021, 121, 6915−6990

nucleophilic addition reaction but not the 1,3-dipolar cycloaddition with alkenes. An et al. synthesized a range of tetrazoles and reported increases in selectivity of the 1,3-dipolar cycloaddition adducts with a variety of alkenes relative to the nucleophilic adducts formed with glutathione (Figure 30).[91] Selectivity was demonstrated in all eight of the alkene

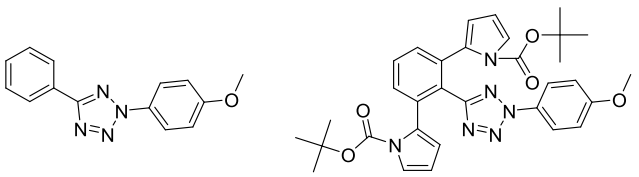

Figure 30. Photoreactive tetrazole (left) and bulky substituent analogue (right). Pendant groups sterically hinder nucleophilic additions and improve selection of 1,3-dipolarcycloaddition adduct with a variety of alkenes.[91]

substrates examined, but the reaction with styrene is a particularly good example of the effect steric hindrance had on the progression of the reaction. While in the presence of equimolar styrene and glutathione, the nonsterically hindered tetrazole showed a preference for the thiol-adduct of 91% to 5%. The sterically hindered tetrazole, in contrast, showed a preference for the styrene cycloadduct, 96% to 2%.

While strategies are available to address the broad reactivity of nitrile imides resulting from the photodecomposition of tetrazoles, these may introduce limitations into the general application of this reaction (e.g., by inclusion of a large chemical moiety that may influence physical as well as chemical properties of the reactant and by requiring additional synthetic steps). Whereas the azide−alkyne chemistries are often touted for their orthogonality, those who employ the tetrazole−alkene photoclick reaction should be cognizant that, in the absence of adequate concentrations of a good dipolarophile, the photogenerated nitrile imine is not functionally inert and will frequently react with other reactive groups present.

2.1.2.2. Azirine−Alkene Reactions. Like tetrazoles, aryl azirines undergo photomediated decomposition to generate a reactive dipole (nitrile ylide moieties in the case of azirines) prone to 1,3-dipolar cycloaddition.[37] As is the case with the tetrazole-alkene reaction, this reaction is favored by strong dipolarophiles including alkenes with proximal electron withdrawing substituents.

The photoactivation of bisaryl azirines as shown in Figure 31 requires exposure to relatively low wavelengths of light (320 nm). However, the pyrene-bound azirine exhibited significant red-shifted absorbance, thus being activatable with visible light at wavelengths from 400 to 410 nm (Figure 32).[98] This reaction was used to link pyrene to a variety of small molecule and electron-deficient alkene terminal polymers with yields ranging from 50% to quantitative.

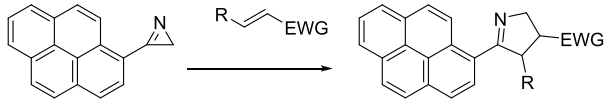

Figure 32. Visible light activation of pyrene azirine and conjugation to electron deficient alkenes. EWG = electron withdrawing group. R = H, COOEt, PEG.[98]

Despite the similarities between the analogous reactions, azirine−alkene photoclick reactions are used much less frequently than the tetrazole-alkene reaction.

2.2. Diels−Alder Reactions

Among the original reactions described by Kolb et al. in their seminal paper laying out the qualifications for click chemistry was the Diels−Alder reaction.[2] Typically, in this cycloaddition, an electron deficient dienophile adds to a relatively electron rich diene. As the π bonds in both the diene and the dienophile are higher energy than the resulting, created σ bonds, the reaction is energetically favorable and is often performed at relatively low temperatures and in the absence of catalysts (although catalysts can be employed to achieve improved rates of reaction). While examples of this reaction are abundant, a very simple case is the reaction of cyclopentadiene with an acrylate (Figure 33), generating a norbornene. Participating π

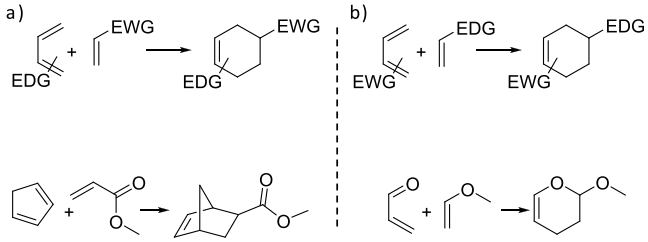

Figure 33. (a) Generalized Diels−Alder reaction between electron rich diene and electron deficient dienophile and example of cyclopentadiene reaction with methyl acrylate. (b) Generalized inverse electron demand Diels−Alder reaction and example of reaction between propenal and methyl vinyl ether.

bonds on either the diene or dienophile need not necessarily be carbon−carbon double bonds. Diels−Alder reactions in which atoms other than carbon are involved in the cycloaddition are referred to as "hetero-Diels−Alder" reactions. Inverse electron demand Diels−Alder reactions (IEDDA) are analogous to Diels−Alder reactions, but where the electron densities of the diene and dienophiles are reversed. The classic example of an IEDDA is the reaction of 2-propenal with a vinyl ether (Figure 33).

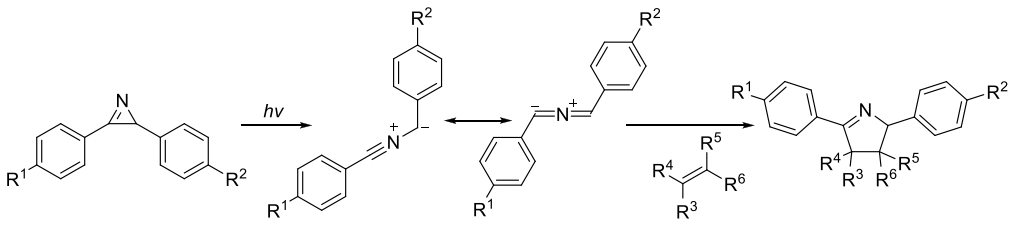

Figure 31. Photogeneration of nitrile ylide from bisaryl azirine and subsequent 1,3-dipolarcycloaddition.[37]

https://doi.org/10.1021/acs.chemrev.0c01212
Chem. Rev. 2021, 121, 6915−6990

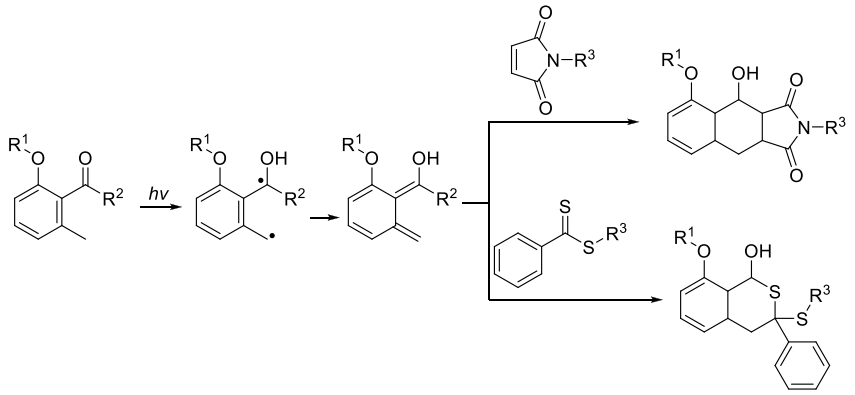

Figure 34. Photoenolization of *ortho*-methyl phenyl aldehyde and subsequent Diels–Alder cycloaddition with dienophilic maleimide (top) or hetero-Diels–Alder cycloaddition with dithiobenzoate (bottom).[38]

2.2.1. Photoenolization DA Reactions. Photoconversion of *ortho*-methyl phenyl ketones and aldehydes to form highly reactive enol dienes via a diradical intermediate was first described many decades ago, achieving high conversions with dienophilic compounds.[99,100] In 2011, Gruendling et al. used this photoenolization to conjugate an *ortho*-methyl phenyl ketone-terminated polycaprolactone to a maleimide-terminated poly(methyl methacrylate) with irradiation at 320 nm for 100 min.[38] While the light source chosen produced a maximum emission at a low wavelength, the authors noted some conversion under exposure to 365 nm or upon exposure to sunlight after "a few hours reaction time." Subsequent reports show effective conjugation with exposure to 382 nm LEDs.[101] A scheme for the photoDA reaction is shown in Figure 34.

Photoenols also readily react with a variety of dienophiles with heteroatoms. For example, Oehlenschlaeger et al. have demonstrated the reactivity of dithiobenzoate with photoenols,[39] a particularly advantageous reaction considering the use of dithiobenzoates and other thiocarbonylthio groups in RAFT chain transfer agents and their consequent presence as RAFT polymer termini. This reaction then allows for direct conjugation to such polymers without any additional modification. In another example of hetero Diels–Alder reactions involving photoenols, triazolinediones have proven effective dienophiles as well. Recently, the orthogonality of this reaction was highlighted in the utilization of light as a reaction-selection tool or "gate" to generate specific products from a mixture of reactants, including triazolinediones and tetrazoles, by selective application of particular stimuli including thermal and multiple wavelengths of light.[101,102]

Coordinated light exposure can provide another aspect of control to the photoenol Diels–Alder reaction. Photoenolization of *o*-methyl benzaldehydes with NIR light via two photon absorption results in a mixture of isomers that, in the absence of a complementary reactive moiety, reketonize via reverse hydrogen transfer to the starting material. Differences in rates of reketonization allow the *E* form of the photoenol, which has a relatively long lifetime (10 μs), to participate in DA addition reactions while the *Z* form with a lifetime 2 orders of magnitude shorter (0.1 μs), is effectively prevented from doing so. Simultaneous exposure with 440 nm light, photoisomerizes the *E* photoenol to the *Z* form, which rapidly reverts to starting material (Figure 35). Researchers have employed this feature to spatially narrow the photoenolization of alpha-methyl benzaldehydes on surfaces in the presence of a maleimide

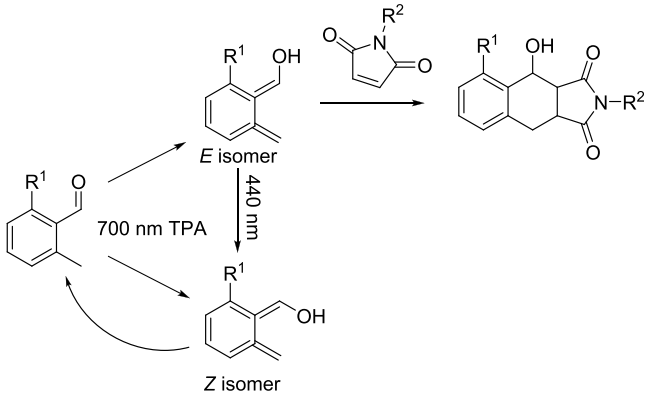

Figure 35. Dual wavelength control over the photoenol DA reaction. Two photon absorption at 700 nm generates a mixture of isomers with differing lifetimes while simultaneous exposure to 440 nm converts a long-lived isomer to a short-lived isomer, preventing effective cycloaddition. Adapted with permission from ref 103. Copyright 2017 American Chemical Society.

dienophile via stimulated-emission depletion (STED) excitation, creating laser written features on size scales below the diffraction limit.[103]

While most common dienophiles employed in Diels–Alder reactions possess double bonds, there is no requirement that precludes the π-bonds in triple bonds from participation. The electron deficient triple bond in dimethyl acetylene dicarboxylate has been shown to be reactive with 2,5-dibenzoyl-*p*-xylene under 24 h of irradiation.[25,104,105] More recently, Feist et al. have performed Diels–Alder reaction with photogenerated *o*-quinodimethanes and electron deficient alkynes within 15–30 min of light exposure, noting that subsequent addition of a catalytic amount of acid resulted in the elimination of the alcohol and the generation of highly fluorescent naphthalene derivatives.[40] A general scheme for these reactions is shown in Figure 36. Notable here is the absorption profile of the nonfluorescent naphthole Diels–Alder product, which does not exhibit significant absorption at those wavelengths most conducive the photogeneration of the diene reactant, absorption which would otherwise attenuate the light necessary to carry out the photoclick reaction. In contrast to the other photoclick reactions described previously that result in the generation of new fluorophores or chromophores, this approach yields such only following the hydroxyl elimination. In addition to preventing attenuation of

https://doi.org/10.1021/acs.chemrev.0c01212
Chem. Rev. 2021, 121, 6915–6990

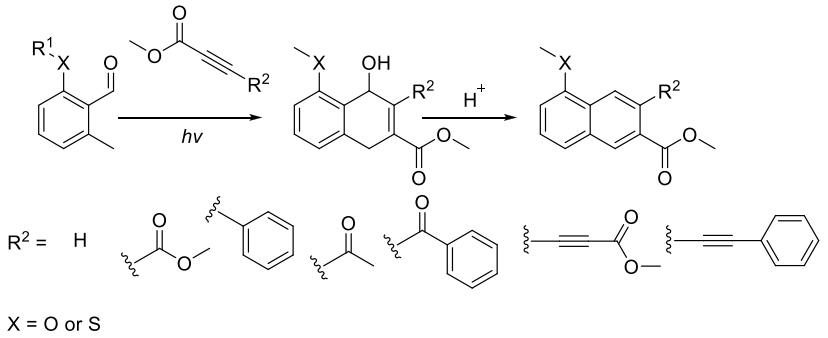

Figure 36. General scheme for the photomediated Diels–Alder reaction with electron deficient alkynes and subsequent hydroxyl elimination to yield fluorescent naphthalene derivative.

the requisite photostimulus, this also mitigates the potential photobleaching of the formed fluorophores and other deleterious light-induced side reactions.

2.2.2. Inverse Electron Demand Diels–Alder. In 2011, Arumugam et al. demonstrated the photoconversion of 3-(hydroxymethyl)-2-naphthol derivatives to 2-naphthoquinone-3-methides, eliminating water and producing effective dienes for IEDDA reactions with appropriate electron deficient alkenes.[41] In an aqueous environment, this photogenerated compound quickly converts back to the starting material (Figure 37). There are two advantageous consequences of the

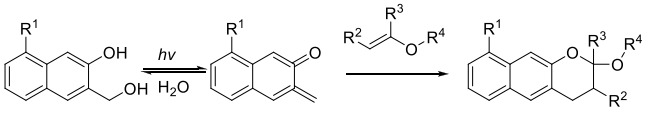

Figure 37. Photodegradation of 3-(hydroxymethly)-2-naphtol to 2-naphthoquinone-3-methide and subsequent IEDDA reaction with vinyl ether.[41]

short-lived (τ = 7 μs in water) diene intermediate in this photoclick reaction. First, the reversion to starting material prevents reaction with all but the most IEDDA-reactive alkenes, vinyl ethers, and enamines. In contrast to, for example, a tetrazole–alkene reaction, there is diminished opportunity for the activated species to react with unintended moieties. With a tetrazole–alkene reaction, even if the dipolarophile is highly reactive and dominates in a competitive reaction with other dipolarophiles and nucleophiles, when consumed, any remaining activated nitrile imide will be free to react with other functional groups. For this particular photo-IEDDA reaction, however, the rate of reversion to starting material outcompetes the IEDDA reaction with any but the most reactive alkenes, preventing off-target conjugations even in the absence of vinyl ethers or eneamines.

The second consequence of this short lifetime of the 2-naphthoquinone-3-methides is the prevention of significant diffusion of the reactive intermediate, improving spatial control over the reaction; IEDDA occurs only in areas that are exposed to light.

However, the product is not stable (Figure 37) because it contains acetals and hemiaminal ethers which are prone to hydrolytic degradation (Figure 38). While the acetal product shows relative stability under neutral pH aqueous conditions, it degrades in the presence of acid. The hemiaminal ether product is even more susceptible to hydrolysis. It should be noted that conjugation of R_3 is maintained even following hydrolysis, indicating that appropriate design of the dienophile

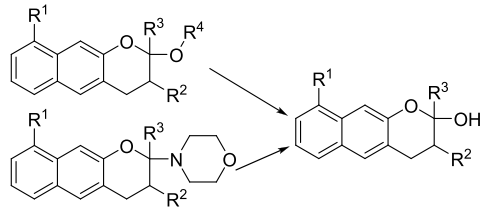

Figure 38. Hydrolysis of IEDDA adducts proceeds in either acidic (acetal, top) or even neutral (hemiaminal ether, bottom) aqueous conditions.

results in effective coupling despite subsequent hydrolysis of the product.

As with other functional groups described previously (e.g., ring strained alkynes, nitrile imides), naphthoquinone methides react with nucleophiles (via a Michael-type addition) in alternative conjugation reactions. Thiols are particularly reactive with a reaction rate approximately five times that of the Diels–Alder reaction (Figure 39). Given this preference,

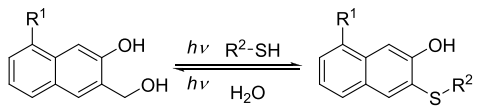

Figure 39. Naphthoquinone methides are also highly reactive toward thiols, although the reaction is reversible.[106]

the naphthoquinone methide–thiol reaction has been described in a previous review as a "photoclick" chemistry.[1] This reaction, however, is reversible in the presence of water and under exposure to the same wavelength of light that produces the naphthoquinone methide in the first place, whereas the Diels–Alder reaction is functionally irreversible. When the photomediated reaction is conducted in the presence of both a vinyl ether and a thiol, the sulfide product is first produced in high yield, although under continued exposure, the fraction of Diels–Alder product increases until all sulfide is consumed. Arumugam et al. have taken advantage of this reversibility to photochemically pattern a thiolated surface by the selective conjugation and replacement of 3-(hydroxymethly)-2-naphthol derivatives.[106]

Among the numerous examples of IEDDA, tetrazine reactions stand out for their specificity and high reaction rates. In 2016, Zhang et al. described the photomediated conversion of a dihydrotetrazine to tetrazine via photo-oxidation with methylene blue as the photocatalyst under irradiation at 660 nm. The tetrazines subsequently reacted with

https://doi.org/10.1021/acs.chemrev.0c01212
Chem. Rev. 2021, 121, 6915–6990

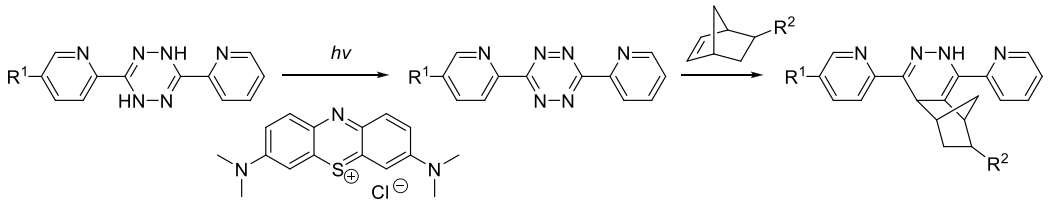

Figure 40. Conversion of dihydrotetrazine to tetrazine via methylene blue-photocatalyzed oxidation and subsequent IEDDA reaction with norbornene.[42]

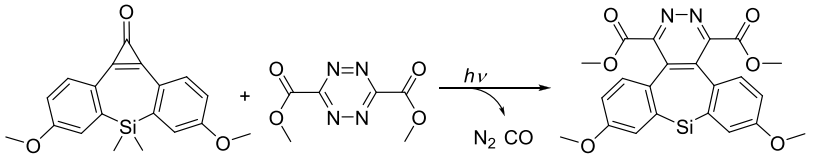

Figure 41. IEDDA reaction between tetrazine and photogenerated cycloheptyne dienophile.[34]

endogenous *trans*-cyclooctene in an IEDDA reaction.[43] Truong et al. employed the same photooxidation of dihydrotetrazine in the presence of the norbornene functional group to accomplish the IEDDA coupling (Figure 40).[42] In contrast to other IEDDA photoreactions, this strategy was able to take advantage of the long wavelength absorbance (600–900 nm) of the catalyst to conduct the reaction with tissue-penetrating red and NIR light and avoid wavelengths that could damage the more light-sensitive biomolecules. Employing this chemistry, the authors performed both polymer conjugation reactions and hydrogel cross-linking, as discussed in section 2.4.5 of this review. Notable in this report was the relative thickness of the cure itself, 0.3 mm for rheometry experiments. While 0.3 mm may not seem like a particularly thick sample, in those reactions employing a one photon, one event mechanism, even such thicknesses are often difficult to react thoroughly or uniformly. The employment of photocatalysts that are regenerated allows researchers to use lower concentrations of the light absorbing species and mitigate light attenuation. This reaction remains a one photon, one event reaction, but in contrast to those IEDDA reactions in which the photochemistry is performed directly on the reactants, the concentration of chromophores is kept well below the reactant concentration.

Ring-strained cycloalkynes may also participate in IEDDA reactions as dienophiles. While described previously in the context of photoSPAAC reactions, the photocaged, bisaryl cycloheptyne shown in Figure 41 was employed in a photomediated IEDDA reaction as a dienophile with a tetrazine moiety, with the reaction exhibiting a rate increase of an order of magnitude greater than that with the unsubstituted cyclooctyne.[34]

As mentioned, another effective dienophile in IEDDA reactions with tetrazine derviatives is the ring strained *trans*-cyclooctene. While synthesis of *trans*-cyclooctenes from their cis-analogues is a viable and efficient production strategy, the conditions under which that photoisomerization takes place are typically not conducive to in situ generation.[107,108] One example that may show promise is the iridium(III) photocatalyzed isomerization of cyclooctene described previously (section 2.1.1.3).[82] It is possible that employment of such a photosensitizer could facilitate an IEDDA reaction by in situ generation of a reactive dienophile rather than the diene shown in the previous example.

2.3. Alternating Radical Propagation Chain Transfer Reactions

Radical chain addition reactions occur when a radical propagates across a π bond, generating a new bond and a radical that subsequently propagates across another π bond. This cycle continues until the radical is terminated by recombination or disproportionation. In contrast, radical alternating propagation chain transfer (APT) reactions result from the addition of a radical across a π bond and subsequent atom abstraction by the resulting radical, regenerating the first radical species (typically intermolecularly).[109] Examples of these reactions include thiol–ene,[45] thiol–yne,[110] iodo–ene,[109] silane–ene,[111] and phosphane–ene[112] reactions. It should be noted here that the term "thiol–ene" and, to a lesser extent, "thiol–yne" are used in the literature to refer to both the radically mediated reactions between thiols and their unsaturated reaction complements, as well as to the anionically mediated reactions between thiols and Michael acceptors. To avoid confusion, the terms "thiol–ene" and "thiol–yne" will be used here to refer only to the radical-mediated reactions and "thiol-Michael" will be used to refer to the Michael-type reactions as has been done previously.[46] As these addition/chain transfer cycles regenerate participating radical species, one initiating radical results in potentially hundreds or thousands of subsequent reactions. However, as radicals are prone to termination, a continuous source of reinitiating radicals is necessary to reach maximum conversion. As these reactions are radically mediated, they may be initiated by nearly any method typically employed to generate appropriate radicals (e.g., thermally with a temperature sensitive initiator, via an electron beam, with a redox initiator, or with a photoinitiator to render the reaction light sensitive). Despite sharing a general mechanism (Figure 42), these distinct APT reactions may vary greatly in terms of efficiency and versatility.

2.3.1. Thiol–ene. While originally reported in 1905,[113] the radical addition of thiols to alkenes has only in the last couple decades been recognized as a particularly powerful tool for the construction of carbon–sulfur bonds. Such conjugations are particularly important because organosulfur moieties are widely represented within natural products, pharmaceutical, and polymeric materials.[114–116] The utility of the reaction comes, in no small part, from the simplicity of its execution, mild reaction conditions, 100% atom economy, high yields, and orthogonality with many other reactions.

https://doi.org/10.1021/acs.chemrev.0c01212
Chem. Rev. 2021, 121, 6915–6990

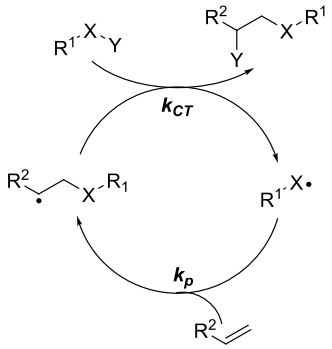

Figure 42. General mechanism for radical alternating propagation, chain transfer reactions wherein radical propagation across a π bond results in generation of a radical that abstracts an atom from a donor molecule to generate the reaction product.

The reaction frequently proceeds by the activation of a photoinitiator which abstracts a hydrogen radical from a thiol to form the thiyl radical, which adds across the alkene carbon−carbon double bond, forming a new carbon−sulfur bond and a carbon-centered radical. Abstraction of the hydrogen from another thiol regenerates the thiyl radical for the cycle to repeat (Figure 43). Alternatively, the initiator may produce a

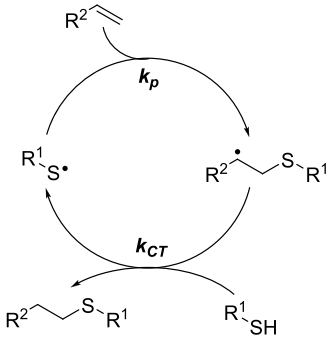

Figure 43. General mechanism of the photoinitiated thiol−ene coupling, consisting of alternating radical propagation and chain transfer reactions, leading to a one-to-one addition between thiols and alkenes.[46]

radical that adds across an alkene carbon−carbon double bond first, generating a carbon centered radical that then abstracts a hydrogen atom from the thiol.

The overall rate of reaction in the thiol−ene addition depends on the rate of propagation (r_p with rate constant k_p) and on the rate of chain transfer (r_{CT} with rate constant k_{CT}) with the overall rate (r) necessarily dictated by the slower of the two constitutive reactions, the rate limiting step, as described by eqs 6−8:[117]

$$\text{for } \frac{k_p}{k_{CT}} \gg 1\text{: } r \propto [\text{SH}]^1 \tag{6}$$

$$\text{for } \frac{k_p}{k_{CT}} \approx 1\text{: } r \propto [\text{SH}]^{1/2}[\text{C=C}]^{1/2} \tag{7}$$

$$\text{for } \frac{k_p}{k_{CT}} \ll 1\text{: } r \propto [\text{C=C}]^1 \tag{8}$$

Although the thiol−ene reaction generally proceeds nearly quantitatively, the characterization of the thiol−ene coupling as a "click" reaction has been challenged due to poor yields in some polymer conjugation reactions under certain reaction conditions.[118] Furthermore, while the relative orthogonality of the reaction has been touted in several reports, the potential reactivity of the nucleophilic thiols with a variety of other functional groups (e.g., Michael acceptors, halides, epoxides) must be a consideration in the application of the thiol−ene coupling reaction, albeit one that is greatly mitigated in the absence of base. Perhaps most significant is the reaction of thiols with themselves under oxidizing conditions to generate disulfides. Nevertheless, radical thiol−ene reactions have been used frequently for effective, selective conjugation reactions under a variety of reaction conditions,[4] in water and open to air, and requiring as little as a few seconds for near quantitative conversions. It is the very high potential reaction rates that allow the thiol−ene reaction to be successfully employed as a click reaction, avoiding undesired competitive reactions. It should be noted that the efficiency of the thiol−ene reaction depends on multiple variables. Reaction parameters that play a particularly influential role in the efficiency of the thiol−ene coupling reaction include the selection of solvent, initiator, thiol, and alkene. This latter factor may not influence just the rate and ultimate conversion but also the degree of participation in competing chain-addition reactions (e.g., acrylate homopolymerization).

The solvent in which the reaction occurs may influence the rate of thiyl radical generation. Although the thiol−ene reaction has been performed in a wide variety of solvents, there are few studies explicitly examining the solvent effects on the reaction.[119] Munar et al. utilized conceptual DFT to model the reactivity of the carbon and sulfur radicals in a thiol−ene reaction in different solvents to elucidate the role of solvent on the propagation and chain transfer steps. The authors noted that solvent ultimately has a negligible influence on the sulfur-centered radical, thus exhibiting little effect on propagation rates.[120] The chain transfer step, however, was significantly more sensitive to the reaction environment, purportedly due to stabilization of the carbon-centered radical intermediate in the presence of a polar solvent.

2.3.1.1. Radical Initiation. Thiol−ene reactions have been initiated via a variety of means. Thermal and redox radical initiation strategies have been employed to conduct thiol−ene couplings. Thiol−ene reactions without traditional radical initiators have also been carried out by generating hydroxyl radicals upon sonication in water.[121] Typically, it has been photoinitiated reactions that have been most advantageous in the application of the chemistry.[4] While the use of photoinitiators to facilitate the reaction is the most commonly employed practice, the photoinitiated reaction can be conducted without initiator by direct photolysis of reactants. In this way, the thiol−ene photoreaction between alkenes and mercaptopropionates has been initiated with both 254 and 365 nm light exposure despite very low absorbance of reactants at that higher wavelength. In such reactions, however, considerably higher light intensities are required and the rates of reaction are considerably lower than in those reactions employing photoinitiators. As described subsequently, however, employment of aryl substituents greatly improves the absorption characteristics of thiols in a thiol−ene reaction to allow more effective initiatorless reaction.[122] The selection of photoinitiators is one of the most consequential in determining the overall rate of reaction in all APT as well as in the previously described photoinitiated photoCuAAC reactions.

https://doi.org/10.1021/acs.chemrev.0c01212
Chem. Rev. 2021, 121, 6915−6990

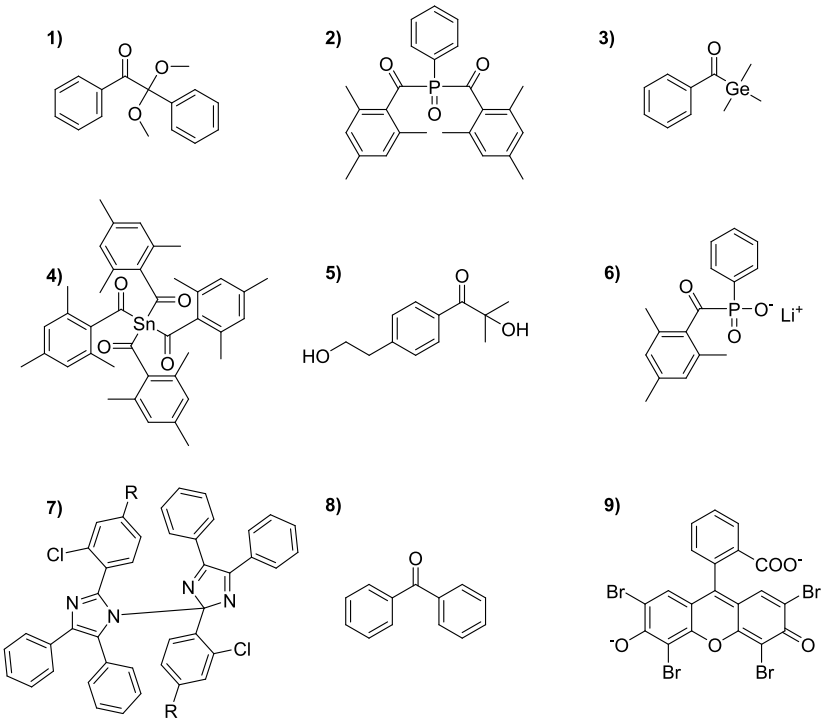

Figure 44. Structures of representative radical photoinitiators that may be used in thiol−ene and other radical APT reactions: (1) hydrophobic type I photoinitiator, 2,2-dimethoxy-2-phenylacetophenone (DMPA); (2) hydrophobic, type I, bis(2,4,6-trimethylbenzoyl)-phenylphosphineoxide (BAPO, I819); (3) hydrophobic type I photoinitiator benzoyltrimethylgermane (BTG); (4) hydrophobic type I photoinitiator tetrakis(2,4,6-trimethylbenzoyl)stannane; (5) hydrophilic, type I, 2-hydroxy-4′-(2-hydroxyethoxy)-2-methylpropiophenone (I2959); (6) hydrophilic, type I, lithium phenyl-2,4,6-trimethylbenzoylphosphinate (LAP); (7) hydrophobic, type I, hexaarylbiimidazole (HABI) photoinitiator; (8) hydrophobic, type II, benzophenone; (9) hydrophilic, type II initiator, eosin Y.

Therefore, a thorough understanding of the available initiators and their salient features is recommended for successful application of such reactions in the various contexts in which they may be employed.

Norrish type I photoinitiators, such as dimethoxyphenylacetophenone (DMPA) and bis(2,4,6-trimethylbenzoyl)-phenylphosphineoxide (BAPO), are the most frequently used class of initiators in thiol−ene and other APT reactions. These initiators, upon absorption of photons, decompose into two or more radical fragments that initiate the reaction as previously described. The initiation rate in a radical polymerization of an optically thin film where the light intensity is nearly constant throughout the film depth is described by eq 9.

$$R_i = \frac{2\phi f \varepsilon I_o[\mathrm{In}]}{N_A h\upsilon} \tag{9}$$

In this expression, φ is the quantum yield of radical generation, f is the efficiency or the fraction of those radicals that initiate reaction, ε is the molar extinction coefficient at the wavelength of exposure, I_o is the intensity of light exposure, [In] is the concentration of photoinitiator, N_A is Avogodro's number, and $h\nu$ is the photonic energy. It is important to highlight the difference between quantum yield of photolysis and efficiency, as not all radicals are equally likely to initiate the reaction and so some radical initiators are better or more poorly suited to thiol−ene reactions regardless of their respective quantum yields. Uygun et al. evaluated a series of photoinitiators and thermal initiators for initiation of thiol−ene reactions and concluded that the type I or cleavage type initiators were most effective. A particularly interesting demonstration of the relative efficiencies of radicals generated by different photoinitiators is the case of hexaarylbiimidazoles (HABI), which are poor initiators for (meth)acrylate chain addition reactions but effective in thiol−ene reactions.[123] Moreover, in contrast to most radicals generated by photodecomposition of an initiator, HABI-based radicals are moderately stable, recombining over the course of several minutes, permitting significant dark cure. HABI is also noteworthy in its high absorption at longer wavelengths of light allowing initiation with 469 nm exposure. Most type I initiators absorb primarily in the UV region of the spectrum, although phosphine oxide,[124] acyl germane,[125] and acylstannane[126] photoinitiators (Figure 44) have extended the absorption spectra of cleavage type radical initiators progressively deeper into the visible spectrum past 500 nm. Despite these advances, use of acylgermane and acylstannane photoinitiators remains somewhat uncommon.

Emerging applications of thiol−ene reactions frequently require performing the reaction in an aqueous environment. While most commercial radical photoinitiators are intended for use in hydrophobic environments and are accordingly poorly water-soluble, a few hydrophilic initiators, such as lithium phenyl-2,4,6-trimethylbenzoylphosphinate (LAP) and 2-hydroxy-4′-(2-hydroxyethoxy)-2-methylpropiophenone (I2959), have been successfully applied to the aqueous thiol−ene reaction (Figure 44).[127−133]

As alluded to previously, direct photolysis of aryl thiols allows for the generation of thiyl radicals with milder wavelengths and intensities. The use of disulfides as type I photoinitiators has been well established.[134] The photoactivation of thiols has received less attention. Such strategy results not only in the direct coupling of aryl thiols to alkenes but also in the photoamplified coupling of other thiols as well,

https://doi.org/10.1021/acs.chemrev.0c01212
Chem. Rev. 2021, 121, 6915−6990

serving the function of effective photoinitiators. Love et al. evaluated the initiating potential for various aromatic thiols, demonstrating near quantitative conversions with divinyl ether under irradiation with modest intensity (10 mW/cm^2) of 405 nm visible light.[122] Reactions reached completion in as little as 5−10 min. The same aromatic thiols were effectively employed to initiate reactions between norbornenes and mercaptopropionates in dilute aqueous reactions. Ortho and para substituted mercaptobenzoic acids and trifluoromethyl thiophenols were particularly effective at initiating the reaction.

One particularly interesting type I, thiol−ene initiating system was developed by Li et al., who attached oxime-ester coumarin groups to the surface of upconverting nanoparticles.[135] Upon absorption of NIR light at 974 nm, these nanoparticles would, through a combination of FRET and photon upconversion, cause cleavage of the oxime ester bond, resulting in the release of phenyl radicals to initiate bulk thiol−ene reaction. The authors compared this release of reactive radicals to the dispersion of dandelion seeds (Figure 45).

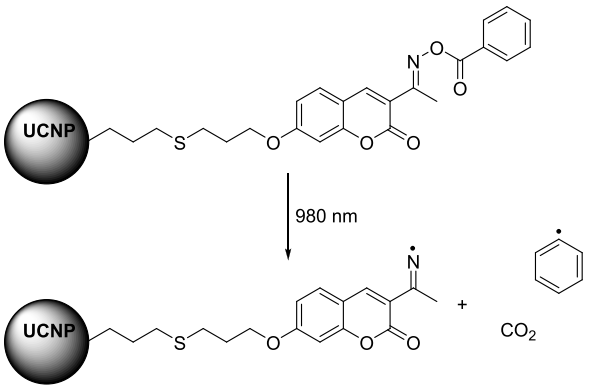

Figure 45. Initiation of thiol−ene reactions with NIR exposure is accomplished by release of initiating radical from upconverting nanoparticles, which, upon absorption of photons, cause the decomposition of the pendant oxime ester coumarin via a combination of FRET and photon upconversion.[135]

Type II initiating systems, in which the initiator, from an excited state, undergoes a multistep electron transfer reaction with a co-initiator (frequently an amine) to generate the initiating radical species, are also frequently used in thiol−ene reactions. In this case, the thiol itself may serve as a co-initiator, donating a hydrogen atom to the excited chromophore, obviating any need for the presence of other co-initiating species. Substantial variability in initiator efficiency when employing type II initiators has been reported, however, with benzophenone, for example, and its derivatives providing for efficient reactions but camphorquinone considerably less so.[136,137]

As cleavage type radical photoinitiators typically absorb in the UV and shorter wavelength visible spectrum in order to conduct the radical thiol−ene reaction at higher wavelengths, other initiating strategies have been and continue to be developed. This can be accomplished by the use of transition metal photoredox catalysts as type II photoinitiators. Upon exposure to visible light, the thiol−ene reaction proceeds by the formation of a strong metal−ligand charge transfer excited state, which undergoes reductive quenching by a thiol to generate the thiyl radical cation. The deprotonation of the radical cation then generates a thiyl radical, which then participates in the thiol−ene reaction cycle as described previously. For example, the most efficient ruthenium catalysis for the thiol−ene click reaction, using $Ru(bpz)_3(PF6)_2$, was found to occur in the presence of an excess of thiol; however, bulkier thiols such as cyclohexyl and *tert*-butyl mercaptan required longer reaction times.[132] Addition of *p*-toluidine, which exhibited thiol-activating capabilities, either via direct hydrogen atom abstraction or sequential electron- and proton-transfer steps to afford the chain-propagating thiyl radical species, improved the rate of reaction by circumventing the slow direct photooxidation of thiol with $Ru^*(bpz)_3^{2+}$.[132,138] Various other metal-based photoredox catalysts, like, $Ru(bpy)_3Cl_2$, *fac*-$Ir(ppy)_3$, and zinc tetraphenylporphyrin (ZnTPP) have been similarly exploited but are often associated with low catalytic efficacy and lower conversion, which has led researchers to explore a metal-free organic photoredox catalyst, eosin-Y.[138−140] An organic photocatalyst, 9-mesityl-10-methylacridinum tetrafluoroborate, designed by Zhao et al., resulted in efficient thiol−ene conjugation involving biomolecules.[127] Although this visible-light-mediated photoredox catalysis under neutral conditions resulted in high yield and few side products, it did require long irradiation times (1−24 h) and high light intensities.

2.3.1.2. Thiol Influence on Rate. The dependence on the rate of reaction of the thiol's molecular structure, although incompletely examined, is significant. Among the most frequently used thiols in thiol−ene reactions are mercaptopropionates, mercaptoacetate, and alkyl and aromatic thiols. Mercaptopropionates are more reactive than mercaptoacetates, which, in turn, are more reactive than aliphatic thiols. This relationship is attributed to the weakening of the S−H bond by intramolecular hydrogen bonding between the thiol proton and the carbonyl that is facilitated by the favorable formation of a six-membered structure in mercaptopropionates and similar thiols.[141,142] Such hydrogen bonding would be considerably less effective in mercaptoacetates and absent entirely from the alkyl thiols.

While secondary and tertiary thiols are infrequently used in thiol−ene reactions, their employment may provide advantages in terms of formulation stability. Varying the thiol substitution from primary to secondary to tertiary has substantial effect on the reaction kinetics due to steric hindrance, although the effect itself is highly dependent on the rate limiting step of the reaction, which varies from alkene to alkene.[143] As increased sterics increase the activation energy more significantly for the chain transfer step, relative to the propagation step, those reactions that are limited by the rate of chain transfer (e.g., reactions with allyl ethers) are particularly affected. However, under most commonly used conditions for thiol−ene reactions, secondary thiols generally perform adequately. Examination of rates in more dilute conditions, however, have not been reported. While the degree of substitution of the thiol has been shown to affect the rate of chain transfer, other evidence indicates that the propagation step can also be negatively influenced by electron withdrawing group substituents proximal to the thiol.[144]

2.3.1.3. Alkene Influence on Rate. Apart from initiator, the most widely explored influence on reaction rate may be the selection of alkene. Early experimental evaluations of the rates of reaction with various alkenes indicated that ring strained (e.g., norbornenes) and electron rich (e.g., vinyl ethers) alkenes reacted most rapidly, while electron poor alkenes such as acrylates and maleimides react more slowly (Figure 46).[145]

https://doi.org/10.1021/acs.chemrev.0c01212
Chem. Rev. 2021, 121, 6915−6990

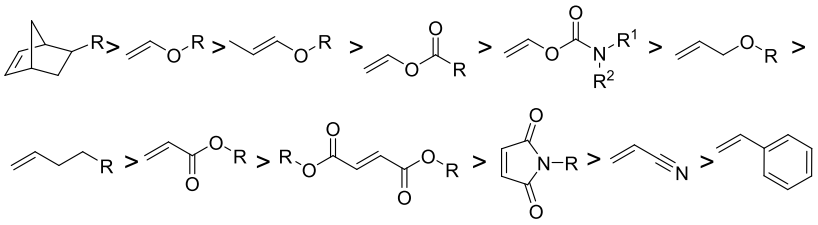

Figure 46. Relative reaction rates of various alkenes as determined experimentally and reported by Roper and Hoyle.[145]

Subsequently, the propagation rate was shown to be directly correlated to the electron density of the alkene, with the chain transfer rate being inversely proportional to the stability of the carbon-centered radical.[146] Computational modeling studies have elucidated the relationship that exists between alkene structure and the activation barrier to propagation and chain-transfer. This kinetic analysis demonstrates the importance of the stability of the carbon-centered radical intermediate, which exhibits direct influence on the chain-transfer activation barrier, as well as the reversibility of the propagation step. It is evident that a small change to the alkene structure would significantly impact the rates of propagation and chain-transfer, as well as the stability of the carbon-centered radical intermediate, which would then directly influence the relative rate constants k_P and k_{CT}.[147,148]

There are other factors that may influence the rate of the thiol−ene coupling reaction. The presence of radical inhibitors or retarding agents, as would be expected, may interfere with the initiation or other steps of the reaction. Interestingly, however, inhibitory effects of oxygen (a considerable problem in acrylic radical chain addition reactions) is muted in most thiol−ene couplings. Additionally, in contrast to thiol-Michael additions, thiol−ene reactions proceed quite rapidly in neutral or acidic conditions. Thiol−ene coupling reactions can also be performed in mildly basic conditions, although deprotonation of the thiol precludes effective chain transfer, so the reaction will not proceed in strongly basic environments. Moreover, even small quantities of generated thiolate can result in the formation of metastable disulfide radical anion species that effectively retard the thiol−ene reaction.[149] Because their generation requires the presence of thiolate anions, the propensity for base-mediated retardation of the thiol−ene reaction is largely dependent on the pK_a of the respective thiols as well as the strength and concentration of the base in the system. In general, the thiol−ene reaction is extremely accommodating to a variety of reaction conditions.

2.3.2. Thiol−yne. The radical thiol−yne reaction is analogous to the thiol−ene click chemistry although considerably less well explored. Recently the reaction has received significant attention, particularly in its suitability for synthesis of dendrimers, modification of peptides and protein, as well as for surface functionalization. An important and distinguishing feature of the thiol−yne reaction compared to thiol−ene reactions is the ability of one equivalent of the alkyne to react with two equivalents of thiol, resulting in a double addition product with 1,2-regioselectivity. As with the radical thiol−ene reaction, radical thiol−yne reactions may be performed open to ambient atmosphere and in aqueous conditions, and like other click reactions, it can be performed at room temperature with relatively high reaction rates. The radical thiol−yne reaction proceeds similarly to two consecutive thiol−ene reactions (Figure 47) and is initiated similarly to the thiol−ene reactions. An initiating radical is generated

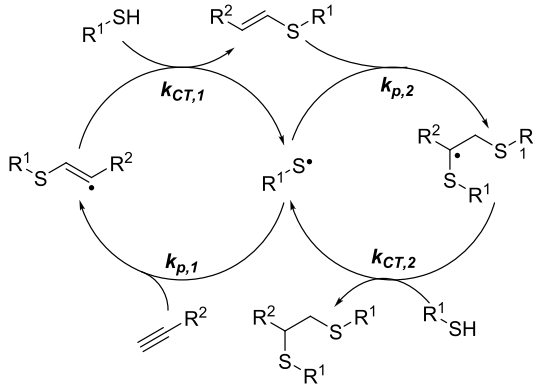

Figure 47. Simplified mechanism of the radical thiol−yne coupling reaction consisting of sequential propagation chain-transfer cycles.[150]

that abstracts a hydrogen atom from a thiol, resulting in the formation of thiyl radical. The sulfur centered radical adds to the carbon−carbon triple-bond, resulting in the formation of a carbon-centered vinyl sulfide radical. Abstraction of a hydrogen from another thiol (chain-transfer) yields the intermediate vinyl sulfide and regenerates the thiyl radical. The vinyl sulfide subsequently undergoes a second addition of thiyl radical, yielding a carbon-centered radical which then undergoes a second chain transfer reaction with thiol, producing the double addition product and another thiyl radical. Fairbanks et al. demonstrated that for the reaction of mercaptopropionates with aliphatic alkynes, the second addition of a thiol to the vinyl-sulfide was approximately three times faster than the initial thiol−yne reaction,[150] an observation that has subsequently been computationally validated.[148] This relationship (i.e., the rate of the second addition exceeding the rate of the first) was observed for other thiol−yne pairs although not universally; reactions with methyl propiolate and propargylamine showed slower thiol−vinyl sulfide reactions than initial thiol−yne reactions. It was also shown that the ring strained cyclooctyne efficiently and quickly undergoes addition by thiyl radical, as a consequence of releasing ring-strain associated with the cyclic alkyne species. However, the addition of a second equivalent of thiol to the cyclic vinyl sulfide is restricted due to steric hindrance.[47,151] Additionally, the spontaneous reaction between the cyclooctyne and thiol were observed in the absence of any light exposure, indicating limits to the orthogonality of both the thiol−yne and SPAAC reactions. Structures of various alkynes with their relative order of reactivity toward mercaptopropionate are shown in Figure 48.

Similar to thiol−ene reactions, thiol−yne chemistry has been successfully accomplished using UV and visible light photoinitiators, which is the most commonly employed methodology. Kritchenkov and co-workers implemented an initiator-free thiol−yne click reaction using ultrasound catalysis to develop antibacterial chitosan derivatives, but only one

https://doi.org/10.1021/acs.chemrev.0c01212
Chem. Rev. 2021, 121, 6915−6990

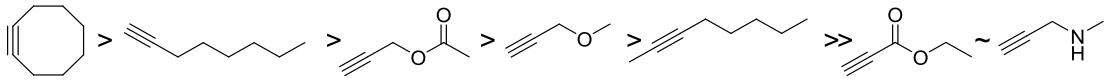

Figure 48. Order of alkyne reactivity toward mercaptopropionates. Notable is that while the initial addition rate is fastest in the ring-strained cyclooctyne, subsequent addition was not observed.[36]

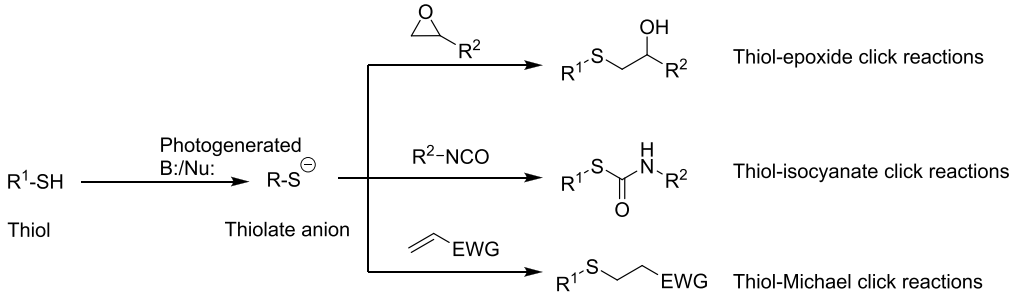

Figure 49. Various photolatent thiolate nucleophile mediated click reactions.

substitution of thiol was observed, although the authors do not speculate as to why this is the case.[152] Similarly, upon use of photoredox catalyst monoadduct vinyl sulfide products predominate, usually as a mixture of *E*:*Z* anti-Markonikov form.[153,154] One plausible explanation for the reaction regioselectivity and stereoselectivity is the concerted effects of single electron oxidation of the thiol moiety from the excited state of eosin Y and the steric influence of the substituent. However, the organic photocatalyst, 9-mesityl-10-methylacridinum tetrafluoroborate, produced diadducts when less sterically hindered thiols were used, providing corresponding adducts in good yields.[155]

Like the thiol−ene reaction, the thiol−yne reaction can be performed open to the air and presumably is similarly affected by the presence of base that results in the generation of disulfide radical anion retardants. While examination of the effects of the thiol substitution on reaction rate have yet to be conducted, given the chain transfer rate dependence of the reported thiol−yne reactions, it may be speculated that secondary and tertiary thiols would have adverse effects on the overall reaction rates.

2.3.3. Other APT Reactions: Iodo−ene, Silane−ene, and Phosphane−ene. Thiols are particularly effective chain transfer agents, making them especially suited to APT reactions. Other chain transfer moieties, however, may also participate in such similar mechanisms. Although these reactions are generally not considered "click" reactions, they warrant mention, in no small part because their examination and applications have been so heavily informed by the study of thiol−ene couplings.

One such example is the iodo−ene reaction wherein iodo compounds add radically to alkenes, the iodine atom filling the role in chain transfer that the hydrogen atom fills in thiol−ene reactions. Obstacles to the wide adoption of the iodo−ene reaction include the relatively poor reactivity of nonfluorinated iodocompounds and the propensity for side reactions of the iodides generally.[156] The presence of fluorine adjacent to iodide results in the enhancement of the chain transfer of iodine due to the electron withdrawing ability of the fluorine. Among many other perfluoro derivatives, perfluoroiodide has been observed to exhibit high efficiency and reactivity. For example, perfluorohexyl iodide exhibits better efficiency as transfer agent when compared to 1,1,2,2-tetrafluoro-3-iodopropane and 1,1,1,3,3-pentafluorobutane, which resulted in lower conversion.[157−159] Although not widely used, the iodo−ene reaction imparts various advantageous properties, depending on the desired application, to materials thus formed due to the presence of the fluorine atoms and conservation of the iodo moiety, which can participate in subsequent reactions.[160,161]

The silane−ene reaction shares many of the features of the other APT reactions described previously, including its insensitivity toward oxygen and the same one-to-one reactivity of the thiol−ene and iodo−ene reactions.[111,162,163] However, the relatively high bond dissociation energy of Si−H bonds disfavor chain transfer reactions to the silane, resulting in relatively slow reactions. This drawback can be overcome by employing silanes with low bond dissociation energies but availability of such suitable silanes is severely limited.

Finally, one more reaction that should be noted is the radical reaction between a primary or secondary phosphine and an alkene.[112,164] Via a mechanism similar to but inverted from that of the thiol−yne reaction, primary phosphines may react consecutively with two alkenes. The limited availability of primary phosphines and their sensitivity to air may prevent more frequent employment of this reaction, although air stable phosphines have been synthesized by Guterman et al.[165] and polymerized via photoinitiation with a phosphine oxide initiator.

2.4. Photoinduced Click Reactions Based on Thiolate Nucleophiles

In addition to the radical mediated thiol−ene click reactions, thiols are particularly effective functional groups for nucleophilic addition click reactions.[45,46,166−168] Chemically, the high reactivity of these soft nucleophiles toward various complementary reactive moieties, high conversions in short time and their broad substrate scope make these click reactions superior over other click chemistries. The very same feature makes them susceptible to multiple simultaneous reactions and thus may be unsuited for some orthogonal strategies. Because the reactivity of thiolate nucleophiles varies based on the nature of the thiolate, a fine-tuning of the reactivity is also possible by wise choice of the substrates. Among the nucleophilic thiolate mediated click strategies, those which are interesting to both chemists and biologists are the thiol−epoxy, thiol−isocyanate, and thiol-Michael additions and are discussed in the following sections with particular emphasis on

https://doi.org/10.1021/acs.chemrev.0c01212
Chem. Rev. 2021, 121, 6915−6990

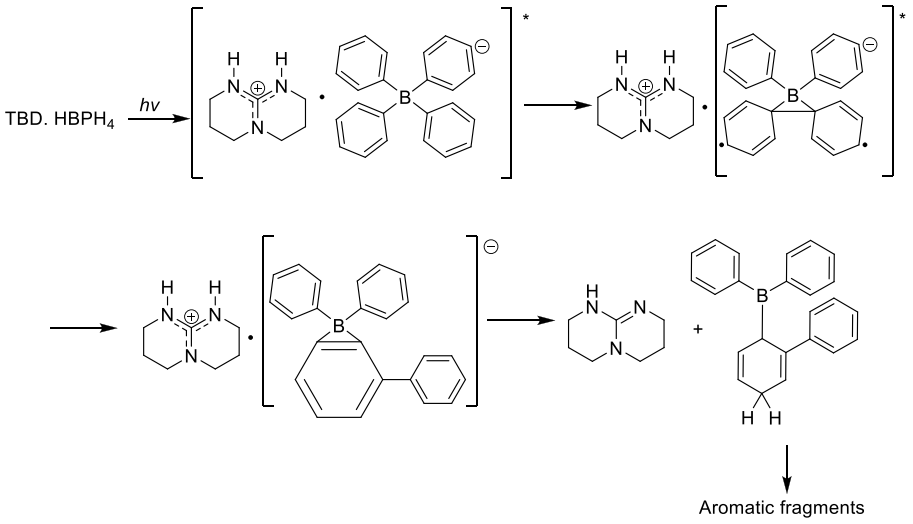

Figure 50. Proposed mechanism of the photogeneration of TBD from TBD·HBPh$_4$. Adapted with permission from ref 180. Copyright 2008 American Chemical Society.

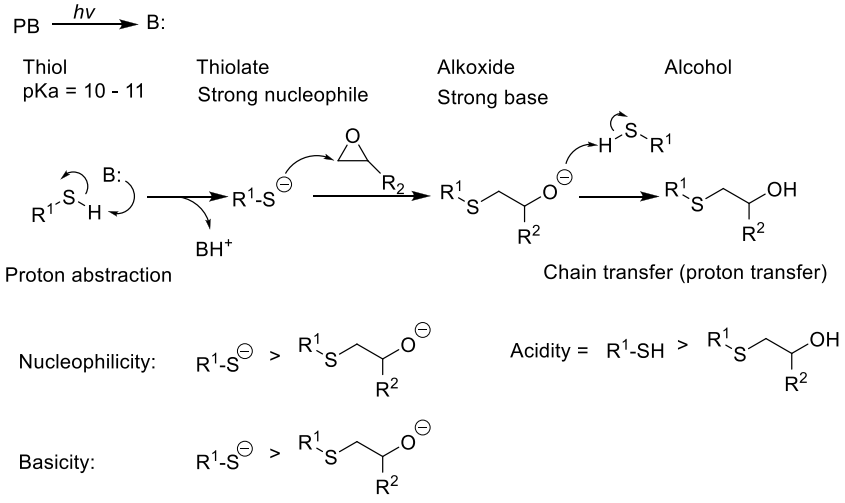

Figure 51. Mechanism and functional group reactivity consideration for base catalyzed thiolate mediated epoxide ring opening click reaction. Figure adapted with permission from ref 187. Copyright 2020 American Chemical Society.

the versatile photoinduced thiol-Michael click reactions (Figure 49).

2.4.1. Photolatent Base/Nucleophile Catalyzed Thiol−Epoxide Click Reactions. Addition of a thiolate nucleophile to a strained ring such as oxirane is among one of the most prominent thiolate-mediated click reactions known.[49,166,169] In general, these ring opening reactions are catalyzed by appropriately strong bases that are capable of deprotonating the thiol more efficiently. To achieve spatial-temporal control, several photobase generators have been developed and their performance in various thiolate mediated click reactions has been extensively studied in recent years.[170,171] Ideally, an efficient photobase generator should have a suitable chromophore for good absorption at a desired wavelength and should be able to produce active species in high yield upon photoexcitation. Thioxanthone,[172] trans-*o*-coumaric acid,[173] *o*-acyloxyime,[174] pthalimidocarbamates,[175] *α*-ketocarbamates,[176] and *o*-nitrobenzyl carbamates[177] are a few among the well-known chromophores used for this purpose. In general, highly efficient photobase generators are often necessary to achieve the thiolate mediated click reactions efficiently. However, there are very few reports on the photobase generators that are capable of releasing robust and stable tertiary amine bases suitable for nucleophilic ring opening click reactions.[172,178,179] For example, Salmi et al. developed a series of photobase generators in the form of a quaternary ammonium salts of phenylglyoxalate that are capable of releasing strong bases such as DBU, DBN, and TMG upon exposure to UV light via photodecarboxylation and were successfully applied in the photo-cross-linking of epoxide-based resins.[178] Thus, by using an appropriate base, near-quantitative conversion could be easily achieved in these reactions without forming any byproducts. Tetraphenyl borate salts of bicyclic guanidinium is another family of short-wave photobase generators that are capable of generating a much stronger base than the strongest base DBU.[180] Upon photoexcitation, the BPh_4^- ion undergoes rearrangement which can abstract a proton from the neighboring TBD·H$^+$ cation to release the free base (TBD) (Figure 50). The trivalent arylborane then decomposes further to aromatic byproducts.

https://doi.org/10.1021/acs.chemrev.0c01212
Chem. Rev. 2021, 121, 6915−6990

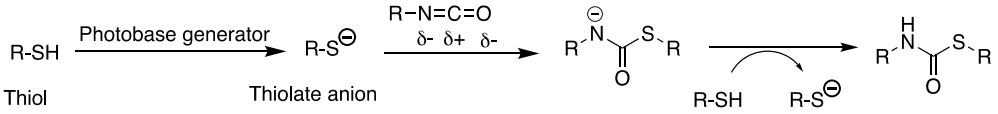

Figure 52. Mechanism of the photolatent base-catalyzed thiol−isocyanate click reaction.

An interesting feature of the base catalyzed thiol−epoxide click reaction is the reduced volumetric shrinkage which is caused by the reduction in free volume during the formation of covalent bonds.[181] Thus, the thiol−epoxy/thiolacrylate hybrid photopolymer produced using a combination of free radical photoinitiator (ITX) and photobase generator (TBD·$HBPh_4$) system exhibited low shrinkage along with enhanced mechanical and physical properties upon increasing the thiol−epoxy content.[182] In another example, Chen et al. used a photogenerated TBD base for delayed photopolymerization of the thiol−epoxy resin to demonstrate an efficient photopolymerization of pigmented or thick composites.[183] In their work, the thiol−epoxy resin formulated with a photoinitiator (ITX) and photobase generator (TBD·$HBPh_4$) system was exposed to UV to release the active tertiary amine base at room temperature. After the release, the resin mixture was mechanically stirred to cause the diffusion of the active base species and then heated at elevated temperature to complete the thiol−epoxy click polymerization. Because no polymerization occurred at room temperature, the liquid resin formulation could be further processed to the desired size and shape.

The general mechanism of photoinduced thiol−epoxide click reactions involve the deprotonation of a thiol by a photogenerated strong base followed by ring opening of the epoxide via the nucleophilic addition of the thiolate anion on the less hindered and most electrophilic site on the epoxide ring. As the secondary alkoxide is the most basic component generated, it autocatalyzes the polymerization via a proton transfer from a new thiol to the secondary alkoxide, producing a new thiolate anion for subsequent reactions. During this process the secondary alkoxide is quenched by a proton transfer from the thiol to the alkoxide, resulting in the quenching of the alkoxide to a secondary hydroxyl group. Reaction rates depend on the reaction conditions and the nature of the thiol and epoxide structure (Figure 51). However, the absence of any acidic protons or strong nucleophiles like a thiol in the system results in homopolymerization of the epoxy groups. The structure of the polymer backbone is thus determined by the proton transfer to alkoxide ion as reported by Frèchet and co-workers and coined the name "proton transfer polymerization."[184−186]

The key benefit of using the thiol−epoxide click reaction in micro- and nanopatterning is the reduced polymerization induced shrinkage, providing dimensional stability especially at lower length scales. Recently, Khan et al. demonstrated the photoinduced proton transfer thiol−epoxide polymerization for micro- and nanopatterning using a photolabile salt prepared by the supramolecular complexation of a guanidine base and DBU with benzoylphenyl propionic acid (ketoprofen).[187] The authors have successfully demonstrated the thiol−epoxide ring opening polymerization and further polymer modification for micro- and macropatterning. The imprinted features were further modified with fluorescent dyes via the $AgBF_4$ mediated alkylation of thioether linkages.

Another key benefit of thiol−epoxide based click reaction is the formation of β-hydroxythio-ether groups with high adhesion properties which further enable the postpolymerization modification for polymer surfaces. Coupled with photolabile *o*-nitrobenzene chemistry, Romano et al. used photoclick thiol−epoxide reaction to alter the bulk and surface properties of thiol−epoxy based network polymers. For this purpose, the authors used a difunctional epoxy monomer containing *o*-nitrobenzylester groups in combination with multifunctional thiol to form the thiol−epoxide network. The thiol−epoxide ring opening was initiated with photolatent 1,5-diazabicyclo-[4.3.0]non-5-ene (DBN). To avoid the interference of the photoexcitation of the base with *o*-NB absorption, the photosensitivity of the base was further extended to the visible region by incorporating the photosensitizer ITX in the resin formulations. Nearly complete conversion of the thiol and epoxide functionalities was achieved upon exposure to the visible light at 400 nm without any damage to the imbedded *o*-NB groups. After the network formation, the wettability, solubility, and the cross-link density of the bulk film were altered via the photo cleavage of the imbedded *o*-NB groups, which upon UV exposure cleaves the ester linkage to release the carboxylate groups.[188]

In summary, the photolatent base catalyzed thiol−epoxide click reaction is certainly a valuable tool for researchers working in both chemistry and biological fields. The commercial availability of a large number of small molecule epoxides and thiols and their ability to reach higher conversion in both aqueous and solvent free conditions make them a frequently employed chemistry for biomedical applications,[189−191] suggesting a potential role for the photomediated reaction. Moreover, the enhancement in material properties such as low polymerization shrinkage and strong adhesion, coupled with spatiotemporal control achieved by photochemical methods and tolerance toward radical reactions, are the key benefits of the photoinduced thiol−epoxide click reaction. However, the requirements for highly efficient photobase generators and the nature of thiol structures are few hindrances to this approach.

2.4.2. Photolatent Base Catalyzed Thiol−Isocyanate Click Reactions. Thiourethanes, the sulfur analogue of urethane, are another prominent class of high yielding click reactions that does not form any byproduct.[166,192] By using appropriate catalysts such as tertiary amines or tryalkyl phosphines, excellent conversions are achieved in short times with no other side reactions. The incorporation of thiourethane groups in the network polymer results in polymeric materials with significantly enhanced material properties through extensive hydrogen bonding interactions. Other key benefits of using thiourethane click chemistry are the significantly higher refractive index and enhanced uniformity, leading to a narrower mechanical transition than the corresponding polyurethanes which makes them suitable for various optical materials development.[50] The mechanism of photoinduced thiol−isocyanate click reactions follows a two-step process identical to that of the radical thiol−ene click

https://doi.org/10.1021/acs.chemrev.0c01212
Chem. Rev. 2021, 121, 6915−6990

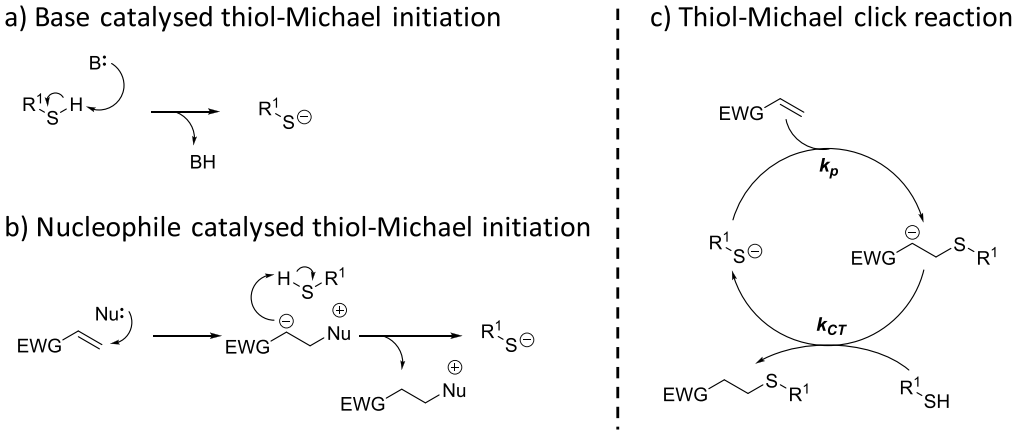

Figure 53. Mechanism of (a) base and (b) nucleophile catalyzed (c) thiol-Michael addition click reaction cycle. In the case of photomediated thiol-Michael addition, the base species, B:, is most often generated by photodecomposition of a photolatent base.

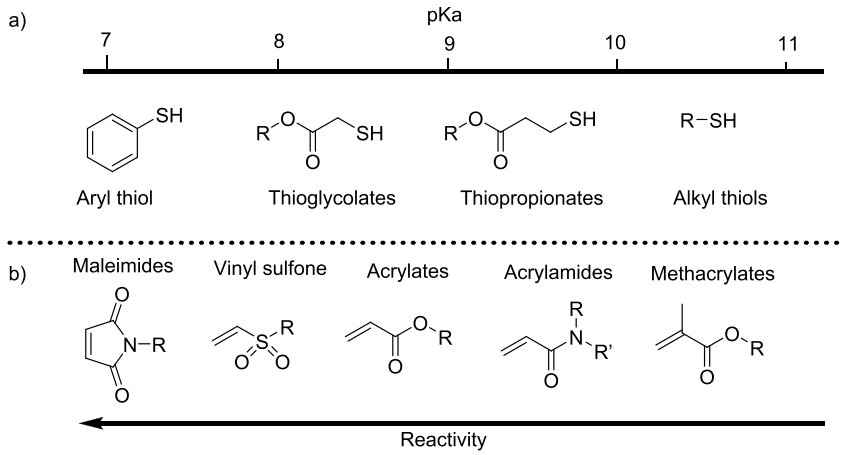

Figure 54. (a) pK_a values of commonly used thiols in Michael addition click reaction, (b) reactivities of commonly used vinyl groups in thiol-Michael addition click reactions.[152,186]

reaction involving the attachment of photogenerated thiolates with carbonyl carbon followed by a chain transfer to a thiol or any proton donating species in the system (Figure 52).

The reaction kinetics of the thiol−isocyanates click reaction are typically fast with primary and secondary thiols adding across aryl isocyanates but at a slower rate with alkyl isocyanates.[166] Another advantage of using the thiol−isocyanate click reaction is the orthogonality of the isocyanates group toward radical polymerization conditions. This key feature has been used in formulating segmented linear polymers[193] and network polymers[194] via the sequential radical thiol−ene and thiol−isocyanate click chemistries and more recently in two-stage holographic photopolymers[195] and surface modification of functional polymeric surfaces.[196] In one recent example reported by Shin et al., fine-tuning of the poly thiourethane network was achieved when thiol−isocyanate click polymerization was initiated by using photolytically generated tributylamine.[51] The photolytically generated tertiary amine was able to initiate the thiol−isocyanate click reaction, reaching nearly quantitative conversion in minutes to form highly elastic polymers with varying cross-linking densities. Furthermore, these materials showed excellent energy damping performance due to a narrow glass transition coupled with the extensive hydrogen bonding interactions.

To summarize, the photoinduced thiol−isocyanate click reaction is an emerging, highly efficient click reaction that has large potential in both synthetic chemistry and biology fields due to its fast reaction kinetics, excellent conversion, and orthogonality toward radical reactions. Moreover, their ability to achieve higher refractive index than comparable polyurethane analogues makes them most suitable for optical materials development. However, the competing reactivity of isocyanates in protic media and low shelf life stability might be the few shortcomings of this click strategy.

2.4.3. Photolatent Base/Nucleophile Catalyzed Thiol-Michael Addition. Although many photolatent base/nucleophile catalysts described in the literature are effective in thiol−epoxide and thiol−isocyanate reactions, they have limited potential in thiol-Michael addition click reactions. The reason for this lack of preference is presumably due to the undesired formation of radical intermediates during the photoinduced dissociation that trigger competitive radical reactions or homopolymerization of activated alkenes such as the common acrylate Michael acceptors.

The Michael addition click reaction involves the facile and selective addition of a nucleophile to an α,β-unsaturated carbonyl, resulting in a Michael adduct with a wide variety of C−X bonds such as C−C, C−N, C−S, and C−O.[197,198] Among these, the Michael addition of a thiolate anion to the α,β-unsaturated carbonyl is considered one of the most

https://doi.org/10.1021/acs.chemrev.0c01212
Chem. Rev. 2021, 121, 6915−6990

explored and widely implemented click reaction, particularly in network polymerization, polymer functionalization, and bioconjugation.[166,168,199] Unlike the radical mediated thiol−ene reaction, the thiol-Michael addition requires an activated carbon−carbon double bond typically employing an electron withdrawing group in conjugation with the double bond. The ability to perform this robust reaction with high efficiency under simple, highly regiospecific, high yielding conditions qualifies the criteria for nearly ideal click reaction. The thiol-Michael addition click reaction occurs typically through one of two distinct pathways: traditional base catalyzed or nucleophile catalyzed. In the base catalyzed reaction protocol, a base such as Et_3N is typically used to deprotonate the thiol generating a thiolate anion. The strongly nucleophilic thiolate anion then reacts with the electron deficient carbon−carbon double bond, producing a carbanion intermediate followed by subsequent deprotonation of the next thiol or the conjugate acid of the base leading to propagation,[199] whereas in the nucleophilic mechanism, the nucleophile first attacks the electron deficient carbon−carbon double bond, generating a carbanion which then deprotonates the thiol, instigating the reaction cycle (Figure 53).

The efficiency of the reaction depends on the nature of the thiols, electron deficient bonds, and chemical environment such as solvent polarity and strength and concentration of the base or the nucleophile catalyst.[200,201] The reactivity of the thiols may vary based on their pK_a and the chemical environment. Similarly, the structure of the ene also plays an important role in the kinetic properties of the click reaction. It has been found that the more electron deficient C−C double bonds are more susceptible to Michael addition click reactions (Figure 54).[168,202] Apart from these prominent electron deficient vinyl functionalities, aklynones[203] have also emerged as efficient and promising Michael acceptors for multiple thiol-Michael addition click reactions. Quite recently, Van Herck et al. explored the utility of this chemistry as a versatile cross-linker for the thiol−yne Michael addition based covalent adaptable polymer network.[204] The kinetic model studies using a small thiol-Michael−yne system revealed that the exchange rates are significantly varied depending on the steric and electronic nature of the alkynone cross-linker. Moreover, this thiol-Michael−yne system has a large potential for photo-induced thiol−yne dynamic systems in the near future.

A general kinetic mechanism supported with mathematical modeling for nonradical 2-(2-nitrophenyl)propyloxycarbon tetramethyl guanidine (NPPOC-TMG, Figure 55) mediated

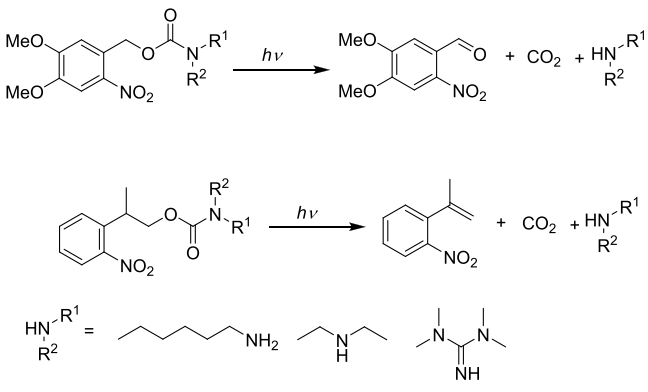

Figure 55. Photolytic pathway of NVOC−amine and NPPOC−amine compounds.[206]

thiol-Michael click reaction, GDMP, and ethyl vinyl sulfone model monomers showed an increase in the reaction kinetics upon increasing the light intensity and/or initial photobase concentration.[205] The reaction kinetics were also found to be more sensitive to the intensity changes at low light intensity when compared to the changes in light intensity at high intensities. Furthermore, minor variations in the initial photobase concentration have a significant impact on the reaction kinetics. These modeling studies indicate that the overall polymerization kinetics follow a pseudo-first-order reaction rate equation in base and coreactant concentrations, determined by k_p/k_{CT}, which in turn depends on the rate limiting step. One of the key features of such photobase catalyzed step-growth thiol-Michael addition click reactions is its unique living nature enabling an extended dark-cure reaction, resulting from the lack of radical mediated termination.

Although there exists earlier reports on photolatent base-induced thiol−epoxide click chemistry, the first photolatent base catalyst mediatedthiol-Michael click chemistry was introduced by Xi et al. in 2013.[52] In their work, 2-(2-nitrophenyl)propyloxycarbonyl (NPPOC) caged photolabile primary amine (hexylamine) was used as the nucleophilic catalyst. Upon irradiation with 320−390 nm UV light, the photocleavage of the NPPOC group released hexylamine via an *aci*-nitro intermediate mediated pathway. The released hexylamine initiated the thiol-Michael addition click reaction of thiol glycolate and methyl acrylate model monomers efficiently, with up to 90% conversion in 30 min. Real-time FTIR revealed that the photoinduced catalysis proceeds in two stages with a delayed upturn nearly at 6 min, which is presumably attributed to the slow formation of hexylamine and anionic intermediates at the initial stages. Furthermore, this photoinduced strategy was utilized in the formation of network polymers by using multifunctional thiols and acrylates. A year later, the same authors expanded the photocaged amines catalysts with more efficient photolabile species.[206] For this purpose a series of NVOC and NPPOC photocaged amines (Figure 55) was synthesized using hexylamine, diethylamine, and TMG as bases. Among those, amines caged with NPPOC exhibited higher quantum yields than that of NVOC caged ones, presumably due to the quenching of released amines with the redox byproduct *o*-nitrobenzaldehyde of NVOC upon irradiation.

The thiol-Michael addition of the model compounds *n*-butylthiolglycolate and ethyl acrylate using photolabile TMG exhibited over 90% conversion within several minutes, exceeding that observed with photoinitiation with latent primary and secondary amines. This behavior was consistent with the higher pK_a of TMG. Additionally, the spatial and temporal control of these catalysts was demonstrated in photopatterning and kinetically controlled two-stage polymer network formation. It should be noted that resolution in photopatterning was achieved by precluding diffusion of catalyst in rapidly cured, glassy networks. Photopatterning would presumably be less effective in rubbery and low cross-link-density materials.

Further to these investigations, Chatani et al. reported visible light initiated thiol-Michael addition polymerization using a ITX/tetraphenylborate system in combination with catalytic amounts TEMPO (Figure 56).[53] In this approach, ITX that possess longer wavelength absorption (>400 nm) was used as a photosensitizer to push the performance of PGBs to longer

https://doi.org/10.1021/acs.chemrev.0c01212
Chem. Rev. 2021, 121, 6915−6990

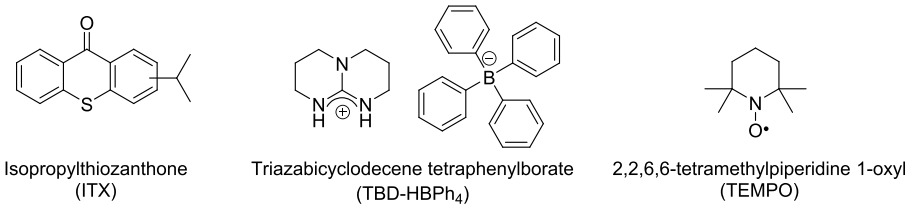

Figure 56. Photosensitization system for photobase-catalyzed thiol-Michael additions with photosensitizer (ITX) photolatent base (TBD-$HBPH_4$) and radical scavenger (TEMPO) to mitigate homopolymerization of acrylate Michael acceptor.[53]

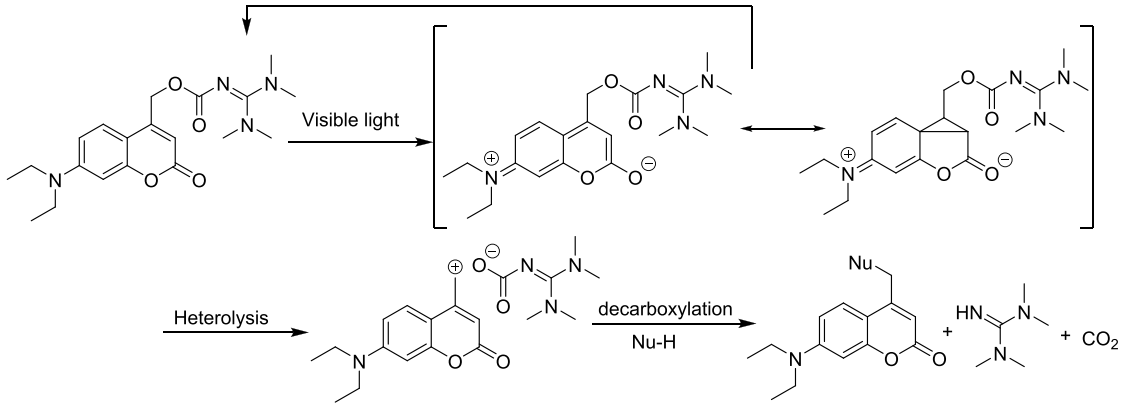

Figure 57. Proposed photolysis mechanism of coumarin−TMG upon visible light irradiation.[207]

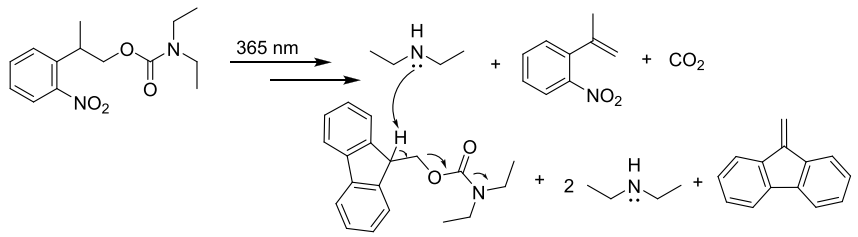

Figure 58. Mechanism of phototriggered base proliferation system for initiating the thiol-Michael addition reaction.[208]

wavelengths via the triplet energy transfer from ITX to PGBs. Such an energy transfer process and the degradation products of tetraphenylborate often involve the generation of radical intermediates, causing the unwanted radical mediated acrylate−acrylate chain growth homopolymerizations to occur.[182,194] The incorporation of catalytic amount of the radical inhibitor, TEMPO, in combination with the photoinitiating system resulted in significantly reduced radical reactions.

Coupling strong bases such as TMG with visible light responsive protecting groups such as coumarin derivatives serves as a highly efficient photobase generator for thiol-Michael and other thiolate anion mediated click reactions. In 2016, Zhang et al. explored the visible light induced photolysis of a coumarin−TMG photobase and successfully demonstrate its catalytic activity in thiol-Michael addition click reactions in small molecules as well as in polymer settings (Figure 57).[207]

This photobase generator with a quantum yield of 0.044 was able to catalyze the Michael addition of various monothiols and DVS to nearly quantitative conversions upon irradiating with 400−500 nm light in a very short period of time (as little as 5 min). Moreover, the thiol-Michael photopolymerization of PETMP and DVS showed faster reaction rates by using a coumarin−TMG photobase compared to that of coumarin−hexylamine analogue which is attributed to the difference in the basicity of the released base.[208]

One major challenge associated with the photobase-induced click reaction is that low quantum yields result in a low concentration of photobase generated via dissociation. One approach that developed to circumvent this shortcoming is the phototriggered base proliferation system.[209] The base proliferation mechanism involves autocatalytic decomposition of a base amplifier, triggered by the catalytic amine generated from a photobase generator, resulting in a dramatic increase in the base concentration. In 2017, Xu et al. reported the use of NPPOC caged hexylamine and Fmoc protected hexyl amine as a photobase and base amplifier, respectively.[210] Upon irradiation with 365 nm UV light, the *n*-hexylamine liberated from NPPOC-hexylamine triggered the base proliferation reaction. Thus, the liberated hexylamine nucleophile diffused further into nonirradiated regions to activate base proliferation and effectively catalyze the thiol-Michael addition reaction of monothiols with acrylic acid to achieve >90% conversion.

Another interesting aspect of the photobase induced thiol-Michael addition click reaction is the possibility for dark curing, i.e., the continuation of the click reaction or curing process even after the light is turned off. Unlike radicals which usually have very short life times due to recombination and disproportionation, the released base/nucleophile remains

https://doi.org/10.1021/acs.chemrev.0c01212
Chem. Rev. 2021, 121, 6915−6990

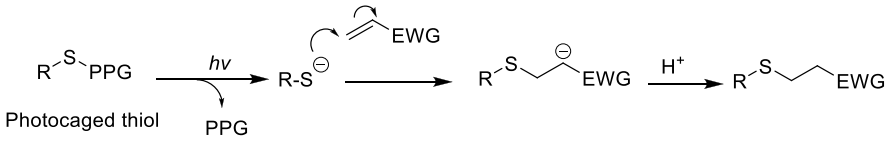

Figure 59. Photouncaging thiol and subsequent thiol-Michael addition click reaction.

active throughout the completion of the reaction and therefore facilitates high conversions, even following termination of light exposure. To this end, Sinha et al. demonstrated an effective, light-activated dark curing possibility of phototriggered base amplification in thiol-Michael click addition (Figure 58).[208] In their work, various combinations of photocaged amine (NPPOC-amine) and base amplifier (Fmoc-amine) were evaluated for the thiol-Michael addition reaction between various thiols and two different Michael acceptors, an acrylate and a vinyl sulfone, and exhibited noticeably higher final conversions for photoinduced thiol-Michael addition reactions. Furthermore, this enhancement in reaction kinetics and conversion was implemented in the preparation of cross-linked network polymers with efficient dark cure rates with limited light exposure.

In summary, photoinduced thiol-Michael click reactions proceed with high efficiency and follow the majority of the criteria recommended for an ideal click reaction, excellent conversions, and fast reaction kinetics. The reactivity of various substrates used in this click reaction can be finely tuned by varying various parameters such as the nature of the thiol, electron beneficent vinyl groups, the light intensity, and pH. However, implementation of the photoinduced thiol-Michael addition is challenging due to undesired photogeneration of radical species along with the intended base catalyst, which often leads to homopolymerization of electron deficient carbon−carbon double bonds such as acrylates and, in biological applications, may adversely affect sensitive biomolecules. The future development of effective and selective photolatent bases and nucleophilic catalysts is therefore an area of continued research.

2.4.4. Click Reactions Based on Photolatent Thiols and Other Nucleophiles. *2.4.4.1. Photolatent Thiol Mediated Michael Addition Click Reactions.* Photomediated thiol-Michael addition can also be facilitated and controlled by employing photoremovable protecting groups or caging groups that have been developed to mask specific click functionalities such as thiols.[211−213] Upon irradiation, with light of suitable wavelength controlled release of highly nucleophilic thiolate anions is achieved, followed by subsequent clicking of the released thiols with their reactive complements (Figure 59). Unlike other photoclick reactions described herein, these reactions frequently release relatively large byproducts from the photodecomposition of the photoprotected thiol. Tetrazole−alkene reactions release only nitrogen, sydnone−alkene reactions release carbon dioxide, and cyclopropenone-based photoSPAAC reactions release carbon monoxide. By contrast, photodeprotection of thiols may release compounds with molecular masses in the hundreds. As the criteria for click chemistry requires the generation of easily removed and inoffensive byproducts, it is justified to question the categorization of such reactions as "photoclick." Their description is included here because nucleophilic Michael additions were among the original click reactions described by Kolb et al,.[2] and in the applications in which these photodeprotection Michael reactions are employed, (e.g., in the context of macromolecular coupling and surface modification), the photocleaved byproducts are frequently small relative to the reactants and either easily removed or tolerated.

The use of photocaged thiols has emerged as an interesting strategy, particularly in the field of biomaterial development and photopatterning. Because of its high nucleophilicity and reactivity toward various click reactions, researchers preferred thiols as photolatent functionality over ubiquitous amine and relatively less reactive alcohols.[212]

The first and the most widely used photoprotecting group for most of the click functionalities including thiols was the *o*-nitrobenzyl derivatives that was developed by Barltrop et al. in the 1960s.[214] These caging groups can be cleaved upon irradiation with UV light at 365 nm and has been proposed as a versatile caging group since the 1970s.[215] The photorelease mechanism of *o*-nitrobenzyl protected groups has been studied by many researchers using time-resolved spectroscopy on the parent *o*-nitro toluene and several other *o*-nitrobenzyl derivatives.[216−219] The primary photoreaction mechanism for the release of *o*-nitrobenzyl protected functional groups proceeds via *aci*-nitro tautomer intermediates in the ground state formed by the hydrogen transfer from the *o*-alkyl substituent to the nitro group. The decay of these *aci*-nitro transient intermediates follows a biexponential rate law due to the formation of both tautomers and vary strongly with substitution, solvent, and pH in aqueous solution.[218] The thus formed *o*-quinonoid intermediate undergoes cyclization to *N*-hydroxybenzisoxazolidine followed by a ring chain tautomerism to release the caged functionality and nitrosobenzaldehyde byproduct (Figure 60).[220,221]

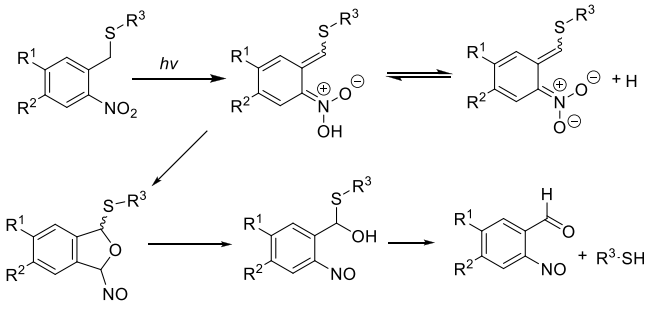

Figure 60. Mechanism of photouncaging of *o*-NB caged thiol.[220,221]

Although there exist several variations in *o*-nitrobenzyl caging groups with varying substituents on the benzene ring as well as on the benzylic methylene, the generic form of this photoprotection group (PPG) with no substitution is usually preferred for thiols in which the leaving thiol is directly attached to the benzylic site. However, for alcohols and amines, the carbonic acid derivatives are preferred as this forms the better leaving group and is easily protected by using commercially available chloroformates. One of the key features of this deprotection-click strategy is that its orthogonality,

https://doi.org/10.1021/acs.chemrev.0c01212
Chem. Rev. 2021, 121, 6915−6990

where the deprotection and the click reaction could be performed in the presence of other catalysts that could be used in the next stage. This versatile deprotection strategy has been used to achieve excellent spatial and temporal in the development advanced biomaterial with tunable material properties.[222,223]

Recently, Pauloehrl et al. explored the feasibility of this highly efficient strategy in ambient temperature polymer end functionalization and backbone modification.[54] The authors attempted the deprotection of ONB capped thiol end functionalized PEG methyl ether in the presence of initiators/catalysts such as α,α-dimethoxy-α-phenylacetophenone (DMPA) for radical thiol−ene and triethylamine (TEA) and dimethylphenylphosphine (DMPP) for thiol-Michael click reaction. Although a complete retardation of thiol-uncaging was observed when the deprotection was carried out in the presence of TEA at 320 nm UV light, a quantitative formation of the desired thiol-end-capped species was achieved in the presence of catalytic amounts of DMPA or DMPP with no noticeable disulfide formation. Moreover, the authors were able to demonstrate a nearly complete backbone modification of an ATRP derived polyacrylate containing thiol-protected pendant groups.

Although *o*-nitrobenzyl derivatives are by far the most commonly used photocaging groups for thiols and other click functionalities, the photolysis of these compounds forms potentially toxic and strongly absorbing byproducts such as *o*-nitrosobenzaldehyde. Another major drawback of this strategy is the formation of nitrosobenzaldehyde derived side products via the condensation of released amines with nitrosobenzaldehyde. The brown-colored byproduct formed via the decomposition of nitrosobenzaldehyde acts as an optical filter by absorbing the incident light. Moreover, these conventional photocaging groups were found to be inefficient in releasing the substrates and lack two-photon sensitivity.[55,224] In this context, the coumarin-derived photocaging groups discovered by Roger Furuta et al. that could be efficiently cleaved by two photon irradiation have become more popular in recent years.[225]

A general uncaging mechanism of coumarin derivatives starts with the relaxation to the lowest excited singlet state (S1) 1[CM-X]*. The decay of the 1[CM-X]* singlet state involved three different processes: fluorescence, nonradiative processes, and a competing heterolytic C−X bond cleavage to form an ion pair intermediate of coumarinylmethyl cation and leaving group conjugate.[226,227] Subsequent separation of the base ion pair by polar solvents followed by the trapping of coumarinylmethyl cation with the polar solvent leads to a new stable coumarylmethyl product and along with uncaged functional groups (Figure 61). Time-resolved absorption studies showed that the heterolytic bond cleavage is the fastest among the most rapid photorelease, with a rate constant reaching 2×10^{10} s^{-1}. However, the recombination of the tight ion pair which leads to the regeneration of the ground-state caged derivative occurs with a reaction rate of 2.3×10^{9} s^{-1} and is 10 times faster than the hydrolysis rate of the separated ion pair by polar solvent molecules.[228] It has been found that the rate of heterolytic bond cleavage and therefore the efficiency of photorelease depends on the stability of the singlet ion pair formed. If both of the components of the singlet ion pair are stabilized, a significant weakening of the C−X bond occurs during the excitation, which in turn depends on the nature of the substituent at the 6,7 position of the coumarin group. Therefore, the substitution of the coumarin ring with electron donating groups to stabilize the cation and the stabilization of released anion by lowering the basicity should enhance the heterolytic cleavage and therefore the uncaging efficiency. In addition, the factors that accelerate the heterolysis also retard the recombination process. For the same reason, the poor leaving groups such as alcohols, phenols, and thiols facilitate heterolysis. In such cases, more efficient release is achieved through the introduction of the carbonate linkages. Heterolysis of these moieties give initially unstable carbonate or thiocarbonates, which undergo decarboxylation to give free alcohol or thiol.

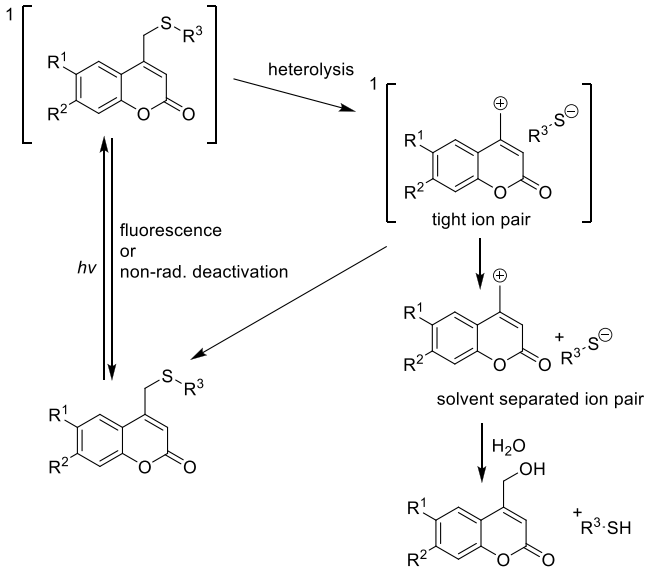

Figure 61. General uncaging mechanism of coumarin derived PPGs.[210,211]

Some of the key features of the coumarin-based photocaging are the large molar absorption coefficients at longer wavelengths and rapid release rates. To improve its absorption maximum, stability, and water solubility, researchers made several modifications at C6 and C7 substituents on the coumaryl group. Among these, the 6-bromo, 7-hydroxy coumarin was found to be the most efficient for photocaging thiols suitable for thiol-Michael type click reaction.

In an interesting inversion of the photoclick paradigm, the nucleophilic thiol-Michael addition may be used to allow subsequent photochemistry to take place. The high regioselectivity of thiol−maleimide click reaction coupled with the fluorescence quenching ability of maleimide has been used to control the photocleavage of the coumarin phototrigger.[229] The phototrigger design involves a photoinduced electron transfer quencher (maleimide) coupled to 7-amino coumarin dye (Figure 62). In the absence of any thiols, the PET takes place from coumarin to the conjugated maleimide moiety deactivating the S1 excited state preventing photocleavage.[230,231] The Michael addition of a thiol to an electron deficient maleimide restores the fluorescence and photocleavage pathways, unlocking the phototrigger to release the previously occluded functional moiety. The photorelease of the thus released biotin was monitored by HPLC and UV−vis absorption and fluorescence emission. The authors also examined the target activation using various biologically relevant compounds including amino acids as routine.

https://doi.org/10.1021/acs.chemrev.0c01212
Chem. Rev. 2021, 121, 6915−6990

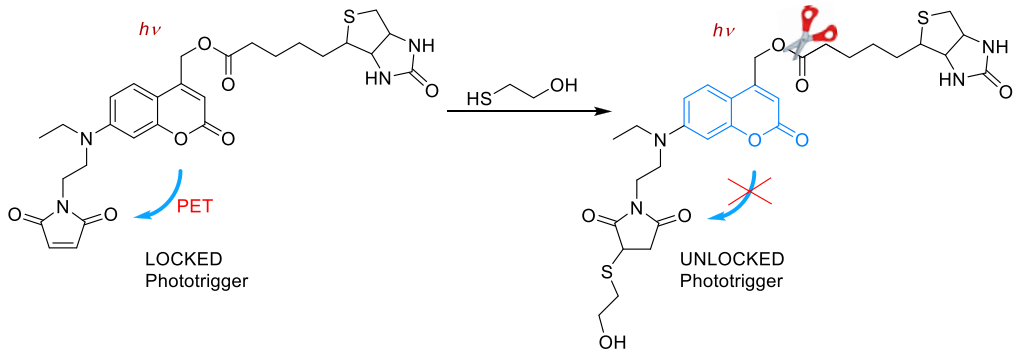

Figure 62. Activation of a locked phototrigger via the reaction with thiol to form an unlocked phototrigger. The reaction of the maleimide substituent with β-mercaptoethanol prevents PET quenching of the phototrigger, allowing subsequent photochemistry to occur. Adapted with permission from ref 229. Copyright 2012 American Chemical Society.

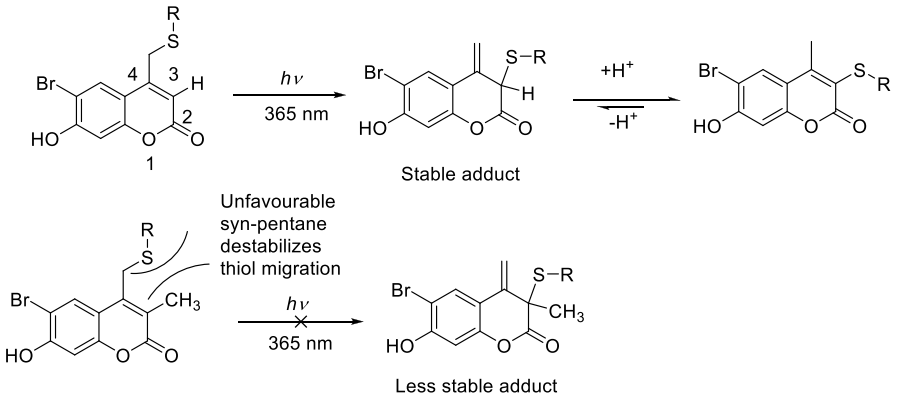

Figure 63. Illustration of potential effects of C-3 substitution on photoisomerization process.[55] A methyl group installed in the C-3 position improves photolysis by preventing the migration of the thioether.

Although the coumarin-based thiol protecting groups such as 7-amino coumarin and 6-bromo-7-hydroxycoumarin are potentially useful and easy to synthesize, their uncaging efficiency is often hampered by the undesired photoisomerization. To address this issue, Distefano et al. developed 6-bromo-7-hydroxy-3-methylcoumarin-4-ylmethyl as an alternative coumarin-based caging group for thiols, in which one of the hydrogens at the C-3 position was replaced by a methyl group. On the basis of the photoisomarization mechanism, the presence of alkyl substituent at the 3-position would prevent the photoisomer formation by blocking the rearomatization of intermediate **1** and the migration of sulfur to the C-3 position due to the *syn*-pentane type interaction between the sulfur and the C-3 methyl group (Figure 63). The one- and two-photon photo uncaging efficiency demonstrated by using mBhc-caged thiol containing peptide showed a clean and efficient photocleavage upon irradiation without any detectable formation of the photoisomer.[55]

Nitrodibenzofuran (NDBF) is another thiol photocaging molecule that does not undergo photoisomerization and is capable of uncaging thiol-containing peptides efficiently with one- and two-photon irradiation (Figure 64).[232] Recently, Fisher et al. compared photuncaging efficiency of NDBF, Bhc, and mBhc and demonstrated the superior efficiency of NDBF biomolecule photopatterning.[233]

Bimane is another interesting compact photocaging group with qualities that are advantageous for biology related studies such as good water solubility, high stability in biological media, and low toxicity to cells. Photocaging of the thiol group is

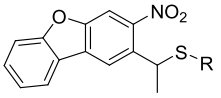

Figure 64. Nitrodibenzofuran has been shown to be an effective photocaging group for thiols.[233]

achieved by efficient reaction of bromobimane in the presence of a base. The high reactivity of bromobimane toward free thiols has been used for fluorescent tagging of proteins.[234−236] Recently Truong et al. utilized this thioether bimane photouncaging strategy for the cross-linking polymerization of multiarm-PEG functionalized with various Michael acceptors such as acrylates, maleimide, and propargyl esters.[237] Upon irradiation with visible light at 420 nm, efficient release of anionic thiols was achieved which spontaneously react with various Michael acceptors efficiently in biological media without the requirement of an additional catalyst (Figure 65). Cross-linking of the photouncaged multiarm thiol occurred even at a pH of 6.9 indicative of the anionic form of the released thiol.

The temporal control of the bimane thioether photodeprotection strategy was further demonstrated by stopping and resuming photouncaging and trapping process by turning the light on and off. Spatial control over the conjugation process was demonstrated by photopatterning the biotin−maleimide and was confirmed by the specific reaction of biotin with TRITC−streptavidin.

Photoinduced thiol−isocyanate click reactions have also been achieved via use of photocaged thiol. Hensarling et al.

https://doi.org/10.1021/acs.chemrev.0c01212
Chem. Rev. 2021, 121, 6915−6990

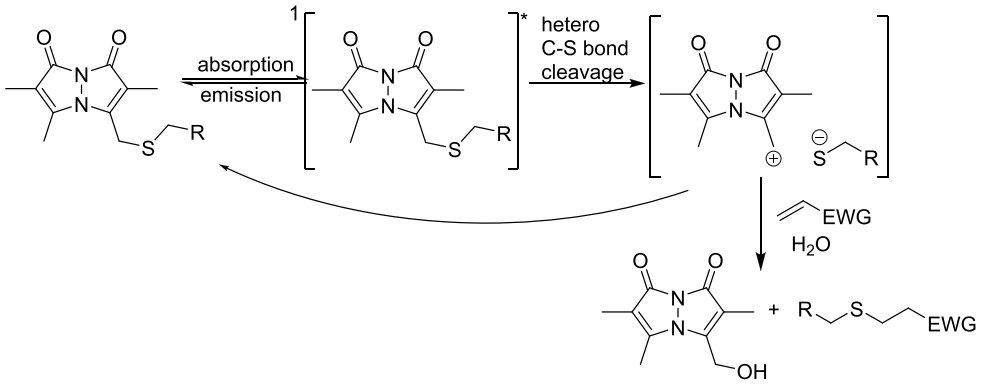

Figure 65. Mechanism for the photouncaging of thiol−bimane in the presence of an electrophile.[237]

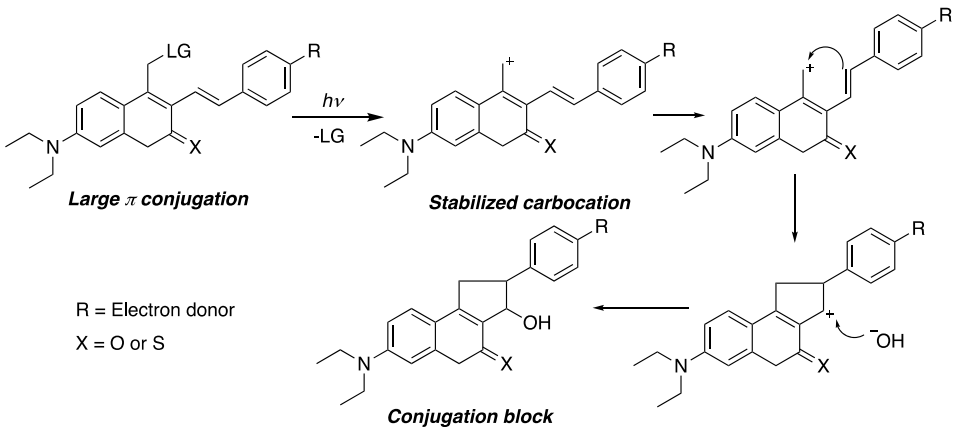

Figure 66. Proposed photolysis mechanism for the electron donor-styryl-conjugated coumarin-based PPGs as reported in ref 239.

employed photocaged thiol strategy to enable postpolymerization modification of pendant thiol polymer brushed using thiol−isocyanate click chemistry.[238] Upon irradiation with UV light the photodeprotection of caged thiols released thiolate anions for subsequent reaction with small molecule isocyanates for surface modification of RAFT derived polymer brushes.

Modification of coumarin photocaging groups with an electron-rich styryl moiety at the 3-postion enabled further enhancement in long wavelength abortion, two photon absorption, and quantum yields, resulting in rapid photocleavage.[239] This enhancement was attributed to the large π-conjugated structure offered by the styryl moiety and stabilization of the carbocation intermediate by electron donors *para* to the styryl group. A comparative study of these styryl modified PPGs displayed an uncaging quantum yield of 0.19−0.7, which is approximately 3−10 times higher than that of the parent diethyl aminocoumarin (0.07). After the photolysis, the carbocation intermediate undergoes intramolecular cyclization rearrangement, forming a five-membered ring (Figure 66). As a result, the conjugation at 3-position is blocked, allowing the byproducts to photobleach after the photolysis. These modified PPGs are therefore well-suited for high concentration samples and thick specimens. The role of electron donating and electron withdrawing substituents on the styryl groups were supported by density functional theory (DFT) calculations, showing that the electron-rich effect significantly stabilizes the carbocation intermediate and enables the styryl conjugated coumarin to undergo intramolecular cyclization rearrangement to enable faster photolysis. In addition, a further enhancement in the photolysis rate was observed for the thione-modified PPGs due to the enhanced intramolecular charge-transfer through the 3d empty atomic orbitals of the sulfur atom.

While discussed previously in connection with the photoclick IEDDA reactions, the photoreversible Michael addition between *o*-naphthoquinone methide and thiols bears mentioning here as well.[106] In contrast to the previously described photomediated thiol-Michael additions, it is the Michael acceptor that bears the chromophore and is generated by absorption of photons rather than the thiol.

2.4.4.2. Other Photolatent Nucleophiles Mediated Click Reactions. Photouncaging strategies have also been used extensively with other functionalities such as aldehydes and amines for subsequent photomediated coupling reactions. One such reaction is the oxime ligation that involves the reaction between an alkoxyamine ($-ONH_2$) and an aldehyde ($-CHO$) or ketone to form oxime linkages.[240,241] The rare occurrence of these two complementary click functional groups in living organisms provides excellent bioorthogonality under physiological conditions. Moreover, the kinetics of oxime ligation are easily controlled by the pH and catalyst concentrations.[240] Two main photouncaging approaches have been employed to afford spatiotemporal control over such ligation involving the photoinduced liberation of one of the complementary reactive species. In the first approach, in situ photogenerated *o*-nitrobenzaldehyde from *o*-nitrobenzyl alcohol was reacted with free hydrazines or amines.[242,243] For example, in 2016, Azagarsamy et al. reported the utilization of phototriggered hydrazone chemistry for the formation of cytocompatibile

https://doi.org/10.1021/acs.chemrev.0c01212
Chem. Rev. 2021, 121, 6915−6990

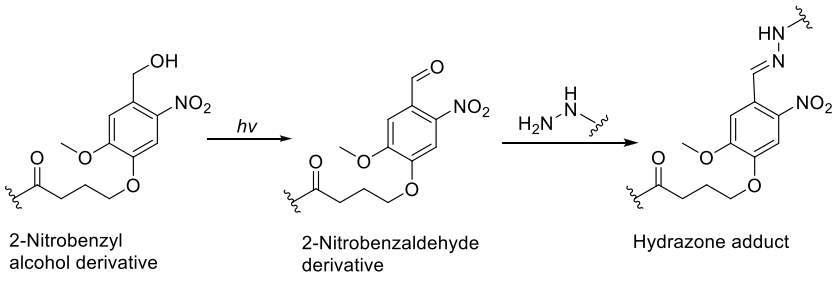

Figure 67. Schematic representation of photoinduced hydrazone reaction.[242]

hydrogels using mutliarm-PEG postfunctionalized with hydrazine and *o*-nitrobenzyl alcohol functionalities. (Figure 67).[242]

Although hydrazone/imine-based click reactions are efficient under physiological conditions, the reversible nature of these chemistries leads to hydrolytic cleavage in just a few days under physiological pH.[244,245] This hydrolytic cleavage is eliminated using an alternative approach. With oxime ligation, the photodeprotected aldehyde reacts with an alkoxy amine, forming an irreversible oxime functionality. In 2012, Pauloehrl et al. implemented this strategy by employing the photouncaging of an *o*-nitrobenzyl acetal under mild irradiation conditions using 370 nm light to achieve rapid, quantitative photouncaging of *o*-nitrobenxzaldehyde patterned on silicon wafers followed by the oxime ligation reaction with amino oxy functionalized biomolecules with excellent spatiotemporal control (Figure 68).[56,57]

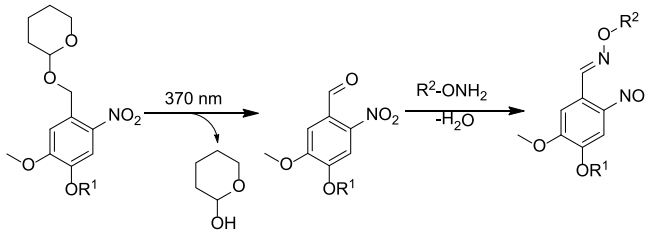

Figure 68. Photoinduced cleavage of a 2-[(4,5-dimethoxy-2-nitrobenzyl)oxy]tetrahydro-2*H*-pyranyl derivative and subsequent oxime ligation with hydroxylamine derivatives. R = C_3H_6COOH.[56]

In a second approach, the photocaging of alkoximes with NPPOC was utilized. The alkoxyamines generated in situ upon photoirradiation directly participate in oxime bond formation with the aldehydes.

2.4.5. Photoinduced Native Chemical Ligation. Native chemical ligation (NCL) introduced by Kent and co-workers in 1994 is one of the more powerful and widely used methodologies for protein chemical synthesis.[246] This reaction involves an initial chemoselective transthioesterification between N-terminal cysteinyl and C-terminal thioester fragments, followed by a rapid intramolecular S to N acyl transfer, to generate a native peptide bond under mild conditions. The ability of NCL to proceed under mild conditions with a wide range of substrates and high chemoselectivity makes it an attractive ligation strategy for highly specific conjugation of biomolecules. The very same features qualify NCL as a click reaction. Beyond the chemical synthesis of peptides and proteins, NCL has also been recognized as a straightforward pathway to bioconjugation and labeling. A review detailing the mechanism, scope, limitations on NCL, and extended methods is available.[247] In 2005, Ueda et al. reported purification free, one-pot sequential native chemical ligation using 4-(dimethylamino)phenacyl-type photolabile amine and thiol protecting groups,[248] where the photocaged amines exhibited adequate stability toward acidic and basic reagents commonly used in protein ligation chemistry. Along with the NCL chemistry, the phototriggered amine release enabled efficient, one-pot sequential NCL reactions under mild conditions without the requirements for purification of the intermediates or change in the ligation conditions. In another example, Aihara et al. used the photocaged *N*-sulfanylethylanilide peptide to synthesize a 41-residue SNX-482 by a one-pot, sequential four-fragment ligation in an N to C direction as

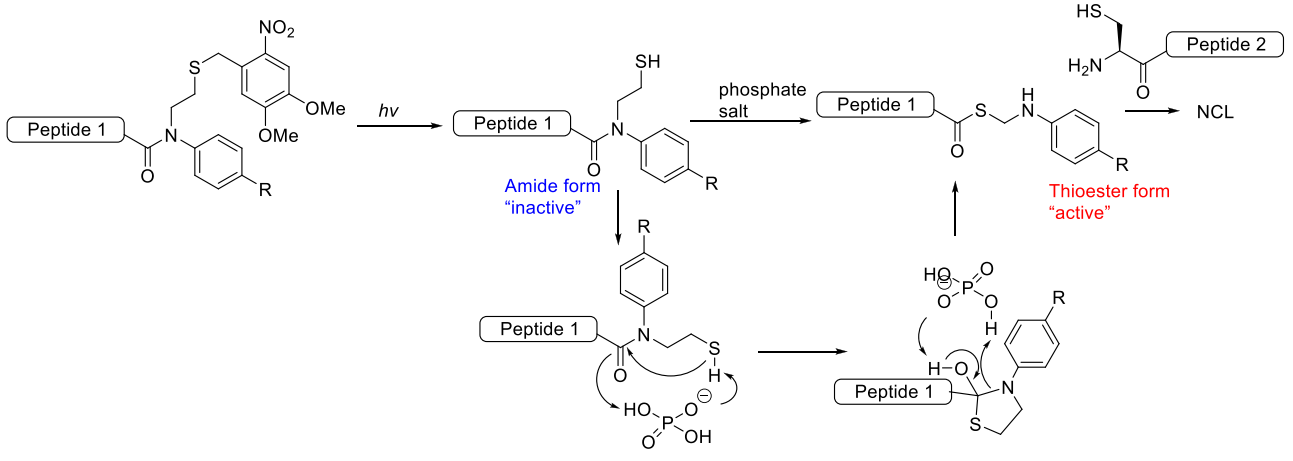

Figure 69. Mechanism and strategy of peptide/protein synthesis using photocaged *N*-sulfanylethylanilide peptide. Adapted with permission from ref 249. Copyright 2016 American Chemical Society.

https://doi.org/10.1021/acs.chemrev.0c01212
Chem. Rev. 2021, 121, 6915−6990

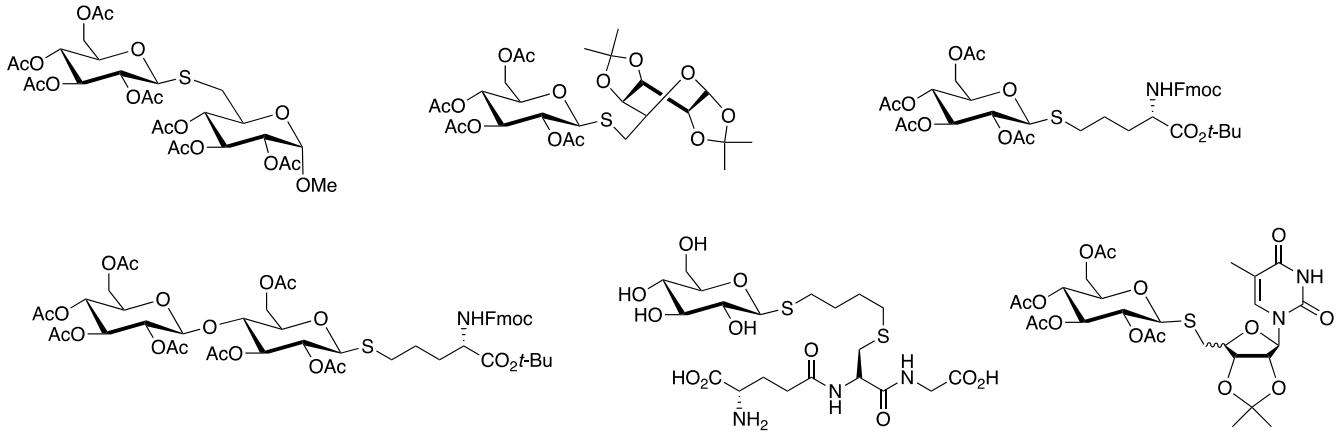

Figure 70. Products generated via thiol−ene coupling of various thiols with unsaturated glycosides.[257]

illustrated in Figure 69. Upon thiol photo uncaging, the inactive amide form undergoes intramolecular rearrangement to an active thioester form in the presence of phosphate salt and subsequent NCL.

To summarize, photouncaging click functionalities is an established concept with continuing improvements moving toward increased efficiencies and implementation as a promising tool for various biological, materials, and synthesis applications. This approach is well suited for temporarily inactivating click functionalities, particularly in the presence of biologically active molecules. Upon light irradiation, stoichiometric uncaging of the functional group facilitates the subsequent click reaction with excellent spatial and temporal control.

3. APPLICATIONS

As click reactions generally have been employed broadly across a wide variety of synthetic applications photoclick reactions specifically have similarly proven advantageous in addressing challenges in diverse fields of (bio)chemical research and development, albeit with distinct advantages and challenges relative to nonphotomediated chemistries. Despite many similar and overlapping benefits that span across nearly all of the reactions discussed herein, photoclick reactions are far from interchangeable; each has its own strengths and weaknesses that determine the applications for which they are best suited. Reactants bearing highly conjugated chromophores may permit the reactions to take place at higher wavelengths of light, but the increase in molecular weight may be deleterious to the intended function of the resulting product. Reactants that are activated by direct photon absorption may benefit from no requirement for photolatent catalyst or photoinitiator, but the requisite, relatively high concentration of the chromophore may hinder scalability of the reaction due to depleted transmittance of light through optically thick samples. Photoamplified reactions, on the other hand, may be conducted on much larger scales but may lack an ability for true spatiotemporal control, depending on the photocatalytic mechanism.

Self-reporting systems, reactions which produce fluorescent products, have recently been shown to be a beneficial feature of some photoclick reactions with obvious advantages in a variety of applications (e.g., fluorescent probes, labeling, and conversion indicators). These reactions represent a significant fraction of present photoclick reactions in many emerging fields and are particularly well represented in biological applications where live cell imaging has become an important focus and biorthorthogonal, spatial, and temporal reactions are key. Self-reporting systems have been highlighted in the relevant application section.

Despite the simplified, popular conception of "click" chemistry as reactions that should work virtually all the time and under any conditions, these practical considerations dictate where and how photoclick reactions can benefit the user. This section of the review surveys the applications of photoclick reactions organized according to the context of the molecular architecture in which these disparate reactions are employed: small molecule synthesis, soluble macromolecule synthesis and modification, functionalization of materials' surfaces, or the development of network polymers.

3.1. Drug Development and Small Biomimetic Molecules

Applications of photoclick reactions are more abundant in those areas of research that frequently require precise management over where and when a desired reaction should occur, i.e., where the most immediate and apparent advantage of photomediated chemistry would have the greatest impact. Typically, these features are not considered of particular importance in the synthesis of small molecules, a situation wherein there is minimal need to spatially limit the reaction within the predetermined confines of the reaction vessel. Additionally, because of the large substituents used to shift absorbance of functional groups, "small" molecule synthesis via many photoclick reactions is often impractical if not impossible. Yet, there are several significant examples of photoclick reactions being employed in drug development and the synthesis of small, biomimetic molecules although the advantages that necessitate such approaches vary. Photoclick reactions are often simply faster and more efficient than alternative synthetic strategies. Temporal control may allow dictation of the order of multiple consecutive reactions and can be used effectively to limit reaction rates for click reactions that may otherwise proceed too rapidly. Ultimately, photoclick reactions are used in small molecule synthesis because they have been proven effective in that arena.

Among photoclick reactions, the thiol−ene and thiol−yne reactions employ perhaps the simplest of reactive groups, resulting in very few superfluous atoms in the resulting linkage. This, along with the insensitivity to water and oxygen, makes these reactions particularly useful in the modification and

https://doi.org/10.1021/acs.chemrev.0c01212
Chem. Rev. 2021, 121, 6915−6990

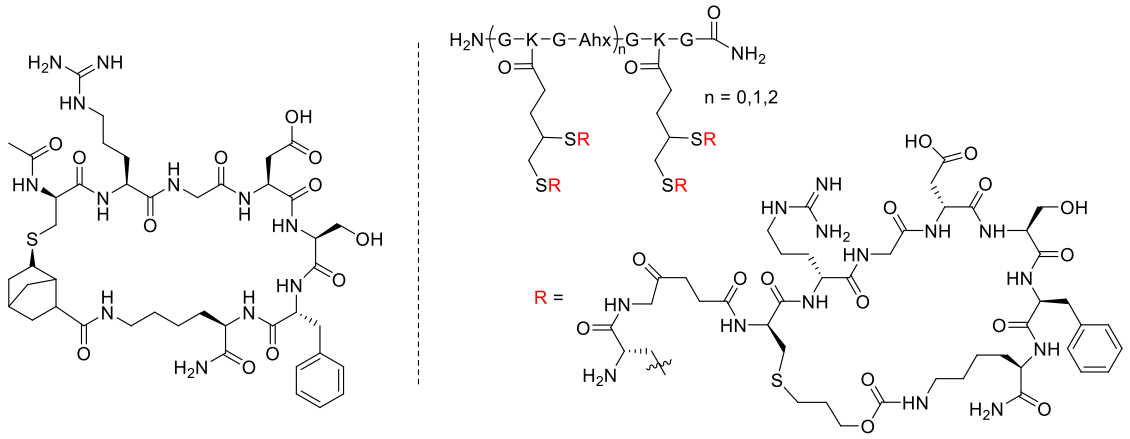

Figure 71. Cyclic peptides formed via intramolecular thiol−ene (left) and thiol−yne (right) reactions.[266]

mimicry of oligomeric biomolecules and their synthetic analogues.

These reactions have been used as a tool for site specific glycosylation for cysteine containing peptides.[250] Dondoni and Marra produced an excellent review on glycoconjugation via thiol−ene chemistry.[250] In brief, the reaction has been used to modify carbohydrates, for amino acid synthesis,[251] assembly of glyoclusters, and peptide and protein glycosylation.[252] In particularly, this reaction has been explored in the construction of carbohydrate mimics such as *S*-glycoside, an unnatural carbohydrate, from readily available peracetylated glucosyl thiol and the diacetonide-protected galactose-derived alkene, yielding abundant and highly diastereoselective 1,6-linked *S*-disaccharides.[253,254] Not limited to carbohydrates, a broad range of 2,3-unsaturated sugars including *O*-, *C*-, *S*-, and *N*-glycosides have been successfully generated. However, different anomeric heteroatoms profoundly affected the reactivity of the 2,3-unsaturated sugars. Hydrothiolation of 2,3-dideoxy *O*-glycosyl enosides efficiently produced the axially C2−S-substituted addition products with high regioselectivity but 2,3-unsaturated *N*-glycosides resulted in a varying regioselectivity and stereoselectivity. No addition was observed onto the endocyclic double bond of *C*-glycosides and addition to 2,3-unsaturated *S*-glycosides resulted in 3-S-substituted glycals (Figure 70).[251,255,256] Researchers have envisioned the application of thiol−ene chemistry to successfully synthesize nucleoside enofuranoside derivatives to produce an array of thio-substituted D-ribo, -arabino, -xylo and L-lyxo-configured pyrimidine nucleosides, which are prime synthetic targets for anticancer and antiviral drug development.[257]

Thiol−ene conjugations provide a versatile strategy to synthesize various models of complex biological systems like cyclic peptides, which have been shown to exhibit improved bioactivity and stability to proteolytic degradation relative to their linear counterparts. Aimetti et al. exploited the use allyl ester-containing building block, Fmoc-Lys(Alloc)-OH, to synthesize peptides with pendant, thiol-reactive alkenes, and pendant thiols resulting from incorporated cysteine residues. Subsequent photoinitiation resulted in the intramolecular thiol−ene conjugation and formation of cyclic peptides. This strategy clearly demonstrated that cyclic peptides could be generated using commercially available amino acids without significant postsynthetic modification, leading to a straightforward synthetic pathway for an important class of biomolecules.[258]

While cyclic peptides may exhibit profound differences in bioactivity relative to their linear analogues, secondary structure within those cyclic peptides also exerts substantial influence over the function thereof. To elucidate the influence of this secondary structure on cyclic peptides, achiral centers in the tether of a stapled peptide were introduced. By utilizing thiol−ene chemistry, optimally tethered cyclic peptides and nontethered linear peptides were synthesized successfully, starting from cyclo-Ac-CAAAS$_5$(2-Me)-NH$_2$ (S$_5$((S)-pentenylglycine), 2-Me (the methyl group located at the b-position with respect to the a-carbon of the amino acid). While the cyclic peptide was found to be a random coil, the linear peptide was found to be in helical form, due to a substituent at the tethered chiral center, suggesting that the substitution group also interacts directly with the binding groove.[259] This simple strategy enabled access to thioether-based constrained peptides, peptide stapling, precisely positioned chiral centers on thioether-based tethers, and thioether-constrained pentapeptides.[260−262] These facile, one-pot reactions recently led to the synthesis of truncated *S*-lipidated teixobactin analogues from commercially sources.[263,264] In one particularly interesting application of the thiol−ene reaction for peptide stapling, Hoppmann et al. employed photoisomerization of a vinyl azobenzene amino acid to facilitate a photocontrollable bridge with the pendant thiol of a cysteine residue.[265]

The thiol−yne reaction has not been employed to the same extent as has the thiol−ene. While this may, in part, be due to the more limited application of the diaddition of thiols to alkynes, this feature of the thiol−yne reaction is advantageous in the synthesis of clustered cyclic peptides. For example, various cyclic and multivalent alkene and alkyne derivatives of Arg-Gly-Asp (RGD) were reacted via the radically photoinitiated thiol−yne chemistry, forming clustered peptides which inhibited the binding of fibrinogen to GPIIb/IIIa relative to linear RGD (Figure 71).[266]

While the thiol−ene and thiol−yne reactions have been successfully employed in the synthesis of small molecules in large part because of the relatively atomically dense reactive functional group structures, few other photoclick reactions exhibit similarly small reactive moieties and so their applications for synthesis on this molecular scale more considerably limited. Another such example is the photo-CuAAC and PcAAC reactions. As described previously, Wu et al. implemented a copperless, visible light, photoredox-mediated azide−alkyne cycloaddition for the synthesis of 1,4-

https://doi.org/10.1021/acs.chemrev.0c01212
Chem. Rev. 2021, 121, 6915−6990

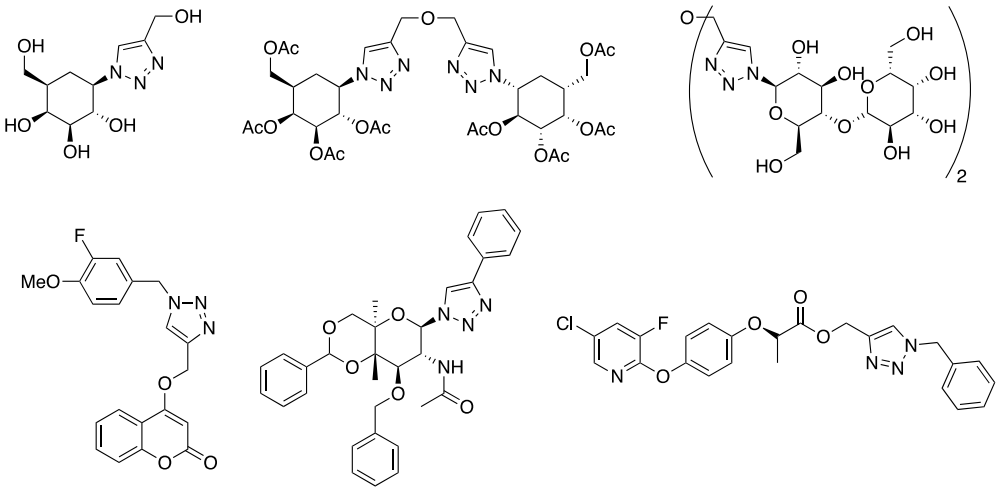

Figure 72. Examples of bioactive molecules and potential drug candidates generated via the photoCuAAC reaction (top) and via the PcAAC reaction (bottom).[268]

disubstituted 1,2,3-triazole derivatives, including bioactive molecules with high regioselectivity and good yield.[267] In another example of implementation of the azide−alkyne cycloaddition employed for the potential synthesis of small therapeutic molecules, Beniazza et al.employed photoCuAAC to drive the alkyne−azide reaction with a variety of protected and nonprotected azide and alkyne-functionalized monosaccharides generating di- and tetrasaccharides in high yield within 10 min of UV irradiation and ∼100 min under daylight illumination (Figure 72).[268]

In limited contexts, spatial and temporal control are advantageous in small molecule synthesis (e.g., the in situ synthesis of self-assembling amphiphilic compounds). Konetski et al. successfully employed photoinitiated CuAAC to produce self-assembled phospholipid vesicles under exposure to visible light. Higher vesicle density via the photomediated reaction was observed relative to that obtained via catalysis with sodium ascorbate and copper sulfate. Additionally, the rate of reaction, tunable via the intensity of light exposure, had a profound impact on the morphology of the self-assembled vesicle structures as shown in Figure 73.[269]

3.2. Oligomerization and Polymerization Reactions

There are two general mechanisms for polymerization: chain addition, wherein monomers add to the active center of a growing chain, and step-growth, wherein complementary functional groups on multifunctional monomers react with each other to form ever larger molecules. While the rapidly increasing molecular weight development in the former may allow for tolerance of some impurities, inefficiencies, or other nonidealities during the polymerization, step-growth polymerizations require highly effective and selective reactions to obtain high molecular weight species. For this reason, click reactions are well suited for step-growth polymerizations.

Several examples of photoclick reactions employed for linear polymerizations have been reported. In one example, Porel and Alabi employed sequential photoinitiated thiol−ene and nucleophile-initiated thiol-Michael reactions to build, unit by unit, a sequence controlled oligomer taking advantage of the semiorthogonality of the two reactions.[270] Difunctional thiols were reacted with heterobifunctional allyl acrylamides (the allyl being radically reactive with thiols and the acrylamide providing the Michael acceptor), bearing various pendant

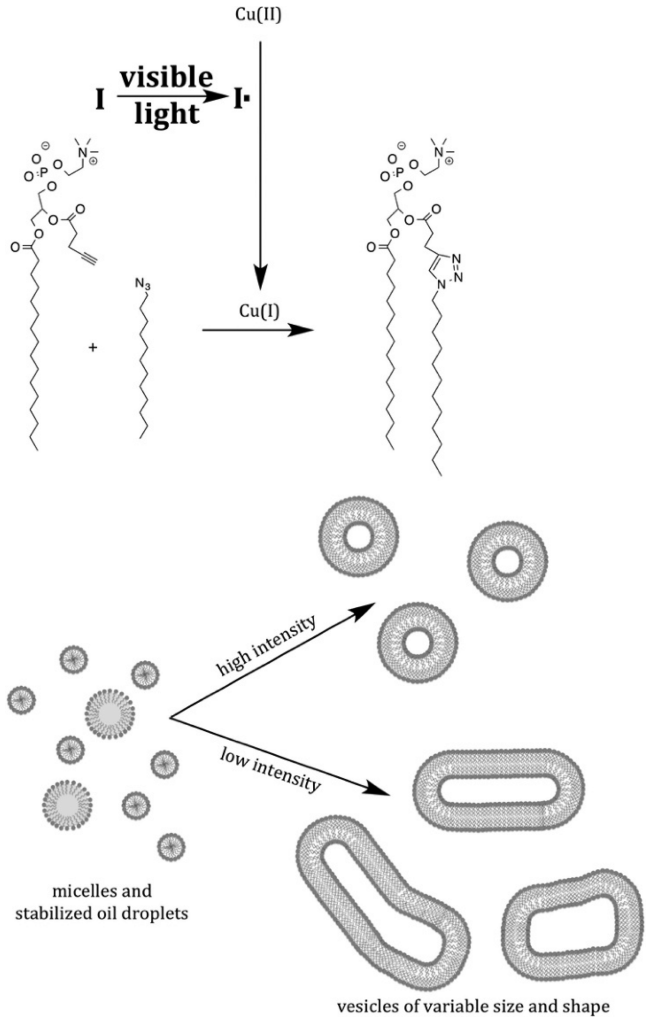

Figure 73. PhotoCuAAC reaction results in in situ synthesized phospholipids that self-assemble into vesicles. Morphology of the resulting vesicles depends on exposure conditions, with high intensity resulting in smaller and more uniform structures. Reproduced with permission from ref 269. Copyright 2016 American Chemical Society.

moieties. Initial reactions with the Michael acceptor allowed for subsequent chain extension radically via the allyl group

https://doi.org/10.1021/acs.chemrev.0c01212
Chem. Rev. 2021, 121, 6915−6990

without the need for deprotection between additions. The reactions were performed in the solution phase; the high efficiency of each reaction and employing a fluorous tag as a liquid phase reaction support allowed for simplified chromatographic purification between each unit extension.

Photoinitiated thiol−ene photoclick chemistry has been used in the development of oligomeric nucleic acid mimics. In 2015, clickable nucleic acids (CNAs), which are single-stranded DNA-mimicking oligonucleotides, were synthesized employing thiol−ene click reactions. Both homooligomers and oligomers of sequence-controlled, periodic repeats were obtained (Figure 74).[271] In contrast to the solid-phase,

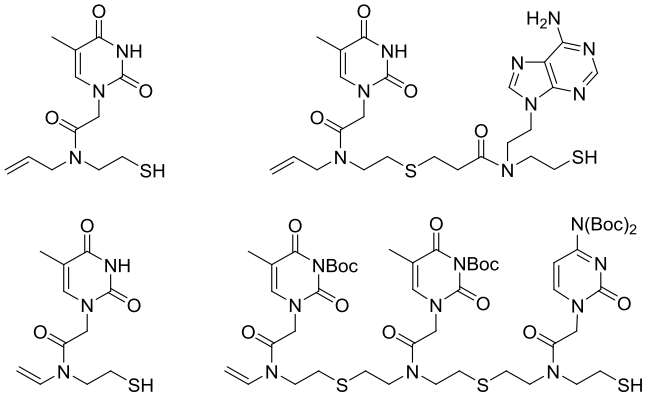

Figure 74. Examples of click nucleic acid (CNA) polymerizable nucleobase monomers including first generation thymine monomer (top left),[271] first-generation polymerizable TA dimer (top right),[271] second-generation thymine monomer (bottom left), and polymerizable TTA trimer (bottom right).[255,256]

sequential addition-based synthesis of oligomers, which may take many hours to obtain the desired product, oligomers of up to 15 nucleobase residues were synthesized in a matter of seconds via the photoinitiated reaction between thiols and eneamides on heterobifunctional monomers. Subsequently, longer sequential patterns such as the precursors of tetramer, pentamer, hexamer, etc., were efficiently synthesized in a simple and scalable manner, leading to highly selective hybridization between these CNA-2G polymers and complementary ssDNA.[272,273] The versatility of this new generation of CNA molecules and the ease of synthesis afforded by the thiol−ene reaction portends applications of artificial nucleic acids and related synthetic bioactive molecules across a wide variety of research fields.

Consecutive photoclick reactions have been used to obtain ordered oligomeric and polymeric structures with high precision. Zydziak et al.[274] achieved sequence-defined macromolecular assembly using a photoenol Diels−Alder reaction between monomers carrying both the photolatent diene (benzaldehyde) and dienophilic alkenes. By sequentially varying introductions of monomer pairs, the authors obtained precise homopolymers, copolymers, and block copolymers. By controlling the structure of the introduced monomers, the physical properties of the resulting macromolecules were able to be tuned, affording user-defined materials with potential use as a molecular information storage system. The efficiency and orthogonality of the photo DA reaction has allowed researchers to employ the reaction in conjunction with other reactions (e.g., the Passerini three component reaction) to generate monodisperse oligomers with precise, alternating sequences via consecutive additions of monomers.[275]

Photoclick reactions have been employed toward the development of linear polymers with advantageous mechanical properties as well. For such application, reactions requiring relatively large functional groups are limited by the influence of those groups on the physical properties of the resulting materials. Photoclick reactions that employ relatively small functional groups are better suited to allow more precise tuning of those properties by monomer design without the concern for disproportionate influence from the reactive groups themselves. For this reason, thiol−ene reactions are particularly suited to this application. Recently, utilizing the thiol−ene reaction, high molecular weight semicrystalline linear and loosely cross-linked polymers were formed from 1,6-hexanedithiol and diallyl terephthalate monomers within a few seconds of irradiation with low intensity light and with demonstrated excellent mechanical properties (tensile strengths of 24 MPa at failure elongations of >800%).[276,277]

Among the described photoclick reactions, the thiol−yne reaction is unusual in its difunctionality. This has allowed it to become particularly useful in the synthesis of dendrimers, highly branched, regularly structured, and frequently fractal macromolecules. The most straightforward synthesis of dendrimers or dendrimer-like materials was conducted by the homopolymerization of a monothiol monoalkyne, which yielded a hyperbranched, polysulfide with many terminal alkynes.[278] The resulting product, however, was polydisperse. Moreover, given the observed homopolmyerization of alkynes upon depletion of thiols, the hyperbranched product may have exhibited considerable structural nonidealities.

By alternating thioglycerol−yne reactions with an orthogonal alkyne coupling reaction, researchers were able to geometrically increase the functionality of each successive generation of dendrimer discretely, generating effectively monodisperse dendrimeric species (Figure 75).[279,280] This strategy had been employed previously with thiol−ene photoclick reactions, employing a reaction to couple pentenoic acid to the hydroxy groups that resulted from coupling of thioglycerol.[281] While the thiol−ene strategy resulted in a doubling of functionality with completion of each set of coupling reactions, the thiol−yne strategy resulted in a theoretical quadrupling of functionality. Such materials have demonstrated utility in drug delivery and as stabilizing contrast agents for CT imaging.

3.3. Macromolecular Modification

3.3.1. Biolabeling. The labeling of biologics in vivo and in vitro allows investigators to better understand structural and functional relationships via the visualization of complex molecular interactions within biological systems.[282,283] Labeling cells, organelles, and biopolymers with fluorescent molecules via biorthogonal click reactions is a popular strategy as it provides generally high sensitivity, minimal invasiveness, and frequently the potential for real-time observation in living systems. The ease and degree of control provided by photomediated reactions with mild reaction conditions, high yields, and high selectivity has incentivized the development of ever new photoactive compounds to label biological polymers and higher-order structures to track and elucidate cellular processes.

While CuAAC reactions have long been the gold standard for click reactions, cytotoxicity, and other deleterious biological

https://doi.org/10.1021/acs.chemrev.0c01212
Chem. Rev. 2021, 121, 6915−6990

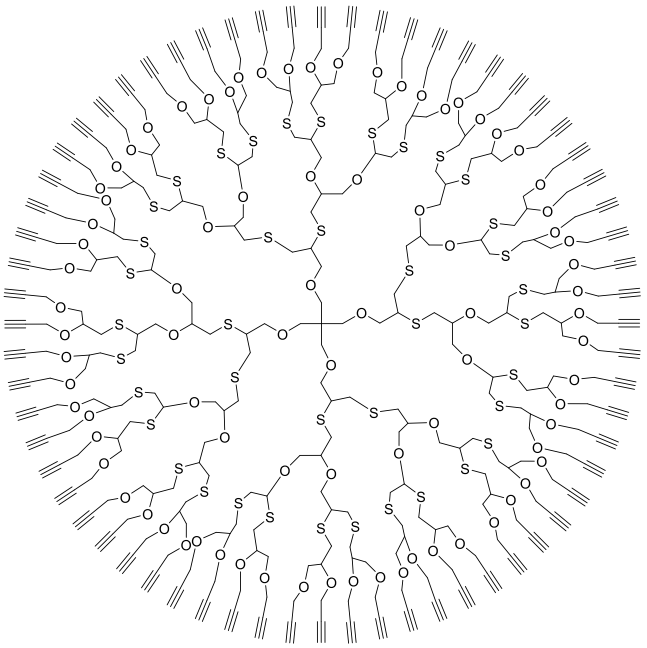

Figure 75. Dendrimer made via alternating thioglyerol−yne and alkyne conjugation reactions. The thioglycerol−yne coupling results in the introduction of two hydroxyl groups per reaction, while the subsequent alkyne coupling replaces the alcohol with the difunctional yne for the next thioglycerol coupling reaction. Each successive reaction pair results in a quadrupling of functionality as each alkyne is difunctional.[279]

interactions associated with the use of copper, have necessitated development of alternative click strategies. Photoactivation of cycloalkynes for copperless azide−alkyne cycloaddition reactions has been particularly successful when applied to labeling in the biological sciences. In an early example, this strategy was employed for the efficient labeling of living cells expressing glycoproteins containing *N*-azidoacetylsialic acid.[33] The authors highlight many advantages of using this phototriggered click reactions for labeling, including the ability to allow for a homogeneous concentration of reagents in the cells before the click reaction is initiated. The relatively high quantum yield for this reaction also improves the biological compatibility of its utilization.

This approach has also been used for the fluorescent labeling of BSA with a rhodamine B dye by using a bis-cyclopropenone to link the two molecules (BSA-DIBOD-rhodamine B). By exploiting the advantages of the photoSPAAC reaction, the labeling occurred in a one-pot reaction with only a few minutes of light exposure (Figure 76).[284] In similar applications, SPAAC photoclick reactions were employed as light-responsive photoaffinity probes for detecting carbohydrate-binding proteins and antibodies.[285−287]

Photoactivated, ring-stained alkynes have also been used in IEDDAC reactions with tetrazines. As demonstrated by Mayer et al., this reaction is efficient for labeling proteins by using a photoactivatable bicyclononyne (BCN) probe, offering spatial and temporal control over the labeling of tetrazine labeled proteins.[44] The authors were able to conduct this photo-triggered reaction in *E. coli*, demonstrating the biorthogonal nature of this reaction (Figure 77). The photo-IEDDAC reaction proceeded with an on-protein rate constant of 50 m^{-1} s^{-1}, on par with the fastest biorthogonal photoinduced reactions. This enables protein labeling within minutes at low concentrations. Although this technique has yet to be explored further, sustained improvements in the design of complementary strained alkenes[288] and new synthetic approaches for derivatives of the tetrazine moiety[289] hold great promise for the future of the photoinduction of tetrazine ligation reactions, particularly in intracellular labeling and conjugation applications by virtue of the bioorthogonality of the reactant chemical species and inverse electron demand cycloaddition mechanism.

Initial work by Lin and co-workers pioneered the tetrazole−ene reaction as a photoclick reaction for biological applications and as a fluorescent self-reporting system.[290] In one approach to the application of this chemistry in the labeling of biopolymers, the tetrazole or alkene moiety was introduced into the protein via genetic encoding of functional group-

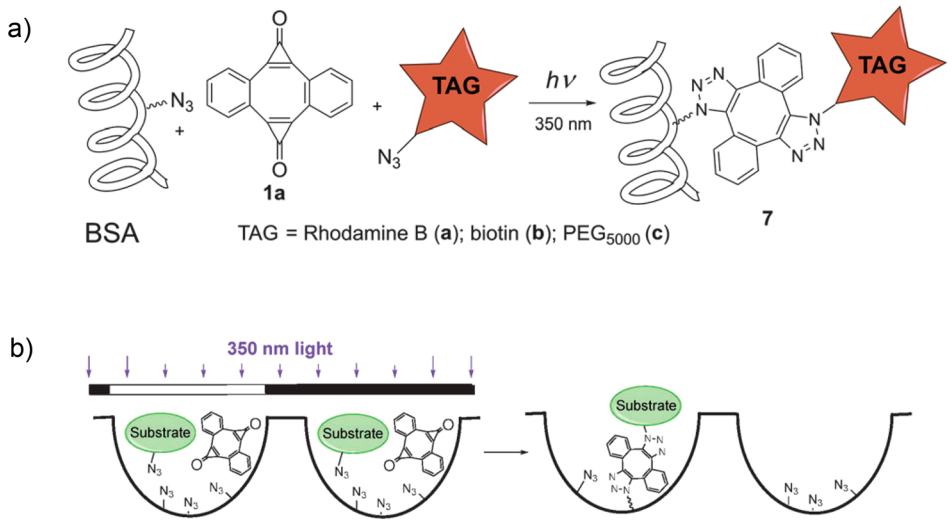

Figure 76. (a) Sequential photolabeling of azido-BSA with photogenerated ring-strained cyclooctadiyne. (b) Selective light-directed Immobilization of rhodamine B on a 96-well plate with photogenerated cyclooctadiyne. In these examples, the photocaged cyclooctadiyne serves as an exogenously activatable cross-linker, permitting the coupling of two azide-containing species. Reproduced with permission from ref 284. Copyright 2016 Royal Society of Chemistry.

https://doi.org/10.1021/acs.chemrev.0c01212
Chem. Rev. 2021, 121, 6915−6990

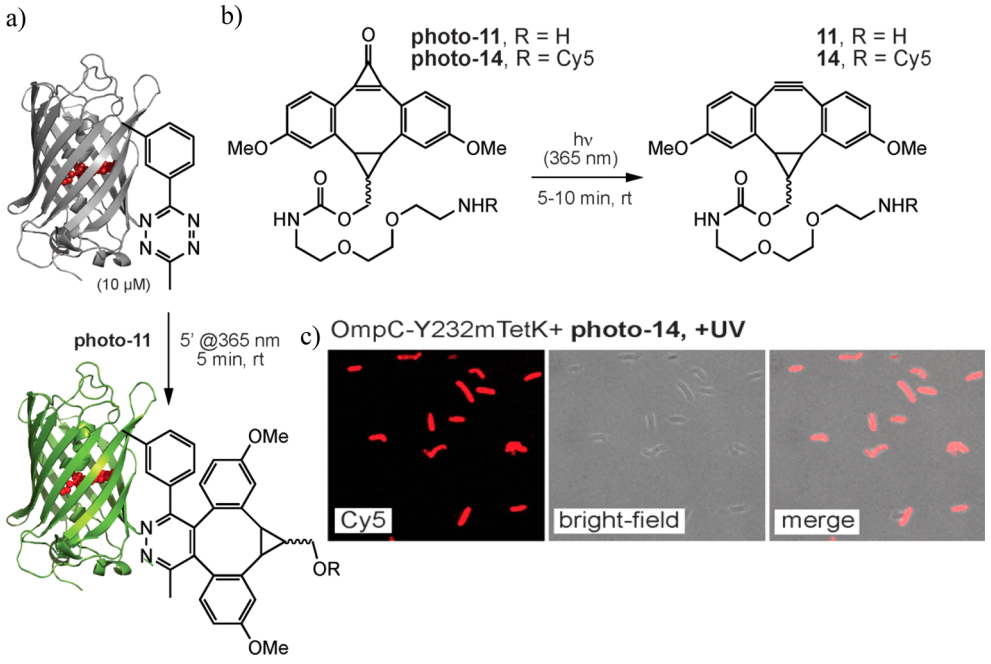

Figure 77. Photo-IEDDAC labeling on living cells. (a) Labeling of sfGFP-N150 mTetK with photo-11. (b) Structures of water-soluble photo-DMBO conjugates. Both photo-11 and the Cy5-conjugate photo-14 are decarbonylated by short irradiation at 365 nm to quantitatively form **11** and **14**, respectively. (c) Fluorescence imaging and fluorescence microscopy show efficient and light-induced labeling of a cell-surface protein in living *Escherichia coli*. Reproduced with permission from ref 44. Copyright 2019 John Wiley and Sons.

bearing, non-natural amino acids.[85,291] A fluorescent moiety was then incorporated in a site selective manner. This was first achieved with a genetically encoded alkene reporter, *O*-allyl tyrosine, for protein labeling in bacteria.[29] However, this reaction was slow (k_2 = 0.00202 ± 0.0007 M^{-1} s^{-1}) because of the low reactivity of the alkene on the reporter. Various routes have been explored to increase the reactivity including the use of an electron-deficient acrylamide-modified lysine side chain. The use of an acrylamide is advantageous as it is relatively small and stable under biological conditions. It was successfully used in a number of cases including the labeling of the membrane protein OmpX on the surface of *Escherichia coli* and successfully incorporated into GFP-TAG-mCherry-HA protein in *Arabidopsis thaliana*, a plant model.[292,293] Norbornene and cyclopropene functional groups have also been incorporated into proteins to increase the reaction rate with tetrazoles.[294−296] For example a cyclopropene-modified lysine was used to direct site specific modifications of green fluorescent protein inside HEK293T cells. The reaction rate increased 5 orders of magnitude to k_2 = 58 ± 16 M^{-1} s^{-1} for cyclopropene, which was reported to be twice as fast as norbornene as a consequence of the increased ring strain.[297] Spiro[2.3]hex-1-ene has also been recognized as another strained alkene that readily reacts with tetrazoles for bioorthogonal protein labeling despite its 3,3-disubstituted conformation.[298]

DNA has also been successfully labeled through the tetrazole−ene reaction. Wagenknecht's group was the first to present tetrazole-modified building blocks for solid state DNA synthesis and a nucleoside triphosphate for the polymerase-based DNA preparation. The ligation with maleimide dyes occurred with LED excitation at 365 nm (k = 23 ± 7 M^{-1} s^{-1}).[299,300] The group developed this technique further by exploiting the fluorescent pyrazoline product that is produced via the tetrazole−ene reaction.[301] By synthesizing tetrazole functionalized 2′-deoxyuridine, a modified DNA structure formed which could then react with a maleimide functional dye for site specific labeling. The researchers also exploited the use of the fluorescent pyrazoline, formed in the tetrazine−ene reaction, and enhanced the fluorescent intensity by enabling energy transfer to the labeled dye. Lehmann et al. indicate that the energy transfer would work on a multitude of dyes and could be tuned to the desired wavelength of choice, demonstrating the versatility of the pyrazoline product. In addition, Yu et al. also exploited the use of the fluorescent pyrazoline product in intramolecular tetrazole−ene cycloaddition.[251] This single reagent approach was demonstrated to be successful as a probe in cancer cells.[290,302] Prefluorescent naphthalene−tetrazole conjugates induced by two-photon excitation at λ = 700 nm for fluorogenic labeling of olefin-tagged intracellular structures have been formed via this photoclick reaction.[303,304]

More recently the reaction has been used in multicellular organisms. Wu et al. incorporated vinyluracil into the DNA of zebrafish to allow for spatially controlled imaging of DNA through the use of a coumarin-linked tetrazole in real time without DNA denaturation (Figure 78).[305] The authors highlight that through the use of the tetrazole−ene reaction a "switch-on" labeling approach was achieved.

Despite these examples of relative bioorthogonality, the high reactivity of the intermediate nitrile imine with many common biological nucleophiles[89,90,306] (e.g., thiols, amines, and acids) may limit its application, although strategies have been developed to improve specificity.[91,307] Utility in this case, however, would effectively be limited to those situations in which labeling with a substantial photoactivatable probe is practical, in contrast to previous examples where biomacromolecules bearing small, alkene functional groups are selectively labeled via photoactivated tetrazoles. Ultimately, the numerous examples of tetrazole−ene photochemistry for

https://doi.org/10.1021/acs.chemrev.0c01212
Chem. Rev. 2021, 121, 6915−6990

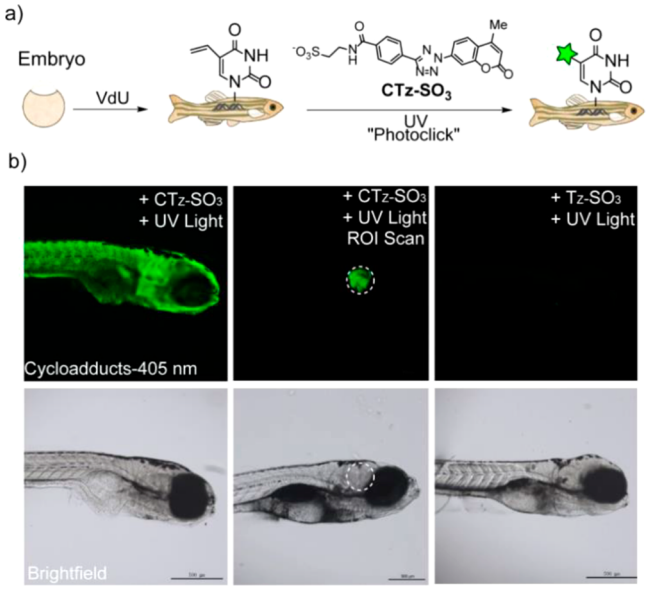

Figure 78. (a) Scheme for labeling DNA of zebrafish via tetrazole−ene photoclick reaction and (b) fluorescence microscopy images of cellular DNA spatially labeled through the tetrazine−ene reaction. Reproduced with permission from ref 305. Copyright 2019 American Chemical Society.

labeling reflects its broad utility for that purpose and suggests extensive continued and future application in biolabeling.

The photomediated 1,3-dipolarcycloaddition via uncaging of nitrile-imine from sydnones form the same pyrazoline cycloaddition adduct as does the reaction with the tetrazole and thus has found similar labeling applications as a fluorescent functional group.[36] Since its introduction in 2018, several examples of labeling reactions between substituted sydnones and variable alkenes and alkynes have been demonstrated.[94,308,309] Included in these was the use of photoisomerizable dipolarophiles, such as dibenzothiadiazepine, the photoinduced ring strain of which allowed dual wavelength control over labeling biomacromolecular structures in live cells.[95]

The azirine−alkene reaction was also used as a bioorthogonal label for lysozymes, although this application required 302 nm UV light, posing a challenge to implementation in living cells.[37] However, this limitation was overcome through the synthesis of an azirine moiety coupled to the visible-light-absorbing chromophore pyrene, resulting in a single molecule for facilitating the azirine−alkene cycloaddition reaction at wavelengths greater than 400 nm. The small size of the functional groups of the bioorthogonal azirine-based photochemistries, in addition to their high reactivity, make them as an attractive albeit underutilized alternative to other photoclick reactions.[310]

Photocycloadditions of 9,10-phenathrenequinones with electron-rich alkenes to form fluorogenic [4 + 2] cycloadducts have also been utilized for labeling proteins in live cells.[311] Li et al. demonstrated the use of a fluorescent self-reporting system that enabled the temporal and spatial surface labeling of A549 cells in a biorthogonal manner using visible light.

Although the photo catalyzed thiol−ene reaction has been used extensively as a bioorthogonal reaction, it has not received the same interest for biolabeling that other photoclick reactions (e.g., tetrazole−ene, photo SPAAC) have. The advantage of using the thiol−ene reaction for labeling proteins is the natural occurrence of cysteine residues that readily react with an alkene functional label.[312] Despite the lack of spatiotemporal control, the thiol−maleimide Michael addition reaction has been a far more popular route for labeling proteins, as it does not require light exposure or the presence of radical initiators. There are, however, examples of modifying biopolymers with the radical thiol−ene reaction. Early examples of using the thiol−ene reaction to react with naturally occurring cysteine residues focused on the glycosylation of proteins in a nonsite-specific manner. Dondoni et al. glycosylated BSA that contains one disulfide bond and one free cysteine using 365 nm light and demonstrated that all three cysteine residues were glycosylated.[250,313] However, if site specific labeling is required, other cysteine groups require modification to avoid also participating in the reaction and thus leading to heterogeneous protein mixtures. More recently, photocatalyzed thiol−ene reactions have been used for paramagnetic tagging of proteins for use in NMR imaging where site specific labeling is not required. Denis et al. have demonstrated, by using an alkene functionalized paramagnetic tag, proteins of interest are labeled through the use of thiol−ene reactions with cysteines present on the protein of interest.[314] The thiol−ene reaction offers high yields and short reaction times enabling stable thioether bonds to form, demonstrating the benefits of the reaction as a route to label proteins with paramagnetic tags.

To allow for site specific labeling of proteins, alkene handles have been incorporated into proteins allowing for reactions with thiol functional labels upon exposure to 365 nm light.[315] This was first demonstrated by Li et al., who synthesized an alkene functional amino acid to genetically incorporate into proteins using alkenyl−pyrrolysine analogues.[316] These proteins demonstrated site specific ligation with thiol modified dyes upon irradiation with 365 nm light. Weinrich et al. used a similar method to immobilize proteins on a thiol functionalized surface.[317] The group functionalized proteins with farnesyl pyrophosphate and were able to immobilize the protein by exposure to UV light, demonstrating a simple method for immobilizing proteins with a high yield using mild conditions.

Although these conditions have been shown to maintain protein structure and activity, relatively few researchers have used photoinitiated radical thiol−ene reactions for protein modification and labeling. In contrast to other photoclick reactions more frequently employed in the labeling of biopolymers and other biological structures, the thiol−ene reaction employs a photoinitiator for the photoamplification of the thiol−ene cycle. Such a mechanism is advantageous in applications wherein the concentration of chromophores is a concern. While photoSPAAC and tetrazole−ene reactions employ functional groups that bear their own chromophores, the concentrations of those groups in labeling reactions is generally so low as to guarantee optically thin samples despite the one photon, one event nature of the reaction. Thus, one of the otherwise primary advantages of the radical thiol−ene reaction is not particularly useful in the context of labeling.

Like the thiol−ene reaction, the thiol−yne reaction can exploit the use of naturally occurring cysteines and disulfides present in proteins to modify and label proteins.[315,318] Dondoni and co-workers demonstrate the ability of attaching two modifications at a single site on BSA using the thiol−yne reaction.[252] They demonstrate the modular addition of alkene functionality that allows for glycosylation and fluorescent labeling at the thiol containing sites on BSA (Figure 79).

https://doi.org/10.1021/acs.chemrev.0c01212
Chem. Rev. 2021, 121, 6915−6990

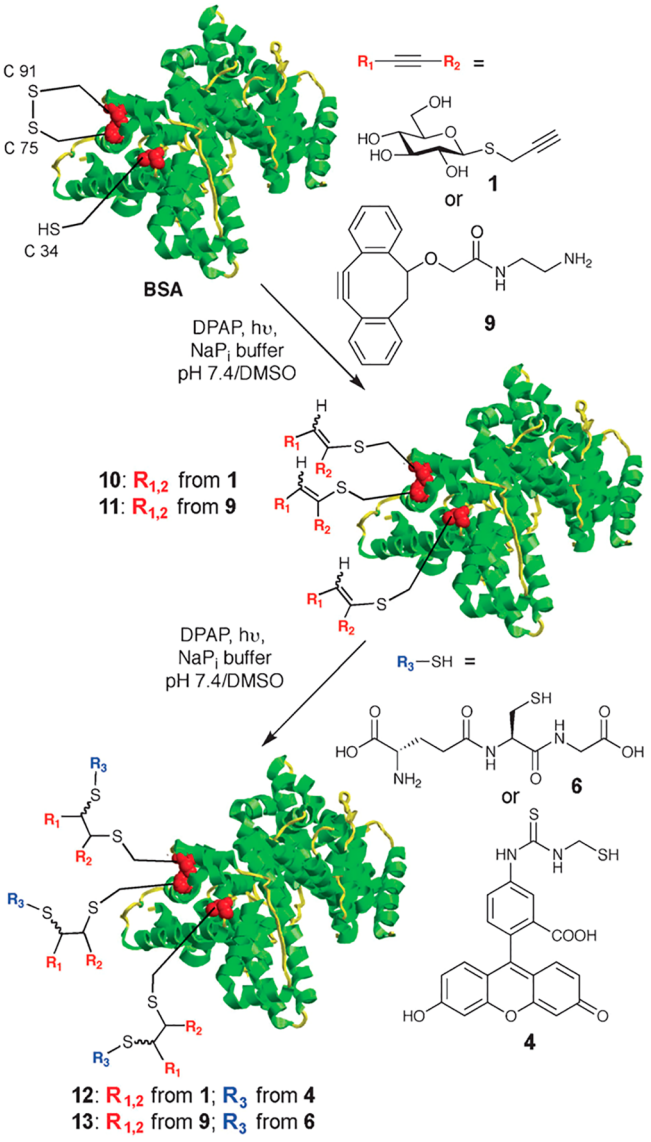

Figure 79. Thiol−yne modification of BSA. Addition of propargyl 1-thio-β-D-glucopyranoside at thiol present sites on BSA to form alkene functional handles, which then react with thiol functional peptide chains and fluorescein. Reproduced with permission from ref 252. Copyright 2011 Royal Society of Chemistry.

However, the researchers note that unanticipated side reactions occurred when the thiol−yne reaction was used in conjugation with other click reactions, most notably cyclo-alkynes. To enable the thiol−yne reaction for site specific labeling, alkyne handles have been genetically incorporated into proteins. Li et al. demonstrated the use of alkyne-containing pyrrolysine derivatives genetically encoded into proteins for site specific labeling with bidansyl−cystamine.[319] They demonstrated that the modification has little effect on the enzyme activity or conformation of the protein and could be expanded on as a dual labeling strategy.

More recently, the thiol−yne reaction has been used in vivo to cross-link proteins. Liu et al. genetically incorporated an alkyne functional amino acid, *S*-propargyl-cysteine (SprC) into a GDT protein in *E. coli*.[320] Through irradiation at 302 nm, a thiol−yne reaction took place between the SprC modified GST and a cysteine residue on the interface of another GST protein because of the compact size of SprC the modification and cross-linking reaction did not affect the protein folding or interactions. Western blot analysis showed covalent cross-linking of the GST dimer, demonstrating an application of the thiol−yne reaction for probing protein interactions in living cells. The photocatalyzed thiol−yne reaction has been applied less than other methods to label proteins potentially as a consequence of the research lacking into the effect radical initiator and irradiation have on protein structure and activity as well as the multifunctional nature of the alkyne itself.

In another example, Luo et al. developed a general strategy that demonstrated the utility of these photoactive and bio-orthogonal chemistries via liposome fusion to cell surfaces for on-demand microtissue assembly and disassembly. In this work, the phototriggered oxime ligation coupled with *o*-nitobenzyl chemistry allowed for the remote-controlled disassembly upon irradiation with UV light and demonstrated the potential of these chemistries for creating engineered photoswitchable cell surfaces for tissue engineering applications (Figure 80).[321]

3.3.2. Polymer−Polymer Conjugation. Block copolymers have a wide variety of applications, both commercially and in research. They are used as thermoplastic elastomers, surfactants, and adhesives.[322] Amphiphilic block copolymers continue to be of great interest for drug delivery, and surface self-assembly of block copolymers results in topographical features of extremely small size (e.g., <10 nm) with great potential for the advance of microchip manufacturing, semiconductor development, and digital media storage.[323]

Such block copolymers are frequently produced via sequential living polymerizations (e.g., anionic polymerization, ROMP, etc.) or controlled radical polymerizations (e.g., RAFT, ATRP), changing constitutive monomers for each successive polymer block. Conjugation of preformed polymers via click reactions is a strategy that obviates the need for blocks to consist of monomers with compatible polymerization mechanisms.

Polymer−polymer conjugation is also a route for designing more complex polymer architectures such as bottle brushes, hyperbranched, and star polymers. Some challenges of polymer−polymer conjugation, include the necessarily dilute conditions required and the potential steric hindrance. In spite of these challenges, macromolecular conjugations require near full conversion between precursors in equimolar conditions, as unconsumed reactants are generally difficult to separate from the conjugated product.

Doran et al.[324] demonstrated sequential photoclick reactions to perform polymer−polymer conjugation and to modify the terminus of a newly formed diblock copolymer. A telechelic poly(caprolactone) with methacrylate and alkyne termini was placed in a flask with an azide-terminal PMMA and an initiating system of copper(I) bromide and radical photo-initiator TPO. Exposure to 350 nm light resulted in the formation of the methacrylate-terminal diblock copolymer. Subsequent addition of *N*-acetyl-L-cysteine and more radical photoinitiator resulted in the conjugation of the cysteine derivative to the free terminus via radical thiol−ene coupling. It should be noted that the methacrylate used here is generally a less reactive alkene in such reactions, perhaps explaining, in part, the abnormally long reaction times employed in this one pot synthesis (16 h).

Though thiol−ene and thiol−yne reactions have been employed for polymer−polymer conjugation reactions, under some reaction conditions, byproducts are obtained in

https://doi.org/10.1021/acs.chemrev.0c01212
Chem. Rev. 2021, 121, 6915−6990

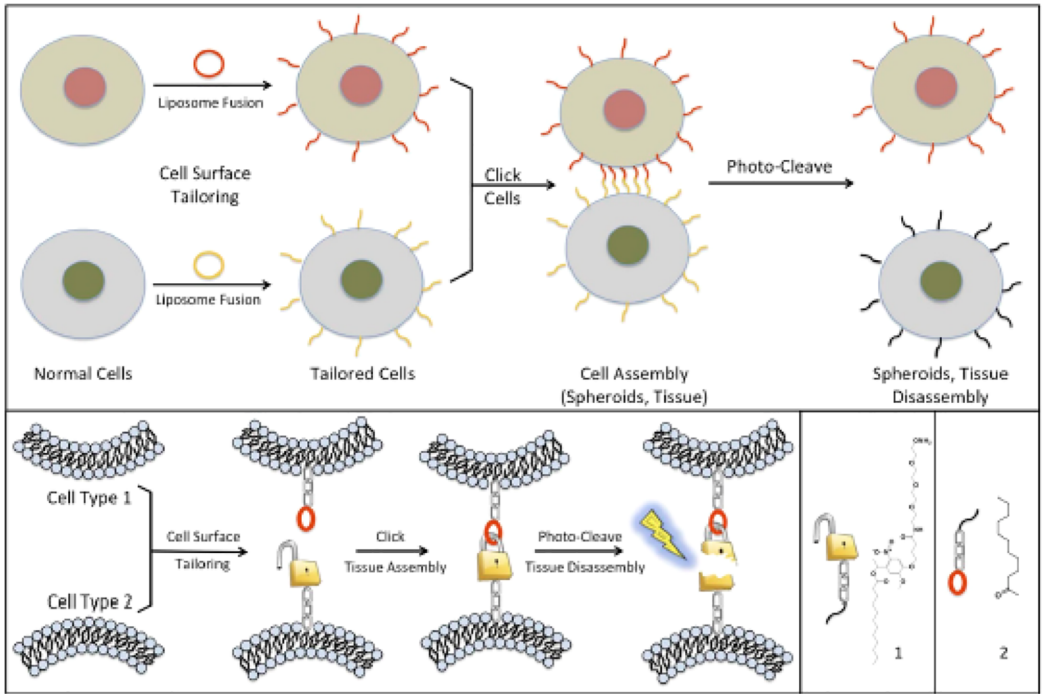

Figure 80. Schematic representation of the molecular level control of tissue assembly and disassembly via the chemoselective, bio-orthogonal, and photoswitchable cell surface engineering approach employing photoinduced oxime ligation and *o*-nitrobenzyl chemistry. Reproduced with permission from ref 321. Copyright 2014 Springer Nature.

significant and even predominant yields. This undesirable outcome is the result of the radical initiation mechanism and the propensity of thiyl radicals to recombine into disulfides. Other byproducts may result from radical termination with radical initiator fragments. Typically, in thiol−ene and thiol−yne coupling reactions, photoinitiators are in such low concentrations and initiate the thiol−ene and thiol−yne reactions so efficiently that any byproduct is negligible. When using low concentrations of thiols and enes such as those found in polymer−polymer conjugation, the concentration of initiators relative to thiol and ene functional groups is generally high and these side reactions become more significant. Another factor that may mitigate the efficacy of polymer−polymer conjugations via thiol−ene reactions is the limited solubility of the polymer with the reactive species.[118,325,326] These limitations are readily addressed with the appropriate selection of reactive alkenes, (e.g., norbornenes), and more reactive thiols (e.g., mercaptopropionate) along with an efficient initiator to ensure that the rate of the thiol−ene reaction exceeds that of competing side reactions. Polymer−polymer conjugations were performed with good yields and relatively high purity by employing mercaptopropionate-terminated PEGs and norbornene-terminated PEGs in both organic and aqueous conditions.[4,327,328] Allyl ether-terminated PEGs, however, resulted in significantly poorer conjugation. Sequential thiol−ene photoclick reactions were conducted to form a three-arm star copolymer. While all polymers in this study were PEG-based, the results indicated the potential to generate heteroarm star copolymers. In the same study, pentynoate-terminal PEG was reacted with the PEG-thiol, resulting in a higher fraction of conjugated polymers than the reaction with the allyl ether. However, the monoaddition product dominated, indicating, contrary to couplings with smaller reactants, that the second addition was significantly less efficient that the first, thereby potentially demonstrating the influence of steric hindrance on the reaction.

Photo Diels−Alder reactions have been used to conjugate dienophile-terminated polymers to *o*-methylbenzaldehyde thioether terminated polymers via photoenolization of the latter to the reactive diene *ortho*-quinodimethane. Feist et al. used illumination with either 365 or 410 nm light in a photoflow reactor to couple hexaethylene glycols with maleimide and methylbenzaldehyde thioether termini within 10 or 20 min (for the UV and visible light irradiation, respectively).[329] The thioether, in place of an ether, improved the absorbance of the benzaldehyde chromophore in the visible region relative to earlier work with this reaction. While the reaction in this example did not employ polymers of high molecular weight, the results suggests that possibility. The authors did, however, employ a similar reaction to generate diblock copolymers via the photo Diels−Alder polymer−polymer conjugation.

Among the most popular current polymerization technologies is the RAFT-mediated polymerization that allows controlled radical polymerization of a wide variety of radically polymerizable monomers. With appropriate RAFT agents, users obtain narrowly dispersed polymers with predefined molecular weight and terminal groups. Polymers synthesized via RAFT-mediated polymerization contain, on one terminus, the thiocarbonylthio moiety common among RAFT agents. Some of these, the dithiobenzoate in particular, have proven effective dienophiles. Generating a poly(methyl methacrylate) via RAFT mediated polymerization with a dithiobenzoate RAFT agent, the authors obtained a polymer with a dienophile terminal functional group that was effectively conjugated to a methylbenzaldehyde thioether-terminated poly(caprolactone) in acetonitrile, with 410 nm light exposure with a residence time of 20 min in a photoflow reactor.

https://doi.org/10.1021/acs.chemrev.0c01212
Chem. Rev. 2021, 121, 6915−6990

3.3.3. Biomacromolecule−Polymer Conjugation. An important subclass of polymer−polymer conjugates are those involving natural biomacromolecules. Protein−polymer conjugates in particular are increasingly utilized in biomedical fields as they exhibit advantageous properties derived from their hybrid composition (e.g., increased stability, improved pharmacokinetics, etc.). Wholly synthetic diblock copolymers are, as stated previously, most frequently synthesized via consecutive living polymerizations with different monomers. Such a synthetic approach is not applicable to biomacromolecule−polymer conjugates. Although the "grafting from" approach employed via ATRP and RAFT is a popular synthetic strategy as reported in the literature for development of protein−polymer conjugates,[330] some researchers have used photoclick reactions to facilitate polymer−biomolecule coupling. This post polymerization coupling is frequently referred to as "grafting to" and offers the advantage of decoupling the polymerization conditions from the requirements of an environment conducive to maintaining the bioactivity of potentially sensitive biomacromolecules.

PEGylation, in particular, increases the hydrodynamic volume of protein-based therapeutics to mitigate their depletion via renal filtration. However, traditional PEGylation reactions are generally not site-specific. Indiscriminate conjugation may result in a heterogeneous mixture of conjugate products and potentially a loss of bioactivity if the polymer chain obstructs or otherwise interferes with the protein's active sites. Purification of the mixed products is time and labor intensive. Incorporating non-natural amino acids with biorthogonal handles allows for site specific PEGylation, potentially increasing the efficiency of the production of their corresponding conjugates. This technique has frequently been used with CuAAC and SPAAC reactions owing to the efficiency and selectivity of these reactions. However, the thiol−ene reaction has also been used as a successful method for PEGylating proteins.

Ye et al. used a reductant to liberate cysteine thiols from their respective disulfide bridges and then grafted mPEG-methacrylate onto the protein via photoinitated thiol−ene coupling.[331] As an alternative to using native cysteine residues in the reactions, thiol−ene conjugations may use non-natural alkene functional amino acids to produce alkene-modified proteins. A thiol functional polymer is then used to react with the alkenes on the protein. This latter approach is advantageous as the thiols on the native cysteine residues are most frequently bound up in disulfide bridges, the reduction of which may interfere with protein structure and function. While reactive in thiol−ene reactions, other thiols demonstrate improved reactivity and less likelihood of participation in side reactions such as disulfide formation.

Siti et al. incorporated allyl-containing nonnative amino acids into bovine β-lactoglobulin (BLG) for photoconjugation of the protein to a diaryl tetrazole-modified PEG.[332] While conjugation was successful, nonspecific coupling was observed and subsequently identified as resulting from the cycloaddition with tryptophan residues on the protein. Additional, nonallyl bearing proteins were reacted with the tetrazole-PEG and conjugation was observed in every case, where there was a tryptophan and at rates and yields comparable to reactions with the allyl, demonstrating the ability to take advantage of native amino acid residues for photoclick conjugations (Figure 81).

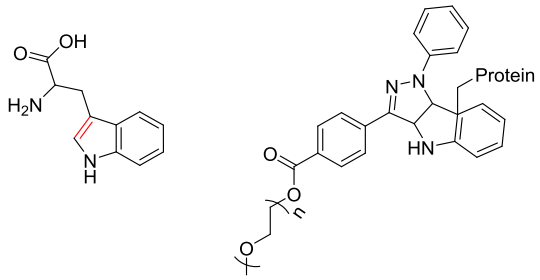

Figure 81. Structure of tryptophan (left) with reactive alkene indicated in red. Proposed conjugate linkage (right) between tryptophan-containing protein and tetrazole-terminated PEG.[332]

While thiol−ene and nitrile imine reactions may take advantage of native amino acid residues for conjugation reactions, in general, the successful application of site-specific protein−polymer coupling relies on the incorporation of non-natural amino acids into the protein structure. The library of reported non-natural amino acids includes those with a variety of pendant moieties capable of participating in photoclick reactions, including alkynes, alkenes, azides, and tetrazoles (Figure 82).

Photoclick reactions have also been used to generate conjugates of different biopolymers. Fruk and co-workers[333,334] used the photo Diels−Alder reaction to couple DNA to proteins by modifying, on CPG, oligomeric single-stranded DNA with a photoenol. Once cleaved from the solid phase, the ssDNA was irradiated in the presence of a maleimide-modified protein (myoglobin and horseradish peroxidase) to generate the biopolymer−biopolymer conjugate.

3.4. Surface Modification and Patterning

Material surface modification provides independent control of the bulk physical properties and interfacial interactions between materials. For example, the hydrophobicity of a material is readily controlled to improve surface fouling resistance or to change the interaction of a substrate with a contacting solution. In biomedical applications, the surface of implant materials that might otherwise elicit a foreign body response may be modified with functional groups that mitigate such a reaction from the host. Alternatively, materials' surfaces may be modified to promote specific in vivo interactions intended to better integrate the material with the host tissue. In diagnostics, surface modification may be desirable to attach a substrate for subsequent detection of an analyte. The spatial control offered by many photoclick reactions makes them particularly well suited to the spatially heterogeneous requirements for many of these surface-level applications.

While photoclick reactions are certainly amenable to the stringent requirements of surface reactions, one challenge to such utility is obtaining surfaces with the requisite functional groups present. For this reason, most surface modifications via photoclick chemistry first require a priming treatment to establish one or the other reactive moieties on the surface. Such surfaces may be thus generated via one or a combination of techniques such as chemical vapor deposition (CVD),[335] layer by layer deposition,[336] polymer grafting via RAFT[337] or ATRP[338] mediated polymerization, or any of many others. Jonkheijm et al. employed plasma enhanced chemical vapor deposition onto silicon oxide surfaces followed by successive coupling reactions to generate a thiolated surface from which the authors were able to write, via 411 nm scanning laser,

https://doi.org/10.1021/acs.chemrev.0c01212
Chem. Rev. 2021, 121, 6915−6990

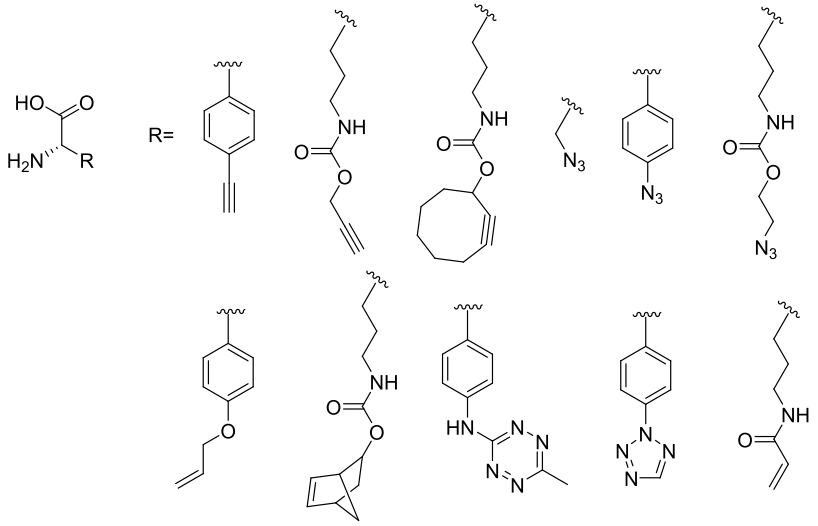

Figure 82. Examples of nonnative amino acids capable of participating in various photoclick reactions.

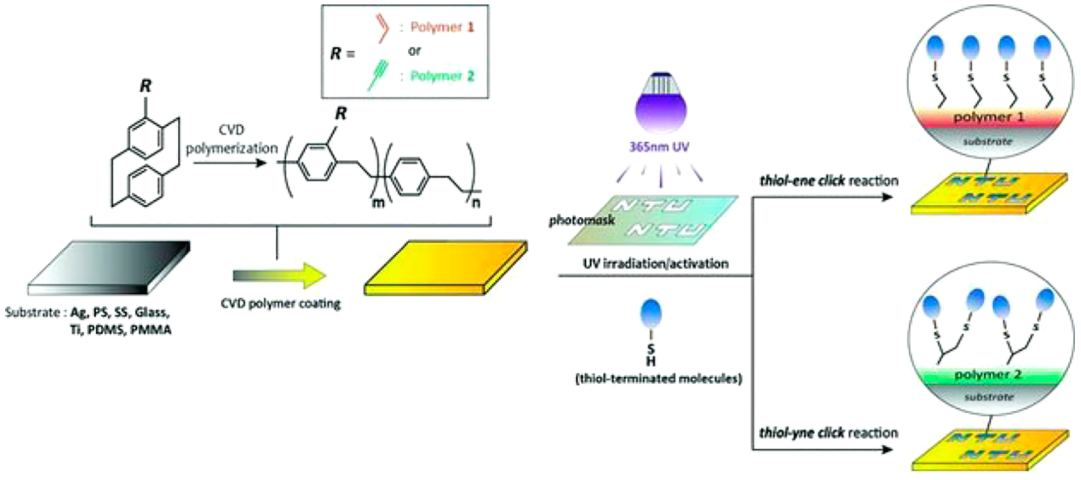

Figure 83. Reactive chemical vapor deposition to prime surface for thiol−ene and thiol−yne surface patterning reactions with thiol-bearing molecules. Reproduced with permission from ref 340. Copyright 2012 John Wiley and Sons.

nanoscale features of covalent attachment of an alkene-modified biotin for subsequent immobilization of streptavidin.[339] Subsequent experiments with alkene-bearing phosphopeptide demonstrated the bioorthgonal patterning of biomacromolecules.

In a demonstration of a particularly versatile surface priming technique, Wu et al. employed a reactive CVD to coat a variety of material surfaces (silver, polystyrene, stainless steel, titanium, PMMA, and PDMS rubber) with alkene and alkyne-pendant polymers onto which were photopatterned either cell-adhesion reducing PEG thiol or cell-adhesion-promoting GRGDYC peptides (Figure 83).[340] Masked exposure of the surface and respective thiols under 365 nm light in the presence of the radical photoinitiator I2959 resulted in controlled cellular adhesion.

While the versatility and availability of alkenes is a particular advantage of this reaction, there are situations in which thiol−yne surface functionalization may be preferred. Bhairamadgi et al. ran a comparative study of surface modification of thiol−ene and thiol−yne reactions and, by XPS, noted a faster rate of reaction at the surface and a higher density of reaction products with the thiol−yne reaction when employing aliphatic, surface bound alkenes, and alkynes.[341] While a more reactive alkene might yield a faster reaction than reported, the authors noted 1.5 times as much sulfur bound to the surface with the thiol−yne reaction as with the thiol−ene at reaction completion.

Surface priming reactions are not always necessary for the covalent modification of materials' surfaces. Endogenous functional groups may result from incomplete conversion or stoichiometric imbalance in the material synthesis itself. This approach is typified by Ma et al., who employed a thiol-Michael reaction to generate a thiolated surface on the surface of a polymeric material formed with an excess of acrylate moieties.[342] Radical thiol−ene photoclick chemistry was then used to pattern peptides on the surface to encourage cell adhesion. Thiol−ene and thiol−yne reactions are particularly amenable to this surface treatment approach as a small stoichiometric imbalance can be well tolerated for maintenance of bulk material properties while providing ample surface-level functionality for subsequent reaction. Alternatively, some materials intrinsically display surface functional groups amenable to photoclick modification directly (e.g., the grafting of thiol-terminated polystyrene to ethylene propylene diene monomer rubber via radical thiol−ene photoclick coupling).[343]

https://doi.org/10.1021/acs.chemrev.0c01212
Chem. Rev. 2021, 121, 6915−6990

The 2D geometry of surface functionalization reactions permits extremely thin samples, which diminishes the concern of light attenuation that may be significant for some photoclick reactions in bulk curing applications. For this reason, reactions involving a one photon, one event type mechanism do not suffer as much from this potential drawback that may mitigate their use in other contexts.

For example, the photoenol DA reaction has been employed for surface functionalization with a variety of surface priming techniques and subsequent surface treatment. In one example, Barner-Kowollik and co-workers[344] synthesized a photoreactive DOPA molecule capable of nonphotomediated polymerization on a variety of surfaces. Subsequent photoenolization in the presence of maleimide-terminal complements resulted in patternable surface attachment. Inverting the surface and soluble reagent functional groups, Vigovskaya et al. modified the 5′ terminus of oligonucleotides with the photocaged diene and patterned surface modification by masked exposure to a maleimide-modified surface.[334]

Many natural materials display abundant functional groups that can be used as functional handles to attach photoclick moieties to their surfaces. Proteins in silk and wool, for example, display a variety of such groups including amines, alcohols, carboxylic acids, and disulfides that have been modified to permit subsequent click and photoclick modifications.[345−347] Cellulose, a polysaccharide with a high concentration of pendant alchohols, is a particularly attractive candidate for such applications given its low cost of production and near ubiquity in consumer goods in the form of paper, cotton, and wood products. In one particularly interesting demonstration of cellulose surface patterning, Wilke et al. employed laser printing to selectively introduce maleimide groups bound to modified cellulose-binding peptides (CBP).[348] Treating the printed paper with toner binding peptides (TBP) occluded maleimide attachment to printed regions. Subsequent photoclick reaction with bisaryl tetrazoles allowed for the patterned attachment of other peptides, suggesting the potential for this chemistry as a means of developing economical medical testing devices.

In addition to the functionalization of flat surfaces,[349] the tetrazole−ene reactions have also been used to surface-functionalize as well as to synthesize particles. Delafresnaye et al. used miniemulsion polymerization of tetrazole-containing acrylic monomers to generated microspheres with surface-pendant tetrazoles, allowing for the subsequent modification with alkenes or other nitrile imide-reactive groups.[350]

A significant challenge in modification of surfaces is obtaining a high surface density of the attached molecule. This is particularly difficult when attaching macromolecular structures to the surface. Increasing the functionality at the surface can often improve the density of attached groups following conjugation. That is, effectively, what employing thiol−yne chemistry accomplished in the previous example due to the higher effective functionality of the yne as compared to the ene. Another option is grafting pendant-functional polymers from the surface to provide a greater number of click groups relative to the area occupied. For example, ATRP has been used to graft a polytetrazole copolymer to the surface of gold, from which either maleimide modified biotin or additional ATRP initiators could be photoclicked to the backbone polymer for subsequent processes (streptavidin immobilization in the former case and ATRP grafting of bottle brush polymers in the latter).[351]

In one interesting example, of PhotoSPAAC-mediated surface modification, Arumugam and Popik used a heterobifunctional SPAAC and photoSPAAC reactive linker to perform consecutive click reactions (one spontaneous and one photomediated) to selectively attach BSA to the surface of azide-modified silicon dioxide particles.[352] In the first click reaction, the cyclooctyne reacts with surface azides, following which the cyclopropenone-protected cyclooctynes is irradiated to promote the coupling of the azide-modified BSA to the surface.

Also worth mentioning, the photochemically generated *o*-naphthoquinone methides have been employed in surface modification via one of two reactions: IEDDA with appropriate dienophile[353] or photoreversible Michael addition with a thiol.[106] Photomediated Michael additions have also been carried out at interfaces of materials via photogeneration of the Michael donor thiols as well. Hensarling et al. grafted functional polymers on silicon dioxide surfaces and then modified pendant groups with *o*-nitrobenzyl and *p*-methoxyphenacyl protected thiols.[238] Photodeprotection and reaction with maleimide or isocyanates was then carried out.

It may be desirable to generate complex, 3D structures with photopatterned or otherwise user-directed hetergenous surface chemistry. This may be the case particularly when attempting to mimic or recreate naturally occurring materials such as biological tissue that exhibits spatially complex architecture on multiple size scales, from the macroscale to the microscale and molecular scale. Here, again, employing photoclick chemistry allows unmatched control over not only the size and shape of the synthesized material, but also over its surface chemistry. Richter et al. demonstrated this by the direct laser surface modification by TPA-mediated photoenol DA click reaction on TPA-generated microstructures.[354]

3.5. Network Polymers

While photopolymerization is infrequently used (previously discussed exceptions notwithstanding) for the generation of linear macromolecules, it is a common method for the generation of cross-linked materials. While acrylic networks comprise the majority of thermosets generated via a photochemical means, some photoclick reactions do exhibit advantages for particular applications of photopolymerized thermosets. These benefits are intrinsically related to those features that make these reactions "click," namely their efficiency and their specificity. The one-to-one reactivity of functional groups dictates a delayed gelation, as described by Flory and Stockmayer.[355] Chain-addition polymerized thermosets may form gels at very low conversions. As soon as the gel point is reached, stress associated with shrinkage due to the reaction begins to accumulate while the diminished diffusion of reactants may result in a significant fraction of unreacted monomer that may subsequently be released from the material. Alternatively, networks polymerized via photoclick reaction between multifunctional thiols and alkenes, for example, form gels at conversions typically much higher in accordance with the functionalities of each reactant. A larger fraction of the reaction occurring prior to gelation allows materials to easily relax and accommodate any shrinkage associated with that conversion, resulting in materials with lower internal stress relative to comparable chain-addition cross-linked materials. At the same time, the delayed gelation and efficiency of the reaction mitigates the quantity of wholly unreacted como-

https://doi.org/10.1021/acs.chemrev.0c01212
Chem. Rev. 2021, 121, 6915−6990

nomers, decreasing the leachable fraction of the resulting materials.

However, not all photoclick reactions are well suited for network polymerization. To take advantage of these features, appropriate photoclick reactions generally must share additional characteristics as well. These include relatively small reactive groups, which otherwise may exert a disproportionate effect on the material properties, and a mechanism for photoamplification, which allows minimal light exposure to initiate the greatest number of reactions while mitigating the attenuation of light penetration through thick samples. Among photoclick reactions, the radically mediated thiol−ene, thiol−yne, photolatent base-catalyzed thiol-Michael, and photoCuAAC in particular exhibit these attributes.

3.5.1. Dental Restoratives. One application of photopolymerizations in the medical industry currently is the curing of dental restorative materials. While most commonly used resins are methacrylate-based, the use of step growth photoinitiated reactions, such as thiol−ene, thiol−yne, thiol-Michael, and photoCuAAC reactions have been studied as potential alternatives.[356−361]

Because of the high conversions of monomers and the regular network organization that their step-growth reaction provides, thiol−ene, thiol−yne, and thiol-Michael resins exhibit several features advantageous to their potential application in dental restoratives including reduced volumetric shrinkage, low development of shrinkage stress, delayed gelation, rapid reaction rates, formation of homogeneous polymer network with advantageous mechanical properties, narrow glass transition, and low leachable fractions. In dental restoratives, stress accompanying polymerization may cause cracking within the materials and is one of the major causes of failure in dental composites.[362] The delayed gelation and reduced volumetric shrinkage per bond reacted, both contribute to the significant reduction in the stress that arises in thiol−ene polymerization.[358,363−365] Despite these advantages, thiol derivatives are often accompanied by a disagreeable odor, which makes its use in this field problematic. Researchers have tried to overcome by preparing thiol functional oligomers and by employing secondary thiol derivatives, which reportedly lack the offensive odor of primary thiols.[363,366]

Another advantage in the application of thiol−ene chemistry for dental materials is the versatility of available chemistries. Water sorption and subsequent degradation of dental restoratives is a concern for materials made with hydrolytically susceptible methacrylate and other ester-containing monomers. The broad availability and ease of synthesis of thiol−ene monomers allows for the formulation of restoratives without such problematic bonds. A few examples of these include ester-free vinyl silanes, cyclotetrasiloxane-based thiol derivatives or vinyl sulfonamide, and vinyl sulfone based alkene derivatives.[358,361,364,366,367] Although methacrylate systems are associated with high shrinkage and stress, the mechanical properties of the resulting resins are difficult to match, and research is still underway to take advantage of thiol−ene, thiol−yne, and photolatent catalyzed thiol-Michael additions reactions for dental restoratives.

PhotoCuAAC reactions have also been explored for their potential in dental restorative materials. The reaction leads to materials with substantially increased material toughness relative to acrylic systems with similar Young's modulus, possibly due, in part, to hydrogen bonding and weak π stacking of the triazole rings.[368] The heat of reaction, however, is significant, and the reaction itself, while complete in as few as 3 min, lags behind that of thiol−ene reactions and the industry standard methacrylic systems, proving yet unresolved obstacles to the application of the chemistry in such a context.

3.5.2. Photolithography and Additive Manufacturing. In contrast to the photoCuAAC and photolatent-base catalyzed thiol-Michael reactions, the radically mediated thiol−ene and thiol−yne reactions are not dependent upon the generation of a catalyst, the persistence and diffusion of which continues to activate reactions even following termination of light exposure. The radicals generated from photoinitiation are, with minimal exceptions, short-lived and therefore reaction outside the limits of light exposure is greatly reduced. This behavior lends these reactions particular efficacy in light-patterned applications including photolithography and additive manufacturing.

Additive manufacturing technologies that employ photochemistry and photopolymerization include stereolithography (SLA) and digital light processing (DLP). In both cases, light exposure is used to polymerize monomer from a reservoir, layer by layer, to build up the desired or preprogrammed structure. While SLA employs a laser to write lines of cured resins and generally provides better spatial resolution, DLP writes plane by plane via projection of two-dimensional images and typically allows for faster printing. As with microfluidic devices and dental restoratives, low shrinkage stress and higher conversion (lower leachables) observed with step growth reactions are advantages to employing photoclick reactions, imparting better control over final dimensions of the printed structure.[369] Another advantage over the use of acrylic resins for 3D printed structures is the ability to generate materials capable of accepting postprinting modifications by the use of off-stoichiometric formulations. Curing with an excess of either reactant results in materials with residual functional groups that may be subsequently reacted with other compounds bearing their respective complementary reactive moieties. This approach enbles the production of materials where the bulk and surface properties may be independently and easily tuned for particular applications. Because the reactions are highly efficient, leaving a fraction of the unreacted moieties does not necessarily greatly increase the fraction of leachables in the printed materials. Ropollo et al. used this strategy while printing thiol−yne formulations to subsequently modify unreacted alkyne groups on the surface with an azide-modified dye.[370] While this demonstration only proved the concept, this approach could be used, for example, to apply a nonfouling surface treatment to printed biomaterials or to attach analytes to surfaces for biodetection or diagnostic purposes.

Achieving highly ductile 3D printed materials has proved challenging. As described previously, recently semicrystalline linear polymers have been prepared via thiol−ene polymerization. The high ductility exhibited by the bulk-polymerized material was, however, diminished in the printed materials. This drawback was overcome by generating low cross-linking density, semicrystalline networks made primarily with hexanedithiol and diallyl terephthalate with small fractions of cross-linkers, yielding 3D printed materials with superior ductility.[371]

The fast reaction kinetics of thiol−ene and thiol−yne photoclick reaction permits the retension of otherwise unstable materials' features. Complex microscopic and macroscopic heterogeneous features generated by phase separation in emulsions and foams can be preserved to create porous

https://doi.org/10.1021/acs.chemrev.0c01212
Chem. Rev. 2021, 121, 6915−6990

Figure 84. General procedure for photomasked image transfer for microfluidic device fabrication. A mask is placed over monomer mixture and exposed to light. Masked regions form channels and other negative features in the generated device.

structures with high surface area to volume ratios.[372,373] Bubbles, for example, generated in more slowly reacting monomer formulations, may merge or pop changing, the volume and density of bubbles in the final, polymerized material. The ability to quickly trap the bubble in place is especially advantageous to the 3D printing of foams, as demonstrated by Amato et al., who used direct writing of multifunctional thiol−ene monomer and initiator and a custom-designed shell−core nozzle to print foams with user-dictated cell size and density.[374] While photopolymerization of larger foam structures may be adversely affected by the scattering and diffusion of light due to the bubbles, this phenomenon is much less significant in the thin streams produced from the nozzle in this direct bubble writing setup.

Photopolymerized emulsions materials have been used in conjunction with additive manufacturing and stereolithographic techniques to generate microfluidic devices with porous, high surface area open cell scaffolds.[375,376]

The relatively low degree of light attenuation achievable with one photon, many event radical polymerization allows researchers and technicians precise control over the absorptive properties of liquid monomer formulations where depth of cure must be precisely tuned. While the photoamplification and small reactive moieties make thiol−ene and thiol−yne particularly attractive reactions for additive manufacturing, other photoclick reactions have also been employed.

In the case of multiphoton absorption-mediated reactions light attenuation is less consequential. The generally very low absorbance of the chromophores at the wavelengths employed generally allow for much greater depth of penetration of the high intensity IR or NIR light and effective reaction in only a minimal volume surrounding the laser focal point. This results in the ability to directly write, within monomers in a liquid or solution state, complex solid, 3D materials with extremely small features. This can be accomplished with photoinitiated systems (two-photon absorption has been employed in the direct writing of microstructures using the thiol−ene reaction[377−379] and acrylate chain addition polymerizations[380−382]) as well as with one photon, one event reactions such as the photo Diels−Alder reaction. In one representative example, Quick et al. employed direct laser writing of microstructures as described by using two-photon absorption at 700 nm to mediate the reaction between multifunctional *o*-quinodimethanes and maleimides.[383] This allowed the researchers to generate structures with features with spacing of 500 nm and allowed for subsequent surface modification via reaction with residual *o*-quinodimethanes.

The temporal control imparted by photomediated reactions can also allow for the generation of regular features while taking advantage of other pattern-generating phenomena. In one such example, Dickey et al. photopolymerized spontaneously generated pillars of thiol−ene monomer formulation, resulting from an electric field-induced force imbalance at the liquid−air interface.[384] While this is not an example of photolithography, this work does present an interesting related strategy, the use of patterned electrodes, to provided spatial control of the generation of the thiol−ene generated pillars.

While the topic of "bioprinting" certainly falls under the category of "additive manufacturing," due to its combining 3D printing technologies with hydrogel chemistry and techniques (described in some detail in section 3.5.5), this subject is presented subsequently in section 3.5.4.3.

3.5.2.1. Microfluidic Applications. A subset of additive manufacturing and photolithography that requires particular mention is microfluidics. While the field of microfluidics involves the study and manipulation of flow of very small volumes and has diverse applications from the design of fuel cells, inkjet printheads, and medical diagnostic devices, the fabrication of those devises is frequently accomplished via additive manufacturing and photolithographic techniques. Microfluidic devices themselves may be tools for the fabrication of monodisperse microspheres or microshells. Capable of mimicking the microfluidic capillary vascularization found in many organs, microfluidic devices have been especially valuable tools in biological research and tissue engineering.

The development of microfluidic devices requires the fabrication of microscale features (e.g., chambers of various dimension, narrow channels that branch or combine) to accommodate the precise transportation, mixing, and splitting of the fluids in question. Thiol−ene coupling reactions have been particularly effective in this area of research. An excellent review by Sticker et al. has recently been published describing the advantages and applications of thiol−ene coupling in microfluidic devices.[385] While there are several techniques for microfluidic fabrication, including casting[386] and 3D printing,[387] one of the most common is the transfer of patterns from a photomask to the device via photolithography (Figure 84).

Unlike many other photoclick reactions, thiol−ene coupling employs small functional groups that exert minimal influence on the mechanical properties of the resulting materials, allowing researchers to dictate those properties via inclusion of soft or rigid monomer cores or pendant groups to generate soft elastomeric materials or hard glassy materials tailored to the particular application of the device.[388−390] Additionally, as the thiol−ene reaction is performed with a diverse selection of thiols and alkenes, development of monomers with desirable attributes may be accomplished with more flexibility in the synthetic routes.

There are other reasons that thiol−ene reactions are particularly suited to microfluidic device fabrication. The

https://doi.org/10.1021/acs.chemrev.0c01212
Chem. Rev. 2021, 121, 6915−6990

photoamplification of radical initiation mitigates light attenuation, while radical termination minimizes the reaction rate of light-activated processes outside areas of illumination enabling precise spatial control. In addition, the delayed gelation of thiol−ene and thiol−yne networks, relative to (meth)acrylate networks, for example, mitigates the development of internal stresses in the material associated with shrinkage, which could cause deformation of device features.[389] These qualities have allowed researchers to generate high resolution channels, pillars and holes with high aspect ratios (∼14), a substantial improvement over acrylic counterparts.[391] Even higher resolution features are obtained with off-stoichiometric formulations as image transfer from the mask is improved by the diffusion of limiting reactant into the exposed area during curing, resulting in a depletion of that reactant in unexposed areas that reduces feature broadening.[392]

Another advantage of employing an excess of one reactant in the monomer formulation is the maintaining of unreacted functional groups following complete cure. These reactive groups bound to the network can be subsequently modified post device fabrication either by diffusing in compounds with the reactive complements or by conducting reactions at the surface of the material (discussed previously in section 3.4).[389] It should be noted, however, that in masked exposure, diffusion of the deficient reactant from unexposed to exposed regions can have a substantial effect on the concentration of functional groups at and near the surface.[392] In addition to allowing modification with chemically dissimilar compounds, the presence of reactive groups at the surface and in the bulk of microfluidic devices may facilitate more effective bonding of subsequent layers during device fabrication, mitigating the chance for solvent or stress mediated delamination.[386,393] This advantage can also be obtained by employing the temporal control of the photoclick reaction to arrest stoichiometrically balanced reactions before full conversion is reached.

Among the many various applications in this field, thiol−ene microfluidic devices have been used for the high throughput screening of immune cells,[394] the culturing of breast cancer spheroids,[395] mimicking intestinal barrier,[396] and the mechanical lysis of cells.[397] In a recent illustration of the versatility of the thiol−ene coupling reaction for microfluidic devices, ene-functionalized temperature-responsive NIPAM was grafted to the surface of a thiol-modified substrate to generate thermally actuatable gates within microfluidics channels for controlled sequestration and release in individual channels.[398] More recently, this versatility was demonstrated in the fabrication of an all-thiol−ene microfluidic enzyme reactor and electrophoretic separator for continuous sample preparation and direct analysis by mass spectrometry,[399] with these applications showing significant promise for thiol−ene photopolymers as materials for numerous lab-on-a-chip technologies with stimuli-responsive behavior to multiple inputs.

Although it shares many features with the thiol−ene reaction, thiol−yne couplings have been used considerably less in the field of microfluidics. This may be because of the moderately slower reaction. One potential advantage of the use of thiol−yne reactions in this area, however, would be the ability to maintain high cross-linking density in off-stoichiometric formulations. Moreover, with a faster second thiol addition, a large fraction of any excess alkyne would likely be maintained at full conversion, leaving a versatile reactive handle for postfabrication modification with another thiol−yne or azide−alkyne cycloaddition reaction.

3.5.3. Optical Materials. Incorporation of more polarizable atoms or groups into the polymer network is one of the well-established strategies to produce high refractive index polymeric materials.[400,401] Owing to the high intrinsic molar refraction of the sulfur atom, the polymers prepared by thiol mediated click reactions received considerable attention in the field of optical material development. Rapid and efficient thiol-X click polymerizations allow for the uniform incorporation of a large number of high refractive index sulfide linkages throughout the polymer network, resulting in photopolymers with high optical quality, thermal stability, and mechanical strength. Advantages of these polymers such as lightweight, low cost, ease of processing, and high impact resistance made them an interesting alternative to silicon and glass for optoelectronic applications. Furthermore, the step-growth mechanism of thiol-X photopolymerization results in polymer network with low intrinsic shrinkage stress with minimum leachable monomers and exceptional resistance to oxygen inhibition. While there exist several recent reports on high refractive index polymers based on radical thiol−ene reactions, a majority of these strategies rely on thermal or self-initiated polymerizations.[402−406] Incorporation of more polarizable groups such as P = S and P = Se and highly polarizable main group elements such as Si, Ge, Sn, etc., enabled these polymers to achieve a refractive index as high as 1.75 with excellent optical transparency.

Use of photoinduced thiol-X click polymerizations allows for the reaction to be performed under ambient conditions to achieve spatial and temporal control over various mechanical properties. For example, in 2003, Natarajan et al. demonstrated the formation of holographic reflection grafting in polymer-dispersed liquid crystals (H-PDLC), offering lower switching fields, higher diffraction efficiencies, better optical properties, and higher thermal stabilities. Upon forming refraction gratings at several wavelengths across the visible spectrum, diffraction efficiency reached up to ∼70% in the blue and green spectral region with no significant polarization dependence. Additionally, implementation of the thiol−ene chemistry reduced the nonuniform shrinkage of the film as a result of higher reactant conversions at much lower viscosities.[407,408]

Peng et al. explored the utilization of a unique sequential orthogonal strategy for two-stage thiol−ene click polymerization, in which an initial thiol−acrylate Michael reaction produced a loosely cross-linked photopolymeric substrate with excess thiol−allyl reactive species.[409] The presence of high-refractive index allyl monomer, 9-(2,3-bis(allyloxy)propyl)-9*H*-carbazole (BAPC), in the matrix allowed for large-index gradients to be developed within the network upon subsequent exposure to coherent laser beams and initiation of the radical-mediated thiol−ene reaction. Upon further investigation, allyl conversion during the thiol−ene reaction was attributed to relatively low volume shrinkage of only ∼3%. Moreover, such shrinkage is further alleviated by introducing additives such as cyclic allyl sulfides or nanoparticles. This novel two-stage system resulted in a holographic material with high Tg, high modulus, diffraction efficiency as high as 82%, and refractive index modulation of 0.004. The novelty and advantage of this two-stage approach lies in the elimination of traditional solvent processing methodologies; these reactions are also rapid and oxygen-tolerant without light scattering or microphase separation, resulting in good optical transparency.

Photoinduced thiol−ene click reactions have been used in UV nanoimprinting lithography application using high

https://doi.org/10.1021/acs.chemrev.0c01212
Chem. Rev. 2021, 121, 6915−6990

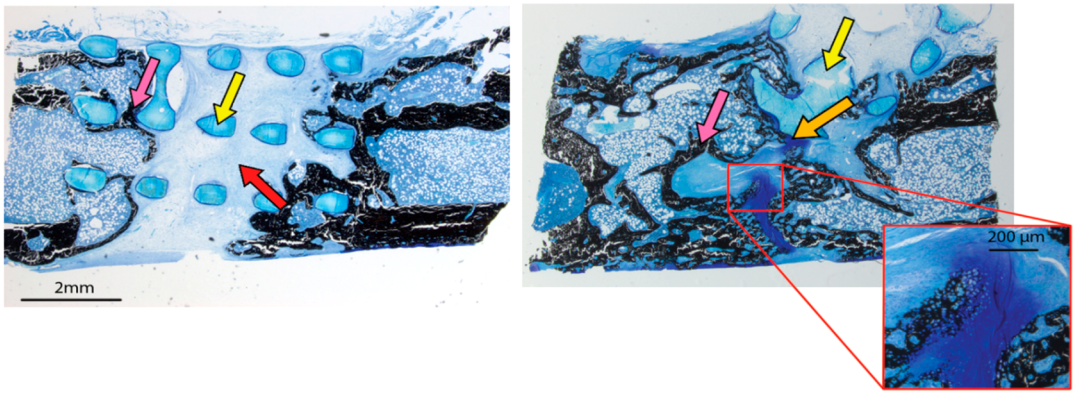

Figure 85. VonKossa MacNeil stained longitudinal sections of the femur defect area at 12 weeks. A sample bridged partially by fibrous tissue (left). A sample bridged by combination of bone and cartilage (right). The poly(propylene fumarate) scaffold stains light blue (indicated by yellow arrows), mineralized tissue stains black (indicated by pink arrow), cartilaginous material stains blue-purple (indicated by orange arrows), and fibrous tissue stains a light blue (red arrow). At the 12 week time point, there was no evidence of the thiol−ene hydrogel macroscopically or microscopically. Endochondral ossification of cartilage is highlighted in the expanded view of the sample on the right. Reproduced with permission from ref 426. Copyright 2019 John Wiley and Sons.

refractive index polythioethers prepared via the radical mediated thiol−ene click reaction of synthesized fluorene-based dithiol monomer with various ene monomers. The nanoimprinted patterns with various features on the order of 100−500 nm were successfully fabricated and characterized by SEM analysis.[410] More recently, McClain et al. carried out a viability study of thiol-ene click derived photopolymers in optical coating applications. A comparative study of optical, thermal, and hydrophilic character of these photopolymers formed by using a common tetrathiol (PETMP) with various multivinyl monomers via photoinduced thiol−ene polymerization resulted in transparent, high refractive index, hydrophilic materials that could be polymerized and molded. Within the comonomers tested, the thiol−ene polymers fabricated using divinyl comonomers showed greater optical transmission but low in refractive index than that of the thiol−ene polymers that contained tetravinyl comonomers.

Incorporation of nanoparticles such as silica nanoparticles in the holographic recording media greatly improved the optical, mechanical, and electrical properties along with leading to a significant reduction in the polymerization shrinkage. To this end, Hata et al. reported the volume holographic recording characteristics of silica nanoparticle−polymer composites using thiol−ene and thiol−yne photopolymer systems.[411,412] While these nanoparticle-(thiol−ene)polymer composites exhibited a high transparency and low shrinkage as low as 0.4−1%, their saturated refractive index modulation were found to be 0.01 and 0.008 for thiol−ene and thiol−yne systems, respectively, and meet the acceptable values for holographic data storage media.

More recently, Alim et al. developed a highly modular synthetic strategy to produce multifunctional thiol and ene monomers with high refractive index cores containing aryl and sulfide groups.[413] The advantage of these low viscosity liquid monomers (<500 cP) with high refractive indices (n_D/20 °C ∼ 1.64) and high optical quality have been demonstrated by fabricating an aspherized plano-convex lens by an overmolding procedure to increase the optical power and numerical aperture. Furthermore, a high-performance holographic recording medium developed by these thiol and ene monomer formulations resulted in a holographic material with high dynamic range of 0.04 with haze as low as 0.2%.[195]

As the refractive index of the thiol-X network is directly proportional to the sulfur content, incorporation of more sulfide linkages by using analogous thiol−yne systems significantly enhances the refractive index development.[414] In combination with orthogonal thiol-Michael addition click reactions, Peng et al. employed the sequential photoinduced thiol-Michael/thiol−yne click polymerization approach to implement direct image patterning with high diffraction efficiency (96%) and index modulation of 0.004 with low volume shrinkage (1.1%).[415]

3.5.4. Hydrogels and Tissue Engineering. *3.5.4.1. Hydrogel Synthesis.* Hydrogels are highly swollen polymer networks that have become useful platforms to study a wide variety of biological systems in vitro and as injectable scaffolds in vivo.[416] The use of light-activated click reactions has allowed for control over the rapid synthesis of hydrogel networks, enabling precise spatiotemporal control over network formation and for the introduction of biomolecules.[417] One of the most popular uses of photoclick hydrogels is for the three-dimensional (3D) encapsulation of cells permitting them to experience a 3D environment which more closely resembles their native extracellular matrix (ECM), allowing researchers to have a better model to understand cell−cell and cell−matrix interactions. With the use of low energy wavelengths of light, photoclick hydrogels have also become popular vehicles for the delivery of biologicals and as platforms to precisely pattered hydrogels with both peptides and proteins. Spatiotemporally controlled hydrogels and their applications in regenerative medicine have been recently comprehensively reviewed by Brown and Anseth.[418] Here, we describe various photoclick reactions that have been used for hydrogel synthesis (e.g., thiol−ene, thiol−yne, thiol-Michael, and tetrazole−ene) and highlight the power of light for their fabrication and for photopattering.

The photoclick thiol−ene reaction has become one of the most popular methods for the synthesis and post modification of hydrogels over the past decade as demonstrated by these recent reviews.[417,419−421] The popularity of the reaction is owed to its many advantages: (1) the thiol−ene step-growth polymerization reaction is frequently preferred over chain-growth polymerization reactions as it allows for the formation of more homogeneous network and is not inhibited by the

https://doi.org/10.1021/acs.chemrev.0c01212
Chem. Rev. 2021, 121, 6915−6990

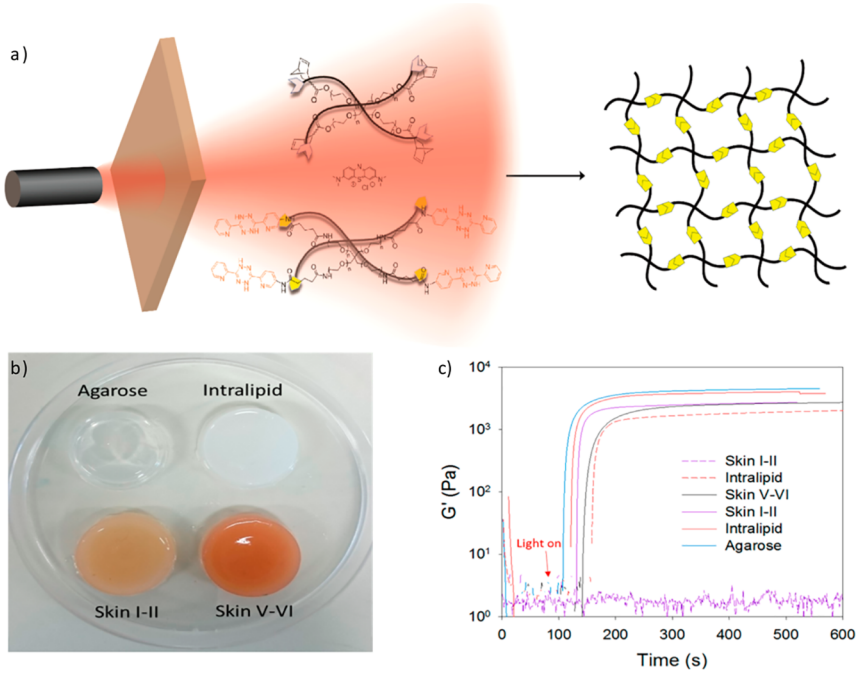

Figure 86. (a) iEDDAC network formation using red light. (b) Picture of agarose gels used as a dermal model. (c) Change in the storage modulus with the exposure to light. Reproduced with permission from ref 42. Copyright 2017 American Chemical Society.

presence of oxygen.[45,422] Therefore, minimal photoinitiator concentrations may be employed leading to a lower concentration of radicals in the presence of cells, improving cytocompatibility, and enabling the encapsulation of cells, tissues, and proteins.[423] (2) The hydrogel formation rate is tuned in various ways by using a range of different photoinitiators, wavelengths of light, light intensities, and photoinitiator concentrations. (3) Facile incorporation of peptides and proteins as cross-links and pendant bioactive moieties is possible via utilization of cysteine thiols. Through the use of photoclick reactions, these fabrication methods are highly tunable and applicable to ranges of cell lines and applications. These advantages allow for milder conditions to be used for encapsulation and lower cell densities compared to chain growth reactions. Recent work using thiol−ene hydrogels has demonstrated the use of these materials for a variety of exciting applications for cartilage development, antimicrobial surfaces, and as controlled drug delivery vehicles (Figure 85).[424−428]

It should be noted that the thiol−ene reaction cannot strictly be considered perfectly biorthogonal as the alkene readily reacts with a thiol-containing natural amino acid, cysteine. However, the natural abundance of cysteine is low and is normally present as disulfides so does not interfere significantly with hydrogel synthesis.[429]

In comparison to its thiol−ene counterpart, the photo-triggered radical thiol−yne reaction has received dramatically less attention as a route to synthesize biomaterials. Through the use of the thiol−yne reaction, the alkyne is able to undergo two consecutive thiol additions to form a dithiol adduct. There are a few accounts of the thiol−yne reaction for hydrogel synthesis. One example demonstrated by Daniele et al. shows the synergistic effects of the step growth and chain growth polymerization reactions.[430] They use a tetrafunctional PEG thiol−yne system with a gelatin methacrylate to tune the characteristics of the interpenetrating network. They state that this system allows for a more representative mimic of the ECM as it mimics the more complex structure and behavior. Although this system does not exploit the advantages of using photoclick reactions, it highlights the ability for this reaction to work alongside other photopolymerization reactions.

Recent advances in the Michael-type thiol−yne reaction have demonstrated the nucleophilic addition reaction with activation using green light. Truong and co-workers have utilized boron−dipyrromethane (BODIPY) moieties with pendant thioether groups that undergo photolysis in the presence of green light (λ = 530 nm) excitation.[431] The liberated free thiolate ion can then undergo a nucleophilic addition with an activated alkyne to form an alkene thioether with controlled stereochemistry. The authors demonstrated this photoclick reaction for hydrogel synthesis using star PEG macromers functionalized with either the BODIPY thioether or alkyne groups, which rapidly forms a hydrogel upon irradiation of light (λ = 530 nm, 30 mW cm^{-2}). The green-light-induced ligation has been shown to pattern hydrogels and for cell encapsulation, demonstrating the low toxicity of green light.

Although the tetrazole−ene reaction has been used extensively for labeling proteins and for molecular probes, it has not been significantly used for hydrogel fabrication. Zhong and co-workers used the reaction to synthesize hydrogels, demonstrating rapid gelation times with low energy light, an advantage of this photoclick reaction.[432] A unique characteristic of these hydrogels is their fluorescent nature through the formation of a pyrazoline ring, aiding the imaging of photopattered regions but could hinder the imaging of cellular structures. The reaction has also been used to modulate self-assembled hydrogels through stacking of short peptide chains with tetrazole functionality.[433] In this study, the tetrazole−ene reaction is used to modulate the properties of the hydrogel with encapsulated hMSCs.

https://doi.org/10.1021/acs.chemrev.0c01212
Chem. Rev. 2021, 121, 6915−6990

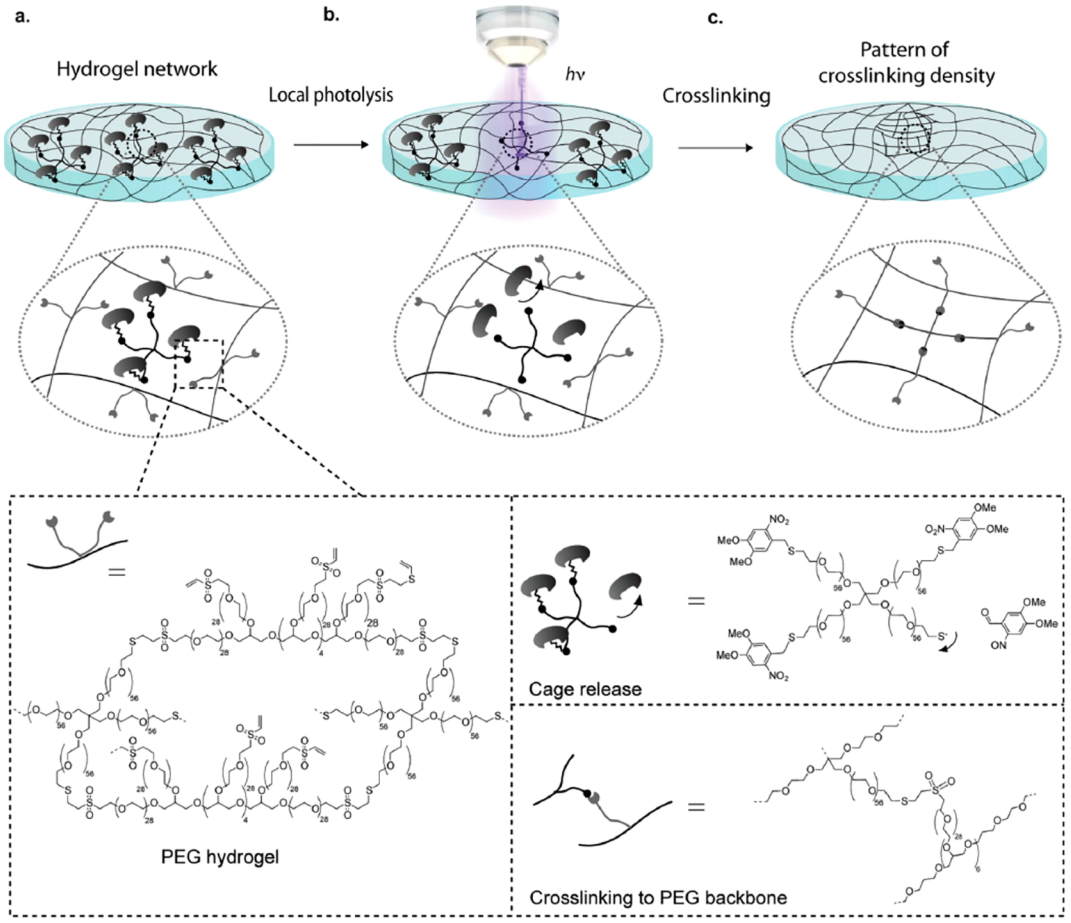

Figure 87. Concept of light-mediated Michael-type addition for spatiotemporally controlled hydrogel cross-linking: (a) a thiol-containing macromer is protected with photolabile caging group and is dissolved in a hydrogel network comprising free vinyl sulfone groups; (b) localized laser illumination causes photocleavage of the caging groups reactivating thiols; (c) activated thiol-containing PEGs react to vinyl sulfone via Michael-type addition reaction creating localized stiffness patterns. Reproduced with permission from ref 445. Copyright 2012 Royal Society of Chemistry.

Although most photoclick reactions utilize UV light, it is not the optimal wavelength to use for biological applications as the high energy wavelengths are damaging to peptides, enzymes, and DNA. For photoclick reactions to become more widely used in biomedical applications, the low energy, long wavelengths of light should be used. The optical therapeutic window is between 600 and 900 nm, where there is minimal adsorption of light by water and tissue. Truong et al. addressed this issue by using 625 nm light for the catalytic activation of IEDDA under physiological conditions (Figure 86).[42] They used multiarm PEGs functionalized with tetrazines and norbornenes and demonstrated the in situ hydrogel formation behind dermal tissue models, suggesting that the system could be used as a controlled injectable hydrogel model into skin. The group stated that this method would allow for better control over gelation than spontaneously forming gels, as the longer wavelengths of light could penetrate deeper into the tissue without damage.

Adzima et al. were the first to demonstrate the synthesis of hydrogels using photoinitiated copper catalyzed azide−alkyne cycloaddition reaction (photo-CuAAC).[434] Cu(II) was reduced to Cu(I) through radicals generated by a photoactivated initiator. Gelation between a multi-arm PEG azide and PEG dialkyne then took place in a controlled manner only in areas which had been exposed to light. By using an excess of alkynes in network formation, the researchers demonstrated in situ fluorescent photopattering through the addition an azide fluorophore. Using this technique, they determined that 25 μm features could be formed with this technique with 50 s of irradiation. This photoclick reaction combined the advantages of CuAAC reactions (i.e., bioorthognal and fast reaction kinetics) and may mitigate its significant drawback, the toxicity of Cu(I), by photogenerating Cu(I) only in user-designated regions. However, as the reaction still relies on the use of Cu(I) catalyst, other photoclick reactions with lower toxicity levels are still preferential for biomaterial applications. This preference notwithstanding, this photoclick reaction has recently been implemented in the synthesis of shape memory hydrogels.[435] The click nature of the reaction allowed for facile control over the thermoresponsive units feed ratio, controlling the mechanical properties of the hydrogel above and below the LCST.

3.5.4.2. Post-cure Modification of Hydrogels. An important application of synthetic hydrogel scaffolds is to create ECM mimics. The ECM is dynamic and responsive to external stresses from the surrounding environment, including increased stiffness with disease progression. To observe these dynamic processes in vitro, hydrogels have been created that respond to external stimuli (e.g., the stiffening of a scaffold to mimic disease progression). Light has been used as an external

https://doi.org/10.1021/acs.chemrev.0c01212
Chem. Rev. 2021, 121, 6915−6990

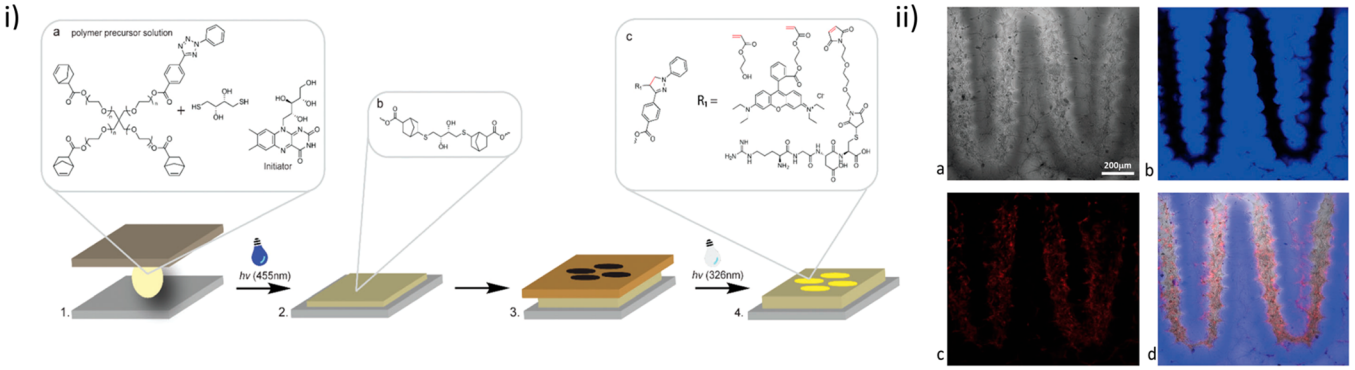

Figure 88. (i) General procedure for the fabrication and functionalization of the PEG-based hydrogels: (1) Precursor solution placed between a methacrylate functional glass slide and PDMS cover; (2) irradiated under blue light to obtain the cross-linked gel; (3) gel swollen with acrylate solution and photomask placed on top; (4) irradiated under UV light to obtain patterned sections (a) hydrogel precursor solution and 1:1 equiv of DTT and norbornene moieties, (b) cross-links consist of a double thioether linkage, and (c) chemistry of the photopatterned areas. (ii) Surface adhesion of NHDF cells: (a) DIC image of NHDF cells after 24 h incubation on the hydrogel surface; (b) fluorescence confocal image of the photopatterned section of the gel (photopatterned areas appear black); (c) fluorescence confocal image of NHDF cells stained with propidium iodide; (d) Merged image of (b) and (c). Reproduced with permission from ref 447. Copyright 2018 Royal Society of Chemistry.

stimulus to increase the stiffness in hydrogels by increasing cross-linking density through various light activated reactions. In particular the radical thiol−ene reaction has been used to in situ stiffen hydrogel materials to mimic disease progression.[436−438] Mabry et al. showed that in situ stiffening hydrogels using subsequent thiol−ene cross-linking enabled a better understanding of myofibroblast to fibroblast transition.[439] Discrete regions of stiffness are also created in hydrogels to further explore mechanobiology.[440−442] The discrete nature of the light activated reaction allows for remarkable control over the stiffness of the material.[443] The popularity of the thiol−ene reaction for postmodification of hydrogels reflects the reputation of this reaction for hydrogel fabrication and the subsequent ease of using these reactive handles for postmodifications.

In situ generation of reactive thiolate functionalities coupled with subsequent thiol-Michael click reactions has been used to control local stiffness in space, time, and intensity of hydrogel matrix.[444,445] To this end, Mosiewicz et al. combined phototriggered uncaging chemistry and subsequent Michael-addition click reaction to spatiotemporally control the physical properties by tuning the cross-linking density of a poly(ethylene glycol) (PEG) hydrogel network, which directly translated to highly localized stiffness patterns of broadly tunable shape and stiffness range (Figure 87). Using this approach, user-defined stiffness patterns in a range of soft tissue microenvironments (i.e., between 3 and 8 kPa) were obtained and shown to influence the migratory behavior of primary human mesenchymal stem cells (hMSC).

Perhaps one of the most popular and valuable postmodification applications of hydrogels is the ability to photopattern proteins and small molecules into the network after formation. The use of photoclick reactions for this process affords spatial control of ligand immobilization through the use of photomasks and the discrete nature of light. In addition, the use of photoclick reaction after cross-linking allows for attachment of sensitive moieties in a homogeneous manner and with high resolution control over patterning.[43] As mentioned in the hydrogel fabrication section, the ability to add cysteine pendant peptides into thiol−ene hydrogel networks has been demonstrated many times to allow for cell adhesion and motility.[446] The use of the thiol−ene reaction for the controlled presentation of biomolecules in hydrogels was reviewed by Grim et al. and highlights the ability to use the reaction for biomolecule patterning and the subsequent photocleavage patterning and reversible patterning that can achieved with these hydrogels.[417]

Hydrogels can also be photopattered through the combination of two photoclick reactions. Batchelor et al. used a thiol−ene reaction to form a hydrogel network and a subsequent tetrazole−ene reaction to further functionalize the hydrogel with peptides to encourage cell attachment (Figure 88).[447] They exploit the use of the self-reporting fluorescent pyrazole ring to show successful ligation of the peptide. The researchers also used riboflavin instead of LAP as the photoinitiator in the thiol−ene reaction to enable the use of visible light (455 nm) to initiate the reaction and UV light (326 nm) to activate the tetrazole−ene reaction. Through the use of lithographic techniques, the hydrogels were functionalized in a spatially resolved fashion, allowing selective cell adhesion in the irradiated sections.

Recently, in 2020, Ma et al. have used the thiol−yne reaction alongside SPAAC and iEDDA photoclick reactions to photopattern proteins into hydrogel networks.[448] The system was used to study the interactive effects of proteins, in particular, transforming growth factor beta (TGF-β), bone morphogenic protein 2 (BMP-2), and fibroblast growth factor 2 (FGF-2), on valvular institute cells (VICs) activation as a model platform to further understand the aortic valve niche. The authors were able to use the photoinitiated thiol−yne reaction to sequentially incorporate moieties for protein immobilization. The thiol−yne reaction was the only choice for this work to allow for the reaction to take place without interfering with the other click reactions, SPAAC and IEDDA.

Spatiotemporally controlled release of caged thiols also promoted specific immobilization of biomolecules including photopatterning.[449] For example, in their earlier studies, Shoichet and co-workers used *S*-2-nitrobenzyl protected cysteine to create spatially defined protein patterns in agarose-based 3D hydrogels by selectively activating the thiol functional groups for thiol−maleimide mediated biomolecule conjugation.[450,451] For this purpose, the pendant primary hydroxyl groups on the dissolved agarose were modified with *o*-nitrobenzyl protected cysteine using carbodiimide coupling

https://doi.org/10.1021/acs.chemrev.0c01212
Chem. Rev. 2021, 121, 6915−6990

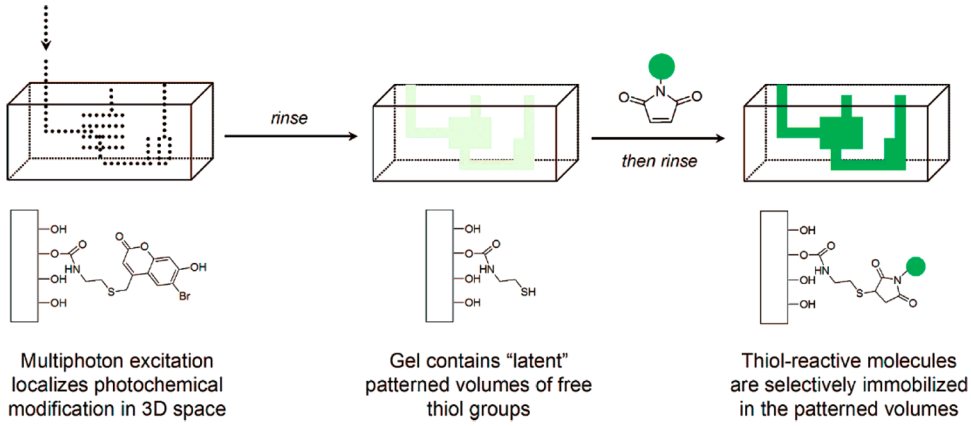

Figure 89. Schematic representation of multiphoton chemical patterning in hydrogel. Reproduced with permission from ref 452. Copyright 2008 American Chemical Society.

chemistry. After the gelation, the photocaged agarose gels were irradiated with 266 nm UV light to release free thiolate functionalities, which were used to immobilize maleimide-functionalized peptides or proteins via a subsequent via thiol-Michael click reactions only at the irradiated regions.

Shoichet and co-workers used 6-bromo,7-hydroxycoumarin sulfide modified agarose hydrogel for highly efficient 3D patterning of maleimide modified Alexa Fluor 488 and other biomolecules without causing any cross-linking or change in physical properties of the hydrogel (Figure 89).[452] The uncaging of the nucleophilic thiolate functionalities was achieved upon irradiation with UV or pulsed multiphoton excitation.

In another work, the authors modified an agarose matrix with the same photolabile 6-bromo-7-hydroxycoumarin-protected thiols in order to photopattern the conjugation of maleimide modified human serum albumin (HSA-maleimide).[453] After binding the HSA to the matrix, FGF2 was immobilized by forming stable complex with ABD fusion protein with the photopatterned HSA.

In another example, Liu et al. demonstrated a highly cytocompatible gelation approach to fabricate 3D ECMs with precisely controlled size, shape, and stiffness via light-controlled thiol-Michael addition cross-linking.[454] In this approach, the authors used a methacrylate copolymer containing pendant macrocyclic 7-amino coumarin-caged thiol and polyethylene glycol side chains. Upon photoexcitation, intramolecular photouncaging of macrocyclic coumarin caged thiol and subsequent reaction of liberated free thiols with multifunctional PEG maleimide produced 3D hydrogels. The combined use of 7-amino coumarin and nitrobenzyl caging groups for thiols was thus used for wavelength selective release of free thiols in a one-pot reaction approach. For example, Liu et al. used the different excitation of coumarin and nitrobenzyl phototriggers at 420 nm and at 365 nm, respectively, to achieve wavelength-selective photodeprotection of thiols at different locations on the same polymer backbone.[455] The different thiols generated this way were used for the bioconjugation of two different functional materials (QDs and proteins) on the same polymer chain to produce QDs−polymer−protein conjugates in one pot (Figure 90).

The authors used a well-defined, hydrophilic polymethacrylate block copolymer in which 7-amino-coumarin and *o*-nitrobenzyl phototriggers were used to protect the end- and

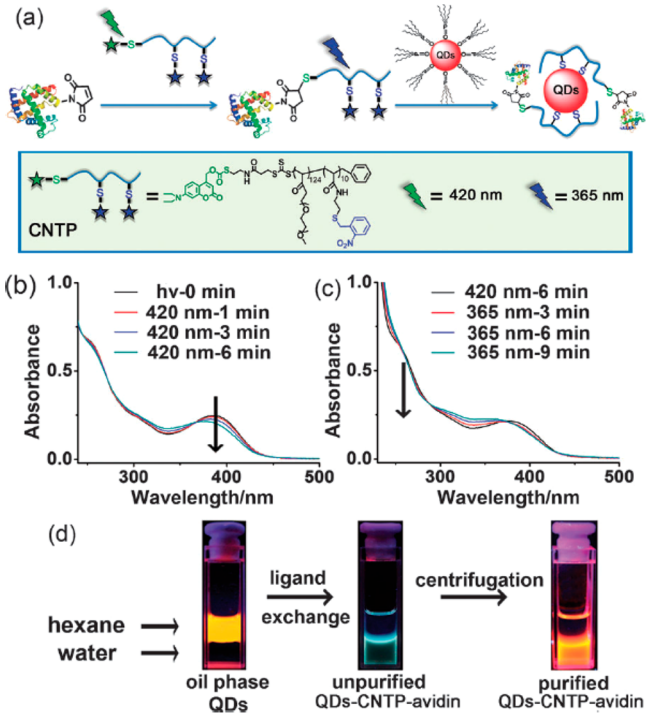

Figure 90. (a) Schematic representation of sequential photorelease of thiols and bioconjugations with protein and QDs in a one-pot process. (b,c) UV−vis spectra of CNTP (PBS, pH = 7.4) upon 420 nm irradiation and followed by 365 nm irradiation. (d) Pictures are TOPO-QDs, unpurified QDs−CNTP−avidin, and purified QDs−CNTP−avidin after centrifugation (from left to right). Reproduced with permission from ref 455. Copyright 2014 Royal Society of Chemistry.

pendant-thiols, respectively. Upon excitation at 420 nm, the absorption of the 7-amino-coumarin phototrigger caused the release of thiol at the end of the polymer chain to trigger the subsequent reaction with maleimide functionalized protein, whereas the *o*-nitrobenzyl phototrigger remained intact. Following this reaction, the exposure to 365 nm light photo released the pendant thiol functionalities via niitrobenzyl photocleavage and subsequently captured the QDs from the oil phase by ligand exchange.

Surface patterning of hydrogels has also been shown using the photoinitated CuAAC reaction. Chen et al. used Irgacure 2959, $CuSO_4 \cdot 5H_2O$ to surface pattern a PEG hydrogel on an

https://doi.org/10.1021/acs.chemrev.0c01212
Chem. Rev. 2021, 121, 6915−6990

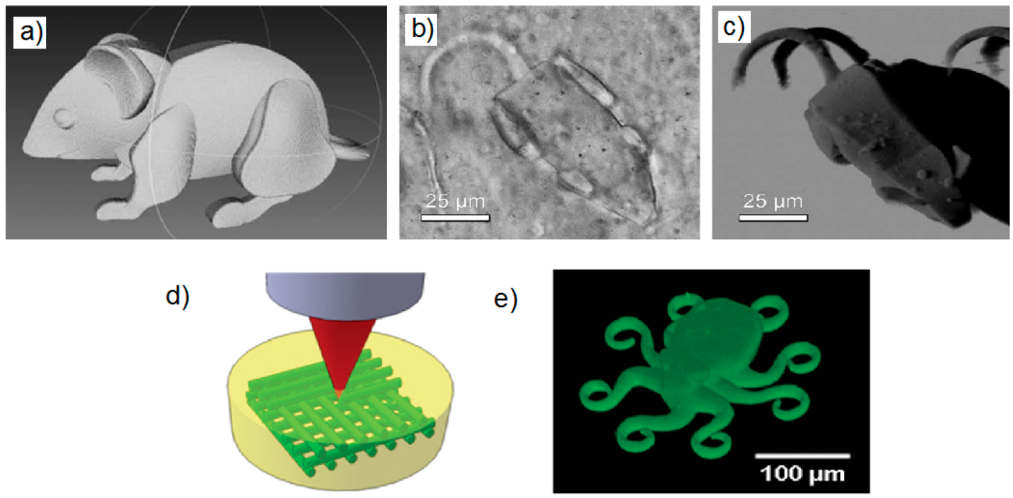

Figure 91. Mouse as a test structure: (a) CAD model, 3D printed N19T06-060 visualized by (b) light microscope and (c) laser scanning microscope using PVA thiol−ene material. Adapted with permission from ref 465. Copyright 2016 John Wiley and Sons. (d) Schematics of the 2PP microfabrication. (e) *z*-Stacked laser scanning microscope image of a 3D "octopus" construct produced by 2PP of HA-VE/DTT. Reproduced with permission from ref 464. Copyright 2014 Royal Society of Chemistry.

azide-functionalized surface.[456] This approach allowed the researchers to control the thickness of the hydrogel and modulate cell attachment using a photomask and UV irradiation.

The photoSPAAC reaction has also been used to pattern hydrogels. Bjerknes et al. selectively labeled hydrogels through incorporation of a cyclopropenone-caged cyclooctyne.[457] The authors demonstrated the uniformed labeling of the network using 365 nm light and an azide functionalized dye, displaying the reaction as a powerful photopatterning tool.

Photopattering hydrogels with photoclick reactions has been demonstrated for a range of applications and cell types, albeit with a significant focus on thiol−ene reactions. Although the area has focused on this reaction, as a consequence of their accessibility and ease of synthesis, the full spectrum of photoclick reactions could be applied to this application. It is envisioned that as the full range of photoclick reactions are increasingly used in hydrogel synthesis, they will also find applications in the orthogonal control of heterogeneous mechanical and biochemical properties of biomimetic hydrogels.

3.5.4.3. Bioprinting. Photoclick reactions lend themselves to applications in bioprinting as a consequence of their biorthogonal nature and spatiotemporal control. Over the past decade, chain growth polymerization reactions have dominated the field, especially through the use of gelatin methacrylate. However, this type of polymerization is affected by oxygen inhibition, heterogeneous polymer networks, and complex polymerization kinetics.[458] In recent years, photoclick reaction has been seen as an alternative route for bioprinting. The thiol−ene, thiol−yne, and thiol-Michael reactions have been used for extrusion-based printing and stereolithography as the step-growth nature of the reactions forms homogeneous polymer networks at high yields with rapid reaction rates.[156]

The thiol−ene reaction is becoming commonly adopted for bioprinting, as its significant advantages over radical chain polymerizations are becoming evident in various applications. Blood vessel-like structures have been printed through cross-linking thiolated hylaronic acid with 4-arm PEG tetra acrylates. The authors used extrusion-based printing enabling the encapsulated of NIH 3T3 cells within the printed tubular tissue constructs. The culture was viable for 4 weeks and demonstrated the feasibility of building controlled bioartificial constructs through the use of light.[459] Norbornene functionalized alginate cross-linked with PEG dithiol has also been used to print scaffolds with ATDC5 and L929 cells.[428] Through the use of the thiol−ene system, they were able to also incorporate a thiol functionalized RGD sequence to improve cell adhesion within the construct.

More recently, Bertlein et al. and Stichler et al. have used thiol−ene biofabrication technology to create scaffolds.[460,461] Stichler used a synthetic poly(allyl glycidyl ether-*co*-glycidyl) (P(AGE-*co*-G)) and poly(glycidol) to create hydrogel precursors with alkene and thiol groups, showing an example of biofabrication with a PEG-based system. The structures were cytocompatible through the use of the photoclick reaction and showed good reproducibility. In 2018, the Burdick group demonstrated 3D extrusion bioprinting of single and double network hydrogels with dynamic covalent cross-links.[462] The authors successfully printed a hyaluronic hydrogel with shear thinning behavior owing to the hydrazine chemistry of the network. The second network used a photoclick reaction and was composed of a norbornene functional hyaluronic acid combined with a tetrathiol cross-linker. This thiol−ene system allowed for patterning and increased mechanics of the original network as a consequence of the spatiotemporal control that the photoclick reaction enables. Although these techniques demonstrate a range of materials and applications of 3D bioprinting, they are restricted to low resolution. Liska and co-workers demonstrate the versatile of alkenes and thiols for two-photon microfabrication, demonstrating that gelatin-vinyl esters, reduced bovine serum albumin (BSA), DTT, or PVA-thiols can be used for biofabrication (Figure 91).[463−465] Recently, Dobos et al. reported the use of a photoclick reaction for lithography-based approaches to enable the production of intrinsic architectures and complex geometries.[466] The group used two-photon polymerizations for submicrometer spatial resolution to print norbornene functionalized gelatin cross-linked with dithiolthreitol (DTT). This was the first example of two-photon polymerization processing while maintaining cell

https://doi.org/10.1021/acs.chemrev.0c01212
Chem. Rev. 2021, 121, 6915−6990

viability, which had previously only been obtained with gelatin methacrylate.

Overall, the photoclick thiol−ene systems offers many advantages to biofabrication, including the ability to form more homogeneous networks in comparison to chain growth polymerization reactions, which are currently widely used in this area. The benefits of this system suggest that it will be used more widely in the future especially for cell laden materials.

The thiol−yne reaction has not been used to its full potential in bioprinting. One rare example was reported by Skardal et al., who used thiol−yne chemistry to form a secondary cross-linking network to form a stable hydrogel structure after printing.[467] The group first used a thiol−acrylate system that reacted spontaneously to form a soft extrudable gel to bioprint. They then added a PEG alkyne and used UV light to photoclick the networks together and increase the stiffness of the network to match tissue (100 Pa to 20 kPa). The use of the thiol−yne reaction here exploits the bifunctionality of each alkyne, enabling a rapid controlled increase in strength. They highlight that the modular nature of this hydrogel bioink could be adapted for multiple tissue types.

Although most of the photoclick reactions have been employed in hydrogel fabrication, they have not been applied to 3D biofabrication. This includes thiol-Michael, photo-strained promoted azide−alkyne cycloadditions, and tetrazole−ene.[468] While diffusion of photoliberated base catalyst in thiol-Michael reactions may mitigate, in some bioprinting applications, the spatial control over the reaction, the spatial resolution offered by nonphotoamplified reactions would seem to be a good fit for such photomediated 3D printing techniques, providing adequate depth of cure for the printing techniques employed. In contrast to the fabrication of thicker materials, the relatively high chromophore concentrations and consequent light attenuation would not preclude the application of such chemistries in thin layers. It is speculated that these reactions have not been used for biofabrication because of the synthetic challenges the precursors present. Many of these photoclick reactions are not commercially available and require many synthetic steps to reach the desired product. The cost and yield of these reaction also prevents large quantities of these reagents to be synthesized. This limits the reaction's use in bioprinting as this application often requires large amounts of reagents. With the increase in popularity and the improvement in commercial availability of easily coupled photoclick moieties, the spatiotemporal advantages of these reactions may be more fully recognized in 3D bioprinting.

3.5.5. Microparticles and Nanoparticles. Polymeric microparticles have broad utility in materials science. They are used in paints and coatings, adhesives, cosmetics, solid supports for chemical syntheses, biomedical diagnostics, drug delivery, as well as many other fields.[469] As described previously, photoclick reactions, including thiol−ene and tetrazole−ene reactions, have been used effectively to modify the surface of microparticles, allowing independent dictation of the surface and bulk chemistry, respectively. Photoclick reactions may also be used to generate microparticles. There are a variety of means of synthesizing microparticles, including emulsion polymerization and microfluidic formation of monomer microdroplets. The quality of the microparticles obtained via these methods is diminished if the polymerization is slow, allowing droplets to fuse or emulsions to break. Rapid rates of reaction make thiol−ene and thiol−yne reactions especially effective in such processes. Microfluidic devices, discussed previously, also provide a means to generate highly uniform droplets of monomer that can be rapidly photocured to create highly uniform microparticles.

This discussion of microparticles and nanoparticles is divided into a description of those materials with relatively high cross-linking density and highly swollen microgels and nanogels.

3.5.5.1. Highly Cross-linked. Some of the earliest work on thiol−ene and thiol−yne microparticles was performed by Prasath et al., who synthesized a variety microparticles by photopolymerization of monomer droplets passing through microfluidic channels.[470] Monomer formulations included a tetrathiol and mono and multifunctional alkenes or alkynes along with a photoinitiator and, in the synthesis of porous microparticles, a porogen. Hydroxy and amine containing alkenes and alkynes permitted subsequent surface attachment, suggesting potential for use in solid-supported chemical synthesis. Similar microparticles with thiol−ene and thiol−yne photoclick reactions have been obtained by Shipp and co-workers[471,472] as well as Gao and co-workers[473] via suspension polymerization, a process generally perceived as more scalable than microfluidic fabrication. Alimohammadi et al. have also used dispersion polymerization, in which a homogeneous solution of monomers phase separates into solvent and microparticles during polymerization, to generate microspheres via thiol−ene and thiol−yne photoclick reactions.[474] Photobase mediated thiol-Michael click reactions have similarly been used to generate very narrowly disperse microparticles via dispersion polymerization.[475]

Tetrazole−ene reactions have also been used to synthesize particles which can be modified postsynthesis. For example, Hooker et al. used tetrazole−alkene reactions to generate surface functionalizable microspheres via the off-stoichiometric cross-linking reaction between complementary tetrazole and acrylate-bearing polystyrene chains,[476] an extension of the groups work generated surface-funtionalizable nanospheres via radical polymerization of acrylic-modified, photoclickable tetrazoles, discussed earlier.[350]

Recently, Barner-Kowollik and co-workers have also developed highly uniform microparticles using Diels−Alder photoclick chemistries (section 2.2.1).[477] The group has also utilized a self-reporting Diels−Alder photoclick reaction between *ortho*-methylbenzaldehydes and electron deficient alkynes using UV light (λ = 320 nm) to generate fluorescent microparticles,[478] a system which that group has pioneered.[40] By using visible light (λ = 525 nm), they were also able to synthesize narrow disperse microparticles using a naphthalene−triazolinedione [2 + 4] photocycloaddition reaction.[479] The group has highlighted the flexibility of the Diels−Alder reaction for the synthesis of materials with small dimensions using a range of different wavelengths of light, highlighting the versatility of these Diels−Alder cycloaddition reaction.

3.5.5.2. Microgels and Nanogels. Water swollen microgels (typically 1−350 μm) and nanogels (typically 20−250 nm) have become popular biomaterials for applications in drug delivery, bionanotechnology, and biomedical implants.[480] Because of their hydrophilic network, nanogels and microgels exhibit high swelling, good biocompatibility, and defined mechanical and diffusional properties.[481] This allows for precise loading and release profiles, which can be further tuned by degradation and postmodification reactions.

https://doi.org/10.1021/acs.chemrev.0c01212
Chem. Rev. 2021, 121, 6915−6990

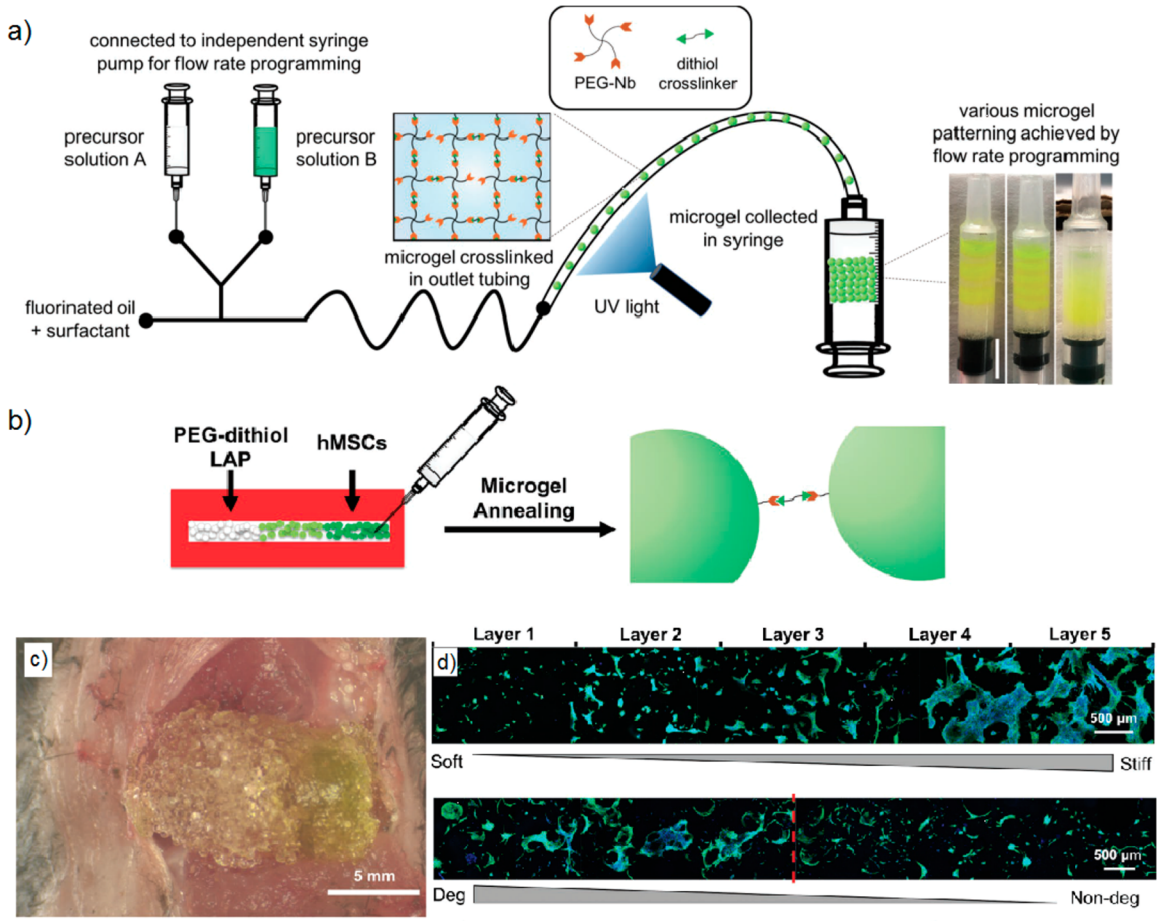

Figure 92. (a) Schematic of the microfluidic device-based microgel production procedure. (b) Schematic illustrating microgel extrusion into a 3 mm rectangular mold and microgel annealing into scaffolds. (c) Image showing gradient MAP scaffolds injected into a mouse femoral defect. (d) *Z* projection images of hMSC proliferation and spreading in MAP scaffolds with either a stiffness gradient (top) or a degradability gradient (bottom). Green represents F-actin and blue represents nuclei. Reproduced with permission from ref 485. Copyright 2020 John Wiley and Sons.

The thiol−ene reaction was first used to make nanoscale hydrogels in 2014 using the aqueous cavity of a liposome to act as a nanoreactor.[482] Hachet et al. demonstrated the synthesis using norbornene functionalized hyaluronic acid and PEG dithiol to form uniform nanogels with tunable swelling properties. Since then, radical thiol−ene reactions have also been used to form peptide functionalized microgels to sequester and release vascular endothelial growth factor (VEGF).[483] This approach, using a water-in-water emulsion to control the size, relies on the rapid kinetics and efficiency of the photoinitiated thiol−ene reaction for batch microparticle synthesis. Building on this work Alge and co-workers used the same photoclick chemistry to form microgels with excess norbornene groups that could be used to functionalize the microgels with tetrazine functionalized proteins.[484] Alkaline phosphatase and glucose-oxidase were used to demonstrate the utility of this process with bioactive proteins and quantitively assess microparticle bioactivity. Recently Xin et al. have developed this work further, using the same thiol−ene chemistry to synthesize microgels but through a microfluidic device to create gradients in microporous annealed particle (MAP) hydrogels.[485] These gradients allowed for a unique insight into cell−material interactions as demonstrated with hMSCs that had differential spreading depending on the degradability and stiffness gradient of the particles (Figure 92).

Thiol−ene microgels have also been postmodified using tetrazole−ene chemistry through utilization of norbornene functionality. Michel et al. synthesized microgels by cross-linking norbornene functionalized chitosan with a PEG dithiol in a low energy water-in-oil nanoemulsion templating method.[486] They demonstrated that the microgels were nontoxic to human dermofibroblasts (HDF). The researchers then exploited the tetrazole−ene reaction to react unreacted norbornenes with a tetrazine coumarin to increase the fluorescence for ease of tracking. The researchers state that the coumarin increases the florescence of the pyrazoles ring by up to 10 times, making the microgels ideal for cell targeting moieties. Alternatively, the thiol−ene reaction can be used to postfunctionalize nanogels and microgels that have been synthesized through other methods. Huang et al. synthesized PMMA microgels using a RAFT-assisted dispersion photopolymerization technique to control the number of vinyl groups present on the particles.[487] A thiolated biotin was conjugated to the surface of the microgels through a photoinduced radical thiol−ene reaction. The biotinylated PMMA microgels could then effectively immobilize fluorescent streptavidin, demonstrating the ability to make controlled monodispersed functional microgels through thiol−ene reactions.

Nanogel postmodification has also been demonstrated using the thiol−yne reaction to form a nanogel coated monolayer.[488]

https://doi.org/10.1021/acs.chemrev.0c01212
Chem. Rev. 2021, 121, 6915−6990

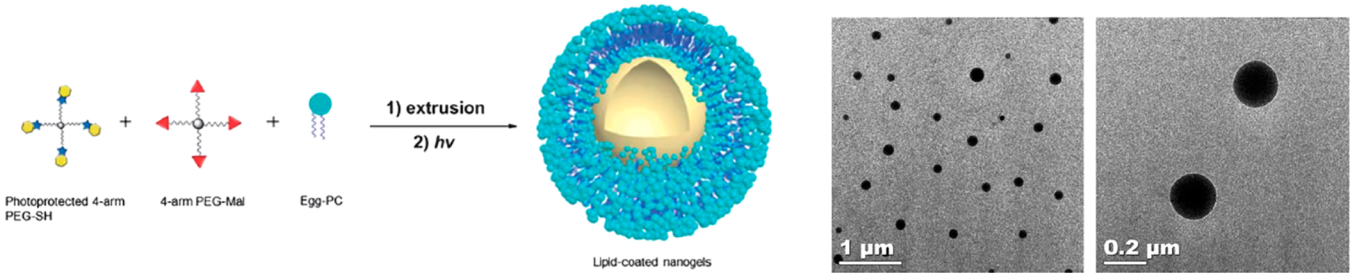

Figure 93. Schematic representation of liposome templated synthesis of PEG-based nanogels via photo triggered thiol−maleimide click reaction in aqueous media: (1) DI water, polycarbonate membrane; (2) 365 nm @ 10 mW/cm^2, 2 h, and TEM images of the lipid-coated nanogels dried from aqueous solution. Reproduced with permission from ref 495. Copyright 2014 Royal Society of Chemistry.

The PEG nanogels were synthesized through a CuAAC cross-linking reaction with excess alkyne groups. A thiol−yne reaction was then carried out between a thiolated surface and the nanogels with exposure to UV light and I-2959 to form a 100% PEG monolayer. The formed layer was superior for producing a protein resistant coting compared to other reaction because of the bioorthogonal nature of the reactions used.

An ideal nanogel application is as drug delivery vehicles with controlled and targeted release.[489] Most drugs are hydrophobic and therefore are cleared out of the body quickly. By trapping drugs within hydrophilic nanogels, they can deliver their load efficiently to an area of interest and release in a controlled manner through a range of degradation routes built into the nanogel structure. This has been demonstrated numerous times in the literature with a range of techniques.[480] However, as clearly demonstrated by Lochhart et al., photoclick reactions enable a facile way to synthesize and load nanogels.[490] Very recently, Graf et al. have also demonstrated this with PEG microgels to deliver therapeutic proteins to the alveolar sacs. Here PEG microgels offer the correct size and hydrophilic surface to prevent a macrophage response enabling efficient delivery. Thiol−ene reactions enabled fast, specific cross-linking in the presence of a therapeutic protein. Furthermore, this photoclick reaction has been used to encapsulate antibodies and growth factors into nanogels for controlled, target delivery.[491,492]

For the production of fluorescent nanogels, the self-reporting tetrazole−ene reaction has the obvious advantage of intrinsic fluorescence. This facilitates tracking nanogels and microgels in vivo without additional synthesis steps to label the material. This photoclick reaction has particularly found an application as a synthetic route to form fluorescent drug delivery vehicles owing to its fast reaction kinetics and specificity, enabling drug encapsulation without side reactions. Zhong and co-workers have used tetrazole−ene nanogels to improve the intracellular target of cancer drugs.[493] The formation of a fluorescent pyrazoles ring through cross-linking enabled the enhanced CT imaging of MCF-7 breast tumor in nude mice compared to iodoxanol, a clinically used contrast agent with nonspecific distribution. The study demonstrated the excellent biocompatibility, high stability, and effective targetability to CD44 overexpressing cells with these tetrazole−ene nanogels and presented the system in vivo for high tumor accumulation and improved survival rate. By loading PTX into the nanogels, the systemic toxicity of the drug was reduced compared to free PTX and the fluorescent nanogels significantly improved imaging.

Phototriggered thiol-Michael reactions have also been used for nanogel synthesis. Gao et al. demonstrated the compatibility of using 400−500 nm light to form nanostructures and 365 nm light to allow for bond exchange.[494] In another example, Liang et al. utilized phototriggered Michael-type additions of *o*-nitrobenzyl caged multiarm PEG thiol and maleimides for liposome-templated production of lipid-coated polymer nanogels.[495] Phototriggered release of PEG−thiols upon irradiation of 365 nm UV light and subsequent cross-linking permitted the formation of well-defined nanogels by providing temporal control of the reaction avoiding the macroscale gelation. The phototriggered formation of nanogels was monitored by oscillatory rheology experiments of bulk hydrogels, and the production of nanogels was confirmed via dynamic light scattering and transmission electron microscopy (Figure 93).

Overall, the synthesis of nanogels and microgels using photoclick reactions is a growing area of research with exciting and impactful applications. The area is still new, with many papers only published in the last several years. Therefore, the current area focuses heavily on thiol−ene and tetrazole−ene reactions because of their ease of synthesis and rapid reaction rates. There is a plethora of alkene and thiol functional groups that can be functionalized onto natural and synthetic polymers, enabling the growth of these two reactions for the synthesis of nano- and microhydrogels. The advantages of photoinitiated CuAAC and SPAAC reactions are less beneficial to the synthesis of nanogels and microgels, as many of the synthetic methods used require oil−water phases and high shear rates. The advantages of discrete areas of a liberated catalyst or ring-strained alkyne are less beneficial for nano- and microhydrogel synthesis in comparison to other photoclick reactions.

3.6. Obstacles in Application of Photoclick Reactions

Despite the successful application of photoclick reactions in such disparate fields of research, there are obstacles to the implementation of these reactions more broadly.

Limited scalability of the reaction has been described briefly, and the requirement for exposure to light in any reaction may mean less effective mediation of that reaction where light cannot penetrate or where it is otherwise obscured by refraction. This may not be as big of an issue where photolatent catalysts that persist in the absence of light are employed (e.g., with photo thiol-Michael reactions), but most of the reactions described herein cease completely in the absence of light. Moreover, light-absorbing chromophores on one or both reactive groups limit the ability to obtain optically thin reactions without extremely low concentrations or very small volumes. Flow reactors, as compared to batch systems,

https://doi.org/10.1021/acs.chemrev.0c01212
Chem. Rev. 2021, 121, 6915−6990

avoid constraints associated with light attenuation and allow for simple scale-up of photoinitiated polymerizations,[496] which can be combined with orthogonal reactions (e.g., thermally driven polymer modifications) within the reactor to produce complex products in unprecedented yield and in essentially one step.[497] Using a photoinduced Diels−Alder cycloaddition between *o*-quinodimethane thioether and maleimide, Feist et al. demonstrated full conversion of starting materials in a photoflow polymerization in aqueous solution and catalyzed by visible light from LEDs, modeling remarkable reagent and catalyst sustainability in a highly efficient polymerization system.[329]

Another obstacle to effective use of photoclick chemistry results from inadequate reporting of the reaction conditions as they apply to light exposure. It is not uncommon for papers to omit relevant information that would assist replication of experimental conditions. Such omissions might consist of the particular exposure wavelength and characteristics of the light source. Instead, general terms like "blue" or "UV light" are often used in the methods description as well as in other sections of the paper. More frequently, however, it is the light intensity (with units of energy per area that is incident on the top surface of the sample) that is omitted. Lamp power may be noted, but that is entirely unuseful for repeating an experiment, hindering reproduction of reported results. Where low intensity, near-UV light is employed in photoclick reactions, mass-produced black lights may be effectively used as a cheap alternative to specialized illumination products. However, the fluorescent tubes of such black lights may use one of two phosphores which, upon excitation, emit light centered at either 352 or 368 nm. Such a difference in emission may not be significant in recreational applications but can be consequential when used to conduct photochemical reactions, as of course is the incident intensity at the sample which must be measured by a reliable radiometer tuned to the wavelengths of light used and reported. Further, reports of solar-initiated reactions frequently omit pertinent wavelength and intensity information. Solar output in terms of intensity and spectral output are subject to season and geography. In addition, details about the sample geometry are also critical as the sample thickness in the direction of exposure, the initiator concentration, and the presence of any other attenuating species must be included.

4. CONCLUSIONS

Rather than having a common mechanism, photoclick reactions are so categorized based on common features that enable their application in a wide variety of chemical and biological contexts: efficiency, selectivity, exogenous control, and so forth. Yet the commonality among these reactions can be overstated. Different photoclick reactions exhibit distinct advantages and disadvantages, the better understanding of which allows more effective implementation of such reactions to address the synthetic and materials challenges at hand for a particular reaction. Perhaps the most fundamental parameter that divides photoclick reactions is the role the chromophore plays in the reaction, whether its activation leads to the generation of the reactive species directly or whether its activation participates in a catalytic or otherwise photoamplified mechanism with the reactive species.

The general orthogonality of click reactions and photoclick reactions drives, to a considerable degree, the varied applications in which they may be employed. While there are many significant advantages to the use of photomediated click reactions, one that holds particular potential, particularly given the recent advances in discrete spectrum LED sources, is the utilization of multiple wavelengths as independent exogenous stimuli. Selective initiation of specific orthogonal photoclick reactions in a predetermined order via consecutive irradiation with different wavelengths has allowed the modular synthesis of complex chemical architectures and holds potential for the development of higher-order structures as well. Expansion of this utility relies on development of chromophores for such reactions with nonoverlapping regions of their respective absorbance spectra. While examples of photoclick reactions conducted with longer wavelengths of light are not exactly rare, it is the near UV and low wavelength, blue regions of the spectra (i.e., 350−420 nm) that are most heavily utilized. Furthermore, many of those reactions conducted at higher wavelengths employ inefficient multiphoton absorption or upconversion techniques that are impractical for all but the most niche applications. Continued development of highly efficient, longer wavelength photolatent catalysts, photoinitiators, and reactive chromophores is key to the broader exploitation of the orthogonality of the sundry photoclick reactions in combination one with another as well as in situations requiring biologically most benign photoexposure.

The concept of photoclick chemistry has expanded the synthetic, polymeric, and biological research toolbox immensely in just a few short years and its continued relevance is anticipated well into the future.

AUTHOR INFORMATION

Corresponding Author

Christopher N. Bowman − *Department of Chemical and Biological Engineering, University of Colorado, Boulder, Colorado 80303, United States; Materials Science and Engineering Program, University of Colorado, Boulder, Colorado 80303, United States;* orcid.org/0000-0001-8458-7723; Email: Christopher.Bowman@Colorado.edu

Authors

Benjamin D. Fairbanks − *Department of Chemical and Biological Engineering, University of Colorado, Boulder, Colorado 80303, United States*

Laura J. Macdougall − *Department of Chemical and Biological Engineering, University of Colorado, Boulder, Colorado 80303, United States*

Sudheendran Mavila − *Department of Chemical and Biological Engineering, University of Colorado, Boulder, Colorado 80303, United States*

Jasmine Sinha − *Department of Chemical and Biological Engineering, University of Colorado, Boulder, Colorado 80303, United States*

Bruce E. Kirkpatrick − *Department of Chemical and Biological Engineering and The BioFrontiers Institute, University of Colorado, Boulder, Colorado 80303, United States; Medical Scientist Training Program, School of Medicine, University of Colorado, Aurora, Coorado 80045, United States*

Kristi S. Anseth − *Department of Chemical and Biological Engineering and The BioFrontiers Institute, University of Colorado, Boulder, Colorado 80303, United States;* orcid.org/0000-0002-5725-5691

Complete contact information is available at: https://pubs.acs.org/10.1021/acs.chemrev.0c01212

https://doi.org/10.1021/acs.chemrev.0c01212
Chem. Rev. 2021, 121, 6915−6990

Notes

The authors declare no competing financial interest.

Biographies

Benjamin D. Fairbanks received his B.S. in Chemical Engineering from the University of Oklahoma in 2004 and his Ph.D. in Chemical Engineering from the University of Colorado in 2009, studying thiol−ene and thiol−yne polymerizations for biomedical applications. He worked on RAFT polymerization as a postdoctoral research fellow and subsequently as a research scientist at CSIRO in Victoria, Australia, until 2015, when he returned to the University of Colorado as a Senior Research Associate.

Laura J. Macdougall received her Ph.D. in Chemistry from the University of Warwick, U.K., in 2018. She earned her Master's degree from the University of York and is currently a postdoctoral researcher in Chemical and Biological Engineering at the University of Colorado Boulder under the mentorship of Professor Kristi Anseth. Her research interests are in the development of click hydrogel biomaterials for tissue engineering.

Sudheendran Mavila received his Ph.D. degree in Polymer Chemistry from the University of Stuttgart, Germany, in 2011. He holds Master's degree in Organic Chemistry from Mahatma Gandhi University, Kerala, India, and worked as Senior Scientist in Synthetic Organic Chemistry for four years at Syngene International Ltd, India. After completing his doctoral studies in Germany, he moved to Israel in the early 2012 as a postdoctoral fellow at the Department of Chemistry at Ben-Gurion University of the Negev. Since January 2016, he has been working as a Postdoctoral Research Associate at the Department of Chemical and Biological engineering, University of Colorado, Boulder. His research interests lie at the interface of Synthetic Organic Chemistry and Material Science.

Jasmine Sinha received her M.Sc. in Chemistry in 2005 from IIT, Guwahati, and Ph.D. in Chemistry in 2011 from the IIT, Bombay, India, studying clickable thiophene and amplified fluorescent polymers for their applications in sensing. After receiving her Ph.D., she moved to Johns Hopkins University as a postdoctoral fellow under the direction of Prof. Howard Katz and focused on organic, hybrid, and interfacial materials for electronic devices. She is currently a postdoctoral associate in the Department of Chemical and Biological Engineering at the University of Colorado, Boulder. Her current research efforts focus on designing monomers for cross-linked polymerizations.

Bruce E. Kirkpatrick is an M.D.−Ph.D. student in the Anseth Research Group at the University of Colorado. He received his B.S. in Chemical and Biological Engineering in 2017 from the University of Colorado, Boulder, where he worked with Prof. Andrew Goodwin on the synthesis of mechanoresponsive click monomers and with Dr. Kavita Jeerage at NIST on quantification assays for biological applications of gold nanoparticles. His research interests involve the design and implementation of engineered systems to stabilize and preserve biological materials.

Kristi S. Anseth is the Tisone Professor of Chemical and Biological Engineering and Associate Director of the BioFrontiers Institute at the University of Colorado, Boulder. Dr Anseth earned her B.S. degree from Purdue University, her Ph.D. degree from the University of Colorado, and completed postdoctoral research at MIT as an NIH fellow. Her research interests lie at the interface between biology and engineering, where she designs new biomaterials for applications in drug delivery and regenerative medicine. She is an elected member of the National Academy of Engineering (2009), National Academy of Medicine (2009), National Academy of Sciences (2013), and the National Academy of Inventors (2016). Dr. Anseth was also recognized with the L'Oreal−UNESCO for Women in Science Award in the Life Sciences in 2020.

Professor Christopher N. Bowman received his B.S. and Ph.D. in Chemical Engineering from Purdue University in 1988 and 1991, respectively. After receiving his Ph.D., he began his academic career at the University of Colorado in January of 1992 as an Assistant Professor. Since that time, Professor Bowman has built a program focused on the fundamentals and applications of cross-linked polymers formed via photopolymerization reactions. He works in the broad areas of the fundamentals of polymerization reaction engineering, polymer chemistry, cross-linked polymers, photopolymerizations, and biomaterials. Professor Bowman is currently the Patten Endowed Chair of the Department of Chemical and Biological Engineering as well as a Clinical Professor of Restorative Dentistry at the University of Colorado at Denver.

ACKNOWLEDGMENTS

This work was supported by grants from the United States Defense Advanced Research Projects Agency (DARPA, grant W911NF-19-2-0024), from the National Science Foundation (NSF, grant CHE 1808484), and from the U.S. National Institutes of Health (NIH, grant R01 DE016523). Graphical abstract created with Biorender.com

ABBREVIATIONS

ABD = albumin binding domain
$AgBF_4$ = silver tetrafluoroborate
APT = alternating propagation and chain transfer
ATRP = atom transfer radical polymerization
BAPC = 9-(2,3-bis(allyloxy)propyl)-9*H*-carbazole
BAPO = bis(2,4,6-trimethylbenzoyl)-phenylphosphineoxide
BCN = bicyclononyne
BMP-2 = bone morphogenic protein 2
BLG = bovine β-lactoglobulin
BSA = bovine serum albumin
CBOA = carbon-bridged octocyclic azobenzene
CNA = click nucleic acid
CNA-2G = click nucleic acid second generation
Coumarin-TMG = coumarin-1,1,3,3-tetramethylguanidine
CPG = controlled pore glass
CT = computed tomography
DA = Diels−Alder
DBN = 1,5-diazabicyclo[4.3.0]non-5-en
DBTD = dibenzo[*b*,*f*][1,4,5]thiadiazepine
DBU = 1,8-diazabicyclo[5.4.0]undec-7-ene
DCM = dichloromethane
DFT = density functional theory
DIBOD = dibenzo[*a*,*e*]cyclooctadiyne
DLP = digital light processing
DMBO = dibenzoannulated bicyclononynes
DMF = dimethylformamide
DMPA = 2,2-dimethoxy-2-phenylacetophenone
DMPP = dimethylphenylphosphine
DMSO = dimethyl sulfoxide
DNA = deoxyribonucleic acid
DTT = dithiolthreitol
DVS = divinyl sulfone
ECM = extracellular matrix
EGFR = epidermal growth factor receptor
EWG = electron withdrawing group
FGF-2 = fibroblast growth factor 2

https://doi.org/10.1021/acs.chemrev.0c01212
Chem. Rev. 2021, 121, 6915−6990

fac-Ir(ppy)$_3$ = (fac-tris(2-phenylpyridine)iridium)
Fmoc = 9-fluorenylmethyl carbamate
GDMP = glycol dimercaptopropionate
GST = glutathione S-transferase
HA = hyaluronic acid
HDF = human dermofibroblasts
HOMO = highest occupied molecular orbital
HPLC = high performance liquid chromatography
HSA = human serum albumin
IEDDA = inverse electron demand Diels−Alder
ISC = intersystem crossing
ITX = isopropylthioxanthone
LAP = lithium phenyl-2,4,6-trimethylbenzoylphosphinate
LED = light emitting Diode
LUMO = lower unoccupied molecular orbital
MAP = microporous annealed particle
MSC = mesenchymal stem cells
NCL = native chemical ligation
NDBF = nitrodibenzofuran
NIR = near-infrared
NMR = nuclear magnetic resonance
NPPOC = 2-(2-nitrophenyl)propyloxycarbonyl
NPPOC-TMG = 2-(nitrophenyl)propoxycarbonyl-1,1,3,3-tetramethylguanidine
NVOC = nitroveratryloxycarbonyl
o-NB = *o*-nitrobenzyl
PBS = phosphate buffered saline
PcAAC = photocatalyzed azide−alkyne cycloaddition
PCL = polycaprolactone
PDLC = polymer-dispersed liquid crystals
PEG = poly(ethylene glycol)
PET = photoinduced electron transfer
PETMP = pentaerythritol tetrakis(3-mercaptopropionate)
PGB = photogenerated base
PMDETA = *N*,*N*,*N*′,*N*″,*N*′′′-pentamethyldiethylenetriamine
PMMA = poly(methyl methacrylate)
pNIPAM = poly(*n*-isopropylacrylamide)
PPE = personal protective equipment
PPG = photoremovable protecting group
PTX = paclitaxel
PVA = poly(vinyl alcohol)
QDs = quantum dots
RAFT = reversible addition−fragmentation chain transfer
ROMP = ring-opening metathesis polymerization
Ru(bpy)$_3$Cl$_2$ = tris(2,2′-bipyridyl)-ruthenium(II) chloride
Ru(bpz)$_3$[PF6]$_2$ = tris(2,2′-bipyrazine)ruthenium bis-(hexafluorophosphate)
RuAAC = ruthenium-catalyzed alkyne−azide cycloaddition
SLA = stereolithography
SPAAC = strain-promoted azide−alkyne click chemistry
ssDNA = single-stranded DNA
TBD = 1,5,7-triazabicyclo[4.4.0]dec-5-ene
TBD·HBPh4 = 1,5,7-triazabicyclo[4.4.0]dec-5-ene tetraphenylborate
TEA = triethylamine
TGF-β = transforming growth factor β
TEMPO = 2,2,6,6-tetramethyl-1-piperidinyloxy
TMEDA = *N*,*N*,*N*′,*N*′-tetramethylethylenediamene
TMG = 1,1,3,3-tetramethylguanidine
TPO = diphenyl(2,4,6-trimethylbenzoyl)phosphine oxide
TRITC = tetramethylrhodamine
UV = ultraviolet
VEGF = vascular endothelial growth factor
VIC = valvular institute cells
YAP/TAZ = yes-associated protein/transcriptional coactivator with pdz-binding motif
Zn-TPP = zinc tetraphenylporphyrin

REFERENCES

(1) Tasdelen, M. A.; Yagci, Y. Light-Induced Click Reactions. *Angew. Chem., Int. Ed.* **2013**, *52*, 5930−5938.
(2) Kolb, H. C.; Finn, M. G.; Sharpless, K. B. Click Chemistry: Diverse Chemical Function from a Few Good Reactions. *Angew. Chem., Int. Ed.* **2001**, *40*, 2004.
(3) Barner-Kowollik, C.; Du Prez, F. E.; Espeel, P.; Hawker, C. J.; Junkers, T.; Schlaad, H.; Van Camp, W. Clicking" Polymers or Just Efficient Linking: What Is the Difference? *Angew. Chem., Int. Ed.* **2011**, *50*, 60−62.
(4) Fairbanks, B. D.; Love, D. M.; Bowman, C. Efficient Polymer-Polymer Conjugation Via Thiol-Ene Click Reaction. *Macromol. Chem. Phys.* **2017**, *218*, 1700073.
(5) Kärkäs, M. D.; Porco, J. A.; Stephenson, C. R. J. Photochemical Approaches to Complex Chemotypes: Applications in Natural Product Synthesis. *Chem. Rev.* **2016**, *116*, 9683−9747.
(6) Turro, N. J., Ramamurthy, V.; Scaiano, J. C. *Principles of Molecular Photochemistry, An Introduction*; University Science Books, Sausalito, CA, 2009.
(7) Yousif, E.; Haddad, R. Photodegradation and Photostabilization of Polymers, Especially Polystyrene: Review. *SpringerPlus* **2013**, *2*, 398.
(8) Song, W.; Wang, Y.; Qu, J.; Madden, M. M.; Lin, Q. A Photoinducible 1,3-Dipolar Cycloaddition Reaction for Rapid, Selective Modification of Tetrazole-Containing Proteins. *Angew. Chem., Int. Ed.* **2008**, *47*, 2832−2835.
(9) Albini, A. Some Remarks on the First Law of Photochemistry. *Photochem. Photobiol.* **2016**, *15*, 319−324.
(10) Einstein, A. Über Die Von Der Molekularkinetischen Theorie Der Wärme Geforderte Bewegung Von in Ruhenden Flüssigkeiten Suspendierten Teilchen. *Ann. Phys.* **1905**, *322*, 549−560.
(11) Mayerhöfer, T. G.; Höfer, S.; Popp, J. Deviations from Beer's Law on the Microscale - Nonadditivity of Absorption Cross Sections. *Phys. Chem. Chem. Phys.* **2019**, *21*, 9793−9801.
(12) Berezin, M. Y.; Achilefu, S. Fluorescence Lifetime Measurements and Biological Imaging. *Chem. Rev.* **2010**, *110*, 2641−2684.
(13) Fleming, K. G., Fluorescence Theory, in *Encyclopedia of Spectroscopy and Spectrometry (Third ed.)*, 3rd ed.; Lindon, J.C., Tranter, G.E., Koppenaal, D.W., Eds.; Academic Press: Oxford, 2017; pp 647−653.
(14) McDonagh, A.; Palma, L.; Lightner, D. Blue Light and Bilirubin Excretion. *Science* **1980**, *208*, 145−151.
(15) Büchi, G.; Goldman, I. M. Photochemical Reactions. Vii.1 the Intramolecular Cyclization of Carvone to Carvonecamphor2. *J. Am. Chem. Soc.* **1957**, *79*, 4741−4748.
(16) Khorana, H. G.; Razzell, W. E.; Gilham, P. T.; Tener, G. M.; Pol, E. H. Syntheses of Dideoxyribonucleotides. *J. Am. Chem. Soc.* **1957**, *79*, 1002−1003.
(17) Schreier, W. J.; Schrader, T. E.; Koller, F. O.; Gilch, P.; Crespo-Hernández, C. E.; Swaminathan, V. N.; Carell, T.; Zinth, W.; Kohler, B. Thymine Dimerization in DNA Is an Ultrafast Photoreaction. *Science* **2007**, *315*, 625−629.
(18) Romero, N. A.; Nicewicz, D. A. Organic Photoredox Catalysis. *Chem. Rev.* **2016**, *116*, 10075−10166.
(19) Worrell, B. T.; McBride, M. K.; Lyon, G. B.; Cox, L. M.; Wang, C.; Mavila, S.; Lim, C.-H.; Coley, H. M.; Musgrave, C. B.; Ding, Y.; Bowman, C. N. Bistable and Photoswitchable States of Matter. *Nat. Commun.* **2018**, *9*, 2804.
(20) Brown, T. E.; Marozas, I. A.; Anseth, K. S. Amplified Photodegradation of Cell-Laden Hydrogels Via an Addition-Fragmentation Chain Transfer Reaction. *Adv. Mater.* **2017**, *29*, 1605001.

https://doi.org/10.1021/acs.chemrev.0c01212
Chem. Rev. 2021, 121, 6915−6990

(21) Li, J.; Kong, H.; Zhu, C.; Zhang, Y. Photo-Controllable Bioorthogonal Chemistry for Spatiotemporal Control of Bio-Targets in Living Systems. *Chem. Sci.* **2020**, *11*, 3390−3396.
(22) Kumar, G. S.; Lin, Q., Light-Triggered Click Chemistry, *Chem. Rev.*, **2020**, DOI: 10.1021/acs.chemrev.0c00799.
(23) Herner, A.; Lin, Q. Photo-Triggered Click Chemistry for Biological Applications. *Top. Curr. Chem.* **2016**, *374*, 1.
(24) Kaur, G.; Singh, G.; Singh, J. Photochemical Tuning of Materials: A Click Chemistry Perspective. *Mater. Today Chem.* **2018**, *8*, 56−84.
(25) Menzel, J. P.; Noble, B. B.; Lauer, A.; Coote, M. L.; Blinco, J. P.; Barner-Kowollik, C. Wavelength Dependence of Light-Induced Cycloadditions. *J. Am. Chem. Soc.* **2017**, *139*, 15812−15820.
(26) Marschner, D. E.; Kamm, P. W.; Frisch, H.; Unterreiner, A.-N.; Barner-Kowollik, C. Photocycloadditions in Disparate Chemical Environments. *Chem. Commun.* **2020**, *56*, 14043−14046.
(27) Arseneault, M.; Wafer, C.; Morin, J.-F. Recent Advances in Click Chemistry Applied to Dendrimer Synthesis. *Molecules* **2015**, *20*, 9263−9294.
(28) Fahrenbach, A. C.; Stoddart, J. F. Reactions under the Click Chemistry Philosophy Employed in Supramolecular and Mechanostereochemical Systems. *Chem. - Asian J.* **2011**, *6*, 2660−2669.
(29) Song, W.; Wang, Y.; Qu, J.; Lin, Q. Selective Functionalization of a Genetically Encoded Alkene-Containing Protein Via "Photoclick Chemistry" in Bacterial Cells. *J. Am. Chem. Soc.* **2008**, *130*, 9654−9655.
(30) Tasdelen, M. A.; Yagci, Y. Light-Induced Copper(I)-Catalyzed Click Chemistry. *Tetrahedron Lett.* **2010**, *51*, 6945−6947.
(31) Adzima, B. J.; Tao, Y. H.; Kloxin, C. J.; DeForest, C. A.; Anseth, K. S.; Bowman, C. N. Spatial and Temporal Control of the Alkyne-Azide Cycloaddition by Photoinitiated Cu(Ii) Reduction. *Nat. Chem.* **2011**, *3*, 256−259.
(32) Wu, Z.-G.; Liao, X.-J.; Yuan, L.; Wang, Y.; Zheng, Y.-X.; Zuo, J.-L.; Pan, Y. Visible-Light-Mediated Click Chemistry for Highly Regioselective Azide-Alkyne Cycloaddition by a Photoredox Electron-Transfer Strategy. *Chem. - Eur. J.* **2020**, *26*, 5694−5700.
(33) Poloukhtine, A. A.; Mbua, N. E.; Wolfert, M. A.; Boons, G.-J.; Popik, V. V. Selective Labeling of Living Cells by a Photo-Triggered Click Reaction. *J. Am. Chem. Soc.* **2009**, *131*, 15769−15776.
(34) Martínek, M.; Filipová, L.; Galeta, J.; Ludvíková, L.; Klán, P. Photochemical Formation of Dibenzosilacyclohept-4-Yne for Cu-Free Click Chemistry with Azides and 1,2,4,5-Tetrazines. *Org. Lett.* **2016**, *18*, 4892−4895.
(35) Wang, Y.; Hu, W. J.; Song, W.; Lim, R. K. V.; Lin, Q. Discovery of Long-Wavelength Photoactivatable Diaryltetrazoles for Bioorthogonal 1,3-Dipolar Cycloaddition Reactions. *Org. Lett.* **2008**, *10*, 3725−3728.
(36) Zhang, L.; Zhang, X.; Yao, Z.; Jiang, S.; Deng, J.; Li, B.; Yu, Z. Discovery of Fluorogenic Diarylsydnone-Alkene Photoligation: Conversion of Ortho-Dual-Twisted Diarylsydnones into Planar Pyrazolines. *J. Am. Chem. Soc.* **2018**, *140*, 7390−7394.
(37) Lim, R. K. V.; Lin, Q. Azirine Ligation: Fast and Selective Protein Conjugation Via Photoinduced Azirine-Alkene Cycloaddition. *Chem. Commun.* **2010**, *46*, 7993−7995.
(38) Gruendling, T.; Oehlenschlaeger, K. K.; Frick, E.; Glassner, M.; Schmid, C.; Barner-Kowollik, C. Rapid Uv Light-Triggered Macromolecular Click Conjugations Via the Use of O-Quinodimethanes. *Macromol. Rapid Commun.* **2011**, *32*, 807−812.
(39) Oehlenschlaeger, K. K.; Mueller, J. O.; Heine, N. B.; Glassner, M.; Guimard, N. K.; Delaittre, G.; Schmidt, F. G.; Barner-Kowollik, C. Light-Induced Modular Ligation of Conventional Raft Polymers. *Angew. Chem., Int. Ed.* **2013**, *52*, 762−766.
(40) Feist, F.; Rodrigues, L. L.; Walden, S. L.; Krappitz, T. W.; Dargaville, T. R.; Weil, T.; Goldmann, A. S.; Blinco, J. P.; Barner-Kowollik, C. Light-Induced Ligation of O-Quinodimethanes with Gated Fluorescence Self-Reporting. *J. Am. Chem. Soc.* **2020**, *142*, 7744−7748.
(41) Arumugam, S.; Popik, V. V. Light-Induced Hetero-Diels-Alder Cycloaddition: A Facile and Selective Photoclick Reaction. *J. Am. Chem. Soc.* **2011**, *133*, 5573−5579.
(42) Truong, V. X.; Tsang, K. M.; Ercole, F.; Forsythe, J. S. Red Light Activation of Tetrazine-Norbornene Conjugation for Bioorthogonal Polymer Cross-Linking across Tissue. *Chem. Mater.* **2017**, *29*, 3678−3685.
(43) Zhang, H.; Trout, W. S.; Liu, S.; Andrade, G. A.; Hudson, D. A.; Scinto, S. L.; Dicker, K. T.; Li, Y.; Lazouski, N.; Rosenthal, J.; et al. Rapid Bioorthogonal Chemistry Turn-on through Enzymatic or Long Wavelength Photocatalytic Activation of Tetrazine Ligation. *J. Am. Chem. Soc.* **2016**, *138*, 5978−5983.
(44) Mayer, S. V.; Murnauer, A.; Wrisberg, v.M.-K.; Jokisch, M.-L.; Lang, K. Photo-Induced and Rapid Labeling of Tetrazine-Bearing Proteins Via Cyclopropenone-Caged Bicyclononynes. *Angew. Chem., Int. Ed.* **2019**, *58*, 15876−15882.
(45) Hoyle, C. E.; Lee, T. Y.; Roper, T. Thiol-Enes: Chemistry of the Past with Promise for the Future. *J. Polym. Sci., Part A: Polym. Chem.* **2004**, *42*, 5301−5338.
(46) Hoyle, C. E.; Bowman, C. N. Thiol-Ene Click Chemistry. *Angew. Chem., Int. Ed.* **2010**, *49*, 1540−1573.
(47) Fairbanks, B. D.; Sims, E. A.; Anseth, K. S.; Bowman, C. N. Reaction Rates and Mechanisms for Radical, Photoinitated Addition of Thiols to Alkynes, and Implications for Thiol-Yne Photopolymerizations and Click Reactions. *Macromolecules* **2010**, *43*, 4113−4119.
(48) Prasath, R. A.; Gokmen, M. T.; Espeel, P.; Du Prez, F. E. Thiol-Ene and Thiol-Yne Chemistry in Microfluidics: A Straightforward Method Towards Macroporous and Nonporous Functional Polymer Beads. *Polym. Chem.* **2010**, *1*, 685−692.
(49) Stuparu, M. C.; Khan, A. Thiol-Epoxy "Click" Chemistry: Application in Preparation and Postpolymerization Modification of Polymers. *J. Polym. Sci., Part A: Polym. Chem.* **2016**, *54*, 3057−3070.
(50) Nakayama, N.; Hayashi, T. Synthesis of Novel Uv-Curable Difunctional Thiourethane Methacrylate and Studies on Organic-Inorganic Nanocomposite Hard Coatings for High Refractive Index Plastic Lenses. *Prog. Org. Coat.* **2008**, *62*, 274−284.
(51) Shin, J.; Lee, J.; Jeong, H. M. Properties of Polythiourethanes Prepared by Thiol-Isocyanate Click Reaction. *J. Appl. Polym. Sci.* **2018**, *135*, 46070.
(52) Xi, W.; Krieger, M.; Kloxin, C. J.; Bowman, C. N. A New Photoclick Reaction Strategy: Photo-Induced Catalysis of the Thiol-Michael Addition Via a Caged Primary Amine. *Chem. Commun.* **2013**, *49*, 4504−4506.
(53) Chatani, S.; Gong, T.; Earle, B. A.; Podgórski, M.; Bowman, C. N. Visible-Light Initiated Thiol-Michael Addition Photopolymerization Reactions. *ACS Macro Lett.* **2014**, *3*, 315−318.
(54) Pauloehrl, T.; Delaittre, G.; Bastmeyer, M.; Barner-Kowollik, C. Ambient Temperature Polymer Modification by in Situ Phototriggered Deprotection and Thiol-Ene Chemistry. *Polym. Chem.* **2012**, *3*, 1740−1749.
(55) Mahmoodi, M. M.; Fisher, S. A.; Tam, R. Y.; Goff, P. C.; Anderson, R. B.; Wissinger, J. E.; Blank, D. A.; Shoichet, M. S.; Distefano, M. D. 6-Bromo-7-Hydroxy-3-Methylcoumarin (Mbhc) Is an Efficient Multi-Photon Labile Protecting Group for Thiol Caging and Three-Dimensional Chemical Patterning. *Org. Biomol. Chem.* **2016**, *14*, 8289−8300.
(56) Pauloehrl, T.; Delaittre, G.; Bruns, M.; Meißler, M.; Börner, H. G.; Bastmeyer, M.; Barner-Kowollik, C. (Bio)Molecular Surface Patterning by Phototriggered Oxime Ligation. *Angew. Chem., Int. Ed.* **2012**, *51*, 9181−9184.
(57) Farahani, P. E.; Adelmund, S. M.; Shadish, J. A.; DeForest, C. A. Photomediated Oxime Ligation as a Bioorthogonal Tool for Spatiotemporally-Controlled Hydrogel Formation and Modification. *J. Mater. Chem. B* **2017**, *5*, 4435−4442.
(58) Huisgen, R. Kinetics and Mechanism of 1,3-Dipolar Cycloadditions. *Angew. Chem., Int. Ed. Engl.* **1963**, *2*, 633−645.
(59) Demko, Z. P.; Sharpless, K. B. A Click Chemistry Approach to Tetrazoles by Huisgen 1,3-Dipolar Cycloaddition: Synthesis of 5-

Sulfonyl Tetrazoles from Azides and Sulfonyl Cyanides. *Angew. Chem., Int. Ed.* **2002**, *41*, 2110−2113.
(60) Rostovtsev, V. V.; Green, L. G.; Fokin, V. V.; Sharpless, K. B. A Stepwise Huisgen Cycloaddition Process: Copper(I)-Catalyzed Regioselective "Ligation" of Azides and Terminal Alkynes. *Angew. Chem., Int. Ed.* **2002**, *41*, 2596−2599.
(61) Worrell, B. T.; Malik, J. A.; Fokin, V. V. Direct Evidence of a Dinuclear Copper Intermediate in Cu(I)-Catalyzed Azide-Alkyne Cycloadditions. *Science* **2013**, *340*, 457−460.
(62) Boren, B. C.; Narayan, S.; Rasmussen, L. K.; Zhang, L.; Zhao, H.; Lin, Z.; Jia, G.; Fokin, V. V. Ruthenium-Catalyzed Azide-Alkyne Cycloaddition: Scope and Mechanism. *J. Am. Chem. Soc.* **2008**, *130*, 8923−8930.
(63) Hong, V.; Udit, A. K.; Evans, R. A.; Finn, M. G. Electrochemically Protected Copper(I)-Catalyzed Azide-Alkyne Cycloaddition. *ChemBioChem* **2008**, *9*, 1481−1486.
(64) Ritter, S. C.; Konig, B. Signal Amplification and Transduction by Photo-Activated Catalysis. *Chem. Commun.* **2006**, 4694−4696.
(65) Song, H. B.; Baranek, A.; Bowman, C. N. Kinetics of Bulk Photo-Initiated Copper(I)-Catalyzed Azide-Alkyne Cycloaddition (Cuaac) Polymerizations. *Polym. Chem.* **2016**, *7*, 603−612.
(66) El-Zaatari, B. M.; Cole, S. M.; Bischoff, D. J.; Kloxin, C. J. Copper Ligand and Anion Effects: Controlling the Kinetics of the Photoinitiated Copper(I) Catalyzed Azide-Alkyne Cycloaddition Polymerization. *Polym. Chem.* **2018**, *9*, 4772−4780.
(67) El-Zaatari, B. M.; Shete, A. U.; Adzima, B. J.; Kloxin, C. J. Towards Understanding the Kinetic Behaviour and Limitations in Photo-Induced Copper(I) Catalyzed Azide-Alkyne Cycloaddition (Cuaac) Reactions. *Phys. Chem. Chem. Phys.* **2016**, *18*, 25504−25511.
(68) Kutahya, C.; Yagci, Y.; Strehmel, B. Near-Infrared Photo-induced Copper-Catalyzed Azide-Alkyne Click Chemistry with a Cyanine Comprising a Barbiturate Group. *ChemPhotoChem.* **2019**, *3*, 1180−1186.
(69) Gschneidtner, T. A.; Moth-Poulsen, K. A Photolabile Protection Strategy for Terminal Alkynes. *Tetrahedron Lett.* **2013**, *54*, 5426−5429.
(70) Tebikachew, B. E.; Börjesson, K.; Kann, N.; Moth-Poulsen, K. Release of Terminal Alkynes Via Tandem Photodeprotection and Decarboxylation of O-Nitrobenzyl Arylpropiolates in a Flow Microchannel Reactor. *Bioconjugate Chem.* **2018**, *29*, 1178−1185.
(71) Sun, X.; Zou, Y.; Jiang, J. Surface Plasmon Resonances Enhanced Click Chemistry through Synergistic Photothermal and Hot Electron Effects. *Chem. Commun.* **2019**, *55*, 4813−4816.
(72) Baskin, J. M.; Prescher, J. A.; Laughlin, S. T.; Agard, N. J.; Chang, P. V.; Miller, I. A.; Lo, A.; Codelli, J. A.; Bertozzi, C. R. Copper-Free Click Chemistry for Dynamic in Vivo Imaging. *Proc. Natl. Acad. Sci. U. S. A.* **2007**, *104*, 16793.
(73) Codelli, J. A.; Baskin, J. M.; Agard, N. J.; Bertozzi, C. R. Second-Generation Difluorinated Cyclooctynes for Copper-Free Click Chemistry. *J. Am. Chem. Soc.* **2008**, *130*, 11486−11493.
(74) Gordon, C. G.; Mackey, J. L.; Jewett, J. C.; Sletten, E. M.; Houk, K. N.; Bertozzi, C. R. Reactivity of Biarylazacyclooctynones in Copper-Free Click Chemistry. *J. Am. Chem. Soc.* **2012**, *134*, 9199−9208.
(75) Jewett, J. C.; Bertozzi, C. R. Cu-Free Click Cycloaddition Reactions in Chemical Biology. *Chem. Soc. Rev.* **2010**, *39*, 1272−1279.
(76) Sutton, D. A.; Popik, V. V. Sequential Photochemistry of Dibenzo[a,E]Dicyclopropa[C,G][8]Annulene-1,6-Dione: Selective Formation of Didehydrodibenzo[a,E][8]Annulenes with Ultrafast Spaac Reactivity. *J. Org. Chem.* **2016**, *81*, 8850−8857.
(77) Sutton, D. A.; Yu, S.-H.; Steet, R.; Popik, V. V. Cyclopropenone-Caged Sondheimer Diyne (Dibenzo[a,E]Cyclooctadiyne): A Photoactivatable Linchpin for Efficient Spaac Crosslinking. *Chem. Commun.* **2016**, *52*, 553−556.
(78) Mishiro, K.; Kimura, T.; Furuyama, T.; Kunishima, M. Phototriggered Active Alkyne Generation from Cyclopropenones with Visible Light-Responsive Photocatalysts. *Org. Lett.* **2019**, *21*, 4101−4105.
(79) Jedináková, P.; Šebej, P.; Slanina, T.; Klán, P.; Hlaváč, J. Study and Application of Noncatalyzed Photoinduced Conjugation of Azides and Cycloocta-1,2,3-Selenadiazoles. *Chem. Commun.* **2016**, *52*, 4792−4795.
(80) Gann, A. W.; Amoroso, J. W.; Einck, V. J.; Rice, W. P.; Chambers, J. J.; Schnarr, N. A. A Photoinduced, Benzyne Click Reaction. *Org. Lett.* **2014**, *16*, 2003−2005.
(81) Huisgen, R.; Ooms, P. H. J.; Mingin, M.; Allinger, N. L. Exceptional Reactivity of the Bicyclo[2.2.1]Heptene Double Bond. *J. Am. Chem. Soc.* **1980**, *102*, 3951−3953.
(82) Singh, K.; Fennell, C. J.; Coutsias, E. A.; Latifi, R.; Hartson, S.; Weaver, J. D. Light Harvesting for Rapid and Selective Reactions: Click Chemistry with Strain-Loadable Alkenes. *Chem.* **2018**, *4*, 124−137.
(83) Huisgen, R.; Seidel, M.; Sauer, J.; McFarland, J.; Wallbillich, G. Communications: The Formation of Nitrile Imines in the Thermal Breakdown of 2,5-Disubstituted Tetrazoles. *J. Org. Chem.* **1959**, *24*, 892−893.
(84) Jamieson, C.; Livingstone, K. The Reactivity of Nitrile Imines. In *The Nitrile Imine 1,3-Dipole: Properties, Reactivity and Applications*; Springer International Publishing: Cham, 2020; pp 37−97.
(85) Ramil, C. P.; Lin, Q. Photoclick Chemistry: A Fluorogenic Light-Triggered in Vivo Ligation Reaction. *Curr. Opin. Chem. Biol.* **2014**, *21*, 89−95.
(86) An, P.; Yu, Z.; Lin, Q. Design of Oligothiophene-Based Tetrazoles for Laser-Triggered Photoclick Chemistry in Living Cells. *Chem. Commun.* **2013**, *49*, 9920−9922.
(87) Lederhose, P.; Wüst, K. N. R.; Barner-Kowollik, C.; Blinco, J. P. Catalyst Free Visible Light Induced Cycloaddition as an Avenue for Polymer Ligation. *Chem. Commun.* **2016**, *52*, 5928−5931.
(88) Lederhose, P.; Chen, Z.; Müller, R.; Blinco, J. P.; Wu, S.; Barner-Kowollik, C. Near-Infrared Photoinduced Coupling Reactions Assisted by Upconversion Nanoparticles. *Angew. Chem., Int. Ed.* **2016**, *55*, 12195−12199.
(89) Li, Z.; Qian, L.; Li, L.; Bernhammer, J. C.; Huynh, H. V.; Lee, J.-S.; Yao, S. Q. Tetrazole Photoclick Chemistry: Reinvestigating Its Suitability as a Bioorthogonal Reaction and Potential Applications. *Angew. Chem., Int. Ed.* **2016**, *55*, 2002−2006.
(90) Zhao, S.; Dai, J.; Hu, M.; Liu, C.; Meng, R.; Liu, X.; Wang, C.; Luo, T. Photo-Induced Coupling Reactions of Tetrazoles with Carboxylic Acids in Aqueous Solution: Application in Protein Labelling. *Chem. Commun.* **2016**, *52*, 4702−4705.
(91) An, P.; Lewandowski, T. M.; Erbay, T. G.; Liu, P.; Lin, Q. Sterically Shielded, Stabilized Nitrile Imine for Rapid Bioorthogonal Protein Labeling in Live Cells. *J. Am. Chem. Soc.* **2018**, *140*, 4860−4868.
(92) Huisgen, R.; Grashey, R.; Seidel, M.; Knupfer, H.; Schmidt, R. 1.3-Dipolare Additionen, Iii. Umsetzungen Des Diphenylnitrilimins Mit Carbonyl Und Thiocarbonyl-Verbindungen. *Liebigs Ann. Chem.* **1962**, *658*, 169−180.
(93) Feng, W.; Li, L.; Yang, C.; Welle, A.; Trapp, O.; Levkin, P. A. Uv-Induced Tetrazole-Thiol Reaction for Polymer Conjugation and Surface Functionalization. *Angew. Chem., Int. Ed.* **2015**, *54*, 8732−8735.
(94) Zhang, X.; Wu, X.; Jiang, S.; Gao, J.; Yao, Z.; Deng, J.; Zhang, L.; Yu, Z. Photo-Accelerated "Click" Reaction between Diarylsydnones and Ring-Strained Alkynes for Bioorthogonal Ligation. *Chem. Commun.* **2019**, *55*, 7187−7190.
(95) Gao, J.; Xiong, Q.; Wu, X.; Deng, J.; Zhang, X.; Zhao, X.; Deng, P.; Yu, Z. Direct Ring-Strain Loading for Visible-Light Accelerated Bioorthogonal Ligation Via Diarylsydnone-Dibenzo[B,F][1,4,5]-Thiadiazepine Photo-Click Reactions. *Commun. Chem.* **2020**, *3*, 29.
(96) Jiang, S.; Wu, X.; Liu, H.; Deng, J.; Zhang, X.; Yao, Z.; Zheng, Y.; Li, B.; Yu, Z. Ring-Strain-Promoted Ultrafast Diaryltetrazole-Alkyne Photoclick Reactions Triggered by Visible Light. *ChemPhotoChem.* **2020**, *4*, 327−331.
(97) Deng, J.; Wu, X.; Guo, G.; Zhao, X.; Yu, Z. Photoisomerization-Enhanced 1,3-Dipolar Cycloaddition of Carbon-Bridged Octocyclic

https://doi.org/10.1021/acs.chemrev.0c01212
Chem. Rev. 2021, 121, 6915−6990

Azobenzene with Photo-Released Nitrile Imine for Peptide Stapling and Imaging in Live Cells. *Org. Biomol. Chem.* **2020**, *18*, 5602−5607.
(98) Mueller, J. O.; Schmidt, F. G.; Blinco, J. P.; Barner-Kowollik, C. Visible-Light-Induced Click Chemistry. *Angew. Chem., Int. Ed.* **2015**, *54*, 10284−10288.
(99) Yang, N. C.; Rivas, C. A New Photochemical Primary Process, the Photochemical Enolization of O-Substituted Benzophenones. *J. Am. Chem. Soc.* **1961**, *83*, 2213−2213.
(100) Sammes, P. G. Photoenolisation. *Tetrahedron* **1976**, *32*, 405−422.
(101) Menzel, J. P.; Feist, F.; Tuten, B.; Weil, T.; Blinco, J. P.; Barner-Kowollik, C. Light-Controlled Orthogonal Covalent Bond Formation at Two Different Wavelengths. *Angew. Chem., Int. Ed.* **2019**, *58*, 7470−7474.
(102) Houck, H. A.; Du Prez, F. E.; Barner-Kowollik, C. Controlling Thermal Reactivity with Different Colors of Light. *Nat. Commun.* **2017**, *8*, 1869.
(103) Mueller, P.; Zieger, M. M.; Richter, B.; Quick, A. S.; Fischer, J.; Mueller, J. B.; Zhou, L.; Nienhaus, G. U.; Bastmeyer, M.; Barner-Kowollik, C.; et al. Molecular Switch for Sub-Diffraction Laser Lithography by Photoenol Intermediate-State Cis-Trans Isomerization. *ACS Nano* **2017**, *11*, 6396−6403.
(104) Porter, G.; Tchir, M. F. Photoenolization of Ortho-Substituted Benzophenones by Flash Photolysis. *J. Chem. Soc. A* **1971**, 3772−3777.
(105) Tyson, D. S.; Carbaugh, A. D.; Ilhan, F.; Santos-Pérez, J.; Meador, M. A. Novel Anthracene Diimide Fluorescent Sensor. *Chem. Mater.* **2008**, *20*, 6595−6596.
(106) Arumugam, S.; Popik, V. V. Attach, Remove, or Replace: Reversible Surface Functionalization Using Thiol-Quinone Methide Photoclick Chemistry. *J. Am. Chem. Soc.* **2012**, *134*, 8408−8411.
(107) Billaud, E. M. F.; Shahbazali, E.; Ahamed, M.; Cleeren, F.; Noël, T.; Koole, M.; Verbruggen, A.; Hessel, V.; Bormans, G. Micro-Flow Photosynthesis of New Dienophiles for Inverse-Electron-Demand Diels-Alder Reactions. Potential Applications for Pretargeted in Vivo Pet Imaging. *Chem. Sci.* **2017**, *8*, 1251−1258.
(108) Svatunek, D.; Denk, C.; Rosecker, V.; Sohr, B.; Hametner, C.; Allmaier, G.; Fröhlich, J.; Mikula, H. Efficient Low-Cost Preparation Of trans-Cyclooctenes Using a Simplified Flow Setup for Photoisomerization. *Monatsh. Chem.* **2016**, *147*, 579−585.
(109) Scott, T. F.; Furgal, J. C.; Kloxin, C. J. Expanding the Alternating Propagation-Chain Transfer-Based Polymerization Toolkit: The Iodo-Ene Reaction. *ACS Macro Lett.* **2015**, *4*, 1404−1409.
(110) Fairbanks, B. D.; Scott, T. F.; Kloxin, C. J.; Anseth, K. S.; Bowman, C. N. Thiol-Yne Photopolymerizations: Novel Mechanism, Kinetics, and Step-Growth Formation of Highly Cross-Linked Networks. *Macromolecules* **2009**, *42*, 211−217.
(111) El-Roz, M.; Lalevée, J.; Allonas, X.; Fouassier, J.-P. The Silane-Ene and Silane-Acrylate Polymerization Process: A New Promising Chemistry? *Macromol. Rapid Commun.* **2008**, *29*, 804−808.
(112) Alvey, L. J.; Rutherford, D.; Juliette, J. J. J.; Gladysz, J. A. Additions of Ph3 to Monosubstituted Alkenes of the Formula H2cch(Ch2)X(Cf2)Ycf3: Convenient, Multigram Syntheses of a Family of Partially Fluorinated Trialkylphosphines with Modulated Electronic Properties and Fluorous Phase Affinities. *J. Org. Chem.* **1998**, *63*, 6302−6308.
(113) Posner, T. Beiträge Zur Kenntniss Der Ungesättigten Verbindungen. Ii. Ueber Die Addition Von Mercaptanen an Ungesättigte Kohlenwasserstoffe. *Ber. Dtsch. Chem. Ges.* **1905**, *38*, 646−657.
(114) Chauhan, P.; Mahajan, S.; Enders, D. Organocatalytic Carbon-Sulfur Bond-Forming Reactions. *Chem. Rev.* **2014**, *114*, 8807−8864.
(115) Clayden, J.; MacLellan, P. Asymmetric Synthesis of Tertiary Thiols and Thioethers. *Beilstein J. Org. Chem.* **2011**, *7*, 582−595.
(116) Tucker-Schwartz, A. K.; Farrell, R. A.; Garrell, R. L. Thiol-Ene Click Reaction as a General Route to Functional Trialkoxysilanes for Surface Coating Applications. *J. Am. Chem. Soc.* **2011**, *133*, 11026−11029.
(117) Cramer, N. B.; Reddy, S. K.; O'Brien, A. K.; Bowman, C. N. Thiol-Ene Photopolymerization Mechanism and Rate Limiting Step Changes for Various Vinyl Functional Group Chemistries. *Macromolecules* **2003**, *36*, 7964−7969.
(118) Koo, S. P. S.; Stamenovic, M. M.; Prasath, R. A.; Inglis, A. J.; Du Prez, F. E.; Barner-Kowollik, C.; Van Camp, W.; Junkers, T. Limitations of Radical Thiol-Ene Reactions for Polymer-Polymer Conjugation. *J. Polym. Sci., Part A: Polym. Chem.* **2010**, *48*, 1699−1713.
(119) Zgrzeba, A.; Andrzejewska, E.; Marcinkowska, A. Ionic Liquid - Containing Ionogels by Thiol-Ene Photopolymerization. Kinetics and Solvent Effect. *RSC Adv.* **2015**, *5*, 100354−100361.
(120) Munar, I.; Findik, V.; Degirmenci, I.; Aviyente, V. Solvent Effects on Thiol-Ene Kinetics and Reactivity of Carbon and Sulfur Radicals. *J. Phys. Chem. A* **2020**, *124*, 2580−2590.
(121) Skinner, E. K.; Whiffin, F. M.; Price, G. J. Room Temperature Sonochemical Initiation of Thiol-Ene Reactions. *Chem. Commun.* **2012**, *48*, 6800−6802.
(122) Love, D. M.; Fairbanks, B. D.; Bowman, C. N. Evaluation of Aromatic Thiols as Photoinitiators. *Macromolecules* **2020**, *53*, 5237−5247.
(123) Ahn, D.; Sathe, S. S.; Clarkson, B. H.; Scott, T. F. Hexaarylbiimidazoles as Visible Light Thiol-Ene Photoinitiators. *Dent. Mater.* **2015**, *31*, 1075−1089.
(124) Kolczak, U.; Rist, G.; Dietliker, K.; Wirz, J. Reaction Mechanism of Monoacyl- and Bisacylphosphine Oxide Photoinitiators Studied by 31p-, 13c-, and 1h-Cidnp and Esr. *J. Am. Chem. Soc.* **1996**, *118*, 6477−6489.
(125) Ganster, B.; Fischer, U. K.; Moszner, N.; Liska, R. New Photocleavable Structures. Diacylgermane-Based Photoinitiators for Visible Light Curing. *Macromolecules* **2008**, *41*, 2394−2400.
(126) Mitterbauer, M.; Knaack, P.; Naumov, S.; Markovic, M.; Ovsianikov, A.; Moszner, N.; Liska, R. Acylstannanes: Cleavable and Highly Reactive Photoinitiators for Radical Photopolymerization at Wavelengths above 500 Nm with Excellent Photobleaching Behavior. *Angew. Chem., Int. Ed.* **2018**, *57*, 12146−12150.
(127) Zhao, G.; Kaur, S.; Wang, T. Visible-Light-Mediated Thiol-Ene Reactions through Organic Photoredox Catalysis. *Org. Lett.* **2017**, *19*, 3291−3294.
(128) Bhat, V. T.; Duspara, P. A.; Seo, S.; Abu Bakar, N. S. B.; Greaney, M. F. Visible Light Promoted Thiol-Ene Reactions Using Titanium Dioxide. *Chem. Commun.* **2015**, *51*, 4383−4385.
(129) Keylor, M. H.; Park, J. E.; Wallentin, C.-J.; Stephenson, C. R. J. Photocatalytic Initiation of Thiol-Ene Reactions: Synthesis of Thiomorpholin-3-Ones. *Tetrahedron* **2014**, *70*, 4264−4269.
(130) Limnios, D.; Kokotos, C. G. Photoinitiated Thiol-Ene "Click" Reaction: An Organocatalytic Alternative. *Adv. Synth. Catal.* **2017**, *359*, 323−328.
(131) Tyson, E. L.; Ament, M. S.; Yoon, T. P. Transition Metal Photoredox Catalysis of Radical Thiol-Ene Reactions. *J. Org. Chem.* **2013**, *78*, 2046−2050.
(132) Tyson, E. L.; Niemeyer, Z. L.; Yoon, T. P. Redox Mediators in Visible Light Photocatalysis: Photocatalytic Radical Thiol-Ene Additions. *J. Org. Chem.* **2014**, *79*, 1427−1436.
(133) Wimmer, A.; Koenig, B. Photocatalytic Formation of Carbon-Sulfur Bonds. *Beilstein J. Org. Chem.* **2018**, *14*, 54−83.
(134) Koyama, D.; Orr-Ewing, A. J. Photochemical Reaction Dynamics of 2,2'-Dithiobis(Benzothiazole): Direct Observation of the Addition Product of an Aromatic Thiyl Radical to an Alkene with Time-Resolved Vibrational and Electronic Absorption Spectroscopy. *Phys. Chem. Chem. Phys.* **2016**, *18*, 12115−12127.
(135) Li, Z.; Zou, X.; Shi, F.; Liu, R.; Yagci, Y. Highly Efficient Dandelion-Like near-Infrared Light Photoinitiator for Free Radical and Thiol-Ene Photopolymerizations. *Nat. Commun.* **2019**, *10*, 3560.
(136) Burget, D.; Mallein, C.; Fouassier, J. P. Photopolymerization of Thiol-Allyl Ether and Thiol-Acrylate Coatings with Visible Light Photosensitive Systems. *Polymer* **2004**, *45*, 6561−6567.

https://doi.org/10.1021/acs.chemrev.0c01212
Chem. Rev. 2021, 121, 6915−6990

(137) Uygun, M.; Tasdelen, M. A.; Yagci, Y. Influence of Type of Initiation on Thiol-Ene "Click" Chemistry. *Macromol. Chem. Phys.* **2010**, *211*, 103−110.
(138) Xu, J.; Boyer, C. Visible Light Photocatalytic Thiol-Ene Reaction: An Elegant Approach for Fast Polymer Postfunctionalization and Step-Growth Polymerization. *Macromolecules* **2015**, *48*, 520−529.
(139) Guerrero-Corella, A.; Maria Martinez-Gualda, A.; Ahmadi, F.; Ming, E.; Fraile, A.; Aleman, J. Thiol-Ene/Oxidation Tandem Reaction under Visible Light Photocatalysis: Synthesis of Alkyl Sulfoxides. *Chem. Commun.* **2017**, *53*, 10463−10466.
(140) Shih, H.; Lin, C.-C. Cross-Linking and Degradation of Step-Growth Hydrogels Formed by Thiol-Ene Photoclick Chemistry. *Biomacromolecules* **2012**, *13*, 2003−2012.
(141) Morgan, C. R.; Magnotta, F.; Ketley, A. D. Thiol-Ene Photo-Curable Polymers. *J. Polym. Sci., Part A: Polym. Chem.* **1977**, *15*, 627−645.
(142) Wutticharoenwong, K.; Soucek, M. D. Influence of the Thiol Structure on the Kinetics of Thiol-Ene Photopolymerization with Time-Resolved Infrared Spectroscopy. *Macromol. Mater. Eng.* **2008**, *293*, 45−56.
(143) Long, K. F.; Bongiardina, N. J.; Mayordomo, P.; Olin, M. J.; Ortega, A. D.; Bowman, C. N. Effects of 1 Degrees, 2 Degrees, and 3 Degrees Thiols on Thiol-Ene Reactions: Polymerization Kinetics and Mechanical Behavior. *Macromolecules* **2020**, *53*, 5805−5815.
(144) Findik, V.; Degirmenci, I.; Catak, S.; Aviyente, V. Theoretical Investigation of Thiol-Ene Click Reactions: A Dft Perspective. *Eur. Polym. J.* **2019**, *110*, 211−220.
(145) Hoyle, C. E.; Lee, T. Y.; Roper, T. Thiol-Enes: Chemistry of the Past with Promise for the Future. *J. Polym. Sci., Part A: Polym. Chem.* **2004**, *42*, 5301−5338.
(146) Cramer, N. B.; Reddy, S. K.; O'Brien, A. K.; Bowman, C. N. Thiol-Ene Photopolymerization Mechanism and Rate Limiting Step Changes for Various Vinyl Functional Group Chemistries. *Macromolecules* **2003**, *36*, 7964−7969.
(147) Northrop, B. H.; Coffey, R. N. Thiol-Ene Click Chemistry: Computational and Kinetic Analysis of the Influence of Alkene Functionality. *J. Am. Chem. Soc.* **2012**, *134*, 13804−13817.
(148) Stolz, R. M.; Northrop, B. H. Experimental and Theoretical Studies of Selective Thiol-Ene and Thiol-Yne Click Reactions Involving N-Substituted Maleimides. *J. Org. Chem.* **2013**, *78*, 8105−8116.
(149) Love, D. M.; Kim, K.; Goodrich, J. T.; Fairbanks, B. D.; Worrell, B. T.; Stoykovich, M. P.; Musgrave, C. B.; Bowman, C. N. Amine Induced Retardation of the Radical-Mediated Thiol-Ene Reaction Via the Formation of Metastable Disulfide Radical Anions. *J. Org. Chem.* **2018**, *83*, 2912−2919.
(150) Fairbanks, B. D.; Scott, T. F.; Kloxin, C. J.; Anseth, K. S.; Bowman, C. N. Thiol-Yne Photopolymerizations: Novel Mechanism, Kinetics, and Step-Growth Formation of Highly Cross-Linked Networks. *Macromolecules* **2009**, *42*, 211−217.
(151) van Geel, R.; Pruijn, G. J. M.; van Delft, F. L.; Boelens, W. C. Preventing Thiol-Yne Addition Improves the Specificity of Strain-Promoted Azide-Alkyne Cycloaddition. *Bioconjugate Chem.* **2012**, *23*, 392−398.
(152) Kritchenkov, A. S.; Egorov, A. R.; Artemjev, A. A.; Kritchenkov, I. S.; Volkova, O. V.; Kurliuk, A. V.; Shakola, T. V.; Rubanik, V. V., Jr.; Rubanik, V. V.; Tskhovrebov, A. G.; et al. Ultrasound-Assisted Catalyst-Free Thiol-Yne Click Reaction in Chitosan Chemistry: Antibacterial and Transfection Activity of Novel Cationic Chitosan Derivatives and Their Based Nanoparticles. *Int. J. Biol. Macromol.* **2020**, *143*, 143−152.
(153) Zalesskiy, S. S.; Shlapakov, N. S.; Ananikov, V. P. Visible Light Mediated Metal-Free Thiol-Yne Click Reaction. *Chem. Sci.* **2016**, *7*, 6740−6745.
(154) Burykina, J. V.; Shlapakov, N. S.; Gordeev, E. G.; König, B.; Ananikov, V. P. Selectivity Control in Thiol-Yne Click Reactions Via Visible Light Induced Associative Electron Upconversion. *Chem. Sci.* **2020**, *11*, 10061−10070.
(155) Kaur, S.; Zhao, G.; Busch, E.; Wang, T. Metal-Free Photocatalytic Thiol-Ene/Thiol-Yne Reactions. *Org. Biomol. Chem.* **2019**, *17*, 1955−1961.
(156) Boyer, C.; Ameduri, B.; Hung, M. H. Telechelic Diiodopoly-(Vdf-Co-Pmve) Copolymers by Iodine Transfer Copolymerization of Vinylidene Fluoride (Vdf) with Perfluoromethyl Vinyl Ether (Pmve). *Macromolecules* **2010**, *43*, 3652−3663.
(157) Boyer, C.; Valade, D.; Sauguet, L.; Ameduri, B.; Boutevin, B. Iodine Transfer Polymerization (Itp) of Vinylidene Fluoride (Vdf). Influence of the Defect of Vdf Chaining on the Control of Itp. *Macromolecules* **2005**, *38*, 10353−10362.
(158) David, G.; Boyer, C.; Tonnar, J.; Ameduri, B.; Lacroix-Desmazes, P.; Boutevin, B. Use of Iodocompounds in Radical Polymerization. *Chem. Rev.* **2006**, *106*, 3936−3962.
(159) Valade, D.; Boyer, C.; Ameduri, B.; Boutevin, B. Poly-(Vinylidene Fluoride)-B-Poly(Styrene) Block Copolymers by Iodine Transfer Polymerization (Itp): Synthesis, Characterization, and Kinetics of Itp. *Macromolecules* **2006**, *39*, 8639−8651.
(160) Scott, T. F.; Furgal, J. C.; Kloxin, C. J. Expanding the Alternating Propagation-Chain Transfer-Based Polymerization Toolkit: The Iodo-Ene Reaction. *ACS Macro Lett.* **2015**, *4*, 1404−1409.
(161) Sinha, J.; Fairbanks, B.; Chen, M.; Song, H. B.; Bowman, C. Phosphate-Based Cross-Linked Polymers from Iodo−ene Photopolymerization: Tuning Surface Wettability through Thiol−ene Chemistry. *ACS Macro Lett.* **2019**, *8*, 213−217.
(162) Steindl, J.; Svirkova, A.; Marchetti-Deschmann, M.; Moszner, N.; Gorsche, C. Light-Triggered Radical Silane-Ene Chemistry Using a Monosubstituted Bis(Trimethylsilyl)Silane. *Macromol. Chem. Phys.* **2017**, *218*, 1600563.
(163) Steindl, J.; Koch, T.; Moszner, N.; Gorsche, C. Silane-Acrylate Chemistry for Regulating Network Formation in Radical Photopolymerization. *Macromolecules* **2017**, *50*, 7448−7457.
(164) Pellon, J. Phosphines: Chain Transfer Studies with Styrene and Methyl Methacrylate. *J. Polym. Sci.* **1960**, *43*, 537−548.
(165) Guterman, R.; Rabiee Kenaree, A.; Gilroy, J. B.; Gillies, E. R.; Ragogna, P. J. Polymer Network Formation Using the Phosphane-Ene Reaction: A Thiol-Ene Analogue with Diverse Postpolymerization Chemistry. *Chem. Mater.* **2015**, *27*, 1412−1419.
(166) Hoyle, C. E.; Lowe, A. B.; Bowman, C. N. Thiol-Click Chemistry: A Multifaceted Toolbox for Small Molecule and Polymer Synthesis. *Chem. Soc. Rev.* **2010**, *39*, 1355−1387.
(167) Kade, M. J.; Burke, D. J.; Hawker, C. J. The Power of Thiol-Ene Chemistry. *J. Polym. Sci., Part A: Polym. Chem.* **2010**, *48*, 743−750.
(168) Lowe, A. B. Thiol-Ene "Click" Reactions and Recent Applications in Polymer and Materials Synthesis. *Polym. Chem.* **2010**, *1*, 17−36.
(169) Fringuelli, F.; Pizzo, F.; Tortoioli, S.; Vaccaro, L. Thiolysis of 1,2-Epoxides by Thiophenol Catalyzed under Solvent-Free Conditions. *Tetrahedron Lett.* **2003**, *44*, 6785−6787.
(170) Dietliker, K.; Hüsler, R.; Birbaum, J. L.; Ilg, S.; Villeneuve, S.; Studer, K.; Jung, T.; Benkhoff, J.; Kura, H.; Matsumoto, A.; et al. Advancements in Photoinitiators—Opening up New Applications for Radiation Curing. *Prog. Org. Coat.* **2007**, *58*, 146−157.
(171) Suyama, K.; Shirai, M. Photobase Generators: Recent Progress and Application Trend in Polymer Systems. *Prog. Polym. Sci.* **2009**, *34*, 194−209.
(172) Dong, X.; Hu, P.; Zhu, G.; Li, Z.; Liu, R.; Liu, X. Thioxanthone Acetic Acid Ammonium Salts: Highly Efficient Photobase Generators Based on Photodecarboxylation. *RSC Adv.* **2015**, *5*, 53342−53348.
(173) Arimitsu, K.; Oguri, A.; Furutani, M. 365nm-Light-Sensitive Photobase Generators Derived from Trans-O-Coumaric Acid. *Mater. Lett.* **2015**, *140*, 92−94.
(174) Ning, X.; Ishida, H. Phenolic Materials Via Ring-Opening Polymerization: Synthesis and Characterization of Bisphenol-a Based Benzoxazines and Their Polymers. *J. Polym. Sci., Part A: Polym. Chem.* **1994**, *32*, 1121−1129.

https://doi.org/10.1021/acs.chemrev.0c01212
Chem. Rev. 2021, 121, 6915−6990

(175) Chae, K. H.; Cho, H. I.; Kim, Y. H.; Yang, U. C. Photo-Crosslinking and Negative-Type Micropattern Formation of a Polymeric Photobase Generator Containing Phthalimido Carbamate Groups. *Eur. Polym. J.* **2012**, *48*, 1186−1194.
(176) Cameron, J. F.; Willson, C. G.; Fréchet, J. M. J. Photogeneration of Amines from A-Keto Carbamates: Photochemical Studies. *J. Am. Chem. Soc.* **1996**, *118*, 12925−12937.
(177) Cameron, J. F.; Frechet, J. M. J. Photogeneration of Organic Bases from O-Nitrobenzyl-Derived Carbamates. *J. Am. Chem. Soc.* **1991**, *113*, 4303−4313.
(178) Salmi, H.; Allonas, X.; Ley, C.; Defoin, A.; Ak, A. Quaternary Ammonium Salts of Phenylglyoxylic Acid as Photobase Generators for Thiol-Promoted Epoxide Photopolymerization. *Polym. Chem.* **2014**, *5*, 6577−6583.
(179) Katogi, S.; Yusa, M. Photobase Generation from Amineimide Derivatives and Their Use for Curing an Epoxide/Thiol System. *J. Polym. Sci., Part A: Polym. Chem.* **2002**, *40*, 4045−4052.
(180) Sun, X.; Gao, J. P.; Wang, Z. Y. Bicyclic Guanidinium Tetraphenylborate: A Photobase Generator and a Photocatalyst for Living Anionic Ring-Opening Polymerization and Cross-Linking of Polymeric Materials Containing Ester and Hydroxy Groups. *J. Am. Chem. Soc.* **2008**, *130*, 8130−8131.
(181) Ye, S.; Cramer, N. B.; Smith, I. R.; Voigt, K. R.; Bowman, C. N. Reaction Kinetics and Reduced Shrinkage Stress of Thiol-Yne-Methacrylate and Thiol-Yne-Acrylate Ternary Systems. *Macromolecules* **2011**, *44*, 9084−9090.
(182) Jian, Y.; He, Y.; Sun, Y.; Yang, H.; Yang, W.; Nie, J. Thiol-Epoxy/Thiol-Acrylate Hybrid Materials Synthesized by Photopolymerization. *J. Mater. Chem. C* **2013**, *1*, 4481−4489.
(183) Chen, L.; Zheng, Y.; Meng, X.; Wei, G.; Dietliker, K.; Li, Z. Delayed Thiol-Epoxy Photopolymerization: A General and Effective Strategy to Prepare Thick Composites. *ACS Omega* **2020**, *5*, 15192−15201.
(184) Chang, H.-T.; Fréchet, J. M. J. Proton-Transfer Polymerization: A New Approach to Hyperbranched Polymers. *J. Am. Chem. Soc.* **1999**, *121*, 2313−2314.
(185) Gong, C.; Fréchet, J. M. J. Proton Transfer Polymerization in the Preparation of Hyperbranched Polyesters with Epoxide Chain-Ends and Internal Hydroxyl Functionalities. *Macromolecules* **2000**, *33*, 4997−4999.
(186) Emrick, T.; Chang, H.-T.; Fréchet, J. M. J. An A2 + B3 Approach to Hyperbranched Aliphatic Polyethers Containing Chain End Epoxy Substituents. *Macromolecules* **1999**, *32*, 6380−6382.
(187) Yeo, H.; Khan, A. Photoinduced Proton-Transfer Polymerization: A Practical Synthetic Tool for Soft Lithography Applications. *J. Am. Chem. Soc.* **2020**, *142*, 3479−3488.
(188) Romano, A.; Roppolo, I.; Giebler, M.; Dietliker, K.; Možina, Š.; Šket, P.; Mühlbacher, I.; Schlögl, S.; Sangermano, M. Stimuli-Responsive Thiol-Epoxy Networks with Photo-Switchable Bulk and Surface Properties. *RSC Adv.* **2018**, *8*, 41904−41914.
(189) Mühlman, A.; Classon, B.; Hallberg, A.; Samuelsson, B. Synthesis of Potent C2-Symmetric, Diol-Based Hiv-1 Protease Inhibitors. Investigation of Thioalkyl and Thioaryl P1/P1' Substituents. *J. Med. Chem.* **2001**, *44*, 3402−3406.
(190) Basuki, J. S.; Esser, L.; Duong, H. T. T.; Zhang, Q.; Wilson, P.; Whittaker, M. R.; Haddleton, D. M.; Boyer, C.; Davis, T. P. Magnetic Nanoparticles with Diblock Glycopolymer Shells Give Lectin Concentration-Dependent Mri Signals and Selective Cell Uptake. *Chem. Sci.* **2014**, *5*, 715−726.
(191) Buerkli, C.; Lee, S. H.; Moroz, E.; Stuparu, M. C.; Leroux, J.-C.; Khan, A. Amphipathic Homopolymers for Sirna Delivery: Probing Impact of Bifunctional Polymer Composition on Transfection. *Biomacromolecules* **2014**, *15*, 1707−1715.
(192) Arnold, R. G.; Nelson, J. A.; Verbanc, J. J. Recent Advances in Isocyanate Chemistry. *Chem. Rev.* **1957**, *57*, 47−76.
(193) Shin, J.; Matsushima, H.; Chan, J. W.; Hoyle, C. E. Segmented Polythiourethane Elastomers through Sequential Thiol-Ene and Thiol-Isocyanate Reactions. *Macromolecules* **2009**, *42*, 3294−3301.
(194) Shin, J.; Matsushima, H.; Comer, C. M.; Bowman, C. N.; Hoyle, C. E. Thiol-Isocyanate-Ene Ternary Networks by Sequential and Simultaneous Thiol Click Reactions. *Chem. Mater.* **2010**, *22*, 2616−2625.
(195) Hu, Y.; Kowalski, B. A.; Mavila, S.; Podgórski, M.; Sinha, J.; Sullivan, A. C.; McLeod, R. R.; Bowman, C. N. Holographic Photopolymer Material with High Dynamic Range (Δn) Via Thiol-Ene Click Chemistry. *ACS Appl. Mater. Interfaces* **2020**, *12*, 44103−44109.
(196) Hensarling, R. M.; Rahane, S. B.; LeBlanc, A. P.; Sparks, B. J.; White, E. M.; Locklin, J.; Patton, D. L. Thiol-Isocyanate "Click" Reactions: Rapid Development of Functional Polymeric Surfaces. *Polym. Chem.* **2011**, *2*, 88−90.
(197) Mather, B. D.; Viswanathan, K.; Miller, K. M.; Long, T. E. Michael Addition Reactions in Macromolecular Design for Emerging Technologies. *Prog. Polym. Sci.* **2006**, *31*, 487−531.
(198) Nising, C. F.; Bräse, S. The Oxa-Michael Reaction: From Recent Developments to Applications in Natural Product Synthesis. *Chem. Soc. Rev.* **2008**, *37*, 1218−1228.
(199) Nair, D. P.; Podgórski, M.; Chatani, S.; Gong, T.; Xi, W.; Fenoli, C. R.; Bowman, C. N. The Thiol-Michael Addition Click Reaction: A Powerful and Widely Used Tool in Materials Chemistry. *Chem. Mater.* **2014**, *26*, 724−744.
(200) Desmet, G. B.; Sabbe, M. K.; D'Hooge, D. R.; Espeel, P.; Celasun, S.; Marin, G. B.; Du Prez, F. E.; Reyniers, M.-F. Thiol-Michael Addition in Polar Aprotic Solvents: Nucleophilic Initiation or Base Catalysis? *Polym. Chem.* **2017**, *8*, 1341−1352.
(201) Chan, J. W.; Hoyle, C. E.; Lowe, A. B.; Bowman, M. Nucleophile-Initiated Thiol-Michael Reactions: Effect of Organocatalyst, Thiol, and Ene. *Macromolecules* **2010**, *43*, 6381−6388.
(202) Chan, J. W.; Yu, B.; Hoyle, C. E.; Lowe, A. B. The Nucleophilic, Phosphine-Catalyzed Thiol-Ene Click Reaction and Convergent Star Synthesis with Raft-Prepared Homopolymers. *Polymer* **2009**, *50*, 3158−3168.
(203) Joshi, G.; Anslyn, E. V. Dynamic Thiol Exchange with B-Sulfido-A,B-Unsaturated Carbonyl Compounds and Dithianes. *Org. Lett.* **2012**, *14*, 4714−4717.
(204) Van Herck, N.; Maes, D.; Unal, K.; Guerre, M.; Winne, J. M.; Du Prez, F. E. Covalent Adaptable Networks with Tunable Exchange Rates Based on Reversible Thiol-Yne Cross-Linking. *Angew. Chem., Int. Ed.* **2020**, *59*, 3609−3617.
(205) Claudino, M.; Zhang, X.; Alim, M. D.; Podgórski, M.; Bowman, C. N. Mechanistic Kinetic Modeling of Thiol-Michael Addition Photopolymerizations Via Photocaged "Superbase" Generators: An Analytical Approach. *Macromolecules* **2016**, *49*, 8061−8074.
(206) Xi, W.; Peng, H.; Aguirre-Soto, A.; Kloxin, C. J.; Stansbury, J. W.; Bowman, C. N. Spatial and Temporal Control of Thiol-Michael Addition Via Photocaged Superbase in Photopatterning and Two-Stage Polymer Networks Formation. *Macromolecules* **2014**, *47*, 6159−6165.
(207) Zhang, X.; Xi, W.; Wang, C.; Podgórski, M.; Bowman, C. N. Visible-Light-Initiated Thiol-Michael Addition Polymerizations with Coumarin-Based Photobase Generators: Another Photoclick Reaction Strategy. *ACS Macro Lett.* **2016**, *5*, 229−233.
(208) Sinha, J.; Podgórski, M.; Tomaschke, A.; Ferguson, V. L.; Bowman, C. N. Phototriggered Base Amplification for Thiol-Michael Addition Reactions in Cross-Linked Photopolymerizations with Efficient Dark Cure. *Macromolecules* **2020**, *53*, 6331−6340.
(209) Arimitsu, K.; Miyamoto, M.; Ichimura, K. Applications of a Nonlinear Organic Reaction of Carbamates to Proliferate Aliphatic Amines. *Angew. Chem., Int. Ed.* **2000**, *39*, 3425−3428.
(210) Xu, R.; Guan, X.; He, M.; Yang, J. Phototriggered Base Proliferation: A Powerful 365 nm Led Photoclick Tool for Nucleophile-Initiated Thiol-Michael Addition Reaction. *RSC Adv.* **2017**, *7*, 914−918.
(211) Bao, C.; Zhu, L.; Lin, Q.; Tian, H. Building Biomedical Materials Using Photochemical Bond Cleavage. *Adv. Mater.* **2015**, *27*, 1647−1662.

https://doi.org/10.1021/acs.chemrev.0c01212
Chem. Rev. 2021, 121, 6915−6990

(212) Klán, P.; Šolomek, T.; Bochet, C. G.; Blanc, A.; Givens, R.; Rubina, M.; Popik, V.; Kostikov, A.; Wirz, J. Photoremovable Protecting Groups in Chemistry and Biology: Reaction Mechanisms and Efficacy. *Chem. Rev.* **2013**, *113*, 119−191.
(213) Kotzur, N.; Briand, B.; Beyermann, M.; Hagen, V. Wavelength-Selective Photoactivatable Protecting Groups for Thiols. *J. Am. Chem. Soc.* **2009**, *131*, 16927−16931.
(214) Barltrop, J. A.; Plant, P. J.; Schofield, P. Photosensitive Protective Groups. *Chem. Commun.* **1966**, *1966*, 822−823.
(215) Patchornik, A.; Amit, B.; Woodward, R. B. Photosensitive Protecting Groups. *J. Am. Chem. Soc.* **1970**, *92*, 6333−6335.
(216) Gravel, D.; Giasson, R.; Blanchet, D.; Yip, R. W.; Sharma, D. K. Photochemistry of the Ortho-Nitrobenzyl System in Solution - Effects of O-H Distance and Geometrical Constraint on the Hydrogen Transfer Mechanism in the Excited-State. *Can. J. Chem.* **1991**, *69*, 1193−1200.
(217) Takezaki, M.; Hirota, N.; Terazima, M. Nonradiative Relaxation Processes and Electronically Excited States of Nitrobenzene Studied by Picosecond Time-Resolved Transient Grating Method. *J. Phys. Chem. A* **1997**, *101*, 3443−3448.
(218) Schwörer, M.; Wirz, J. Photochemical Reaction Mechanisms of 2-Nitrobenzyl Compounds in Solution, I. 2-Nitrotoluene: Thermodynamic and Kinetic Parameters of the Aci-Nitro Tautomer. *Helv. Chim. Acta* **2001**, *84*, 1441−1458.
(219) Schmierer, T.; Laimgruber, S.; Haiser, K.; Kiewisch, K.; Neugebauer, J.; Gilch, P. Femtosecond Spectroscopy on the Photochemistry of Ortho-Nitrotoluene. *Phys. Chem. Chem. Phys.* **2010**, *12*, 15653−15664.
(220) Il'ichev, Y. V.; Schwörer, M. A.; Wirz, J. Photochemical Reaction Mechanisms of 2-Nitrobenzyl Compounds: Methyl Ethers and Caged Atp. *J. Am. Chem. Soc.* **2004**, *126*, 4581−4595.
(221) Walker, J. W.; Reid, G. P.; McCray, J. A.; Trentham, D. R. Photolabile 1-(2-Nitrophenyl)Ethyl Phosphate Esters of Adenine Nucleotide Analogs. Synthesis and Mechanism of Photolysis. *J. Am. Chem. Soc.* **1988**, *110*, 7170−7177.
(222) Kloxin, A. M.; Kasko, A. M.; Salinas, C. N.; Anseth, K. S. Photodegradable Hydrogels for Dynamic Tuning of Physical and Chemical Properties. *Science* **2009**, *324*, 59−63.
(223) Tsurkan, M. V.; Wetzel, R.; Pérez-Hernández, H. R.; Chwalek, K.; Kozlova, A.; Freudenberg, U.; Kempermann, G.; Zhang, Y.; Lasagni, A. F.; Werner, C. Photopatterning of Multifunctional Hydrogels to Direct Adult Neural Precursor Cells. *Adv. Healthcare Mater.* **2015**, *4*, 516−521.
(224) Brown, E. B.; Shear, J. B.; Adams, S. R.; Tsien, R. Y.; Webb, W. W. Photolysis of Caged Calcium in Femtoliter Volumes Using Two-Photon Excitation. *Biophys. J.* **1999**, *76*, 489−499.
(225) Furuta, T.; Wang, S.S.-H.; Dantzker, J. L.; Dore, T. M.; Bybee, W. J.; Callaway, E. M.; Denk, W.; Tsien, R. Y. Brominated 7-Hydroxycoumarin-4-Ylmethyls: Photolabile Protecting Groups with Biologically Useful Cross-Sections for Two Photon Photolysis. *Proc. Natl. Acad. Sci. U. S. A.* **1999**, *96*, 1193−1200.
(226) Schmidt, R.; Geissler, D.; Hagen, V.; Bendig, J. Mechanism of Photocleavage of (Coumarin-4-Yl)Methyl Esters. *J. Phys. Chem. A* **2007**, *111*, 5768−5774.
(227) Schade, B.; Hagen, V.; Schmidt, R.; Herbrich, R.; Krause, E.; Eckardt, T.; Bendig, J. Deactivation Behavior and Excited-State Properties of (Coumarin-4-Yl)Methyl Derivatives. 1. Photocleavage of (7-Methoxycoumarin-4-Yl)Methyl-Caged Acids with Fluorescence Enhancement. *J. Org. Chem.* **1999**, *64*, 9109−9117.
(228) Schmidt, R.; Geissler, D.; Hagen, V.; Bendig, J. Kinetics Study of the Photocleavage of (Coumarin-4-Yl)Methyl Esters. *J. Phys. Chem. A* **2005**, *109*, 5000−5004.
(229) Lin, Q.; Bao, C.; Cheng, S.; Yang, Y.; Ji, W.; Zhu, L. Target-Activated Coumarin Phototriggers Specifically Switch on Fluorescence and Photocleavage Upon Bonding to Thiol-Bearing Protein. *J. Am. Chem. Soc.* **2012**, *134*, 5052−5055.
(230) Girouard, S.; Houle, M.-H.; Grandbois, A.; Keillor, J. W.; Michnick, S. W. Synthesis and Characterization of Dimaleimide Fluorogens Designed for Specific Labeling of Proteins. *J. Am. Chem. Soc.* **2005**, *127*, 559−566.
(231) Chen, X.; Zhou, Y.; Peng, X.; Yoon, J. Fluorescent and Colorimetric Probes for Detection of Thiols. *Chem. Soc. Rev.* **2010**, *39*, 2120−2135.
(232) Mahmoodi, M. M.; Abate-Pella, D.; Pundsack, T. J.; Palsuledesai, C. C.; Goff, P. C.; Blank, D. A.; Distefano, M. D. Nitrodibenzofuran: A One- and Two-Photon Sensitive Protecting Group That Is Superior to Brominated Hydroxycoumarin for Thiol Caging in Peptides. *J. Am. Chem. Soc.* **2016**, *138*, 5848−5859.
(233) Fisher, S. A.; Tam, R. Y.; Fokina, A.; Mahmoodi, M. M.; Distefano, M. D.; Shoichet, M. S. Photo-Immobilized Egf Chemical Gradients Differentially Impact Breast Cancer Cell Invasion and Drug Response in Defined 3d Hydrogels. *Biomaterials* **2018**, *178*, 751−766.
(234) Hu, L. Q.; Colman, R. F. Monobromobimane as an Affinity Label of the Xenobiotic Binding-Site of Rat Glutathione-S-Transferase-3−3. *J. Biol. Chem.* **1995**, *270*, 21875−21883.
(235) Lavis, L. D.; Raines, R. T. Bright Ideas for Chemical Biology. *ACS Chem. Biol.* **2008**, *3*, 142−155.
(236) Kosower, N. S.; Kosower, E. M.; Newton, G. L.; Ranney, H. M. Bimane Fluorescent Labels: Labeling of Normal Human Red Cells under Physiological Conditions. *Proc. Natl. Acad. Sci. U. S. A.* **1979**, *76*, 3382−3386.
(237) Truong, V. X.; Li, F.; Forsythe, J. S. Visible Light Activation of Nucleophilic Thiol-X Addition Via Thioether Bimane Photocleavage for Polymer Cross-Linking. *Biomacromolecules* **2018**, *19*, 4277−4285.
(238) Hensarling, R. M.; Hoff, E. A.; LeBlanc, A. P.; Guo, W.; Rahane, S. B.; Patton, D. L. Photocaged Pendent Thiol Polymer Brush Surfaces for Postpolymerization Modifications Via Thiol-Click Chemistry. *J. Polym. Sci., Part A: Polym. Chem.* **2013**, *51*, 1079−1090.
(239) Lin, Q.; Yang, L.; Wang, Z.; Hua, Y.; Zhang, D.; Bao, B.; Bao, C.; Gong, X.; Zhu, L. Coumarin Photocaging Groups Modified with an Electron-Rich Styryl Moiety at the 3-Position: Long-Wavelength Excitation, Rapid Photolysis, and Photobleaching. *Angew. Chem., Int. Ed.* **2018**, *57*, 3722−3726.
(240) Lin, F.; Yu, J.; Tang, W.; Zheng, J.; Defante, A.; Guo, K.; Wesdemiotis, C.; Becker, M. L. Peptide-Functionalized Oxime Hydrogels with Tunable Mechanical Properties and Gelation Behavior. *Biomacromolecules* **2013**, *14*, 3749−3758.
(241) Grover, G. N.; Lam, J.; Nguyen, T. H.; Segura, T.; Maynard, H. D. Biocompatible Hydrogels by Oxime Click Chemistry. *Biomacromolecules* **2012**, *13*, 3013−3017.
(242) Azagarsamy, M. A.; Marozas, I. A.; Spaans, S.; Anseth, K. S. Photoregulated Hydrazone-Based Hydrogel Formation for Biochemically Patterning 3d Cellular Microenvironments. *ACS Macro Lett.* **2016**, *5*, 19−23.
(243) Yang, Y.; Zhang, J.; Liu, Z.; Lin, Q.; Liu, X.; Bao, C.; Wang, Y.; Zhu, L. Tissue-Integratable and Biocompatible Photogelation by the Imine Crosslinking Reaction. *Adv. Mater.* **2016**, *28*, 2724−2730.
(244) Boehnke, N.; Cam, C.; Bat, E.; Segura, T.; Maynard, H. D. Imine Hydrogels with Tunable Degradability for Tissue Engineering. *Biomacromolecules* **2015**, *16*, 2101−2108.
(245) Kalia, J.; Raines, R. T. Hydrolytic Stability of Hydrazones and Oximes. *Angew. Chem., Int. Ed.* **2008**, *47*, 7523−7526.
(246) Dawson, P.; Muir, T.; Clark-Lewis, I.; Kent, S. Synthesis of Proteins by Native Chemical Ligation. *Science* **1994**, *266*, 776−779.
(247) Agouridas, V.; El Mahdi, O.; Diemer, V.; Cargoët, M.; Monbaliu, J.-C. M.; Melnyk, O. Native Chemical Ligation and Extended Methods: Mechanisms, Catalysis, Scope, and Limitations. *Chem. Rev.* **2019**, *119*, 7328−7443.
(248) Ueda, S.; Fujita, M.; Tamamura, H.; Fujii, N.; Otaka, A. Photolabile Protection for One-Pot Sequential Native Chemical Ligation. *ChemBioChem* **2005**, *6*, 1983−1986.
(249) Aihara, K.; Yamaoka, K.; Naruse, N.; Inokuma, T.; Shigenaga, A.; Otaka, A. One-Pot/Sequential Native Chemical Ligation Using Photocaged Crypto-Thioester. *Org. Lett.* **2016**, *18*, 596−599.
(250) Dondoni, A.; Marra, A. Recent Applications of Thiol-Ene Coupling as a Click Process for Glycoconjugation. *Chem. Soc. Rev.* **2012**, *41*, 573−586.

https://doi.org/10.1021/acs.chemrev.0c01212
Chem. Rev. 2021, 121, 6915−6990

(251) Fiore, M.; Lo Conte, M.; Pacifico, S.; Marra, A.; Dondoni, A. Synthesis of S-Glycosyl Amino Acids and S-Glycopeptides Via Photoinduced Click Thiol-Ene Coupling. *Tetrahedron Lett.* **2011**, *52*, 444−447.
(252) Conte, M. L.; Staderini, S.; Marra, A.; Sanchez-Navarro, M.; Davis, B. G.; Dondoni, A. Multi-Molecule Reaction of Serum Albumin Can Occur through Thiol-Yne Coupling. *Chem. Commun.* **2011**, *47*, 11086−11088.
(253) Fiore, M.; Marra, A.; Dondoni, A. Photoinduced Thiol-Ene Coupling as a Click Ligation Tool for Thiodisaccharide Synthesis. *J. Org. Chem.* **2009**, *74*, 4422−4425.
(254) Limnios, D.; Kokotos, C. G. Photoinitiated Thiol-Ene "Click" Reaction: An Organocatalytic Alternative. *Adv. Synth. Catal.* **2017**, *359*, 323−328.
(255) Kelemen, V.; Csavas, M.; Hotzi, J.; Herczeg, M.; Poonam; Rathi, B.; Herczegh, P.; Jain, N.; Borbas, A. Photoinitiated Thiol-Ene Reactions of Various 2,3-Unsaturated O-, C- S- and N-Glycosides - Scope and Limitations Study. *Chem. - Asian J.* **2020**, *15*, 876−891.
(256) Lázár, L.; Csávás, M.; Herczeg, M.; Herczegh, P.; Borbás, A. Synthesis of S-Linked Glycoconjugates and S-Disaccharides by Thiol-Ene Coupling Reaction of Enoses. *Org. Lett.* **2012**, *14*, 4650−4653.
(257) Bege, M.; Bereczki, I.; Herczeg, M.; Kicsák, M.; Eszenyi, D.; Herczegh, P.; Borbás, A. A Low-Temperature, Photoinduced Thiol-Ene Click Reaction: A Mild and Efficient Method for the Synthesis of Sugar-Modified Nucleosides. *Org. Biomol. Chem.* **2017**, *15*, 9226−9233.
(258) AAimetti, A. A.; KShoemaker, R. K.; Lin, C.-C.; Anseth, K. S. On-Resin Peptide Macrocyclization Using Thiol - Ene Click Chemistry. *Chem. Commun.* **2010**, *46*, 4061−4063.
(259) Hu, K.; Geng, H.; Zhang, Q.; Liu, Q.; Xie, M.; Sun, C.; Li, W.; Lin, H.; Jiang, F.; Wang, T.; et al. An in-Tether Chiral Center Modulates the Helicity, Cell Permeability, and Target Binding Affinity of a Peptide. *Angew. Chem., Int. Ed.* **2016**, *55*, 8013−8017.
(260) Wang, Y.; Chou, D.H.-C. A Thiol-Ene Coupling Approach to Native Peptide Stapling and Macrocyclization. *Angew. Chem., Int. Ed.* **2015**, *54*, 10931−10934.
(261) Tian, Y.; Yang, D.; Ye, X.; Li, Z. Thioether-Derived Macrocycle for Peptide Secondary Structure Fixation. *Chem. Rec.* **2017**, *17*, 874−885.
(262) Choi, H.; Kim, M.; Jang, J.; Hong, S. Visible-Light-Induced Cysteine-Specific Bioconjugation: Biocompatible Thiol-Ene Click Chemistry. *Angew. Chem., Int. Ed.* **2020**, *59*, 22514−22522.
(263) Yim, V. V.; Cameron, A. J.; Kavianinia, I.; Harris, P. W. R.; Brimble, M. A. Thiol-Ene Enabled Chemical Synthesis of Truncated S-Lipidated Teixobactin Analogs. *Front. Chem.* **2020**, *8*, 568.
(264) Yim, V. V.; Kavianinia, I.; Cameron, A. J.; Harris, P. W. R.; Brimble, M. A. Direct Synthesis of Cyclic Lipopeptides Using Intramolecular Native Chemical Ligation and Thiol-Ene Clippa Chemistry. *Org. Biomol. Chem.* **2020**, *18*, 2838−2844.
(265) Hoppmann, C.; Schmieder, P.; Heinrich, N.; Beyermann, M. Photoswitchable Click Amino Acids: Light Control of Conformation and Bioactivity. *ChemBioChem* **2011**, *12*, 2555−2559.
(266) Aimetti, A. A.; Feaver, K. R.; Anseth, K. S. Synthesis of Cyclic, Multivalent Arg-Gly-Asp Using Sequential Thiol - Ene/Thiol - Yne Photoreactions. *Chem. Commun.* **2010**, *46*, 5781−5783.
(267) Wu, Z.-G.; Liao, X.-J.; Yuan, L.; Wang, Y.; Zheng, Y.-X.; Zuo, J.-L.; Pan, Y. Visible-Light-Mediated Click Chemistry for Highly Regioselective Azide-Alkyne Cycloaddition by a Photoredox Electron-Transfer Strategy. *Chem. - Eur. J.* **2020**, *26*, 5694−5700.
(268) Beniazza, R.; Lambert, R.; Harmand, L.; Molton, F.; Duboc, C.; Denisov, S.; Jonusauskas, G.; McClenaghan, N. D.; Lastecoueres, D.; Vincent, J.-M. Sunlight-Driven Copper-Catalyst Activation Applied to Photolatent Click Chemistry. *Chem. - Eur. J.* **2014**, *20*, 13181−13187.
(269) Konetski, D.; Gong, T.; Bowman, C. N. Photoinduced Vesicle Formation Via the Copper-Catalyzed Azide-Alkyne Cycloaddition Reaction. *Langmuir* **2016**, *32*, 8195−8201.
(270) Porel, M.; Alabi, C. A. Sequence-Defined Polymers Via Orthogonal Allyl Acrylamide Building Blocks. *J. Am. Chem. Soc.* **2014**, *136*, 13162−13165.
(271) Xi, W.; Pattanayak, S.; Wang, C.; Fairbanks, B.; Gong, T.; Wagner, J.; Kloxin, C. J.; Bowman, C. N. Clickable Nucleic Acids: Sequence-Controlled Periodic Copolymer/Oligomer Synthesis by Orthogonal Thiol-X Reactions. *Angew. Chem., Int. Ed.* **2015**, *54*, 14462−14467.
(272) Han, X.; Domaille, D. W.; Fairbanks, B. D.; He, L.; Culver, H. R.; Zhang, X.; Cha, J. N.; Bowman, C. N. New Generation of Clickable Nucleic Acids: Synthesis and Active Hybridization with DNA. *Biomacromolecules* **2018**, *19*, 4139−4146.
(273) Han, X.; Fairbanks, B. D.; Sinha, J.; Bowman, C. N. Sequence-Controlled Synthesis of Advanced Clickable Synthetic Oligonucleotides. *Macromol. Rapid Commun.* **2020**, *41*, 2000327.
(274) Zydziak, N.; Konrad, W.; Feist, F.; Afonin, S.; Weidner, S.; Barner-Kowollik, C. Coding and Decoding Libraries of Sequence-Defined Functional Copolymers Synthesized Via Photoligation. *Nat. Commun.* **2016**, *7*, 13672.
(275) Konrad, W.; Bloesser, F. R.; Wetzel, K. S.; Boukis, A. C.; Meier, M. A. R.; Barner-Kowollik, C. A Combined Photochemical and Multicomponent Reaction Approach to Precision Oligomers. *Chem. - Eur. J.* **2018**, *24*, 3413−3419.
(276) Alim, M. D.; Childress, K. K.; Baugh, N. J.; Martinez, A. M.; Davenport, A.; Fairbanks, B. D.; McBride, M. K.; Worrell, B. T.; Stansbury, J. W.; McLeod, R. R.; et al. A Photopolymerizable Thermoplastic with Tunable Mechanical Performance. *Mater. Horiz.* **2020**, *7*, 835−842.
(277) Childress, K. K.; Alim, M. D.; Hernandez, J. J.; Stansbury, J. W.; Bowman, C. N. Additive Manufacture of Lightly Crosslinked Semicrystalline Thiol-Enes for Enhanced Mechanical Performance. *Polym. Chem.* **2020**, *11*, 39−46.
(278) Konkolewicz, D.; Gray-Weale, A.; Perrier, S. Hyperbranched Polymers by Thiol-Yne Chemistry: From Small Molecules to Functional Polymers. *J. Am. Chem. Soc.* **2009**, *131*, 18075−18077.
(279) Li, N.; Tsoi, T.-H.; Lo, W.-S.; Gu, Y.-J.; Wan, H.-Y.; Wong, W.-T. An Efficient Approach to Synthesize Glycerol Dendrimers Via Thiol-Yne "Click" Chemistry and Their Application in Stabilization of Gold Nanoparticles with X-Ray Attenuation Properties. *Polym. Chem.* **2017**, *8*, 6989−6996.
(280) Chen, G.; Kumar, J.; Gregory, A.; Stenzel, M. H. Efficient Synthesis of Dendrimersvia a Thiol-Yne and Esterification Process and Their Potential Application in the Delivery of Platinum Anti-Cancer Drugs. *Chem. Commun.* **2009**, 6291−6293.
(281) Killops, K. L.; Campos, L. M.; Hawker, C. J. Robust, Efficient, and Orthogonal Synthesis of Dendrimers Via Thiol-Ene "Click" Chemistry. *J. Am. Chem. Soc.* **2008**, *130*, 5062−5064.
(282) Debets, M. F.; van Hest, J. C. M.; Rutjes, P. J. T. Bioorthogonal Labelling of Biomolecules: New Functional Handles and Ligation Methods. *Org. Biomol. Chem.* **2013**, *11*, 6439−6455.
(283) Ivancová, I.; Leone, D.-L.; Hocek, M. Reactive Modifications of DNA Nucleobases for Labelling, Bioconjugations, and Cross-Linking. *Curr. Opin. Chem. Biol.* **2019**, *52*, 136−144.
(284) Sutton, D. A.; Yu, S.-H.; Steet, R.; Popik, V. V. Cyclopropenone-Caged Sondheimer Diyne (Dibenzo[a, E]-Cyclooctadiyne): A Photoactivatable Linchpin for Efficient Spaac Crosslinking. *Chem. Commun.* **2016**, *52*, 553−556.
(285) Chang, T.-C.; Adak, A. K.; Lin, T.-W.; Li, P.-J.; Chen, Y.-J.; Lai, C.-H.; Liang, C.-F.; Chen, Y.-J.; Lin, C.-C. A Photo-Cleavable Biotin Affinity Tag for the Facile Release of a Photo-Crosslinked Carbohydrate-Binding Protein. *Bioorg. Med. Chem.* **2016**, *24*, 1216−1224.
(286) Arts, R.; Ludwig, S. K. J.; van Gerven, B. C. B.; Estirado, E. M.; Milroy, L.-G.; Merkx, M. Semisynthetic Bioluminescent Sensor Proteins for Direct Detection of Antibodies and Small Molecules in Solution. *ACS Sens.* **2017**, *2*, 1730−1736.
(287) Sadiki, A.; Kercher, E. M.; Lu, H.; Lang, R. T.; Spring, B. Q.; Zhou, Z. S. Site-Specific Bioconjugation and Convergent Click

https://doi.org/10.1021/acs.chemrev.0c01212
Chem. Rev. 2021, 121, 6915−6990

Chemistry Enhances Antibody-Chromophore Conjugate Binding Efficiency. *Photochem. Photobiol.* **2020**, *96*, 596−603.
(288) Ramil, C. P.; Dong, M.; An, P.; Lewandowski, T. M.; Yu, Z.; Miller, L. J.; Lin, Q. Spirohexene-Tetrazine Ligation Enables Bioorthogonal Labeling of Class B G Protein-Coupled Receptors in Live Cells. *J. Am. Chem. Soc.* **2017**, *139*, 13376−13386.
(289) Wang, L.; Zhang, J.; Zhao, J.; Yu, P.; Wang, S.; Hu, H.; Wang, R. Recent Synthesis of Functionalized S-Tetrazines and Their Application in Ligation Reactions under Physiological Conditions: A Concise Overview. *Catal. Rev. Sci. Eng.* **2020**, 1−42.
(290) Yu, Z.; Ho, L. Y.; Lin, Q. Rapid, Photoactivatable Turn-on Fluorescent Probes Based on an Intramolecular Photoclick Reaction. *J. Am. Chem. Soc.* **2011**, *133*, 11912−11915.
(291) Wang, J.; Zhang, W.; Song, W.; Wang, Y.; Yu, Z.; Li, J.; Wu, M.; Wang, L.; Zang, J.; Lin, Q. A Biosynthetic Route to Photoclick Chemistry on Proteins. *J. Am. Chem. Soc.* **2010**, *132*, 14812−14818.
(292) Lee, Y.-J.; Wu, B.; Raymond, J. E.; Zeng, Y.; Fang, X.; Wooley, K. L.; Liu, W. R. A Genetically Encoded Acrylamide Functionality. *ACS Chem. Biol.* **2013**, *8*, 1664−1670.
(293) Li, F.; Zhang, H.; Sun, Y.; Pan, Y.; Zhou, J.; Wang, J. Expanding the Genetic Code for Photoclick Chemistry in E. Coli, Mammalian Cells, and A. Thaliana. *Angew. Chem., Int. Ed.* **2013**, *52*, 9700−9704.
(294) Yu, Z.; Lim, R. K. V.; Lin, Q. Synthesis of Macrocyclic Tetrazoles for Rapid Photoinduced Bioorthogonal 1,3-Dipolar Cycloaddition Reactions. *Chem. - Eur. J.* **2010**, *16*, 13325−13329.
(295) Lang, K.; Davis, L.; Torres-Kolbus, J.; Chou, C.; Deiters, A.; Chin, J. W. Genetically Encoded Norbornene Directs Site-Specific Cellular Protein Labelling Via a Rapid Bioorthogonal Reaction. *Nat. Chem.* **2012**, *4*, 298−304.
(296) Kaya, E.; Vrabel, M.; Deiml, C.; Prill, S.; Fluxa, V. S.; Carell, T. A Genetically Encoded Norbornene Amino Acid for the Mild and Selective Modification of Proteins in a Copper-Free Click Reaction. *Angew. Chem., Int. Ed.* **2012**, *51*, 4466−4469.
(297) Yu, Z.; Pan, Y.; Wang, Z.; Wang, J.; Lin, Q. Genetically Encoded Cyclopropene Directs Rapid, Photoclick-Chemistry-Mediated Protein Labeling in Mammalian Cells. *Angew. Chem., Int. Ed.* **2012**, *51*, 10600−10604.
(298) Yu, Z.; Lin, Q. Design of Spiro[2.3]Hex-1-Ene, a Genetically Encodable Double-Strained Alkene for Superfast Photoclick Chemistry. *J. Am. Chem. Soc.* **2014**, *136*, 4153−4156.
(299) Arndt, S.; Wagenknecht, H.-A. Photoclick" Postsynthetic Modification of DNA. *Angew. Chem., Int. Ed.* **2014**, *53*, 14580−14582.
(300) Merkel, M.; Arndt, S.; Ploschik, D.; Cserép, G. B.; Wenge, U.; Kele, P.; Wagenknecht, H.-A. Scope and Limitations of Typical Copper-Free Bioorthogonal Reactions with DNA: Reactive 2'-Deoxyuridine Triphosphates for Postsynthetic Labeling. *J. Org. Chem.* **2016**, *81*, 7527−7538.
(301) Lehmann, B.; Wagenknecht, H.-A. Fluorogenic "Photoclick" Labelling of DNA Using a Cy3 Dye. *Org. Biomol. Chem.* **2018**, *16*, 7579−7582.
(302) Zhou, Z.; Xie, X.; Yi, Q.; Yin, W.; Kadi, A. A.; Li, J.; Zhang, Y. Enzyme-Instructed Self-Assembly with Photo-Responses for the Photo-Regulation of Cancer Cells. *Org. Biomol. Chem.* **2017**, *15*, 6892−6895.
(303) Yu, Z.; Ohulchanskyy, T. Y.; An, P.; Prasad, P. N.; Lin, Q. Fluorogenic, Two-Photon-Triggered Photoclick Chemistry in Live Mammalian Cells. *J. Am. Chem. Soc.* **2013**, *135*, 16766−16769.
(304) Zhou, M.; Hu, J.; Zheng, M.; Song, Q.; Li, J.; Zhang, Y. Photo-Click Construction of a Targetable and Activatable Two-Photon Probe Imaging Protease in Apoptosis. *Chem. Commun.* **2016**, *52*, 2342−2345.
(305) Wu, Y.; Guo, G.; Zheng, J.; Xing, D.; Zhang, T. Fluorogenic "Photoclick" Labeling and Imaging of DNA with Coumarin-Fused Tetrazole in Vivo. *ACS Sens.* **2019**, *4*, 44−51.
(306) Zhu, B.; Ge, J.; Yao, S. Q. Developing New Chemical Tools for DNA Methyltransferase 1 (Dnmt 1): A Small-Molecule Activity-Based Probe and Novel Tetrazole-Containing Inhibitors. *Bioorg. Med. Chem.* **2015**, *23*, 2917−2927.
(307) An, P.; Lin, Q. Sterically Shielded Tetrazoles for a Fluorogenic Photoclick Reaction: Tuning Cycloaddition Rate and Product Fluorescence. *Org. Biomol. Chem.* **2018**, *16*, 5241−5244.
(308) Yao, Z.; Wu, X.; Zhang, X.; Xiong, Q.; Jiang, S.; Yu, Z. Synthesis and Evaluation of Photo-Activatable B-Diarylsydnone- L -Alanines for Fluorogenic Photo-Click Cyclization of Peptides. *Org. Biomol. Chem.* **2019**, *17*, 6777−6781.
(309) Favre, C.; Friscourt, F. Fluorogenic Sydnone-Modified Coumarins Switched-on by Copper-Free Click Chemistry. *Org. Lett.* **2018**, *20*, 4213−4217.
(310) Krell, K.; Harijan, D.; Ganz, D.; Doll, L.; Wagenknecht, H.-A. Postsynthetic Modifications of DNA and Rna by Means of Copper-Free Cycloadditions as Bioorthogonal Reactions. *Bioconjugate Chem.* **2020**, *31*, 990−1011.
(311) Li, J.; Kong, H.; Huang, L.; Cheng, B.; Qin, K.; Zheng, M.; Yan, Z.; Zhang, Y. Visible Light-Initiated Bioorthogonal Photoclick Cycloaddition. *J. Am. Chem. Soc.* **2018**, *140*, 14542−14546.
(312) Jung, S.; Kwon, I. Expansion of Bioorthogonal Chemistries Towards Site-Specific Polymer-Protein Conjugation. *Polym. Chem.* **2016**, *7*, 4584−4598.
(313) Dondoni, A.; Massi, A.; Nanni, P.; Roda, A. A New Ligation Strategy for Peptide and Protein Glycosylation: Photoinduced Thiol-Ene Coupling. *Chem. - Eur. J.* **2009**, *15*, 11444−11449.
(314) Denis, M.; Softley, C.; Giuntini, S.; Gentili, M.; Ravera, E.; Parigi, G.; Fragai, M.; Popowicz, G.; Sattler, M.; Luchinat, C.; et al. The Photocatalyzed Thiol-Ene Reaction: A New Tag to Yield Fast, Selective and Reversible Paramagnetic Tagging of Proteins. *ChemPhysChem* **2020**, *21*, 863−869.
(315) Gunnoo, S. B.; Madder, A. Chemical Protein Modification through Cysteine. *ChemBioChem* **2016**, *17*, 529−553.
(316) Li, Y.; Yang, M.; Huang, Y.; Song, X.; Liu, L.; Chen, P. R. Genetically Encoded Alkenyl-Pyrrolysine Analogues for Thiol-Ene Reaction Mediated Site-Specific Protein Labeling. *Chem. Sci.* **2012**, *3*, 2766−2770.
(317) Weinrich, D.; Lin, P.-C.; Jonkheijm, P.; Nguyen, U. T. T.; Schröder, H.; Niemeyer, C. M.; Alexandrov, K.; Goody, R.; Waldmann, H. Oriented Immobilization of Farnesylated Proteins by the Thiol-Ene Reaction. *Angew. Chem., Int. Ed.* **2010**, *49*, 1252−1257.
(318) Minozzi, M.; Monesi, A.; Nanni, D.; Spagnolo, P.; Marchetti, N.; Massi, A. An Insight into the Radical Thiol/Yne Coupling: The Emergence of Arylalkyne-Tagged Sugars for the Direct Photoinduced Glycosylation of Cysteine-Containing Peptides. *J. Org. Chem.* **2011**, *76*, 450−459.
(319) Li, Y.; Pan, M.; Li, Y.; Huang, Y.; Guo, Q. Thiol-Yne Radical Reaction Mediated Site-Specific Protein Labeling Via Genetic Incorporation of an Alkynyl-L-Lysine Analogue. *Org. Biomol. Chem.* **2013**, *11*, 2624−2629.
(320) Liu, J.; Cheng, R.; Wu, H.; Li, S.; Wang, P. G.; DeGrado, W. F.; Rozovsky, S.; Wang, L. Building and Breaking Bonds Via a Compact S-Propargyl-Cysteine to Chemically Control Enzymes and Modify Proteins. *Angew. Chem., Int. Ed.* **2018**, *57*, 12702−12706.
(321) Luo, W.; Pulsipher, A.; Dutta, D.; Lamb, B. M.; Yousaf, M. N. Remote Control of Tissue Interactions Via Engineered Photo-Switchable Cell Surfaces. *Sci. Rep.* **2015**, *4*, 6313.
(322) Lodge, T. P. Block Copolymers: Past Successes and Future Challenges. *Macromol. Chem. Phys.* **2003**, *204*, 265−273.
(323) Hu, H.; Gopinadhan, M.; Osuji, C. O. Directed Self-Assembly of Block Copolymers: A Tutorial Review of Strategies for Enabling Nanotechnology with Soft Matter. *Soft Matter* **2014**, *10*, 3867−3889.
(324) Doran, S.; Murtezi, E.; Barlas, F. B.; Timur, S.; Yagci, Y. One-Pot Photo-Induced Sequential Cuaac and Thiol-Ene Click Strategy for Bioactive Macromolecular Synthesis. *Macromolecules* **2014**, *47*, 3608−3613.
(325) Derboven, P.; D'Hooge, D. R.; Stamenovic, M. M.; Espeel, P.; Marin, G. B.; Du Prez, F. E.; Reyniers, M.-F. Kinetic Modeling of Radical Thiol-Ene Chemistry for Macromolecular Design: Importance of Side Reactions and Diffusional Limitations. *Macromolecules* **2013**, *46*, 1732−1742.

https://doi.org/10.1021/acs.chemrev.0c01212
Chem. Rev. 2021, 121, 6915−6990

(326) Colak, B.; Da Silva, J. C. S.; Soares, T. A.; Gautrot, J. E. Impact of the Molecular Environment on Thiol-Ene Coupling for Biofunctionalization and Conjugation. *Bioconjugate Chem.* **2016**, *27*, 2111−2123.
(327) Stamenovic, M. M.; Espeel, P.; Van Camp, W.; Du Prez, F. E. Norbornenyl-Based Raft Agents for the Preparation of Functional Polymers Via Thiol-Ene Chemistry. *Macromolecules* **2011**, *44*, 5619−5630.
(328) Walker, C. N.; Sarapas, J. M.; Kung, V.; Hall, A. L.; Tew, G. N. Multiblock Copolymers by Thiol Addition across Norbornene. *ACS Macro Lett.* **2014**, *3*, 453−457.
(329) Feist, F.; Menzel, J. P.; Weil, T.; Blinco, J. P.; Barner-Kowollik, C. Visible Light-Induced Ligation Via O-Quinodimethane Thioethers. *J. Am. Chem. Soc.* **2018**, *140*, 11848−11854.
(330) Niu, J.; Lunn, D. J.; Pusuluri, A.; Yoo, J. I.; O'Malley, M. A.; Mitragotri, S.; Soh, H. T.; Hawker, C. J. Engineering Live Cell Surfaces with Functional Polymers Via Cytocompatible Controlled Radical Polymerization. *Nat. Chem.* **2017**, *9*, 537−545.
(331) Ye, X.; Yuan, J.; Jiang, Z.; Wang, S.; Wang, P.; Wang, Q.; Cui, L. Thiol-Ene Photoclick Reaction: An Eco-Friendly and Facile Approach for Preparation of Mpeg-G-Keratin Biomaterial. *Eng. Life Sci.* **2020**, *20*, 17−25.
(332) Siti, W.; Khan, A. K.; de Hoog, H.-P. M.; Liedberg, B.; Nallani, M. Photo-Induced Conjugation of Tetrazoles to Modified and Native Proteins. *Org. Biomol. Chem.* **2015**, *13*, 3202−3206.
(333) Bauer, D. M.; Rogge, A.; Stolzer, L.; Barner-Kowollik, C.; Fruk, L. Light Induced DNA-Protein Conjugation. *Chem. Commun.* **2013**, *49*, 8626−8628.
(334) Vigovskaya, A.; Abt, D.; Ahmed, I.; Niemeyer, C. M.; Barner-Kowollik, C.; Fruk, L. Photo-Induced Chemistry for the Design of Oligonucleotide Conjugates and Surfaces. *J. Mater. Chem. B* **2016**, *4*, 442−449.
(335) Asatekin, A.; Barr, M. C.; Baxamusa, S. H.; Lau, K. K. S.; Tenhaeff, W.; Xu, J.; Gleason, K. K. Designing Polymer Surfaces Via Vapor Deposition. *Mater. Today* **2010**, *13*, 26−33.
(336) Decher, G.; Hong, J. D. Buildup of Ultrathin Multilayer Films by a Self-Assembly Process: Ii. Consecutive Adsorption of Anionic and Cationic Bipolar Amphiphiles and Polyelectrolytes on Charged Surfaces. *Ber. Bunsen Ges. Phys. Chem.* **1991**, *95*, 1430−1434.
(337) Ohno, K.; Ma, Y.; Huang, Y.; Mori, C.; Yahata, Y.; Tsujii, Y.; Maschmeyer, T.; Moraes, J.; Perrier, S. Surface-Initiated Reversible Addition-Fragmentation Chain Transfer (Raft) Polymerization from Fine Particles Functionalized with Trithiocarbonates. *Macromolecules* **2011**, *44*, 8944−8953.
(338) Yan, W.; Dadashi-Silab, S.; Matyjaszewski, K.; Spencer, N. D.; Benetti, E. M. Surface-Initiated Photoinduced Atrp: Mechanism, Oxygen Tolerance, and Temporal Control During the Synthesis of Polymer Brushes. *Macromolecules* **2020**, *53*, 2801−2810.
(339) Jonkheijm, P.; Weinrich, D.; Köhn, M.; Engelkamp, H.; Christianen, P. C. M.; Kuhlmann, J.; Maan, J. C.; Nüsse, D.; Schroeder, H.; Wacker, R.; et al. Photochemical Surface Patterning by the Thiol-Ene Reaction. *Angew. Chem., Int. Ed.* **2008**, *47*, 4421−4424.
(340) Wu, J.-T.; Huang, C.-H.; Liang, W.-C.; Wu, Y.-L.; Yu, J.; Chen, H.-Y. Reactive Polymer Coatings: A General Route to Thiol-Ene and Thiol-Yne Click Reactions. *Macromol. Rapid Commun.* **2012**, *33*, 922−927.
(341) Bhairamadgi, N. S.; Gangarapu, S.; Caipa Campos, M. A.; Paulusse, J. M. J.; van Rijn, C. J. M.; Zuilhof, H. Efficient Functionalization of Oxide-Free Silicon(111) Surfaces: Thiol-Yne Versus Thiol-Ene Click Chemistry. *Langmuir* **2013**, *29*, 4535−4542.
(342) Ma, S. J.; Ford, E. M.; Sawicki, L. A.; Sutherland, B. P.; Halaszynski, N. I.; Carberry, B. J.; Wagner, N. J.; Kloxin, A. M.; Kloxin, C. J. Surface Chemical Functionalization of Wrinkled Thiol-Ene Elastomers for Promoting Cellular Alignment. *ACS Appl. Bio Mater.* **2020**, *3*, 3731−3740.
(343) Liang, H.; Gagné, J. D.; Faye, A.; Rodrigue, D.; Brisson, J. Ground Tire Rubber (Gtr) Surface Modification Using Thiol-Ene Click Reaction: Polystyrene Grafting to Modify a Gtr/Polystyrene (Ps) Blend. *Prog. Rubber, Plast. Recycl. Technol.* **2020**, *36*, 81−101.
(344) Preuss, C. M.; Tischer, T.; Rodriguez-Emmenegger, C.; Zieger, M. M.; Bruns, M.; Goldmann, A. S.; Barner-Kowollik, C. A Bioinspired Light Induced Avenue for the Design of Patterned Functional Interfaces. *J. Mater. Chem. B* **2014**, *2*, 36−40.
(345) Zhang, X. N.; Liang, J. W.; Chen, Z. Y.; Donley, C.; Zhang, X. L.; Cheng, G. T. Surface Modification of Bombyx Mori Silk Fibroin Film Via Thiol-Ene Click Chemistry. *Processes* **2020**, *8*, 498.
(346) Zhang, P.; Wang, Q.; Shen, J.; Wang, P.; Yuan, J.; Fan, X. Enzymatic Thiol-Ene Click Reaction: An Eco-Friendly Approach for Mpegma-Grafted Modification of Wool Fibers. *ACS Sustainable Chem. Eng.* **2019**, *7*, 13446−13455.
(347) Hu, Y.; Wang, W.; Xu, L.; Yu, D. Surface Modification of Keratin Fibers through Step-Growth Dithiol-Diacrylate Thiol-Ene Click Reactions. *Mater. Lett.* **2016**, *178*, 159−162.
(348) Wilke, P.; Abt, D.; Große, S.; Barner-Kowollik, C.; Börner, H. G. Selective Functionalization of Laser Printout Patterns on Cellulose Paper Sheets Coated with Surface-Specific Peptides. *J. Mater. Chem. A* **2017**, *5*, 16144−16149.
(349) Blasco, E.; Piñol, M.; Oriol, L.; Schmidt, B. V. K. J.; Welle, A.; Trouillet, V.; Bruns, M.; Barner-Kowollik, C. Photochemical Generation of Light Responsive Surfaces. *Adv. Funct. Mater.* **2013**, *23*, 4011−4019.
(350) Delafresnaye, L.; Zaquen, N.; Kuchel, R. P.; Blinco, J. P.; Zetterlund, P. B.; Barner-Kowollik, C. A Simple and Versatile Pathway for the Synthesis of Visible Light Photoreactive Nanoparticles. *Adv. Funct. Mater.* **2018**, *28*, 1800342.
(351) de los Santos Pereira, A.; Kostina, N. Y.; Bruns, M.; Rodriguez-Emmenegger, C.; Barner-Kowollik, C. Phototriggered Functionalization of Hierarchically Structured Polymer Brushes. *Langmuir* **2015**, *31*, 5899−5907.
(352) Arumugam, S.; Popik, V. V. Sequential "Click" - "Photo-Click" Cross-Linker for Catalyst-Free Ligation of Azide-Tagged Substrates. *J. Org. Chem.* **2014**, *79*, 2702−2708.
(353) Arumugam, S.; Orski, S. V.; Locklin, J.; Popik, V. V. Photoreactive Polymer Brushes for High-Density Patterned Surface Derivatization Using a Diels-Alder Photoclick Reaction. *J. Am. Chem. Soc.* **2012**, *134*, 179−182.
(354) Richter, B.; Pauloehrl, T.; Kaschke, J.; Fichtner, D.; Fischer, J.; Greiner, A. M.; Wedlich, D.; Wegener, M.; Delaittre, G.; Barner-Kowollik, C.; et al. Three-Dimensional Microscaffolds Exhibiting Spatially Resolved Surface Chemistry. *Adv. Mater.* **2013**, *25*, 6117−6122.
(355) Stockmayer, W. H. Theory of Molecular Size Distribution and Gel Formation in Branched Polymers Ii. General Cross Linking. *J. Chem. Phys.* **1944**, *12*, 125−131.
(356) Lu, H.; Carioscia, J. A.; Stansbury, J. W.; Bowman, C. N. Investigations of Step-Growth Thiol-Ene Polymerizations for Novel Dental Restoratives. *Dent. Mater.* **2005**, *21*, 1129−1136.
(357) Reinelt, S.; Tabatabai, M.; Moszner, N.; Fischer, U. K.; Utterodt, A.; Ritter, H. Synthesis and Photopolymerization of Thiol-Modified Triazine-Based Monomers and Oligomers for the Use in Thiol-Ene-Based Dental Composites. *Macromol. Chem. Phys.* **2014**, *215*, 1415−1425.
(358) Podgorski, M.; Becka, E.; Claudino, M.; Flores, A.; Shah, P. K.; Stansbury, J. W.; Bowman, C. N. Ester-Free Thiol-Ene Dental Restoratives-Part A: Resin Development. *Dent. Mater.* **2015**, *31*, 1255−1262.
(359) Song, H. B.; Sowan, N.; Shah, P. K.; Baranek, A.; Flores, A.; Stansbury, J. W.; Bowman, C. N. Reduced Shrinkage Stress Via Photo-Initiated Copper(I)-Catalyzed Cycloaddition Polymerizations of Azide-Alkyne Resins. *Dent. Mater.* **2016**, *32*, 1332−1342.
(360) El-Zaatari, B.; Shete, A.; Kloxin, C. Photo-Cuaac Applications in Dental Restorative Materials. *Abst. Pap. Am. Chem. Soc.* **2017**, *253*, 1.
(361) Huang, S.; Podgorski, M.; Zhang, X.; Sinha, J.; Claudino, M.; Stansbury, J. W.; Bowman, C. N. Dental Restorative Materials Based on Thiol-Michael Photopolymerization. *J. Dent. Res.* **2018**, *97*, 530−536.

https://doi.org/10.1021/acs.chemrev.0c01212
Chem. Rev. 2021, 121, 6915−6990

(362) Lovell, L. G.; Berchtold, K. A.; Elliott, J. E.; Lu, H.; Bowman, C. N. Understanding the Kinetics and Network Formation of Dimethacrylate Dental Resins. *Polym. Adv. Technol.* **2001**, *12*, 335−345.
(363) Carioscia, J. A.; Lu, H.; Stanbury, J. W.; Bowman, C. N. Thiol-Ene Oligomers as Dental Restorative Materials. *Dent. Mater.* **2005**, *21*, 1137−1143.
(364) Podgorski, M.; Becka, E.; Claudino, M.; Flores, A.; Shah, P. K.; Stansbury, J. W.; Bowman, C. N. Ester-Free Thiol-Ene Dental Restoratives-Part B: Composite Development. *Dent. Mater.* **2015**, *31*, 1263−1270.
(365) Ye, S.; Azarnoush, S.; Smith, I. R.; Cramer, N. B.; Stansbury, J. W.; Bowman, C. N. Using Hyperbranched Oligomer Functionalized Glass Fillers to Reduce Shrinkage Stress. *Dent. Mater.* **2012**, *28*, 1004−1011.
(366) Roth, M.; Oesterreicher, A.; Mostegel, F. H.; Moser, A.; Pinter, G.; Edler, M.; Piock, R.; Griesser, T. Silicon-Based Mercaptans: High-Performance Monomers for Thiol-Ene Photopolymerization. *J. Polym. Sci., Part A: Polym. Chem.* **2016**, *54*, 418−424.
(367) Sinha, J.; Dobson, A.; Bankhar, O.; Podgorski, M.; Shah, P. K.; Zajdowicz, S. L. W.; Alotaibi, A.; Stansbury, J. W.; Bowman, C. N. Vinyl Sulfonamide Based Thermosetting Composites Via Thiol-Michael Polymerization. *Dent. Mater.* **2020**, *36*, 249−256.
(368) Song, H. B.; Wang, X.; Patton, J. R.; Stansbury, J. W.; Bowman, C. N. Kinetics and Mechanics of Photo-Polymerized Triazole-Containing Thermosetting Composites Via the Copper(I)-Catalyzed Azide-Alkyne Cycloaddition. *Dent. Mater.* **2017**, *33*, 621−629.
(369) Leonards, H.; Engelhardt, S.; Hoffmann, A.; Pongratz, L.; Schriever, S.; Blasius, J.; Wehner, M.; Gillner, A. Advantages and Drawbacks of Thiol-Ene Based Resins for 3d-Printing. In *Laser 3D Manufacturing II*, Helvajian, H., et al., Eds.; Spie-Int Soc Optical Engineering: Bellingham. 2015.
(370) Roppolo, I.; Frascella, F.; Gastaldi, M.; Castellino, M.; Ciubini, B.; Barolo, C.; Scaltrito, L.; Nicosia, C.; Zanetti, M.; Chiappone, A. Thiol-Yne Chemistry for 3d Printing: Exploiting an Off-Stoichiometric Route for Selective Functionalization of 3d Objects. *Polym. Chem.* **2019**, *10*, 5950−5958.
(371) Childress, K. K.; Alim, M. D.; Hernandez, J. J.; Stansbury, J. W.; Bowman, C. N. Additive Manufacture of Lightly Crosslinked Semicrystalline Thiol-Enes for Enhanced Mechanical Performance. *Polym. Chem.* **2020**, *11*, 39−46.
(372) Lovelady, E.; Kimmins, S. D.; Wu, J.; Cameron, N. R. Preparation of Emulsion-Templated Porous Polymers Using Thiol-Ene and Thiol-Yne Chemistry. *Polym. Chem.* **2011**, *2*, 559−562.
(373) Chen, C.; Eissa, A. M.; Schiller, T. L.; Cameron, N. R. Emulsion-Templated Porous Polymers Prepared by Thiol-Ene and Thiol-Yne Photopolymerisation Using Multifunctional Acrylate and Non-Acrylate Monomers. *Polymer* **2017**, *126*, 395−401.
(374) Amato, D. N.; Amato, D. V.; Sandoz, M.; Weigand, J.; Patton, D. L.; Visser, C. W. Programmable Porous Polymers Via Direct Bubble Writing with Surfactant-Free Inks. *ACS Appl. Mater. Interfaces* **2020**, *12*, 42048−42055.
(375) Svejdal, R. R.; Dickinson, E. R.; Sticker, D.; Kutter, J. P.; Rand, K. D. Thiol-Ene Microfluidic Chip for Performing Hydrogen/Deuterium Exchange of Proteins at Subsecond Time Scales. *Anal. Chem.* **2019**, *91*, 1309−1317.
(376) Jönsson, A.; Svejdal, R. R.; Bøgelund, N.; Nguyen, T. T. T. N.; Flindt, H.; Kutter, J. P.; Rand, K. D.; Lafleur, J. P. Thiol-Ene Monolithic Pepsin Microreactor with a 3d-Printed Interface for Efficient Uplc-Ms Peptide Mapping Analyses. *Anal. Chem.* **2017**, *89*, 4573−4580.
(377) Quick, A. S.; Fischer, J.; Richter, B.; Pauloehrl, T.; Trouillet, V.; Wegener, M.; Barner-Kowollik, C. Preparation of Reactive Three-Dimensional Microstructures Via Direct Laser Writing and Thiol-Ene Chemistry. *Macromol. Rapid Commun.* **2013**, *34*, 335−340.
(378) Kumpfmueller, J.; Stadlmann, K.; Li, Z.; Satzinger, V.; Stampfl, J.; Liska, R. Two-Photon-Induced Thiol-Ene Polymerization as a Fabrication Tool for Flexible Optical Waveguides. *Des. Monomers Polym.* **2014**, *17*, 390−400.
(379) Griesser, T.; Wolfberger, A.; Daschiel, U.; Schmidt, V.; Fian, A.; Jerrar, A.; Teichert, C.; Kern, W. Cross-Linking of Romp Derived Polymers Using the Two-Photon Induced Thiol-Ene Reaction: Towards the Fabrication of 3d-Polymer Microstructures. *Polym. Chem.* **2013**, *4*, 1708−1714.
(380) Nguyen, L. H.; Straub, M.; Gu, M. Acrylate-Based Photopolymer for Two-Photon Microfabrication and Photonic Applications. *Adv. Funct. Mater.* **2005**, *15*, 209−216.
(381) Wu, S.; Straub, M.; Gu, M. Single-Monomer Acrylate-Based Resin for Three-Dimensional Photonic Crystal Fabrication. *Polymer* **2005**, *46*, 10246−10255.
(382) Batchelor, R.; Messer, T.; Hippler, M.; Wegener, M.; Barner-Kowollik, C.; Blasco, E. Two in One: Light as a Tool for 3d Printing and Erasing at the Microscale. *Adv. Mater.* **2019**, *31*, 1904085.
(383) Quick, A. S.; Rothfuss, H.; Welle, A.; Richter, B.; Fischer, J.; Wegener, M.; Barner-Kowollik, C. Fabrication and Spatially Resolved Functionalization of 3d Microstructures Via Multiphoton-Induced Diels-Alder Chemistry. *Adv. Funct. Mater.* **2014**, *24*, 3571−3580.
(384) Dickey, M. D.; Collister, E.; Raines, A.; Tsiartas, P.; Holcombe, T.; Sreenivasan, S. V.; Bonnecaze, R. T.; Willson, C. G. Photocurable Pillar Arrays Formed Via Electrohydrodynamic Instabilities. *Chem. Mater.* **2006**, *18*, 2043−2049.
(385) Sticker, D.; Geczy, R.; Häfeli, U. O.; Kutter, J. P. Thiol-Ene Based Polymers as Versatile Materials for Microfluidic Devices for Life Sciences Applications. *ACS Appl. Mater. Interfaces* **2020**, *12*, 10080−10095.
(386) Tähkä, S. M.; Bonabi, A.; Jokinen, V. P.; Sikanen, T. M. Aqueous and Non-Aqueous Microchip Electrophoresis with on-Chip Electrospray Ionization Mass Spectrometry on Replica-Molded Thiol-Ene Microfluidic Devices. *J. Chromatogr. A* **2017**, *1496*, 150−156.
(387) Waheed, S.; Cabot, J. M.; Macdonald, N. P.; Lewis, T.; Guijt, R. M.; Paull, B.; Breadmore, M. C. 3d Printed Microfluidic Devices: Enablers and Barriers. *Lab Chip* **2016**, *16*, 1993−2013.
(388) Mongkhontreerat, S.; Öberg, K.; Erixon, L.; Löwenhielm, P.; Hult, A.; Malkoch, M. Uv Initiated Thiol-Ene Chemistry: A Facile and Modular Synthetic Methodology for the Construction of Functional 3d Networks with Tunable Properties. *J. Mater. Chem. A* **2013**, *1*, 13732−13737.
(389) Carlborg, C. F.; Haraldsson, T.; Öberg, K.; Malkoch, M.; van der Wijngaart, W. Beyond Pdms: Off-Stoichiometry Thiol-Ene (Oste) Based Soft Lithography for Rapid Prototyping of Microfluidic Devices. *Lab Chip* **2011**, *11*, 3136−3147.
(390) Good, B. T.; Reddy, S.; Davis, R. H.; Bowman, C. N. Tailorable Low Modulus, Reversibly Deformable Elastomeric Thiol-Ene Materials for Microfluidic Applications. *Sens. Actuators, B* **2007**, *120*, 473−480.
(391) Ashley, J. F.; Cramer, N. B.; Davis, R. H.; Bowman, C. N. Soft-Lithography Fabrication of Microfluidic Features Using Thiol-Ene Formulations. *Lab Chip* **2011**, *11*, 2772−2778.
(392) Hillmering, M.; Pardon, G.; Vastesson, A.; Supekar, O.; Carlborg, C. F.; Brandner, B. D.; van der Wijngaart, W.; Haraldsson, T. Off-Stoichiometry Improves the Photostructuring of Thiol-Enes through Diffusion-Induced Monomer Depletion. *Microsyst. Nanoeng.* **2016**, *2*, 15043.
(393) Zhou, X. C.; Sjöberg, R.; Druet, A.; Schwenk, J. M.; van der Wijngaart, W.; Haraldsson, T.; Carlborg, C. F. Thiol-Ene-Epoxy Thermoset for Low-Temperature Bonding to Biofunctionalized Microarray Surfaces. *Lab Chip* **2017**, *17*, 3672−3681.
(394) Zurgil, N.; Afrimzon, E.; Deutsch, A.; Namer, Y.; Shafran, Y.; Sobolev, M.; Tauber, Y.; Ravid-Hermesh, O.; Deutsch, M. Polymer Live-Cell Array for Real-Time Kinetic Imaging of Immune Cells. *Biomaterials* **2010**, *31*, 5022−5029.
(395) Markovitz-Bishitz, Y.; Tauber, Y.; Afrimzon, E.; Zurgil, N.; Sobolev, M.; Shafran, Y.; Deutsch, A.; Howitz, S.; Deutsch, M. A Polymer Microstructure Array for the Formation, Culturing, and High Throughput Drug Screening of Breast Cancer Spheroids. *Biomaterials* **2010**, *31*, 8436−8444.

https://doi.org/10.1021/acs.chemrev.0c01212
Chem. Rev. 2021, 121, 6915−6990

(396) Tan, H.-Y.; Trier, S.; Rahbek, U. L.; Dufva, M.; Kutter, J. P.; Andresen, T. L. A Multi-Chamber Microfluidic Intestinal Barrier Model Using Caco-2 Cells for Drug Transport Studies. *PLoS One* **2018**, *13*, No. e0197101.
(397) Burke, J. M.; Pandit, K. R.; Goertz, J. P.; White, I. M. Fabrication of Rigid Microstructures with Thiol-Ene-Based Soft Lithography for Continuous-Flow Cell Lysis. *Biomicrofluidics* **2014**, *8*, 056503.
(398) D'Eramo, L.; Chollet, B.; Leman, M.; Martwong, E.; Li, M.; Geisler, H.; Dupire, J.; Kerdraon, M.; Vergne, C.; Monti, F.; et al. Microfluidic Actuators Based on Temperature-Responsive Hydrogels. *Microsyst. Nanoeng.* **2018**, *4*, 17069.
(399) Lu, N.; Sticker, D.; Kretschmann, A.; Petersen, N. J.; Kutter, J. P. A Thiol-Ene Microfluidic Device Enabling Continuous Enzymatic Digestion and Electrophoretic Separation as Front-End to Mass Spectrometric Peptide Analysis. *Anal. Bioanal. Chem.* **2020**, *412*, 3559−3571.
(400) Macdonald, E. K.; Shaver, M. P. Intrinsic High Refractive Index Polymers. *Polym. Int.* **2015**, *64*, 6−14.
(401) Liu, J.-g.; Ueda, M. High Refractive Index Polymers: Fundamental Research and Practical Applications. *J. Mater. Chem.* **2009**, *19*, 8907−8919.
(402) Bhagat, S. D.; Filho, E. B. D. S.; Stiegman, A. E. High Refractive Index Polymer Composites Synthesized by Cross-Linking of Oxozirconium Clusters through Thiol-Ene Polymerization. *Macromol. Mater. Eng.* **2015**, *300*, 580−585.
(403) Su, Y.; Filho, E. B. D. S.; Peek, N.; Chen, B.; Stiegman, A. E. High Refractive Index Polymers (N > 1.7), Based on Thiol-Ene Cross-Linking of Polarizable P-S and P-Se Organic/Inorganic Monomers. *Macromolecules* **2019**, *52*, 9012−9022.
(404) Fang, L.; Sun, J.; Chen, X.; Tao, Y.; Zhou, J.; Wang, C.; Fang, Q. Phosphorus- and Sulfur-Containing High-Refractive-Index Polymers with High Tg and Transparency Derived from a Bio-Based Aldehyde. *Macromolecules* **2020**, *53*, 125−131.
(405) Chen, X.; Fang, L.; Wang, J.; He, F.; Chen, X.; Wang, Y.; Zhou, J.; Tao, Y.; Sun, J.; Fang, Q. Intrinsic High Refractive Index Siloxane-Sulfide Polymer Networks Having High Thermostability and Transmittance Via Thiol-Ene Cross-Linking Reaction. *Macromolecules* **2018**, *51*, 7567−7573.
(406) Bhagat, S. D.; Chatterjee, J.; Chen, B.; Stiegman, A. E. High Refractive Index Polymers Based on Thiol-Ene Cross-Linking Using Polarizable Inorganic/Organic Monomers. *Macromolecules* **2012**, *45*, 1174−1181.
(407) Natarajan, L. V.; Shepherd, C. K.; Brandelik, D. M.; Sutherland, R. L.; Chandra, S.; Tondiglia, V. P.; Tomlin, D.; Bunning, T. J. Switchable Holographic Polymer-Dispersed Liquid Crystal Reflection Gratings Based on Thiol-Ene Photopolymerization. *Chem. Mater.* **2003**, *15*, 2477−2484.
(408) Natarajan, L. V.; Brown, D. P.; Wofford, J. M.; Tondiglia, V. P.; Sutherland, R. L.; Lloyd, P. F.; Bunning, T. J. Holographic Polymer Dispersed Liquid Crystal Reflection Gratings Formed by Visible Light Initiated Thiol-Ene Photopolymerization. *Polymer* **2006**, *47*, 4411−4420.
(409) Peng, H.; Nair, D. P.; Kowalski, B. A.; Xi, W.; Gong, T.; Wang, C.; Cole, M.; Cramer, N. B.; Xie, X.; McLeod, R. R.; et al. High Performance Graded Rainbow Holograms Via Two-Stage Sequential Orthogonal Thiol-Click Chemistry. *Macromolecules* **2014**, *47*, 2306−2315.
(410) Nakabayashi, K.; Sobu, S.; Kosuge, Y.; Mori, H. Synthesis and Nanoimprinting of High Refractive Index and Highly Transparent Polythioethers Based on Thiol-Ene Click Chemistry. *J. Polym. Sci., Part A: Polym. Chem.* **2018**, *56*, 2175−2182.
(411) Hata, E.; Mitsube, K.; Momose, K.; Tomita, Y. Holographic Nanoparticle-Polymer Composites Based on Step-Growth Thiol-Ene Photopolymerization. *Opt. Mater. Express* **2011**, *1*, 207−222.
(412) Mitsube, K.; Nishimura, Y.; Nagaya, K.; Takayama, S.; Tomita, Y. Holographic Nanoparticle-Polymer Composites Based on Radical-Mediated Thiol-Yne Photopolymerizations: Characterization and Shift-Multiplexed Holographic Digital Data Page Storage. *Opt. Mater. Express* **2014**, *4*, 982−996.
(413) Alim, M. D.; Mavila, S.; Miller, D. B.; Huang, S.; Podgórski, M.; Cox, L. M.; Sullivan, A. C.; McLeod, R. R.; Bowman, C. N. Realizing High Refractive Index Thiol-X Materials: A General and Scalable Synthetic Approach. *ACS Materials Letters* **2019**, *1*, 582−588.
(414) Chan, J. W.; Zhou, H.; Hoyle, C. E.; Lowe, A. B. Photopolymerization of Thiol-Alkynes: Polysulfide Networks. *Chem. Mater.* **2009**, *21*, 1579−1585.
(415) Peng, H.; Wang, C.; Xi, W.; Kowalski, B. A.; Gong, T.; Xie, X.; Wang, W.; Nair, D. P.; McLeod, R. R.; Bowman, C. N. Facile Image Patterning Via Sequential Thiol-Michael/Thiol-Yne Click Reactions. *Chem. Mater.* **2014**, *26*, 6819−6826.
(416) Slaughter, B. V.; Khurshid, S. S.; Fisher, O. Z.; Khademhosseini, A.; Peppas, N. A. Hydrogels in Regenerative Medicine. *Adv. Mater.* **2009**, *21*, 3307−3329.
(417) Grim, J. C.; Marozas, I. A.; Anseth, K. S. Thiol-Ene and Photo-Cleavage Chemistry for Controlled Presentation of Biomolecules in Hydrogels. *J. Controlled Release* **2015**, *219*, 95−106.
(418) Brown, T.; Anseth, K. Spatiotemporal Hydrogel Biomaterials for Regenerative Medicine. *Chem. Soc. Rev.* **2017**, *46*, 6532−6552.
(419) Lin, C.-C.; Ki, C. S.; Shih, H. Thiol-Norbornene Photoclick Hydrogels for Tissue Engineering Applications. *J. Appl. Polym. Sci.* **2015**, *132*, 41563.
(420) Kharkar, P. M.; Rehmann, M. S.; Skeens, K. M.; Maverakis, E.; Kloxin, A. M. Thiol-Ene Click Hydrogels for Therapeutic Delivery. *ACS Biomater. Sci. Eng.* **2016**, *2*, 165−179.
(421) Kharkar, P. M.; Kiick, K. L.; Kloxin, A. M. Designing Degradable Hydrogels for Orthogonal Control of Cell Microenvironments. *Chem. Soc. Rev.* **2013**, *42*, 7335−7372.
(422) Polizzotti, B. D.; Fairbanks, B. D.; Anseth, K. S. Three-Dimensional Biochemical Patterning of Click-Based Composite Hydrogels Via Thiolene Photopolymerization. *Biomacromolecules* **2008**, *9*, 1084−1087.
(423) McCall, J. D.; Anseth, K. S. Thiol-Ene Photopolymerizations Provide a Facile Method to Encapsulate Proteins and Maintain Their Bioactivity. *Biomacromolecules* **2012**, *13*, 2410−2417.
(424) Shih, H.; Lin, C.-C. Photoclick Hydrogels Prepared from Functionalized Cyclodextrin and Poly(Ethylene Glycol) for Drug Delivery and in Situ Cell Encapsulation. *Biomacromolecules* **2015**, *16*, 1915−1923.
(425) Cleophas, R. T. C.; Riool, M.; Quarles van Ufford, H. C.; Zaat, S. A. J.; Kruijtzer, J. A. W.; Liskamp, R. M. J. Convenient Preparation of Bactericidal Hydrogels by Covalent Attachment of Stabilized Antimicrobial Peptides Using Thiol-Ene Click Chemistry. *ACS Macro Lett.* **2014**, *3*, 477−480.
(426) Wojda, S. J.; Marozas, I. A.; Anseth, K. S.; Yaszemski, M. J.; Donahue, S. W. Thiol-Ene Hydrogels for Local Delivery of Pth for Bone Regeneration in Critical Size Defects. *J. Orthop. Res.* **2020**, *38*, 536−544.
(427) Hunckler, M. D.; Medina, J. D.; Coronel, M. M.; Weaver, J. D.; Stabler, C. L.; García, A. J. Linkage Groups within Thiol-Ene Photoclickable Peg Hydrogels Control in Vivo Stability. *Adv. Healthcare Mater.* **2019**, *8*, 1900371.
(428) Ooi, H. W.; Mota, C.; Ten Cate, A. T.; Calore, A.; Moroni, L.; Baker, M. B. Thiol-Ene Alginate Hydrogels as Versatile Bioinks for Bioprinting. *Biomacromolecules* **2018**, *19*, 3390−3400.
(429) Deng, J.-R.; Chung, S.-F.; Leung, A.S.-L.; Yip, W.-M.; Yang, B.; Choi, M.-C.; Cui, J.-F.; Kung, K.K.-Y.; Zhang, Z.; Lo, K.-W.; et al. Chemoselective and Photocleavable Cysteine Modification of Peptides and Proteins Using Isoxazoliniums. *Commun. Chem.* **2019**, *2*, 93.
(430) Daniele, M. A.; Adams, A. A.; Naciri, J.; North, S. H.; Ligler, F. S. Interpenetrating Networks Based on Gelatin Methacrylamide and Peg Formed Using Concurrent Thiol Click Chemistries for Hydrogel Tissue Engineering Scaffolds. *Biomaterials* **2014**, *35*, 1845−1856.
(431) Li, M.; Dove, A. P.; Truong, V. X. Additive-Free Green Light-Induced Ligation Using Bodipy Triggers. *Angew. Chem., Int. Ed.* **2020**, *59*, 2284−2288.

https://doi.org/10.1021/acs.chemrev.0c01212
Chem. Rev. 2021, 121, 6915−6990

(432) Fan, Y.; Deng, C.; Cheng, R.; Meng, F.; Zhong, Z. In Situ Forming Hydrogels Via Catalyst-Free and Bioorthogonal "Tetrazole-Alkene" Photo-Click Chemistry. *Biomacromolecules* **2013**, *14*, 2814−2821.
(433) He, M.; Li, J.; Tan, S.; Wang, R.; Zhang, Y. Photodegradable Supramolecular Hydrogels with Fluorescence Turn-on Reporter for Photomodulation of Cellular Microenvironments. *J. Am. Chem. Soc.* **2013**, *135*, 18718−18721.
(434) Adzima, B. J.; Tao, Y.; Kloxin, C. J.; DeForest, C. A.; Anseth, K. S.; Bowman, C. N. Spatial and Temporal Control of the Alkyne-Azide Cycloaddition by Photoinitiated Cu(Ii) Reduction. *Nat. Chem.* **2011**, *3*, 256−259.
(435) Maiti, B.; Abramov, A.; Franco, L.; Puiggalí, J.; Enshaei, H.; Alemán, C.; Díaz, D. D. Thermoresponsive Shape-Memory Hydrogel Actuators Made by Phototriggered Click Chemistry. *Adv. Funct. Mater.* **2020**, *30*, 2001683.
(436) Arkenberg, M. R.; Nguyen, H. D.; Lin, C.-C. Recent Advances in Bio-Orthogonal and Dynamic Crosslinking of Biomimetic Hydrogels. *J. Mater. Chem. B* **2020**, *8*, 7835−7855.
(437) Munoz-Robles, B. G.; Kopyeva, I.; DeForest, C. A. Surface Patterning of Hydrogel Biomaterials to Probe and Direct Cell-Matrix Interactions. *Adv. Mater. Interfaces* **2020**, *7*, 2001198.
(438) Petrou, C. L.; D'Ovidio, T. J.; Bölükbas, D. A.; Tas, S.; Brown, R. D.; Allawzi, A.; Lindstedt, S.; Nozik-Grayck, E.; Stenmark, K. R.; Wagner, D. E.; et al. Clickable Decellularized Extracellular Matrix as a New Tool for Building Hybrid-Hydrogels to Model Chronic Fibrotic Diseases in Vitro. *J. Mater. Chem. B* **2020**, *8*, 6814−6826.
(439) Mabry, K. M.; Lawrence, R. L.; Anseth, K. S. Dynamic Stiffening of Poly(Ethylene Glycol)-Based Hydrogels to Direct Valvular Interstitial Cell Phenotype in a Three-Dimensional Environment. *Biomaterials* **2015**, *49*, 47−56.
(440) Aziz, A. H.; Wahlquist, J.; Sollner, A.; Ferguson, V.; DelRio, F. W.; Bryant, S. J. Mechanical Characterization of Sequentially Layered Photo-Clickable Thiol-Ene Hydrogels. *J. Mech. Behav. Biomed. Mater.* **2017**, *65*, 454−465.
(441) Hui, E.; Gimeno, K. I.; Guan, G.; Caliari, S. R. Spatiotemporal Control of Viscoelasticity in Phototunable Hyaluronic Acid Hydrogels. *Biomacromolecules* **2019**, *20*, 4126−4134.
(442) Tong, X.; Jiang, J.; Zhu, D.; Yang, F. Hydrogels with Dual Gradients of Mechanical and Biochemical Cues for Deciphering Cell-Niche Interactions. *ACS Biomater. Sci. Eng.* **2016**, *2*, 845−852.
(443) Carberry, B. J.; Rao, V. V.; Anseth, K. S. Phototunable Viscoelasticity in Hydrogels through Thioester Exchange. *Ann. Biomed. Eng.* **2020**, *48*, 2053−2063.
(444) Mosiewicz, K. A.; Kolb, L.; van der Vlies, A. J.; Martino, M. M.; Lienemann, P. S.; Hubbell, J. A.; Ehrbar, M.; Lutolf, M. P. In Situ Cell Manipulation through Enzymatic Hydrogel Photopatterning. *Nat. Mater.* **2013**, *12*, 1072−1078.
(445) Mosiewicz, K. A.; Kolb, L.; van der Vlies, A. J.; Lutolf, M. P. Microscale Patterning of Hydrogel Stiffness through Light-Triggered Uncaging of Thiols. *Biomater. Sci.* **2014**, *2*, 1640−1651.
(446) Fairbanks, B. D.; Schwartz, M. P.; Halevi, A. E.; Nuttelman, C. R.; Bowman, C. N.; Anseth, K. S. A Versatile Synthetic Extracellular Matrix Mimic Via Thiol-Norbornene Photopolymerization. *Adv. Mater.* **2009**, *21*, 5005−5010.
(447) Batchelor, R. R.; Blasco, E.; Wuest, K. N. R.; Lu, H.; Wegener, M.; Barner-Kowollik, C.; Stenzel, M. H. Spatially Resolved Coding of Λ-Orthogonal Hydrogels by Laser Lithography. *Chem. Commun.* **2018**, *54*, 2436−2439.
(448) Ma, H.; Caldwell, A. S.; Azagarsamy, M. A.; Gonzalez Rodriguez, A.; Anseth, K. S. Bioorthogonal Click Chemistries Enable Simultaneous Spatial Patterning of Multiple Proteins to Probe Synergistic Protein Effects on Fibroblast Function. *Biomaterials* **2020**, *255*, 120205.
(449) Horn-Ranney, E. L.; Khoshakhlagh, P.; Kaiga, J. W.; Moore, M. J. Light-Reactive Dextran Gels with Immobilized Guidance Cues for Directed Neurite Growth in 3d Models. *Biomater. Sci.* **2014**, *2*, 1450−1459.
(450) Luo, Y.; Shoichet, M. S. A Photolabile Hydrogel for Guided Three-Dimensional Cell Growth and Migration. *Nat. Mater.* **2004**, *3*, 249−253.
(451) Luo, Y.; Shoichet, M. S. Light-Activated Immobilization of Biomolecules to Agarose Hydrogels for Controlled Cellular Response. *Biomacromolecules* **2004**, *5*, 2315−2323.
(452) Wosnick, J. H.; Shoichet, M. S. Three-Dimensional Chemical Patterning of Transparent Hydrogels. *Chem. Mater.* **2008**, *20*, 55−60.
(453) Wylie, R. G.; Shoichet, M. S. Three-Dimensional Spatial Patterning of Proteins in Hydrogels. *Biomacromolecules* **2011**, *12*, 3789−3796.
(454) Liu, Z.; Lin, Q.; Sun, Y.; Liu, T.; Bao, C.; Li, F.; Zhu, L. Spatiotemporally Controllable and Cytocompatible Approach Builds 3d Cell Culture Matrix by Photo-Uncaged-Thiol Michael Addition Reaction. *Adv. Mater.* **2014**, *26*, 3912−3917.
(455) Liu, Z.; Liu, T.; Lin, Q.; Bao, C.; Zhu, L. Photoreleasable Thiol Chemistry for Facile and Efficient Bioconjugation. *Chem. Commun.* **2014**, *50*, 1256−1258.
(456) Chen, R. T.; Marchesan, S.; Evans, R. A.; Styan, K. E.; Such, G. K.; Postma, A.; McLean, K. M.; Muir, B. W.; Caruso, F. Photoinitiated Alkyne-Azide Click and Radical Cross-Linking Reactions for the Patterning of Peg Hydrogels. *Biomacromolecules* **2012**, *13*, 889−895.
(457) Bjerknes, M.; Cheng, H.; McNitt, C. D.; Popik, V. V. Facile Quenching and Spatial Patterning of Cyloоctynes Via Strain-Promoted Alkyne-Azide Cycloaddition of Inorganic Azides. *Bioconjugate Chem.* **2017**, *28*, 1560−1565.
(458) Yu, C.; Schimelman, J.; Wang, P.; Miller, K. L.; Ma, X.; You, S.; Guan, J.; Sun, B.; Zhu, W.; Chen, S. Photopolymerizable Biomaterials and Light-Based 3d Printing Strategies for Biomedical Applications. *Chem. Rev.* **2020**, *120*, 10695.
(459) Skardal, A.; Zhang, J.; Prestwich, G. D. Bioprinting Vessel-Like Constructs Using Hyaluronan Hydrogels Crosslinked with Tetrahedral Polyethylene Glycol Tetracrylates. *Biomaterials* **2010**, *31*, 6173−6181.
(460) Stichler, S.; Jungst, T.; Schamel, M.; Zilkowski, I.; Kuhlmann, M.; Böck, T.; Blunk, T.; Teßmar, J.; Groll, J. Thiol-Ene Clickable Poly(Glycidol) Hydrogels for Biofabrication. *Ann. Biomed. Eng.* **2017**, *45*, 273−285.
(461) Bertlein, S.; Brown, G.; Lim, K. S.; Jungst, T.; Boeck, T.; Blunk, T.; Tessmar, J.; Hooper, G. J.; Woodfield, T. B. F.; Groll, J. Thiol-Ene Clickable Gelatin: A Platform Bioink for Multiple 3d Biofabrication Technologies. *Adv. Mater.* **2017**, *29*, 1703404.
(462) Wang, L. L.; Highley, C. B.; Yeh, Y.-C.; Galarraga, J. H.; Uman, S.; Burdick, J. A. Three-Dimensional Extrusion Bioprinting of Single- and Double-Network Hydrogels Containing Dynamic Covalent Crosslinks. *J. Biomed. Mater. Res., Part A* **2018**, *106*, 865−875.
(463) Qin, X.-H.; Torgersen, J.; Saf, R.; Mühleder, S.; Pucher, N.; Ligon, S. C.; Holnthoner, W.; Redl, H.; Ovsianikov, A.; Stampfl, J.; et al. Three-Dimensional Microfabrication of Protein Hydrogels Via Two-Photon-Excited Thiol-Vinyl Ester Photopolymerization. *J. Polym. Sci., Part A: Polym. Chem.* **2013**, *51*, 4799−4810.
(464) Qin, X.-H.; Gruber, P.; Markovic, M.; Plochberger, B.; Klotzsch, E.; Stampfl, J.; Ovsianikov, A.; Liska, R. Enzymatic Synthesis of Hyaluronic Acid Vinyl Esters for Two-Photon Microfabrication of Biocompatible and Biodegradable Hydrogel Constructs. *Polym. Chem.* **2014**, *5*, 6523−6533.
(465) Baudis, S.; Bomze, D.; Markovic, M.; Gruber, P.; Ovsianikov, A.; Liska, R. Modular Material System for the Microfabrication of Biocompatible Hydrogels Based on Thiol-Ene-Modified Poly(Vinyl Alcohol). *J. Polym. Sci., Part A: Polym. Chem.* **2016**, *54*, 2060−2070.
(466) Dobos, A.; Van Hoorick, J.; Steiger, W.; Gruber, P.; Markovic, M.; Andriotis, O. G.; Rohatschek, A.; Dubruel, P.; Thurner, P. J.; Van Vlierberghe, S.; Baudis, S.; Ovsianikov, A. Thiol-Gelatin-Norbornene Bioink for Laser-Based High-Definition Bioprinting. *Adv. Healthcare Mater.* **2020**, *9*, 1900752.
(467) Skardal, A.; Devarasetty, M.; Kang, H.-W.; Mead, I.; Bishop, C.; Shupe, T.; Lee, S. J.; Jackson, J.; Yoo, J.; Soker, S.; et al. A

https://doi.org/10.1021/acs.chemrev.0c01212
Chem. Rev. 2021, 121, 6915−6990

Hydrogel Bioink Toolkit for Mimicking Native Tissue Biochemical and Mechanical Properties in Bioprinted Tissue Constructs. *Acta Biomater.* **2015**, *25*, 24−34.
(468) Lee, M.; Rizzo, R.; Surman, F.; Zenobi-Wong, M. Guiding Lights: Tissue Bioprinting Using Photoactivated Materials. *Chem. Rev.* **2020**, *120*, 10950.
(469) Campos, E.; Branquinho, J.; Carreira, A. S.; Carvalho, A.; Coimbra, P.; Ferreira, P.; Gil, M. H. Designing Polymeric Microparticles for Biomedical and Industrial Applications. *Eur. Polym. J.* **2013**, *49*, 2005−2021.
(470) Prasath, R. A.; Gokmen, M. T.; Espeel, P.; Du Prez, F. E. Thiol-Ene and Thiol-Yne Chemistry in Microfluidics: A Straightforward Method Towards Macroporous and Nonporous Functional Polymer Beads. *Polym. Chem.* **2010**, *1*, 685−692.
(471) Durham, O. Z.; Norton, H. R.; Shipp, D. A. Functional Polymer Particles Via Thiol-Ene and Thiol-Yne Suspension "Click" Polymerization. *RSC Adv.* **2015**, *5*, 66757−66766.
(472) Durham, O. Z.; Krishnan, S.; Shipp, D. A. Polymer Microspheres Prepared by Water-Borne Thiol-Ene Suspension Photopolymerization. *ACS Macro Lett.* **2012**, *1*, 1134−1137.
(473) Cai, S.; Weng, Z.; Zheng, Y.; Zhao, B.; Gao, Z.; Gao, C. High Porosity Microspheres with Functional Groups Synthesized by Thiol-Yne Click Suspension Polymerization. *Polym. Chem.* **2016**, *7*, 7400−7407.
(474) Alimohammadi, F.; Wang, C.; Durham, O. Z.; Norton, H. R.; Bowman, C. N.; Shipp, D. A. Radical Mediated Thiol-Ene/Yne Dispersion Polymerizations. *Polymer* **2016**, *105*, 180−186.
(475) Wang, C.; Zhang, X.; Podgórski, M.; Xi, W.; Shah, P.; Stansbury, J.; Bowman, C. N. Monodispersity/Narrow Polydispersity Cross-Linked Microparticles Prepared by Step-Growth Thiol-Michael Addition Dispersion Polymerizations. *Macromolecules* **2015**, *48*, 8461−8470.
(476) Hooker, J. P.; Delafresnaye, L.; Barner, L.; Barner-Kowollik, C. With Polymer Photoclicks to Fluorescent Microspheres. *Mater. Horiz.* **2019**, *6*, 356−363.
(477) Hooker, J. P.; Feist, F.; Delafresnaye, L.; Barner, L.; Barner-Kowollik, C. Precisely Controlled Microsphere Design Via Visible-Light Cross-Linking of Functional Prepolymers. *Adv. Funct. Mater.* **2020**, *30*, 1905399.
(478) Hooker, J. P.; Feist, F.; Delafresnaye, L.; Cavalli, F.; Barner, L.; Barner-Kowollik, C. On-Demand Acid-Gated Fluorescence Switch-on in Photo-Generated Nanospheres. *Chem. Commun.* **2020**, *56*, 4986−4989.
(479) Schmitt, C. W.; Walden, S. L.; Delafresnaye, L.; Houck, H. A.; Barner, L.; Barner-Kowollik, C. The Bright and the Dark Side of the Sphere: Light-Stabilized Microparticles. *Polym. Chem.* **2021**, *12*, 449−457.
(480) Jiang, Y.; Chen, J.; Deng, C.; Suuronen, E. J.; Zhong, Z. Click Hydrogels, Microgels and Nanogels: Emerging Platforms for Drug Delivery and Tissue Engineering. *Biomaterials* **2014**, *35*, 4969−4985.
(481) Gruber, A.; Navarro, L.; Klinger, D. Reactive Precursor Particles as Synthetic Platform for the Generation of Functional Nanoparticles, Nanogels, and Microgels. *Adv. Mater. Interfaces* **2020**, *7*, 1901676.
(482) Hachet, E.; Sereni, N.; Pignot-Paintrand, I.; Ravaine, V.; Szarpak-Jankowska, A.; Auzély-Velty, R. Thiol-Ene Clickable Hyaluronans: From Macro-to Nanogels. *J. Colloid Interface Sci.* **2014**, *419*, 52−55.
(483) Belair, D. G.; Khalil, A. S.; Miller, M. J.; Murphy, W. L. Serum-Dependence of Affinity-Mediated Vegf Release from Biomimetic Microspheres. *Biomacromolecules* **2014**, *15*, 2038−2048.
(484) Jivan, F.; Yegappan, R.; Pearce, H.; Carrow, J. K.; McShane, M.; Gaharwar, A. K.; Alge, D. L. Sequential Thiol-Ene and Tetrazine Click Reactions for the Polymerization and Functionalization of Hydrogel Microparticles. *Biomacromolecules* **2016**, *17*, 3516−3523.
(485) Xin, S.; Dai, J.; Gregory, C. A.; Han, A.; Alge, D. L. Creating Physicochemical Gradients in Modular Microporous Annealed Particle Hydrogels Via a Microfluidic Method. *Adv. Funct. Mater.* **2020**, *30*, 1907102.
(486) Michel, S. E. S.; Dutertre, F.; Denbow, M. L.; Galan, M. C.; Briscoe, W. H. Facile Synthesis of Chitosan-Based Hydrogels and Microgels through Thiol-Ene Photoclick Cross-Linking. *ACS Appl. Bio Mater.* **2019**, *2*, 3257−3268.
(487) Huang, Y.; Yuan, J.; Tang, J.; Yang, J.; Zeng, Z. One Step Synthesis of Monodisperse Thiol-Ene Clickable Polymer Microspheres and Application on Biological Functionalization. *Eur. Polym. J.* **2019**, *110*, 22−30.
(488) Donahoe, C. D.; Cohen, T. L.; Li, W.; Nguyen, P. K.; Fortner, J. D.; Mitra, R. D.; Elbert, D. L. Ultralow Protein Adsorbing Coatings from Clickable Peg Nanogel Solutions: Benefits of Attachment under Salt-Induced Phase Separation Conditions and Comparison with Peg/Albumin Nanogel Coatings. *Langmuir* **2013**, *29*, 4128−4139.
(489) Huang, D. C.; Qian, H. L.; Qiao, H. S.; Chen, W.; Feijen, J.; Zhong, Z. Y. Bioresponsive Functional Nanogels as an Emerging Platform for Cancer Therapy. *Expert Opin. Drug Delivery* **2018**, *15*, 703−716.
(490) Lockhart, J. N.; Beezer, D. B.; Stevens, D. M.; Spears, B. R.; Harth, E. One-Pot Polyglycidol Nanogels Via Liposome Master Templates for Dual Drug Delivery. *J. Controlled Release* **2016**, *244*, 366−374.
(491) Impellitteri, N. A.; Toepke, M. W.; Lan Levengood, S. K.; Murphy, W. L. Specific Vegf Sequestering and Release Using Peptide-Functionalized Hydrogel Microspheres. *Biomaterials* **2012**, *33*, 3475−3484.
(492) Gregoritza, M.; Abstiens, K.; Graf, M.; Goepferich, A. M. Fabrication of Antibody-Loaded Microgels Using Microfluidics and Thiol-Ene Photoclick Chemistry. *Eur. J. Pharm. Biopharm.* **2018**, *127*, 194−203.
(493) Chen, J.; Zou, Y.; Deng, C.; Meng, F.; Zhang, J.; Zhong, Z. Multifunctional Click Hyaluronic Acid Nanogels for Targeted Protein Delivery and Effective Cancer Treatment in Vivo. *Chem. Mater.* **2016**, *28*, 8792−8799.
(494) Gao, G.; Han, X.; Sowan, N.; Zhang, X.; Shah, P. K.; Chen, M.; Bowman, C. N.; Stansbury, J. W. Stress Relaxation Via Covalent Dynamic Bonds in Nanogel-Containing Thiol-Ene Resins. *ACS Macro Lett.* **2020**, *9*, 713−719.
(495) Liang, Y.; Kiick, K. L. Multifunctional Lipid-Coated Polymer Nanogels Crosslinked by Photo-Triggered Michael-Type Addition. *Polym. Chem.* **2014**, *5*, 1728−1736.
(496) Janssens, P.; Debrouwer, W.; Van Aken, K.; Huvaere, K. Thiol-Ene Coupling in a Continuous Photo-Flow Regime. *ChemPhotoChem.* **2018**, *2*, 884−889.
(497) Junkers, T.; Wenn, B. Continuous Photoflow Synthesis of Precision Polymers. *React. Chem. Eng.* **2016**, *1*, 60−64.

https://doi.org/10.1021/acs.chemrev.0c01212
Chem. Rev. 2021, 121, 6915−6990